HYDROGEN BONDING AS IT RELATES TO MISCIBILITY OF HIGH PERFORMANCE POLY(ARYLENE ETHER)S WITH EPOXY RESINS

by

Katherine W. Stickney

Dissertation submitted to the faculty of

the Virginia Polytechnic Institute and State University

in partial fulfillment of the requirements for the degree of
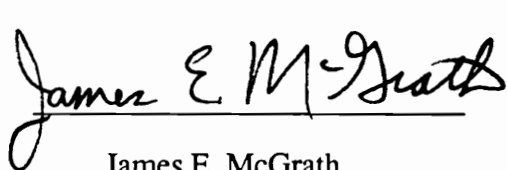
DOCTOR OF PHILOSOPHY

in

Chemistry

APPROVED:
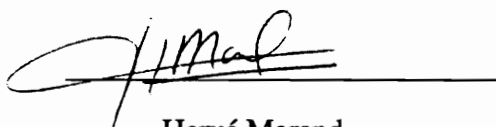
Judy S. Riffle
Judy S. Riffle, Chairman

James E. McGrath   _Harry W. Gibson_

James E. McGrath   Harry W. Gibson

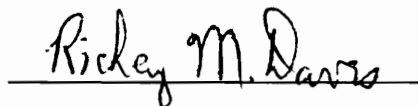_Hervé Marand_   _Richey M. Davis_

Hervé Marand   Richey M. Davis

July, 1995

Blacksburg, VA

C.2

LD
5655
V856
1995
5753
C.2

HYDROGEN BONDING AS IT RELATES TO MISCIBILITY OF HIGH PERFORMANCE POLY(ARYLENE ETHER)S WITH EPOXY RESINS

by

Katherine W. Stickney

Committee Chairman: Dr. J. S. Riffle

Department of Chemistry

(ABSTRACT)

The overall goal of this research project was to synthesize poly(arylene ether)s with electron rich functional groups for use as tougheners in epoxy thermosets followed by evaluation of the miscibility of the poly(arylene ether) materials in cured epoxy thermosets. Poly(arylene ether)s were synthesized by reaction of bisphenol A with a variety of dihalo monomers including 4,4'-difluorodiphenylsulfoxide, 4,4'-difluorodiphenylphenylphosphine oxide, 2,6-dichloropyridine, and 4,4'-dichlorodiphenylsulfone. A novel monomer, 2,3-bis(4-fluorophenyl)quinoxaline was also synthesized and utilized to make quinoxaline-containing homopolymers and copolymers. The bisphenol A based poly(arylene ether)s: poly(arylene ether sulfoxide), poly(arylene ether pyridine) and poly(arylene ether phosphine oxide) were found to be miscible with the amine cured epoxy thermosets. Poly(arylene ether sulfone) and poly(arylene ether quinoxaline) were immiscible with the epoxy thermosets.

Polymer-polymer miscibility is governed in large part by intermolecular attractive forces. To evaluate better the role that hydrogen bonding plays in the miscibility of the

poly(arylene ether)/epoxy blends, a fundamental investigation of hydrogen bonding between model compounds possessing functional groups of interest (e. g. diphenylsulfone, diphenylsulfoxide, pyridine, triphenylphosphine oxide, and diphenylmethylphosphine oxide) and water was undertaken. ^{1}H NMR spectroscopy of model compounds in DMSO-d_6/water (97/3) solutions was performed to ascertain the effect of the mole fraction of model compound in solution on the shift of the water peak in the ^{1}H NMR spectrum. In all cases, increasing mole fractions of the electron rich model compound caused the water resonance to move downfield, revealing the existence of hydrogen bonding interactions between the model compound and water.

The ^{1}H NMR shift data were used to calculate the equilibrium constants of formation of the water-model compound hydrogen bonded complex and the shift of the proton hydrogen bonded to the model compound. The phosphine oxide containing model compounds followed no trend; however, the other model compounds were ranked as: pyridine > diphenylsulfoxide > diphenylsulfone in hydrogen bonding strength. This supports the thermal analysis data which showed that the poly(arylene ether sulfone) was immiscible with the epoxy thermoset while the poly(arylene ether sulfoxide)/epoxy system was miscible.

ACKNOWLEDGEMENTS

TABLE OF CONTENTS

LIST OF FIGURES

LIST OF TABLES

CHAPTER 1

Introduction

Epoxy-graphite fiber composites are currently of great interest in advanced technology fields such as aerospace engineering (1-3). Composite materials possess high strength to weight ratios; incorporation of composite technology in aircraft manufacturing processes could lead to improved structural strength coupled with decreased fuel consumption. There are drawbacks, however, to current epoxy-graphite fiber composite manufacturing processes. Construction of composite pieces is labor intensive; the entire preform must be laid up by hand and thereafter cured in an oven the size of the preform piece. Furthermore, the epoxy-graphite fiber composites can be brittle and can experience catastrophic failure under certain conditions.

In an effort to improve the mechanical properties of epoxy-graphite fiber composites, the effect of using different sizing materials to coat the graphite fibers before prepregging with the epoxy resin will be investigated. It is anticipated that this interlayer material should act as a toughener for the epoxy and also improve adhesion between the epoxy matrix and the graphite fiber. The optimum interlayer sizing should be miscible (or reactive) with the epoxy resin and also will have good adhesion to the normally acidic surface of the graphite fiber. This is accomplished by using a sizing with basic groups that will not only hydrogen bond to the pendant hydroxyl groups on the epoxy backbone but also to the graphite fiber. Possible functional group candidates are shown in Figure 1-1. All of these functional groups possess lone pairs of electrons and π bonds which are available for hydrogen bond formation.

Initial work by Lesko et al. (4, 5) demonstrated that poly(vinylpyrrolidinone) or PVP, an amorphous polymer possessing pendant electron rich polyamide groups, could be used as a sizing material for graphite fibers. It was found that the mechanical properties of

the composites made with PVP sized graphite fibers were superior to the mechanical

properties of composites made with unsized fibers. Use of PVP sized fibers in carbon

fiber-epoxy composites improved the static compressive strength by 51 % and increased

the notched cross ply R = -1 fatigue by two orders of magnitude over epoxy/bisphenol A

sizings (4, 5). Although the PVP was both miscible with the epoxy resin and adhered

well to the graphite fiber, composites made using this method would have compromised

thermal stability due to the aliphatic nature of the poly(vinylpyrrolidinone) backbone.

Aromatic, thermally stable polymers with analogous electron rich functional groups

(Figure 1-1) are now being evaluated as interlayer materials. Because the sizings must be

stable at the elevated epoxy cure temperatures, candidates in this research include

amorphous poly(arylene ether)s with basic functional groups, such as poly(arylene ether
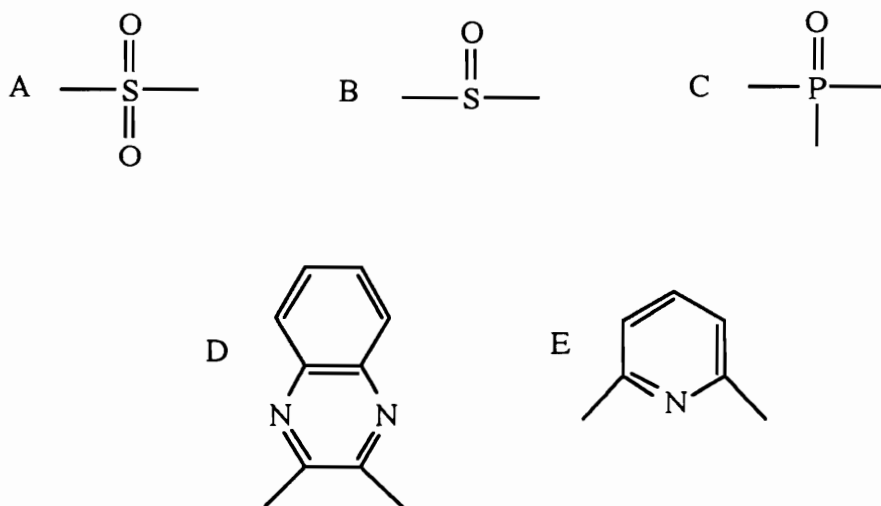
Figure 1-1: Functional group candidates for interlayer sizing materials: A: sulfone; B: sulfoxide; C: phosphine oxide; D: quinoxaline; and E: pyridine

sulfone), poly(arylene ether phosphine oxide), poly(arylene ether pyridine), and poly(arylene ether sulfoxide). Initial blend studies of these bisphenol A based poly(arylene ether)s with epoxy resins were performed to determine miscibility of each modifier in the epoxy resin. Then ^{1}H nuclear magnetic resonance (NMR) spectroscopy studies were performed on ternary solutions containing deuterated dimethyl sulfoxide (DMSO-d_6), water, and model compounds. Polymers containing strongly hydrogen bonding functional groups should show excellent performance as adhesives and tougheners in epoxy based materials. The calculation of the hydrogen bonding ability of the functional group contained in each model compound (phosphine oxide, sulfoxide, sulfone, and pyridine) was an adaptation of the method developed by Lin (6). Here, ^{1}H NMR was employed to evaluate the extent of hydrogen bonding ability of each of the functional groups to water. The shift of the water proton hydrogen bonded to the model compound as well as the equilibrium constant of the water-model compound complex formation may be calculated from the ^{1}H NMR shift data and concentrations of each of the components in the series of hydrogen bonding solutions.

CHAPTER 2

Poly(arylene ether)s: high performance engineering thermoplastics
for epoxy resin blend studies

2.1.   Literature review of poly(arylene ether)s

2.1.1. Electron withdrawing groups in poly(arylene ether) synthesis

Poly(arylene ether)s, thermoplastics with glass transition temperatures in excess of 150 °C, are endowed with exceptional toughness and thermooxidative stability (7). These materials are generally prepared from aromatic bisphenates and dihalo or dinitro monomers (8) or from A-B monomers possessing one phenol and one halo (or nitro) group. The electronegative halogen atom creates an electrophilic (electron poor) site on the aromatic ring; an electron withdrawing group must be in an ortho or para position to this electrophilic site. Attack of the bisphenate nucleophile at this position permits the formation of the resonance stabilized Meisenheimer intermediate as the electron withdrawing group stabilizes the negative charge. The halogen is a better leaving group than the aromatic phenoxy and correspondingly the aromatic ether linkage remains intact as the halide leaves. The displacement of a fluoro, chloro, or nitro group by a nucleophile is referred to as nucleophilic aromatic substitution (9). Electron withdrawing functionalities that activate a dihalo monomer to nucleophilic substitution include: sulfone (10), sulfoxide (11), phosphine oxide (12), quinoxaline (13), benzil (14), ketone (15), ketimine (16), benzoxazole (17), oxadiazoles and triazoles (18, 19), pyridine (20), and phthalimides (21). Detailed information on poly(arylene ether quinoxaline)s and poly(arylene ether sulfoxide)s will be discussed here. Information pertaining to the poly(arylene ether

4

phosphine oxide) (22) poly(arylene ether pyridine) (23), and poly(arylene ether sulfone) (24) materials used in this study has been detailed elsewhere.

2.1.2. Poly(arylene ether quinoxaline)s

2.1.2.1.　　　Classical poly(phenyl quinoxaline) synthesis methods

Poly(phenyl quinoxaline)s are an important family of materials due to their solubility, thermal stability (25), low dielectric constant (26), and excellent mechanical properties (27). Potential uses for these materials include films, coatings, or structural adhesives that require a chemically resistant or insulating resin (28, 29). The quinoxaline moiety was first synthesized in 1884 by Hinsberg and Korner (30), via condensation of o-phenylene diamine with a 1,2-dicarbonyl compound. The first polyquinoxaline was synthesized in 1964 by reaction with a tetraamine and bisglyoxal monomer (31). Poly(phenyl quinoxaline)s were subsequently polymerized from aromatic bis(phenyl-α-diketone)s and aromatic tetraamines (32). The reaction, illustrated in Figure 2-1, progresses at room temperature due to the favorable formation of the aromatic heterocyclic quinoxaline ring over the course of the reaction. Disadvantages of this classical poly(phenyl quinoxaline) synthesis include the multistep synthesis of the tetraketone monomer, making commercial processes difficult, and toxicity of the tetraamines.

2.1.2.2.　　　Polyquinoxalines via the nucleophilic aromatic substitution synthesis route

In the late 1980's, researchers at IBM and NASA Langley spearheaded an effort to achieve the desirable polyquinoxaline thermal and adhesive properties without the

expensive and toxic starting materials. Their work involved preparation of polyphenylquinoxalines via nucleophilic aromatic substitution. This method not only circumvented the expensive tetraketone monomers but provided more facile chemical structure variation (33).
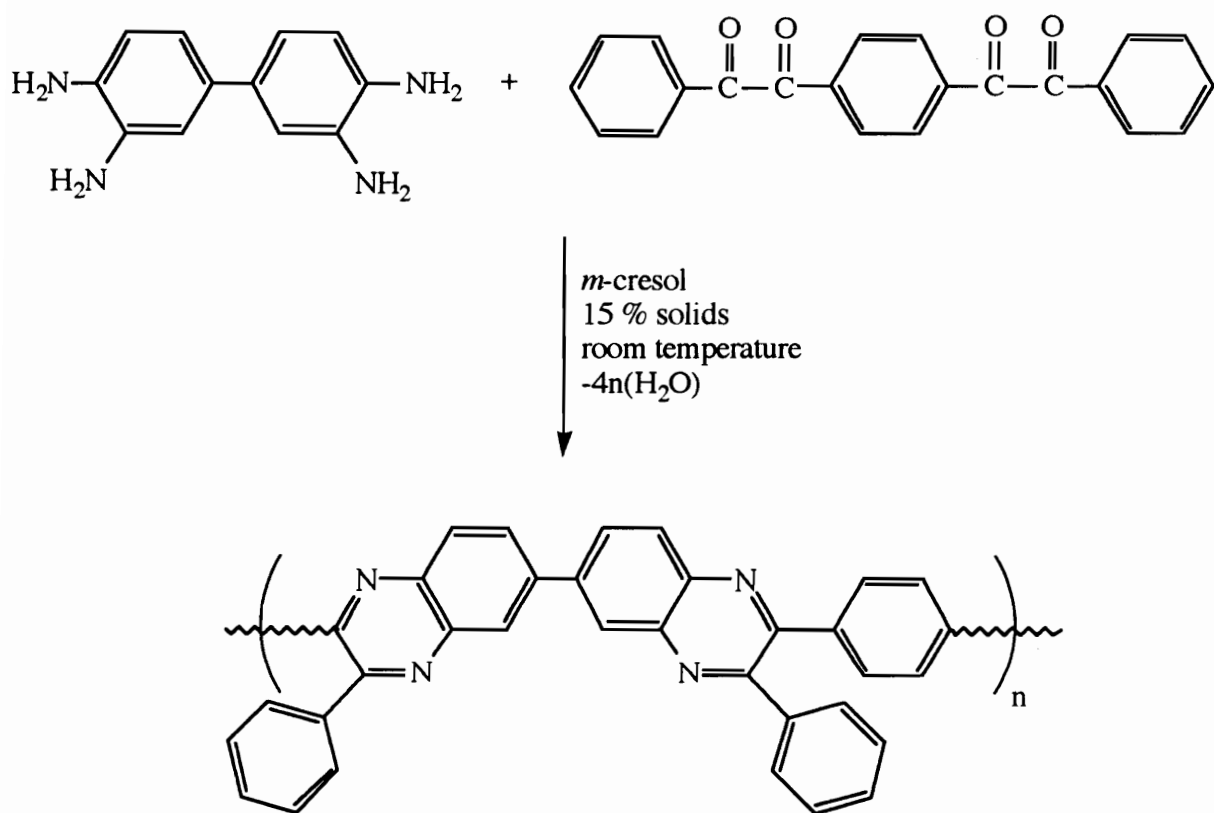
Figure 2-1: Classical poly(phenyl quinoxaline) synthesis route showing the formation of a "cis" repeat unit (pendant phenyl groups are "cis" to each other)

2.1.2.2a.   Quinoxaline-containing bisphenol monomers

The first reported quinoxaline-containing monomer for poly(arylene ether) synthesis was 2,3-bis(4-hydroxyphenyl)quinoxaline, obtained by reaction of 4,4'-dihydroxybenzil with o-phenylene diamine (33). This monomer, containing a preformed quinoxaline ring structure, was subsequently reacted with 4,4'-difluorobenzophenone, 4,4'-difluorodiphenylsulfone, and other dihalo compounds. The polymers prepared from 2,3-bis(4-hydroxyphenyl)quinoxaline precipitated during synthesis from the N,N-dimethylacetamide solvent but inherent viscosities of the polymers, obtained from 0.5 % solutions in m-cresol at 25 °C, ranged from 0.34 to 1.30 dL/g. Glass transition temperatures of the poly(arylene ether quinoxaline)s ranged from 179 to 240 °C. Films of several of these poly(arylene ether quinoxaline)s cast from m-cresol were opaque and showed evidence of low levels of crystallinity by WAXS (34).

2.1.2.2b.   Nucleophilic substitution reactions displacing fluorine at the 6-position on
             the quinoxaline ring

Hedrick and Labadie first ascertained that the electron deficient pyrazine ring component of the quinoxaline ring system could be used to stabilize the negative charge developed in the transition state through a Meisenheimer-like complex in polymerization reactions (35). This discovery provoked the synthesis of dihalo monomers containing preformed quinoxaline moeities. Evidence for the electronic effect of the pyrazine ring on the 6 and 7 positions on the quinoxaline ring included ^{1}H NMR spectroscopy measurements indicating that the shift of the proton ortho to the pyrazine ring was 8.2 ppm

(36). Reaction of 4-fluoro-1,2-phenylene diamine with 1,4-bis(phenylglyoxalyl)benzene produced 1,4-bis(6-fluoro-3-phenyl-2-quinoxalinyl)benzene, a diquinoxaline monomer with fluorines at the 6 position on each of the quinoxaline rings. This monomer, depicted in Figure 2-2, possessed three stereoisomers and when solution polymerized with a variety of bisphenols, including bisphenol A and 3F-bisphenol, produced soluble poly(arylene
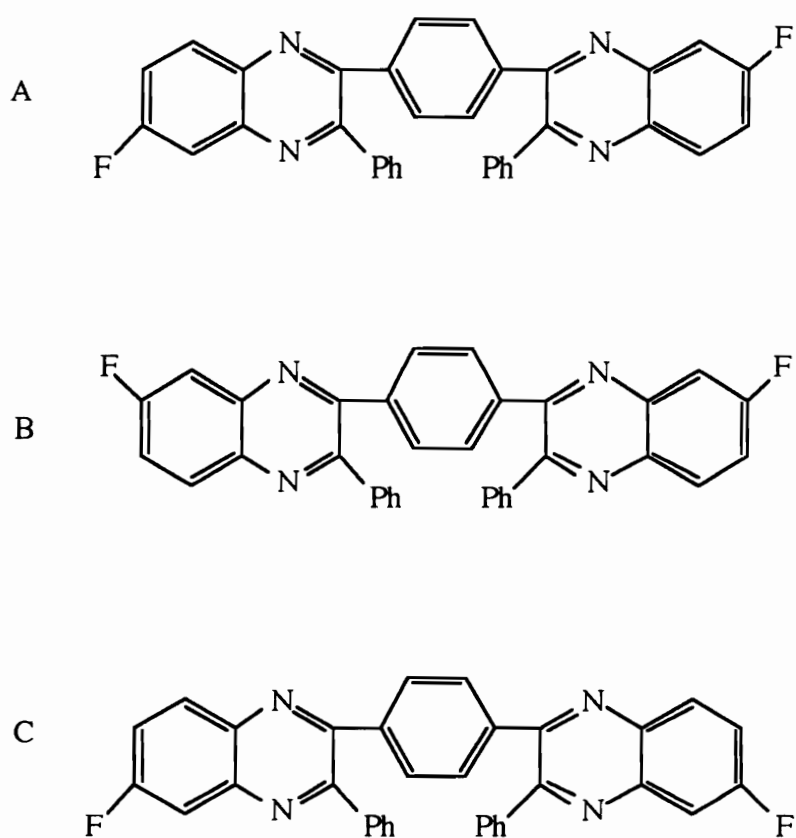
Figure 2-2: The three stereoisomers of 1,4-bis(6-fluoro-3-phenyl-2-quinoxalinyl)benzene:
A: one pendant phenyl group is "trans" and the other pendant phenyl group is "cis" to the fluorine on the same heterocyclic fused ring system; B: the pendant phenyl groups are "trans" to the fluorines; and C: the pendant phenyl groups are "cis" to the fluorines

8

ether quinoxaline)s with glass transition temperatures ranging from 255 to 275 °C (37). Although facile, this method required expensive tetraketone and fluorine substituted o-phenylene diamine starting materials, and as such was not appropriate for commercial scale up. Hedrick and Labadie also evaluated chlorine and nitro functionalities as leaving groups in the quinoxaline activated nucleophilic aromatic substitution and found that chlorine was not quantitatively displaced and that displacement of the nitro group occurred with the generation of many side products (38). Labadie et al. (39) prepared an A-B monomer, 2-(4-hydroxyphenyl)-3-phenyl-6-fluoroquinoxaline, through reaction of 4-methoxybenzil with 4-fluoro-1,2-phenylene diamine, followed by deprotection of the hidden phenol functionality. Self polymerization of this monomer yielded an N-methyl-2-pyrrolidinone soluble polymer with a glass transition temperature of 255 °C. Once again, 4-fluoro-1,2-phenylene diamine was requisite in this poly(arylene ether quinoxaline) synthesis route.

2.1.2.2c.   Remote activation of fluorine to nucleophilic substitution reaction by the
             quinoxaline moiety

A more cost effective route to a difluoro monomer possessing a preformed quinoxaline ring was developed in the early 1990's with the synthesis of the novel compound, 2,3-bis(4-fluorophenyl)quinoxaline (40, 41). This material, obtained from the reaction of 4,4'difluorobenzil with o-phenylene diamine, combined inexpensive starting materials via a facile synthetic pathway. The chemical shift of the proton ortho to the quinoxaline group on the fluorinated aromatic ring of 2,3-bis(4-fluorophenyl)quinoxaline was 7.55 ppm, suggesting that this monomer would have reduced activity relative to the difluoro monomer wherein the fluorine was directly attached to the fused heterocyclic ring structure. However, nucleophilic aromatic substitution polymerization reactions using

similarly unreactive dihalo monomers have been known to proceed under certain conditions. The relatively unreactive triazole-based heterocyclic difluoro monomer, 2,5-bis(4'-fluorophenyl)-4-phenyl-1,2,4-triazole, wherein the shift of the proton ortho to the activating group was 7.38 ppm, was successfully polymerized, albeit under vigorous conditions (42).

The polymers prepared from 2,3-bis(4-fluorophenyl)quinoxaline showed limited solubility in N-methyl-2-pyrrolidinone so Hedrick et al. (40) conducted the polymerizations in 1,3-dimethyl-3,4,5,6-tetrahydro-2(1H)-pyrimidinone (DMPU), an excellent high temperature solvent for polyether syntheses of materials only marginally soluble in other polar aprotic solvents (43). Reaction of 2,3-bis(4-fluorophenyl)quinoxaline with bisphenol A produced an amorphous poly(arylene ether quinoxaline) with a glass transition temperature of 195 °C. Stickney et al. reported a T_g of 200 °C for the same material (41).

2.1.2.3.   Poly(arylene ether quinoxaline) copolymers

Copolymers have been prepared with quinoxaline functionalities randomly distributed along the backbone to improve solubility of the poly(arylene ether quinoxaline)s while maintaining the desirable high temperature and adhesive capabilities of this heterocyclic polymer. Labadie et al. (43) systematically replaced 2,3-bis(4-fluorophenyl)quinoxaline with 4,4'-difluorodiphenylsulfone in reactions with 6F-bisphenol. The resulting poly(arylene ether quinoxaline-co-sulfone)s had equivalent glass transition temperatures to the homopoly(arylene ether quinoxaline)s but had improved solubility in polar aprotic solvents such as NMP and DMAc. Connell et al. (44) synthesized poly(arylene ether quinoxaline-co-phosphine oxide)s to evaluate lightweight, atomic oxygen resistant heterocycle-containing polymers. The resultant materials had

significantly improved oxygen plasma resistance compared to Kapton™, confirming the earlier discovery of Smith (44).

Poly(arylene ether quinoxaline-co-imide) random copolymers have been prepared by first synthesizing an amine functionalized poly(arylene ether quinoxaline) using a 3-aminophenol endcapping reagent, and subsequently mixing this oligomer with a diamine and dianhydride in an imidization reaction (45, 46). After thermal cure, the resulting poly(arylene ether quinoxaline-co-imide)s based on a pyromellitic dianhydride/oxydianiline mixture displayed glass transition temperatures in the 300 °C range with high moduli and improved auto-adhesion relative to the homopolyimides (46). Hergenrother and Havens devised a procedure for poly(arylene ether quinoxaline-co-imide) synthesis from the dihydroxyquinoxaline-containing monomer developed at NASA Langley (47).

2.1.3. Alternate routes to polyquinoxaline materials

Yamamoto et al. developed a novel route to poly(thiophene-co-quinoxaline) materials using a palladium catalyzed polycondensation between 2,5-bis(trimethylstannyl) thiophene and 5,8-dibromoquinoxaline derivatives (48). The quinoxaline has stronger electron accepting properties than pyridine; by UV spectroscopy the perfectly alternating π-conjugated poly(thiophene-co-quinoxaline) showed charge transfer between occupied orbitals of the thiophene donor and unoccupied orbitals of the quinoxaline acceptor.

Chmil and Scherf (49) used the route devised by Suzuki et al. (50) to couple 4,4'-dibromobenzil with 2,5-dihexyl-1,4-phenylenediboronic acid. The palladium catalyzed reaction yielded an aromatic poly(1,2-diketone) of molecular weight 15,000 g/mole, which was quantitatively reacted with 1,2-phenylenediamine in acetic acid to yield a conjugated polyquinoxaline.

2.1.3. Poly(arylene ether sulfoxide)s

Poly(arylene ether sulfoxide) materials were first synthesized by Johnson et al. in 1967 (51). Poly(arylene ether sulfoxides) have also been synthesized by selective oxidation of poly(p-phenoxyphenyl sulfide) to poly(sulfoxide) using hydrogen peroxide (52). Under carefully controlled conditions, the oxidation reaction quantitatively oxidized the thio linkages to sulfoxides without concomitant formation of the polysulfone. The amorphous polysulfoxide product was soluble in a variety of solvents including chloroform, pyridine, and polar aprotic solvents such as N,N-dimethylacetamide.

Babu et al. reported the synthesis of high molecular weight poly(arylene ether sulfoxide)s as amorphous precursors to semicrystalline poly(arylene ether sulfide)s (53). The difluoro monomer, 4,4'-difluorodiphenylsulfoxide, was synthesized using an aluminum chloride catalyzed Friedel-Crafts acylation of fluorobenzene with thionyl chloride (54). The electron withdrawing sulfoxide linkage activated the difluoro compound toward nucleophilic aromatic substitution. Reaction of this monomer with hydroquinone, bisphenol A, or 4,4'-biphenol in the presence of a monofunctional endcapping reagent resulted in preparation of controlled molecular weight poly(arylene ether sulfoxides) with nonreactive endgroups. The poly(arylene ether sulfoxide)s demonstrated interesting thermal properties. By thermogravimetric analysis, the polymer underwent a sharp weight loss corresponding to about 5 weight percent at 400 °C before a more gradual but comprehensive degradation occurring at 500 °C. The glass transition temperatures of the poly(arylene ether sulfoxide)s ranged from 169 to 216 °C, less than those of poly(arylene ether sulfone)s of analogous structures.

2.2.   Introduction

In this research a series of controlled molecular weight high performance poy(arylene ether)s with nonreactive endgroups was synthesized. The dihalo monomer used in the poly(arylene ether) syntheses was systematically varied to provide a series of polymers of the same molecular weight with different functionalities incorporated into the backbone structure. The goal of the research was to identify the relationship between the ability of the poly(arylene ether) to form intermolecular interactions and the polarity and hydrogen bonding ability of various functional groups.

Poly(arylene ether)s utilized in this research were synthesized by reaction of dihalo monomers possessing phosphine oxide, sulfoxide, sulfone, quinoxaline, and pyridine moieties with 2,2-(4-hydroxyphenyl)propane (bisphenol A). The novel synthesis of the quinoxaline-containing monomer, 2,3-bis(4-fluorophenyl)quinoxaline, is also discussed. The synthesis method used was the general nucleophilic aromatic substitution route using potassium carbonate to deprotonate the bisphenol under azeotroping toluene conditions. Reaction of the phenolate with the activated dihalide occurred in polar aprotic solvents at high reaction temperatures. Use of the monofunctional endcapping reagent, t-butyl phenol, not only controlled the molecular weight but permitted approximate number average molecular weight determination by ^{1}H NMR studies. The poly(arylene ether)s were characterized and then evaluated as blend modifiers for epoxy resins.

2.3. Synthesis of poly(arylene ether)s

2.3.1. Synthesis of 2,3-bis(4-fluorophenyl)quinoxaline monomer

2.3.1.1. Materials for monomer preparation

1,2-Phenylenediamine was obtained from Aldrich and sublimed prior to use. 4-Fluorobenzaldehyde (Aldrich) was stirred over calcium hydride and vacuum distilled prior to use. Copper(II) acetate, ammonium nitrate, potassium cyanide, and trifluoroacetic acid were obtained from Aldrich and used as received. The reaction solvents, HPLC grade chloroform and glacial acetic acid (Fisher) and absolute ethanol (Aaper Alcohol and Chemical Co.), were used as received.

2.3.1.2. Synthesis of 4,4'-difluorobenzoin

4-Fluorobenzaldehyde (15 g, 0.12 moles), potassium cyanide (1.5 g, 23 mmoles), 60 mL of absolute ethanol, and 15 mL of deionized water were charged to a one neck roundbottom flask fitted with a condenser. The benzaldehyde coupling progresses via a series of equilibria and thus the bright orange mixture must be stirred and refluxed for about 24 hours. Reaction progress was measured using ^{1}H NMR spectroscopy in CDCl$_3$ by monitoring the disappearance of the aldehyde proton at 10 ppm with concurrent appearance of the benzoin methine proton at 5.9 ppm. When the reaction was complete, the reaction mixture was cooled and dissolved in chloroform. The solution was placed in a separatory funnel and the material was washed five times with water to remove the residual potassium cyanide salt. Finally the ethanol and chloroform were removed under reduced pressure to yield 4,4'-difluorobenzoin, a pale yellow solid possessing a melting point of

74.5 to 76.5 °C. Infrared spectroscopy of the substituted benzoin showed a strong carbonyl stretch at 1683 cm^{-1} and a broad alcohol stretch at 3450 cm^{-1}.

2.3.1.3.   Synthesis of 4,4'-difluorobenzil

4,4'-Difluorobenzoin (10 g, 40 mmoles) was placed in a 100 mL roundbottom flask equipped with a condenser. 30 mL of glacial acetic acid, 5 mL of a 2% aqueous copper(II) acetate solution (0.5 mmoles copper(II) acetate), and 5 g (62 mmoles) of ammonium nitrate was added to the flask. The green reaction mixture was stirred and reluxed for 8 hours, cooled, and dissolved in chloroform. This solution containing the product was washed 2 times with water, one time with saturated aqueous sodium bicarbonate solution, and three more times with water. The chloroform was thereafter removed under reduced pressure, and the yellow solid that was obtained was recrystallized from ethanol/water (80/20). The melting point of the purified 4,4'-difluorobenzil was 156 to 158 °C. The ^{1}H NMR spectrum of 4,4'-difluorobenzil in CDCl$_3$ consisted of two multiplets at δ 8.0 ppm and δ 7.2 ppm.

2.3.1.4.   Synthesis of 2,3-bis(4-fluorophenyl)quinoxaline

The quinoxaline was synthesized according to the procedure of Labadie et al. (39) which was used for a quinoxaline of a different structure. One equivalent of 4,4'-difluorobenzil along with 1.35 equivalents of 1,2-phenylenediamine were dissolved in chloroform at 5% solids in a roundbottom flask fitted with a condenser. Approximately 0.1 mL of trifluoroacetic acid was added per 100 mL chloroform utilized. The reaction

mixture was stirred and refluxed for 24 hours, then diluted with chloroform, washed once with water, twice with 5% aqueous HCl, and three times with water. The chloroform was removed under reduced pressure and the resulting 2,3-bis(4-fluorophenyl)quinoxaline was first recrystallized from ethanol/water (80/20) and dried, then recrystallized from hexane and dried, followed by a third recrystallization from ethanol/water (80/20). The yellow monomer was dried *in vacuo* to constant weight before use and possessed a melting point of 132 to 134 °C (literature melting point: 133.5 to 134 °C (40)). The structure was confirmed by ^{1}H NMR spectroscopy; the spectrum consisted of 4 multiplets at δ 7.0 ppm (protons ortho to fluorine), δ 7.5 ppm (protons ortho to the withdrawing quinoxaline moiety), and δ 7.8 ppm and δ 8.2 ppm corresponding to the 5 and 6 positions on the quinoxaline ring.

2.3.2. Poly(arylene ether quinoxaline) synthesis

The 2,3-bis(4-fluorophenyl)quinoxaline monomer was successfully used in homopolymer and copolymer synthesis reactions. Specific reaction details are described below.

2.3.2.1.   Synthesis of poly(arylene ether quinoxaline) homopolymers

Equal molar amounts (1:1 stoichiometry) of 2,2'-(4-hydroxyphenyl)propane (bisphenol A, 0.03 moles) and 2,3-bis(4-fluorophenyl)quinoxaline (0.03 moles) were charged to a 500 mL 4-neck roundbottom flask equipped with a nitrogen inlet/thermometer adapter, a stopper, a motorized overhead stirrer, and a Dean Stark trap topped with a

condenser leading to a nitrogen bubbler. N,N-dimethylacetamide (70 mL) was added to render the solution 20 weight percent solids. Subsequently 60 mL toluene and 1.5 equivalents of potassium carbonate were added. The reaction flask was placed in an oil bath equipped with a thermometer, and heating tape was wrapped around the arm of the Dean Stark trap. The reaction mixture was heated with stirring to a reflux temperature of 135 to 140 °C. After the Dean Stark trap was filled with toluene, the temperature was maintained for a period of 2 to 4 hours in order to dehydrate the system. After the dehydration period, the toluene was drained from the Dean Stark trap. The reaction temperature was then increased to, and maintained at, 165 to 170 °C. The polymer precipitated from the reaction solution after a period of 12 to 18 hours. The reaction mixture was then cooled and poured into a 50:50 mixture of methanol and water, vigorously agitating in a blender, to remove the solvent and potassium carbonate.

2.3.2.2.   Synthesis of poly(arylene ether quinoxaline) copolymers

Copolymers of poly(arylene ether quinoxaline-co-sulfoxide) and poly(arylene ether quinoxaline-co-sulfone) were synthesized across a systematically varied composition range to evaluate the effect of structure on the solubility of the polyquinoxaline-based materials. The synthesis procedure was the same as above except for variations in the composition of the dihalo monomer. 4,4'-Dichlorodiphenylsulfone (or 4,4'-difluorodiphenylsulfoxide) monomer was mixed with 2,3-bis(4-fluorophenyl)quinoxaline to synthesize copolymers. In all cases the diol monomer was bisphenol A and the stoichimetry between diol and dihalide was 1:1. Copolymer compositions ranged from 0.0 molar equivalent quinoxaline and 1.0 molar equivalent sulfone (homopoly(arylene ether sulfone)) or sulfoxide (homopoly(arylene ether sulfoxide), to 1.0 molar equivalent quinoxaline and 0.0 molar

equivalent sulfone (or sulfoxide) to form homopoly(arylene ether quinoxaline), and several compositions in between these extremes.

2.3.3. Synthesis of poly(arylene ether)s comprising phosphine oxide, sulfoxide, sulfone, and pyridine functionalities

Several other poly(arylene ether)s were synthesized in the same manner as the poly(arylene ether quinoxaline)s, including poly(arylene ether phosphine oxide) (22), poly(arylene ether sulfoxide) (53), poly(arylene ether sulfone), poly(bis 3F-sulfone), poly(bis 6F-sulfone) (24), and poly(arylene ether pyridine) (23). The details of these monomer and polymer syntheses are outlined elsewhere (22-24, 53).

2.3.4. Characterization of monomers and polymers

All ^{1}H NMR spectroscopy measurements were conducted on a Varian Unity NMR spectrometer operating at 400 MHz. Thermogravimetric analyses were performed using a Perkin-Elmer TGA-7 operating under a nitrogen atmosphere with a heating rate of 10 °C/minute from room temperature to 700 °C. Differential scanning calorimetry results were obtained using a Perkin-Elmer DSC-7 operating under a nitrogen atmosphere from 50 ° to 300 °C with a heating rate of 10 °C/minute. Two heats for each DSC sample were obtained under these conditions, with quench cooling of the sample between heats. Intrinsic viscosity measurements were made in N-methyl-2-pyrrolidinone at 25 °C using a Ubbelhohde type viscometer. Gel permeation chromatography was performed using a Waters 150-C chromatograph operating at 60 °C with a µ-Styragel column set comprised of

500 Å and 100 Å pore size columns. HPLC grade NMP containing 0.5 % w/w LiBr was used as the mobile phase at 1 mL/min. Dual concentration and viscosity detectors were employed, and a universal calibration method calibrated with polystyrene standards was used to calculate absolute molecular weights. Fourier transform infrared spectroscopy (FTIR) was performed with a Nicolet Impact 400 FTIR. FTIR samples of poly(arylene ether)s were made by casting 1 % (w/w) solutions of poly(arylene ether) in $CHCl_3$ onto KBr plates and evaporating the solvent to form a thin, transparent film of polymer on the salt plate.

2.4.   Results and Discussion

Detailed results obtained for the synthesis and characterization of quinoxaline-containing monomers and polymers will be discussed here. Syntheses of the bisphenol A poly(arylene ether)s based on phosphine oxide, sulfone, sulfoxide, and pyridine are discussed in detail elsewhere (22-24, 53) so will be discussed only briefly here.

2.4.1. Poly(arylene ether quinoxaline) monomer, homopolymers, and copolymers

2.4.1.1.   Synthesis of 2,3-bis(4-fluorophenyl)quinoxaline monomer

The 3-step monomer synthesis, shown in Figure 2-3, was facile and produced a 45 % yield of monomer grade 2,3-bis(4-fluorophenyl)quinoxaline after three recrystallization steps. The first step of the reaction, the synthesis of 4,4'-difluorobenzoin, is a complex series of equilibria involving multiple hydrogen transfers in the reactive substrate. The equilibrium steps leading to formation of 4,4'-difluorobenzoin are shown in Figure 2-4. The low final yield of the monomer synthesis reaction may be attributable to the equilibrium in the first step, which produced 85 % conversion of fluorobenzaldehyde to 4,4'-difluorobenzoin under the reaction conditions employed. The ^{1}H NMR spectra of the 2,3-bis(4-fluorophenyl)quinoxaline monomer as well as the two precursor materials, 4,4'-difluorobenzoin and 4,4'difluorobenzil are shown in Figures 2-5 to 2-7. The 4,4-difluorobenzoin was pale yellow with a melting point of 74.5 to 76.5 °C. The 2,3-bis(4-fluorophenyl)quinoxaline monomer was medium yellow in color with melting point of 132-134 °C. The 4,4'-difluorobenzil was bright yellow with a melting point of 156-158 °C.
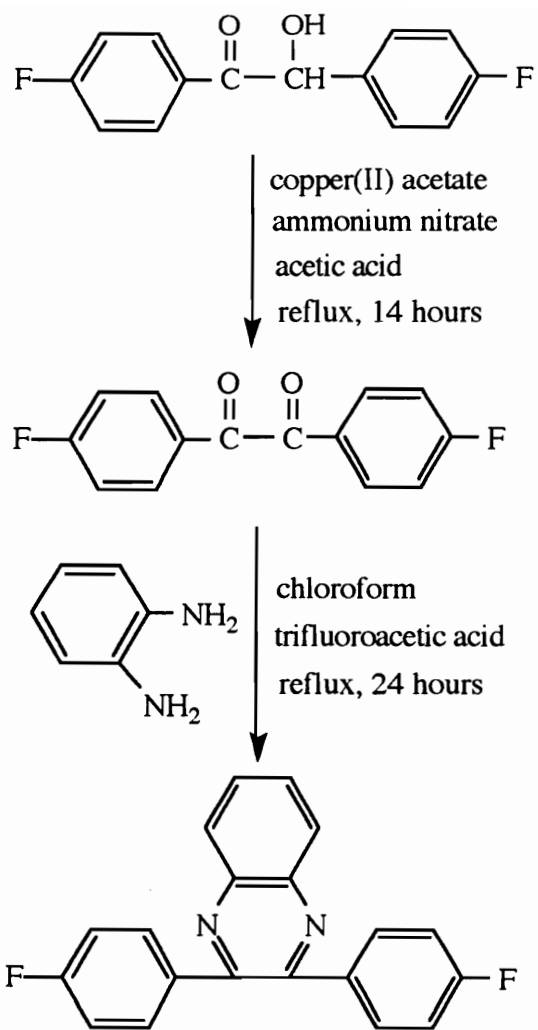
Figure 2-3: 3-step synthesis of 2,3-bis(4-fluorophenyl)quinoxaline
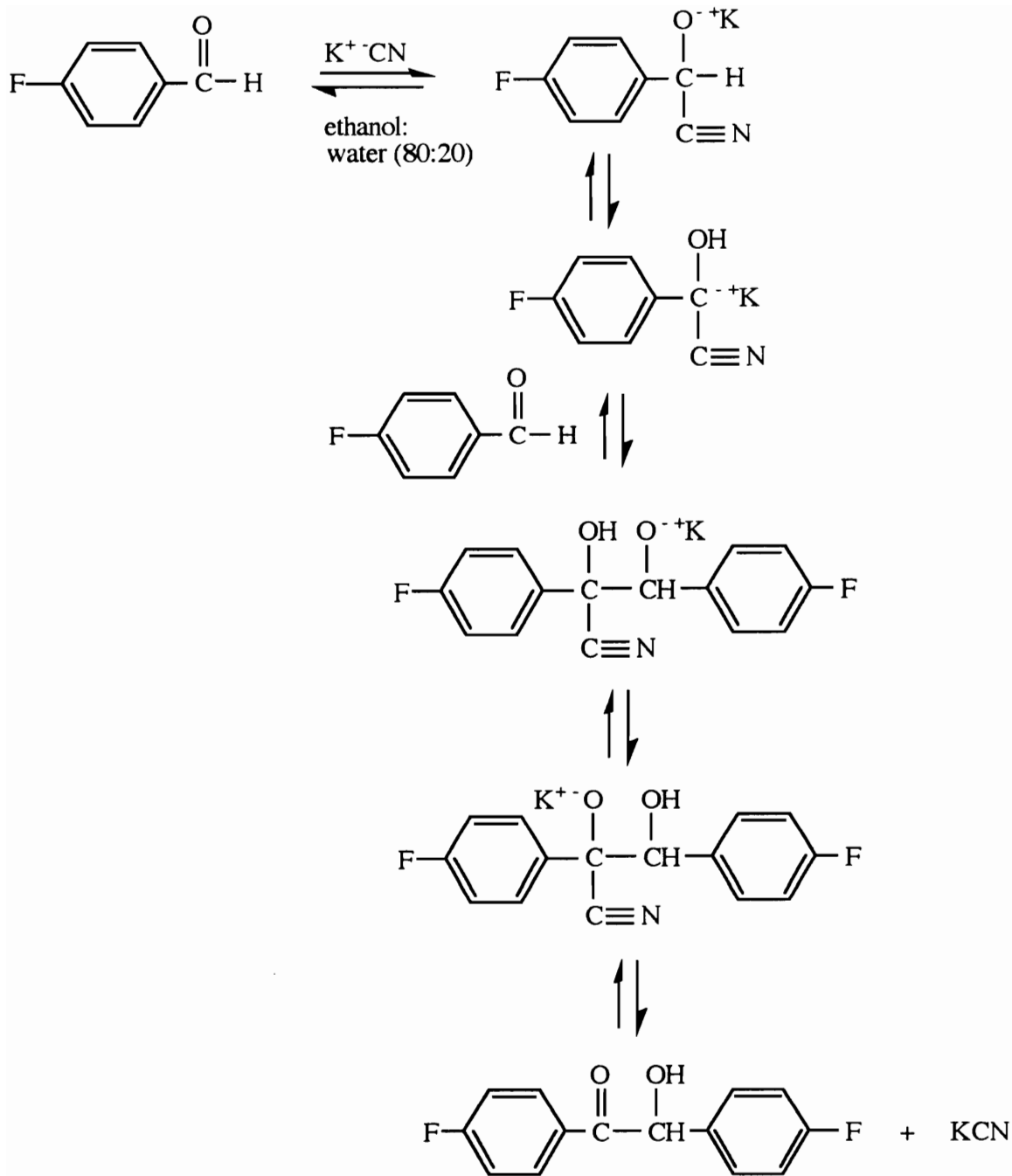
Figure 2-4: Synthesis of 4,4'-difluorobenzoin
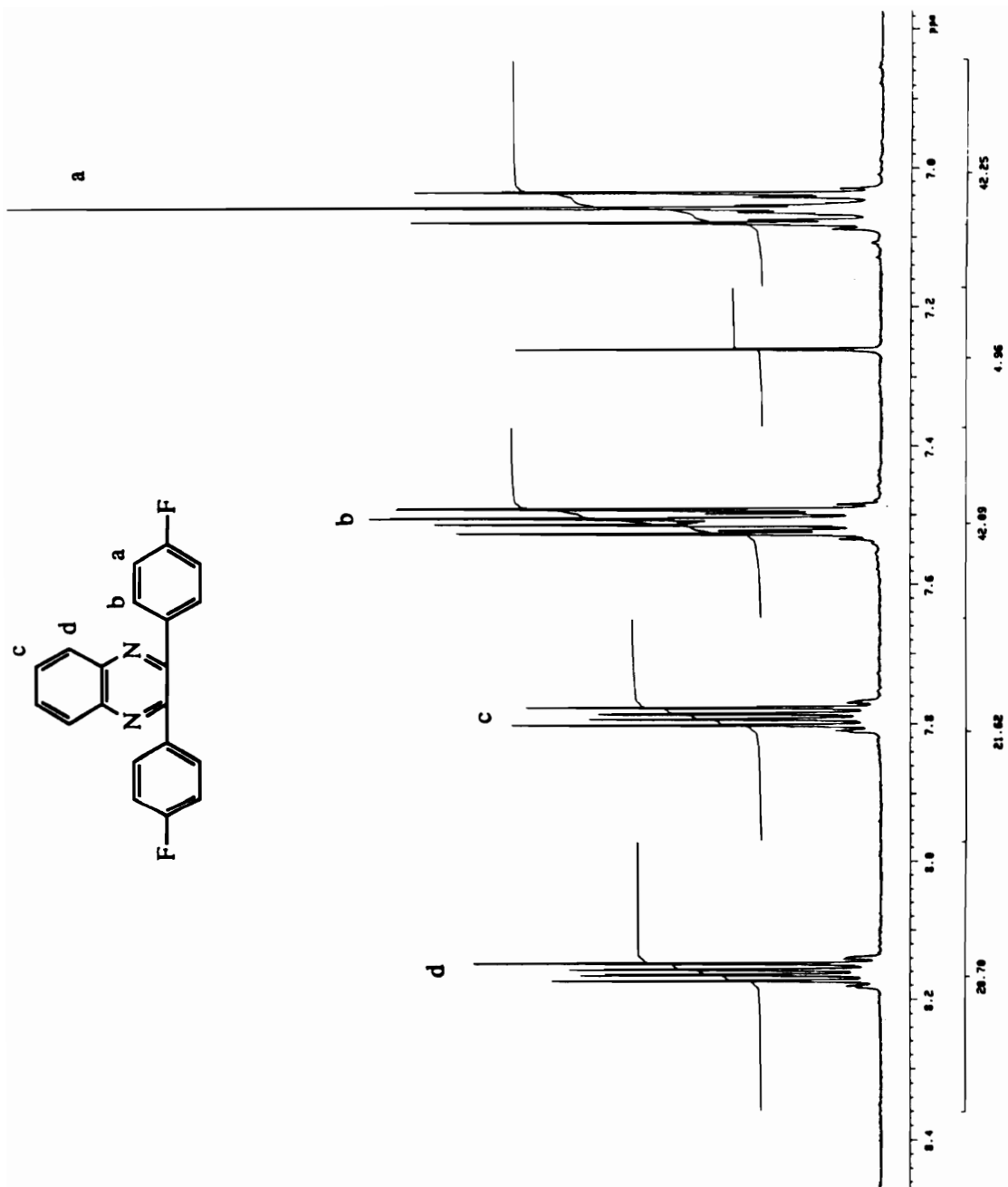
Figure 2-5: ^{1}H NMR spectrum of 2,3-bis(4-fluorophenyl)quinoxaline in CDCl$_3$

23
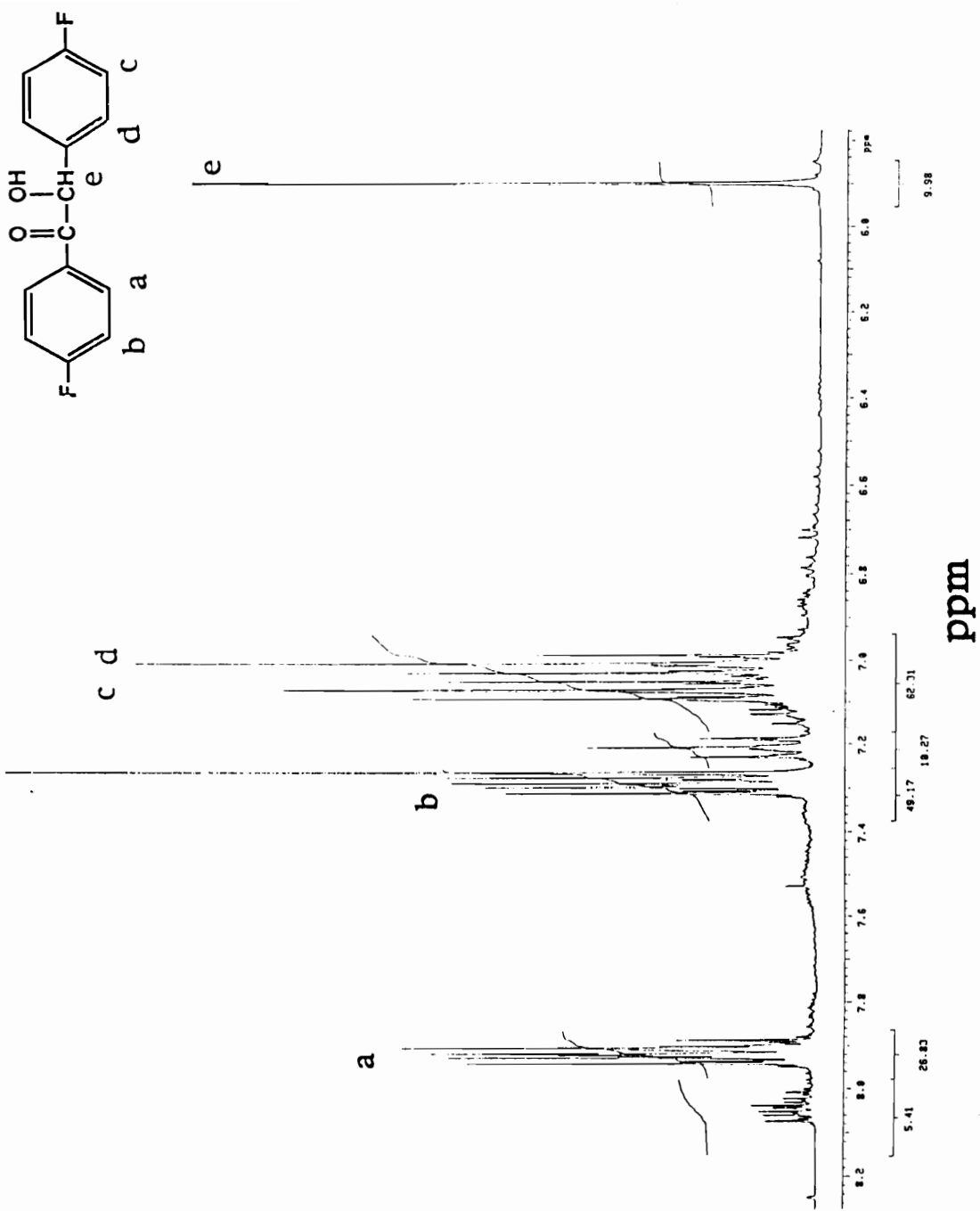
Figure 2-6: ^{1}H NMR spectrum of 4,4'-difluorobenzoin in CDCl$_3$

24
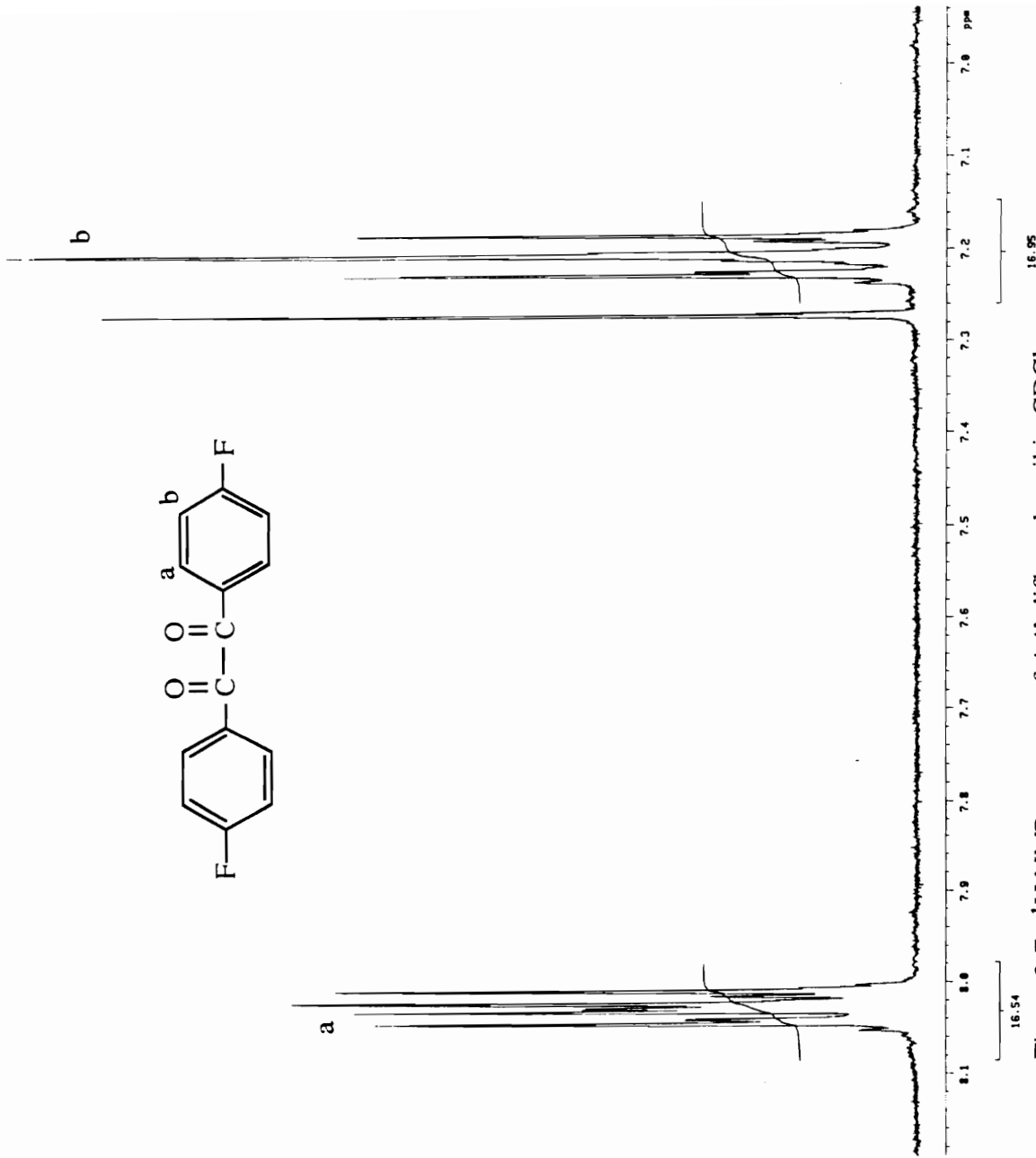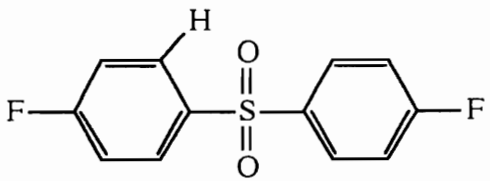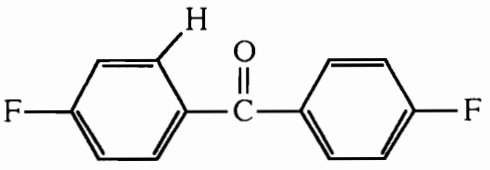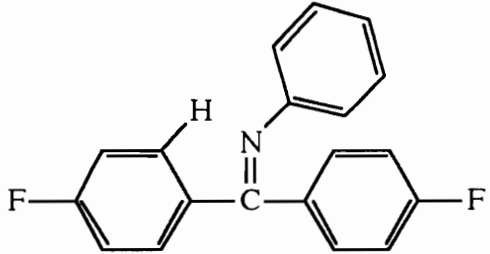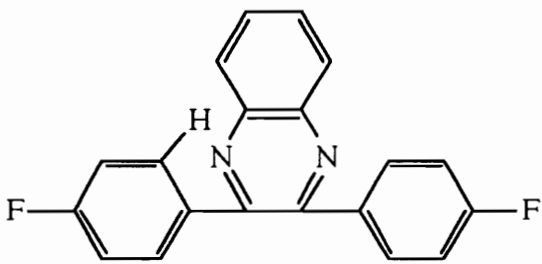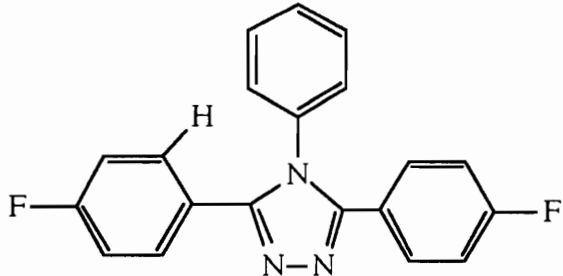
Figure 2-7: ^{1}H NMR spectrum of 4,4'-difluorobenzil in CDCl$_3$

25

The monomer was evaluated for reactivity to nucleophilic aromatic substitution by measuring the shift of the proton ortho to the quinoxaline group. The withdrawing ability of the functional group is directly linked to monomer reactivity because the more electron withdrawing the central group of the monomer, the more stable the Meisenheimer complex, the key reaction intermediate in the nucleophilic aromatic substitution synthesis mechanism. The more downfield the shift of the proton ortho to this group, the more electron withdrawing the substituent. This leads to increased electrophilicity of the carbon attached to the halogen and increased reactivity of the monomer to nucleophilic aromatic substitution. Shifts of some known monomers are compared to that of 2,3-bis(4-fluorophenyl)quinoxaline in Figure 2-8. The shift of the proton ortho to the quinoxaline group is 7.5 ppm, indicating that 2,3-bis(4-fluorophenyl)quinoxaline is rather unreactive toward nucleophilic aromatic substitution by this technique. Note, however, Carter et al. (19) were successful in polymerizing the less reactive difluorotriazole monomer under rigorous conditions.

The dihydroxy monomer, 2,3-bis(4-hydroxyphenyl)quinoxaline, was also synthesized and evaluated in poly(arylene ether) syntheses. The monomer synthesis protocol was similar to that used for the synthesis of 2,3-bis(4-fluorophenyl)quinoxaline. 4-Methoxybenzaldehyde was coupled using the cyanide catalyzed benzoin condensation reaction, and the resulting 4,4'-dimethoxybenzoin was oxidized to 4,4'-dimethoxybenzil using copper acetate/ammonium nitrate in acetic acid. The dimethoxybenzil was converted to 2,3-bis(4-methoxyphenyl)quinoxaline through reaction with o-phenylene diamine. The diol monomer was obtained through deprotection of the 2,3-bis(4-methoxyphenyl)quinoxaline using HBr in refluxing acetic acid. This monomer synthesis was more complex than that of the 2,3-bis(4-fluorophenyl)quinoxaline. Moreover, when reacted with monomers such as 4,4'-dichlorodiphenylsulfone, the polymers obtained were

8.04

7.81

7.7

7.5

7.38*

* K. R. Carter, H. Jonsson, R. Twieg, R. D. Miller, and J. L. Hedrick, Polym. Prepr., 33(1), 288, 1992

Figure 2-8: Effect of electron withdrawing group on the chemical shift of the ortho proton in monomers used in poly(arylene ether) syntheses
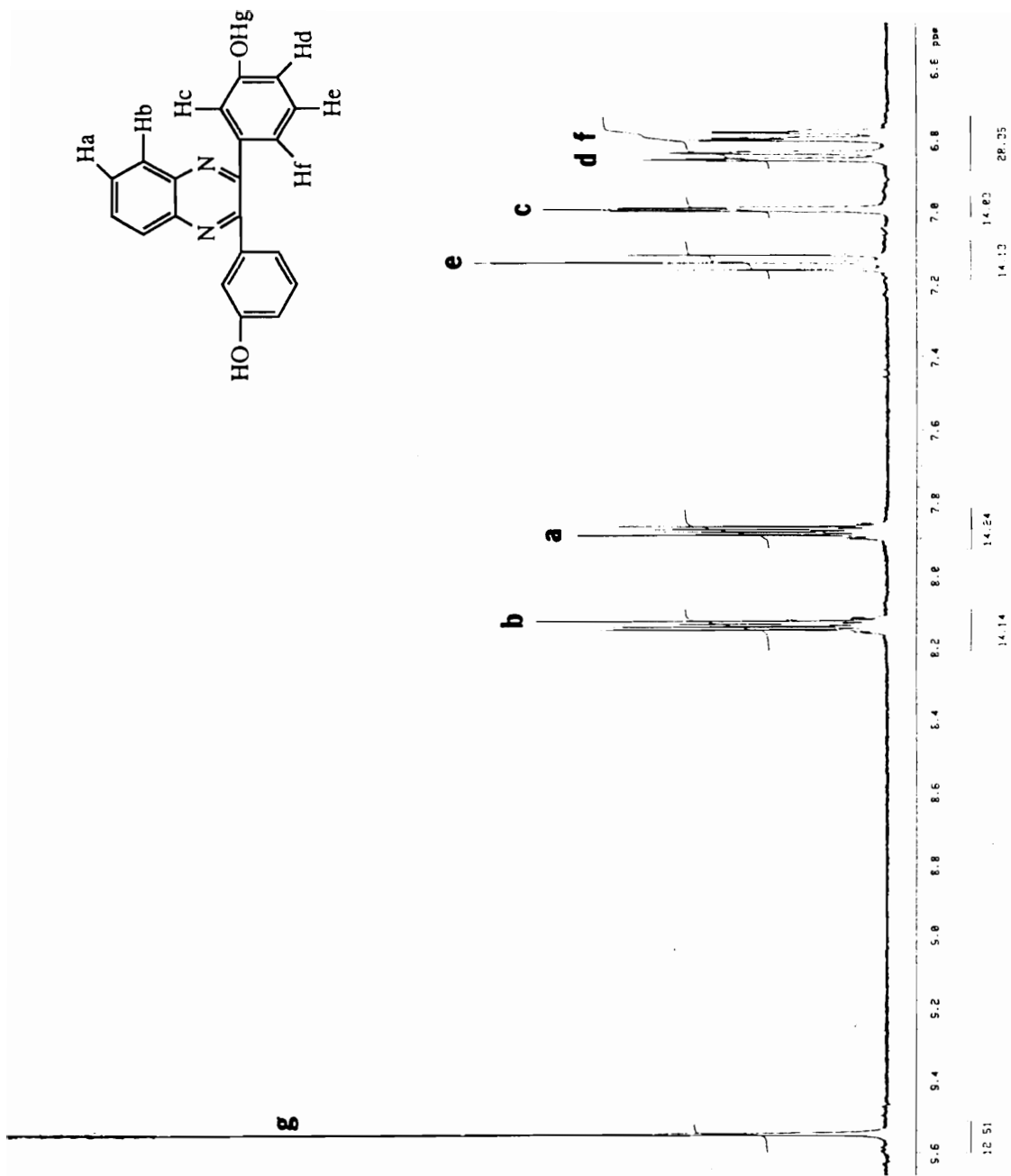
Figure 2-9: ^{1}H NMR spectrum of 2,3-bis(4-hydroxyphenyl)quinoxaline in DMSO-d$_6$

28

sparingly soluble in both NMP and DMAc, and, thus the investigation was abandoned. The ^{1}H NMR spectrum of 2,3-bis(4-hydroxyphenyl)quinoxaline is shown in Figure 2-9.

2.4.1.2.   Poly(arylene ether quinoxaline)s

Figure 2-10 depicts the method used to synthesize poly(arylene ether quinoxaline)s. The molecular weight of the polymer formed by reaction of bisphenol A and 2,3- bis(4-fluorophenyl)quinoxaline was limited in all synthesis attempts by poor solubility of the resulting poly(arylene ether quinoxaline) in the polar aprotic reaction solvents. All synthesis reactions used 1:1 stoichiometry of the monomers in an effort to obtain high molecular weight materials, but the polymer precipitated out of solution after several hours at the reaction temperature. The molecular weights of the poly(arylene ether quinoxaline)s were evaluated by gel permeation chromatography in N-methyl-2-pyrrolidinone. A representative GPC trace is shown in Figure 2-11. The number average molecular weights of the polymers was usually 18,000 to 20,000 g/mol and the molecular weight distribution was about 2. The chemical structure of the polymer was confirmed with ^{1}H NMR (Figure 2-12). Qualitative solubility tests of the poly(arylene ether quinoxaline) yielded the results shown in Table 2-1. Note that the polymer is only sparingly soluble in typical nucleophilic aromatic substitution reaction solvents such as N,N-dimethylacetamide and N-methyl-2-pyrrolidone. The insolubility of the polymer seems to be due more to polarity rather than rigidity because the polymer is quite soluble in slightly less polar solvents such as chloroform and chlorobenzene. This indicates that insolublity due to rigidity of the structure is not a factor. Thus the insolubility is probably due to the poly(arylene ether quinoxaline) structure being less polar than that of polymers such as poly(arylene ether sulfone) and poly(arylene ether ketimine). Hedrick et al. reported low levels of crystallinity

DMAc/toluene (80/20)
K₂CO₃
dehydrate 4 hr at 140 °C
165 °C, 24 hours
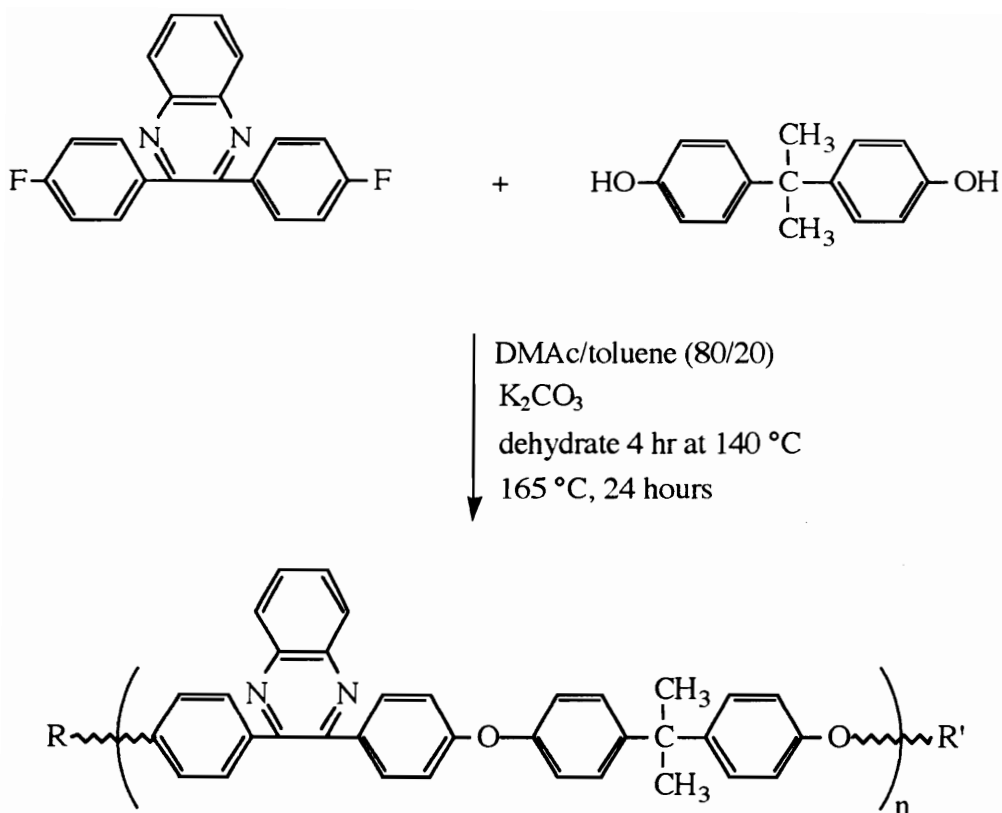
- $T_g \approx 200\ ^\circ C$
- Sparingly soluble in polar aprotic solvents such as NMP and DMAc
- Soluble in halogenated solvents such as chloroform and tetrachloroethane
- Precipitates during polymerization from DMAc solution at $M_n \approx 20{,}000$ g/mol

Figure 2-10: Synthesis of poly(arylene ether quinoxaline) materials

in the poly(arylene ether quinoxaline) by WAXS measurements (40). The material was

also soluble in DMPU and chloroform. An attempt was made to synthesize the

poly(arylene ether quinoxaline) with the less polar N-cyclohexyl-2-pyrrolidone as the

reaction solvent. This reaction was also unsuccessful and yielded low molecular weight

material. This may have been due to the low reactivity of the 2,3-bis(4-

fluorophenyl)quinoxaline monomer coupled with the "tight" ion pairs on the bisphenate as well as the inability of the less polar solvent to support the polar Meisenheimer complex intermediate.

Thermal gravimetric analysis (TGA) performed on the poly(arylene ether quinoxaline)s demonstrated that the polymer lost 5 percent of its original weight at about 510 °C under a nitrogen atmosphere. Differential scanning calorimetry (DSC) showed that the polymer was amorphous and possessed a glass transition temperature of about 200 °C (Figure 2-13).
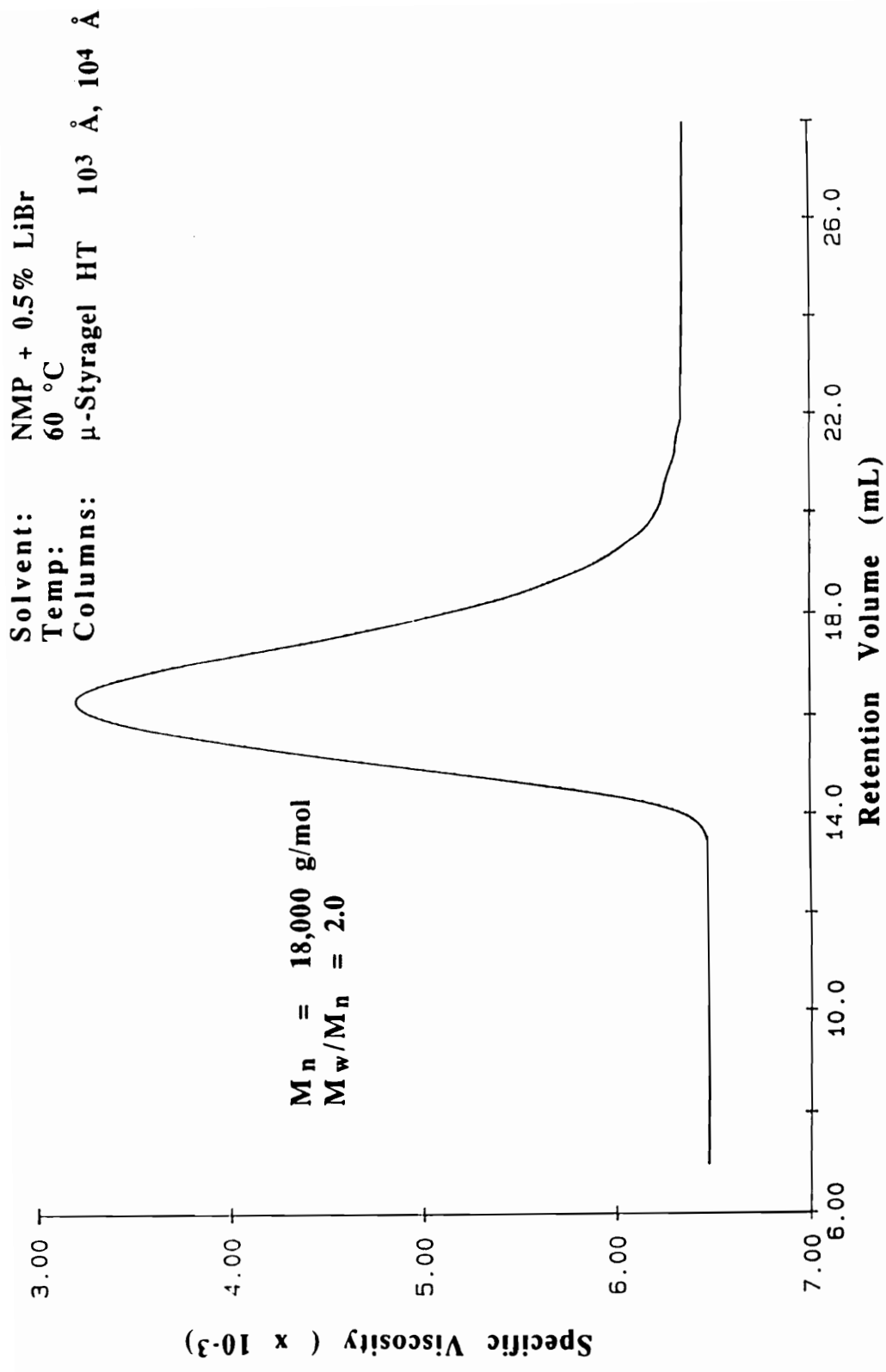
Figure 2-11: Gel permeation chromatography of poly(arylene ether quinoxaline)

Solvent: NMP + 0.5% LiBr
Temp: 60 °C
Columns: μ-Styragel HT 10^3 Å, 10^4 Å

M_n = 18,000 g/mol
M_w/M_n = 2.0

Retention Volume (mL)

Specific Viscosity (x 10^{-3})
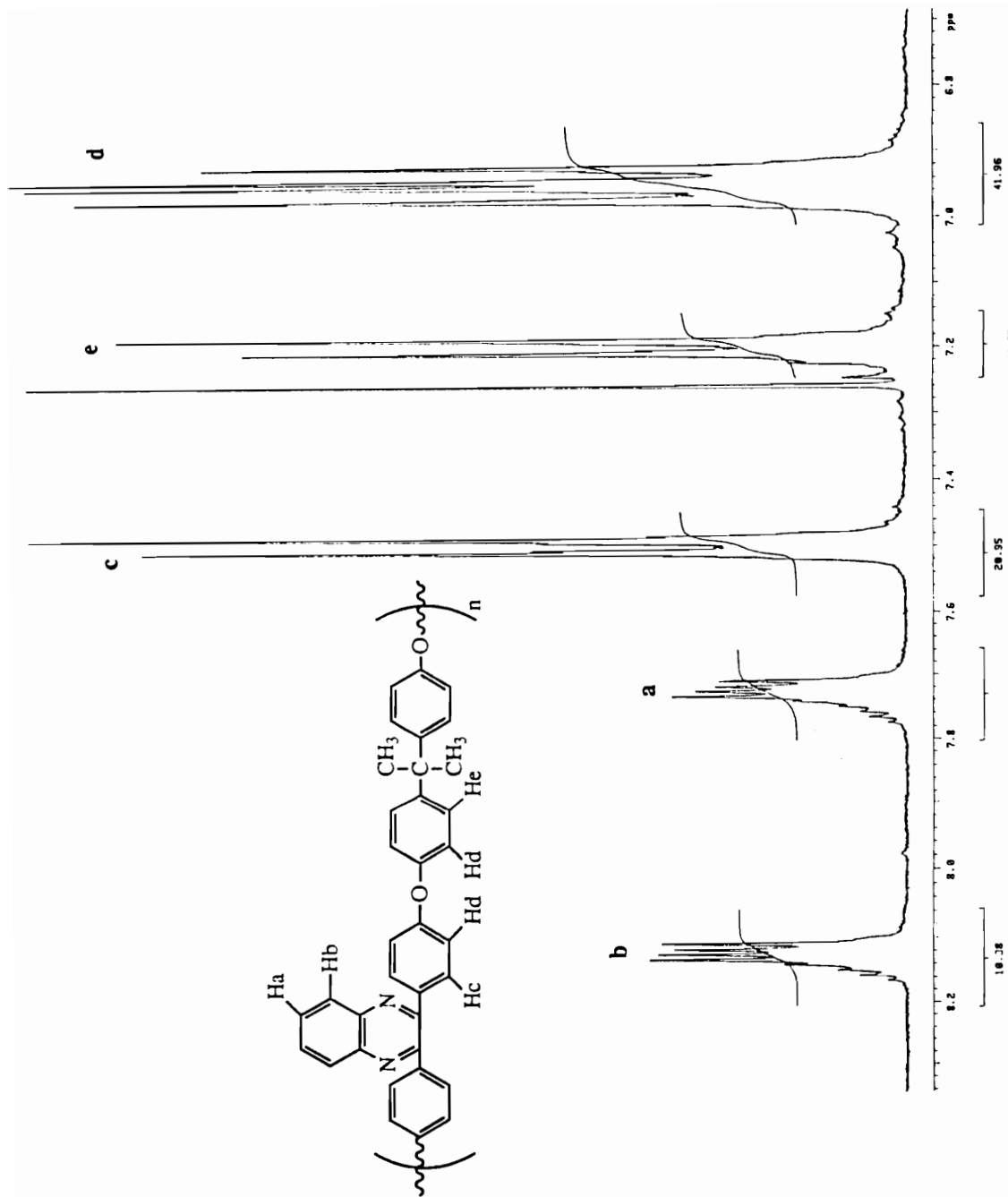
Figure 2-12: ^{1}H NMR spectrum of bisphenol A based poly(arylene ether quinoxaline) in CDCl$_3$

Table 2-1: Solubility of poly(arylene ether quinoxaline) and solubility parameter values of solvents (55)

solvent	solubility of (PAEQ)	δ (MPa)$^{1/2}$
N-cyclohexyl-2-pyrrolidinone	soluble	----
dimethyltetrahydropyrimidone	soluble	----
tetrachloroethane	soluble	19.8
chloroform	soluble	19.0
o-dichlorobenzene	soluble	20.5
chlorobenzene	soluble	19.4
toluene	sparingly soluble	18.2
N,N-dimethylacetamide	sparingly soluble	22.1
N-methyl-2-pyrrolidinone	sparing soluble	23.1
tetrahydrofuran	insoluble	18.6
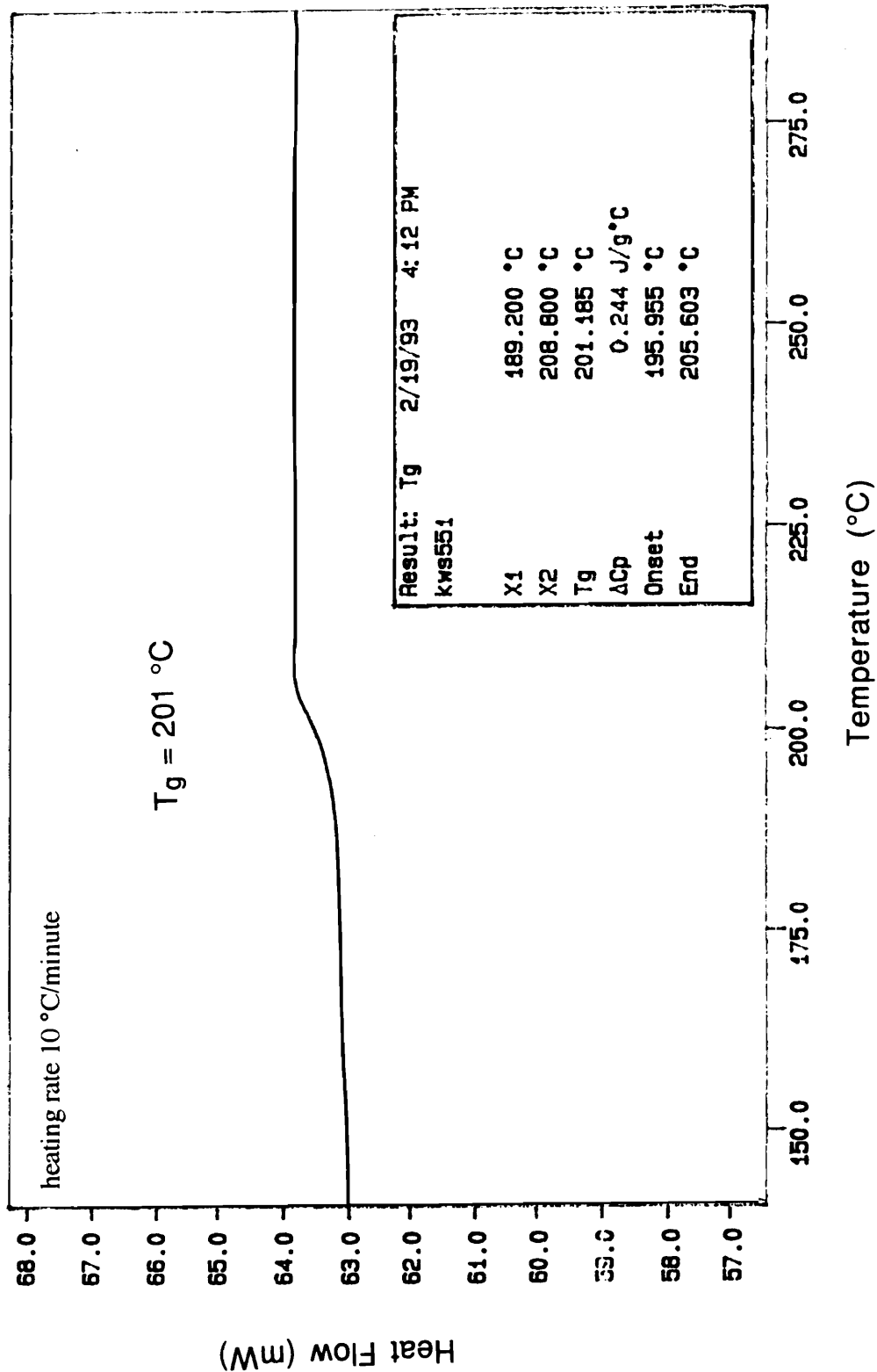
Figure 2-13: Differential scanning calorimetry of poly(arylene ether quinoxaline) under nitrogen atmosphere

35

2.4.1.3.   Copolymers of poly(arylene ether quinoxaline)s and sulfones or sulfoxides

In order to synthesize high molecular weight polymers with the quinoxaline functionality incorporated along the backbone, copolymers were prepared from mixtures of 2,3-bis(4-fluorophenyl)quinoxaline and 4,4'-difluorodiphenylsulfoxide or 4,4'-dichlorodiphenylsulfone, in an attempt to break up the regular nature of the poly(arylene ether quinoxaline) and thus promote solubility in the polar aprotic reaction solvents such as NMP or DMAc. All reactions were performed with a 1:1 stoichiometry of bisphenol with dihalide in order to obtain high molecular weight materials for the characterization methods. The random copolymers were synthesized and characterized across the composition range shown in Table 2-2. The high molecular weights obtained using 2,3-bis(4-fluorophenyl)quinoxaline as a comonomer with either 4,4'-dichlorodiphenylsulfone or 4,4'-difluorodiphenylsulfoxide demonstrates that the three step synthesis of the quinoxaline monomer yielded high purity material. However, the polymers became insoluble in the reaction solvent when the dihalo monomer mixture was about 0.4 molar equivalents quinoxaline to 0.6 molar equivalents of either 4,4'-dichlorodiphenylsulfone or 4,4'-difluorodiphenylsulfoxide. This reflected the increasing rigidity of the backbone with increasing quinoxaline content, corroborated by increasing glass transition temperatures of the copolymers with increased quinoxaline content.

The glass transition temperatures of the sulfoxide-containing polymers were lower than those of the corresponding sulfone-containing polymers. This may be a result of the reduced rigidity of the backbone structure of the poly(arylene ether sulfoxide) relative to the poly(arylene ether sulfone). While both the sulfoxide and sulfone linkage are tetrahedral, the lone pair in the nonbonding sulfoxide orbital occupies less space than the corresponding sulfur-oxygen molecular orbital present in the sulfone. Furthermore, the chiral sulfoxide functionality produces an atactic polymer system which will also promote solubility.

Table 2-2: Characterization of random poly(quinoxaline-co-sulfone) and poly(quinoxaline-co-sulfoxide) bisphenol A based poly(arylene ether)s
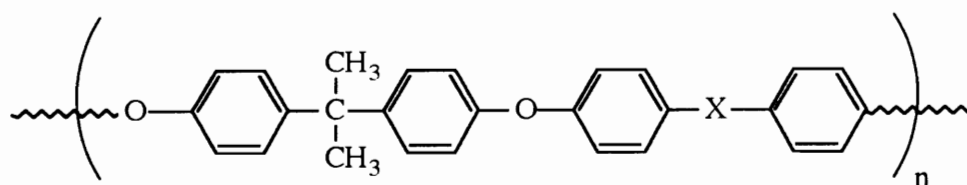
$X = SO_2$ and/or SO and/or (Q)
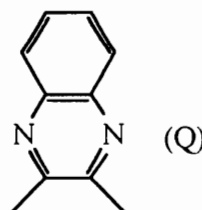
composition	$\langle M_n \rangle$ [1]	M_w/M_n	$[\eta]^{25°C}$(NMP) dL/g	T_g (°C)	Comments
0 Q/ 1 SO$_2$	253.3 K	1.51	1.4	195	polysulfone
0.1 Q/0.9 SO$_2$	62.7 K	1.99	0.58	194	
0.2 Q/0.8 SO$_2$	57.7 K	1.98	0.53	195	
0.3 Q/0.7 SO$_2$	77.9 K	1.86	0.64	--	
0.4 Q/0.6 SO$_2$	69.6 K	2.00	0.63	195	pptd from rxn
0.9 Q/0.1SO$_2$	19.7 K	2.06	insoluble	197	pptd from rxn
1.0 Q / 0 SO$_2$	11.5 K [2]	2.48	0.2	200	pptd from rxn
0 Q/ 1.0 SO	24.3 K [3]	1.89	0.34	169	polysulfoxide
0.2 Q/ 0.8 SO	100.1 K	1.80	0.74	179	
0.4 Q / 0.6 SO	25.2 K	1.97	0.34	173	pptd from rxn
1.0 Q / 0 SO	11.5 K [2]	2.48	0.2	200	pptd from rxn

[1] Determined by GPC in chloroform at 30 °C, relative to polystyrene standards

[2] M_n was 20 K by GPC in NMP with Viscotek detector

[3] M_n was 20 K by GPC in NMP with Viscotek detector

2.4.2. Poly(arylene ether sulfoxide) synthesis

Controlled molecular weight poly(arylene ether sulfoxide)s with nonreactive endgroups were synthesized using bisphenol A and 4,4'-difluorodiphenylsufloxide with t-butylphenol as the endcapping reagent. The targeted molecular weight was 25,000 g/mole, and the monomer amounts were calculated using the Carother's equation. A gel permeation chromatogram of a representative poly(arylene ether sulfoxide) is shown in Figure 2-14. The number average molecular weight of the poly(arylene ether sulfoxide) was approximated by comparing the high resolution ^{1}H NMR integrations of the protons in the t-butyl endgroups with the isopropylidene backbone protons. Using this method, the $<M_n>$ of the polymer was 24,200 g/mole while by GPC (relative to polystyrene standards) the $<M_n>$ was determined to be 16,000 g/mole.

2.5   Conclusions

The novel monomer, 2,3-bis(4-fluorophenyl)quinoxaline, was successfully synthesized. Reaction of this monomer with bisphenol A yielded a polymer which precipitated out of solution when the molecular weight grew to approximately 18,000 to 20,000 g/mol. The insolubility of the poly(arylene ether quinoxaline) is possibly a result of the rigid nature or low polarity of the fused heterocyclic backbone. Quinoxaline based copolymers using 4,4'-difluorodiphenylsulfoxide or 4,4'-dichlorodiphenylsulfone as comonomers with 2,3-bis(4-fluorophenyl)quinoxaline remained soluble until the quinoxaline content of the dihalo monomer combination exceeded 0.4 equivalents quinoxaline per 0.6 equivalents sulfone or sulfoxide. All poly(arylene ether)s synthesized

Solvent: THF
Temp.:   30 °C
Detector: R. I.

Elution Volume: 12.1 cm
Theor. <Mn>:   25,000 g/mol

Calculated <Mn>:   16,500 g/mol
Calculated PDI: 2.09
with respect to polystyrene standards

Elution Volume (cm)
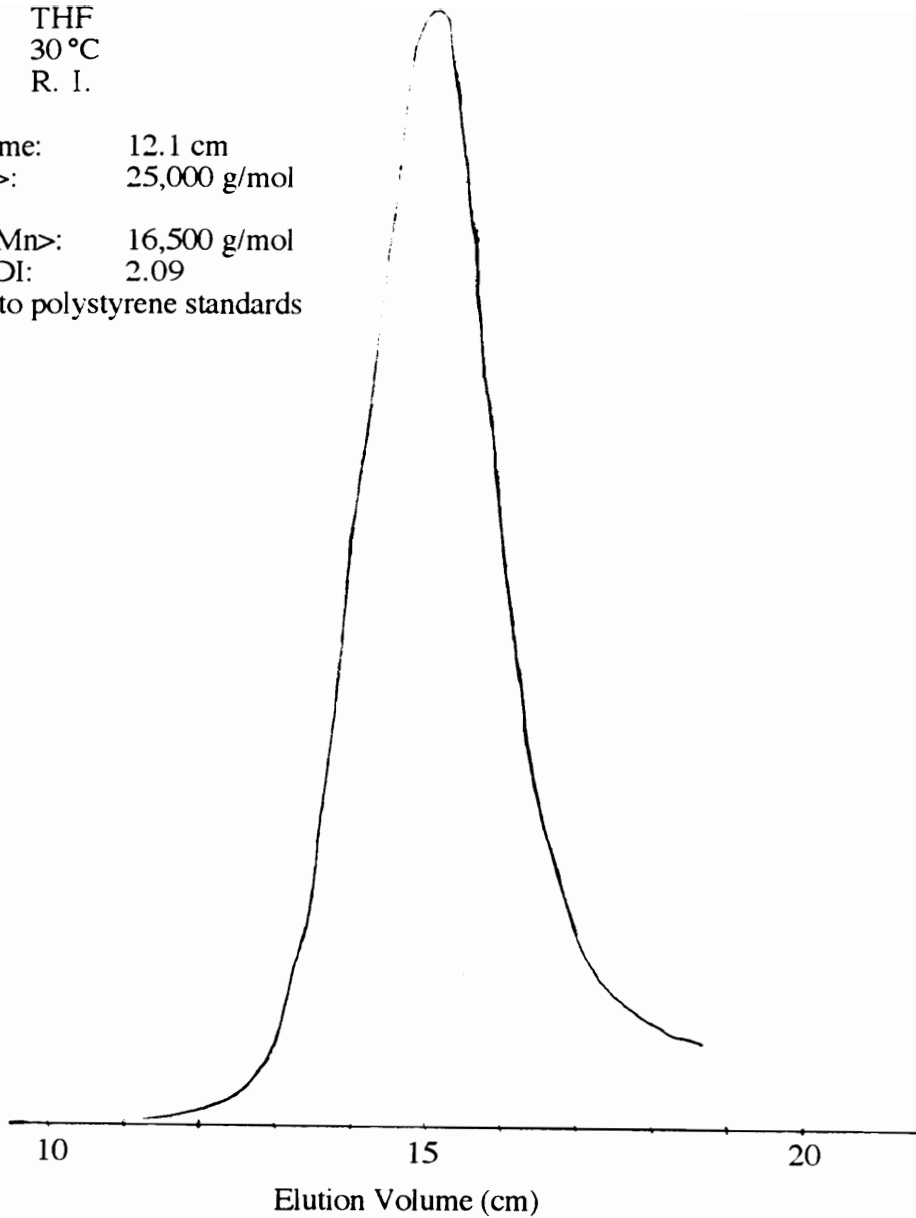
Figure 2-14: Gel permeation chromatography of t-butylphenol endcapped bisphenol A based poly(arylene ether sulfoxide)

demonstrated high glass transition temperatures with the T_g increasing with incorporation of quinoxaline segments.

Poly(arylene ether sulfoxide)s with controlled molecular weights were synthesized. The molecular weights were evaluated using ^{1}H NMR spectroscopy and gel permeation chromatography. Poly(arylene ether sulfoxide)s have lower glass transition temperatures than analogous poly(arylene ether sulfone)s, due to increased flexibility present in the sulfoxide linkage relative to the sulfone linkage.

CHAPTER 3

Epoxy-polymer blend miscibility

3.1. Literature review: toughened epoxy materials

Epoxy resin thermosets possess excellent chemical and corrosion resistance, good mechanical and thermal properties, outstanding adhesion to various substrates, and are ideally suited for a number of applications including coatings, structural adhesives, and advanced composite materials (56). Unfortunately, the highly crosslinked system which imparts strength to these materials results in inherent brittleness and poor fracture toughness (57). This toughness deficiency opens the door to stress cracking; a highly destructive phenomenon possibly leading to catastrophic failure of a crucial epoxy composite part. In order to create epoxy composite materials suitable for high performance applications, a serious effort is being made today to identify and evaluate methods to toughen epoxy thermosets. This literature review comprises information on rubber toughened epoxies, intermolecular forces in polymer blends, engineering thermoplastic toughened epoxies, and organometallic toughened epoxies.

3.1.1. Rubber toughened epoxies

In the late 1960's, rubber toughened epoxy materials were developed (58). The toughening arose via addition of elastomeric carboxyl functionalized poly(butadiene-co-acrylonitrile)s (CTBNs) to the epoxy resin before the cure cycle (59). The carboxyl endgroup of the rubbery oligomer reacts with the epoxide groups of the diglycidyl

prepolymer and is chemically bonded into the matrix. The nonpolar, aliphatic CTBN separates from the aromatic epoxy resin during the curing cycle to form a two phase morphology consisting of small (0.1 to 1 μm) rubbery particles dispersed in the continuous epoxy phase (60-63). It is well known that the fracture toughness of epoxy resins is greatly improved by the presence of these discrete rubbery particles that are chemically bonded to the matrix. (64). The proposed model is one of energy dissipation.

Epoxy matrices have more recently been rubber toughened by addition of partially epoxidized hydroxyl terminated polybutadiene oligomers (65, 66). Because chemical bonding between rubber particles and the epoxy matrix is required for efficient stress transfer, Bussi and Ishida (65, 66) proposed that the polybutadiene elastomers systematically epoxidized along the backbone would be more efficient tougheners than carboxyl terminated poly(butadiene-co-acrylonitrile). Although the reaction rate of internal oxirane groups was less than that of the terminal oxirane groups of the epoxy prepolymer, the rubber was effectively incorporated into the diglycidyl ether of bisphenol A epoxy resin. Bussi and Ishida found that blends containing 9 to 12 percent rubber exhibit a value of the critical stress intensity factor K_{IC} higher by about 40 percent relative to the pure epoxy, and that this improvement was due to the flexibilizing effect of the rubber rather than the presence of a second phase. However, despite enhancement of the fracture toughness, rubber toughening of epoxy resins is accompanied by a significant deterioration of elastic modulus and glass transition temperature (67).

Other rubbers evaluated as epoxy tougheners include: carboxyl terminated polyisobutylene (68), polysiloxanes (69), n-butyl acrylate rubbers (70), fluoroelastomers (71), and linear polysulfide rubbers (72). Kemp et al. (72) reported that polysulfide rubber modified epoxy resin had improved ductility, even in systems not exhibiting disperse particles. These results agreed with the results of Bussi and Ishida (65, 66) for the

polybutadiene toughened epoxies. Thus a modifier present as a solution or as aggregates of submicroscopic dimensions also enhances properties.

3.1.2. Intermolecular forces in polymer blends

Specific attractive interactions (such as hydrogen bonding, dipole-dipole forces, Van der Waals forces, and charge transfer complexes) play a major role in the miscibility of polymers. These intermolecular forces provide a favorable negative enthalpy of mixing to the system, compensating for the usually negligible entropy of mixing, and render the Gibbs free energy of mixing negative (73, 74). It is well established that hydrogen bonds, the strongest of the intermolecular attractive forces, play a particularly important role in polymer-polymer miscibility (75).

Hydrogen bonding occurs between a hydrogen atom bonded to a nitrogen or oxygen (e. g. hydroxy, carboxyl, amine, amide, urea, or urethane functionality) and an electronegative atom such as oxygen, nitrogen, or occasionally a halogen (e. g. fluorine) (76). Hydrogen bond energies in polymers typically range between 12 to 30 kJ/mol per repeat unit in dissociation energy and between 2.4 and 3.2 Å in length (77). It is well known that hydrogen bonds greatly influence the physical properties of the polymers in which they appear (78). The glass transition temperature and melting temperature of a polymer are affected by attractive forces between polymer chains; hydrogen bonding decreases the mobility and entropy of amorphous polymer chains. Thus more energy (heat) is required to break the intermolecular forces and glass and melting transitions are elevated.

Intermolecular hydrogen bonding between functional groups in blends leads to cohesiveness between chains and good physical properties. Often polymers that hydrogen

bond to one another are capable of forming a miscible polymer blend. Hydrogen bonding in blends has been evaluated by spectroscopic techniques including Fourier Transform infrared spectroscopy (FTIR) (79-82), high resolution solid state ^{13}C nuclear magnetic resonance spectroscopy (NMR) (83-86), and two dimensional solid state NMR (87, 88). It is well known that the formation of intermolecular hydrogen bonds often results in a change of chemical shifts of the atoms and groups involved (89). Detailed information about the miscibility, intermolecular interaction, and morphology of polymer blends can be obtained through examining FTIR parameters such as frequency and line width as well as NMR parameters such as the chemical shift, line width, and relaxation parameters (83). More importantly, specific interactions in polymer-polymer blends have been quantified by FTIR, and equilibrium constants of inter-and intramolecular hydrogen bonding have been calculated using a method developed by Coleman's group at Pennsylvania State University. Quantitative FTIR studies of blend systems with hydrogen bonding sites are discussed below.

3.1.2.1.   Occurence of hydrogen bonds in polymer-polymer blends: FTIR studies

The study of intermolecular interactions in polymer blends represents a very important tool in the comprehension of the miscibility mechanism (90). Classic examples of hydrogen bond accepting polymers include poly(vinylpyridine), poly(N-vinyl-2-pyrrolidinone), polyesters, poly(vinyl methyl ketone), and poly(ethylene oxide). Hydrogen bond donor polymers include poly(vinyl alcohol), poly(vinylphenol), and poly(methacrylic acid). Hydrogen bonding in blends can be evaluated by ^{13}C solid state NMR, ^{1}H NMR, FTIR, and differential scanning calorimetry. Some examples of spectroscopic characterization of hydrogen bonding in polymer blends are listed below.

Coleman's group at Pennsylvania State University pioneered the research linking infrared spectral results to equilibrium constants of specific interactions in polymer-polymer blends (91). In a recent report (92), Coleman et al. emphasized that problems may occur when transferring a set of equilbrium constants derived from low molecular weight analogues to polymer blends. Accurate calculations of miscibility and phase behavior using low molecular weight compounds may be limited by three factors: limited accessiblity of functional groups, reduction of rotational freedom in a hydrogen bonded polymer, and entropy changes that occur upon hydrogen bond formation. In this paper, Coleman et al. evaluated hydrogen bonding interactions between phenolic hydroxyl functionalities and ester carbonyl groups for four different systems with analogous functional groups: low molecular weight liquid model compounds (4-ethylphenol and ethyl isobutyrate), different composition copolymers (poly(4-vinylphenol-co-ethyl methacrylate)), a physical blend of poly(4-vinylphenol) and poly(ethyl methacrylate), and poly(4-vinylphenol) dissolved in ethyl isobutyrate. Using FTIR to calculate fractions of free carbonyl groups (1729 cm^{-1}) and hydrogen bonded carbonyl groups (1705 cm^{-1}), Coleman et al. calculated equilibrium constants of interassociation between the phenolic hydroxyls and the methacrylate carbonyl groups (K_A) for each system. The K_A values are shown in parantheses for each system and were: polymer blend (38.4), copolymer (67.4), polymer solution (168), and solvent/solvent (172). The hydrogen bond associations were significantly less in the polymer blend than in the copolymer.

Cesteros et al. (93) evaluated hydrogen bonding in a blend of poly(4-vinylpyridine) and poly(vinyl acetate-co-vinyl alcohol) using FTIR. Poly(4-vinylpyridine) is more readily miscible with hydrogen bond donating polymers relative to poly(2-vinylpyridine) due to the better accessibility of the nitrogen in the para position relative to the ortho position (93). In the poly(4-vinyl pyridine) and poly(vinyl acetate-co-vinyl alcohol) system, hydrogen bonding occurs between the pendant hydroxyl group of the poly(vinyl acetate-co-vinyl

alcohol) and the nitrogen of the poly(4-vinylpyridine). Furthermore, competitive hydrogen bonding arises between two hydroxyl groups or between the hydroxyl group and the acetate group of the copolymer. Using the Painter and Coleman model (91), Cesteros et al. quantitatively evaluated equilibrium constants for the different competitive hydrogen bonding associations shown below in Figure 3-1. K_2 is the equilibrium constant for the self association of two vinyl alcohol moeities, K_B is the equilibrium constant for the "chain-like" self association of several vinyl alcohol moieties, K_C is the equilibrium constant for the hydrogen bond formation between the vinyl alcohol cluster and vinyl acetate, and K_A is the equilibrium constant of hydrogen bond formation between the vinyl alcohol cluster and pyridine. Cesteros et al. found the hydrogen bonding equilbrium constants values to be: K_2 (109 L/mol), K_B (197 L/mol), K_C (52 L/mol), and K_A (60 L/mol). The results indicate that the hydroxyl-pyridine association prevails over the hydroxyl-carbonyl associations (60 > 52), but that the intramolecular vinyl alcohol self association was the strongest hydrogen bond in the system.
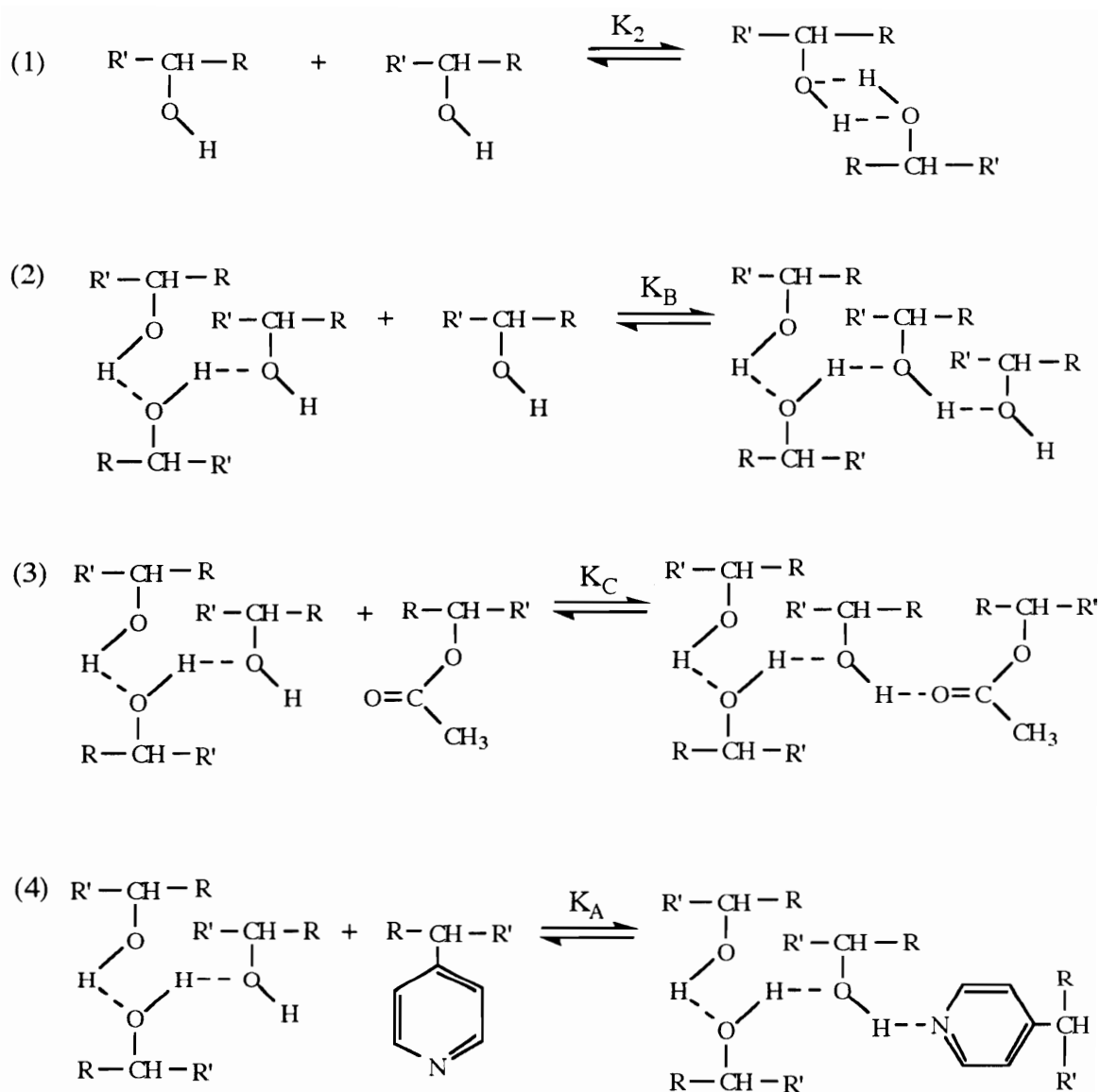
Figure 3-1: Possible hydrogen bonding associations between the moieties: (1) self association of two vinyl alcohol functionalities; (2) "chain-like" self association of several vinyl alcohol functionalities; (3) association between a vinyl alcohol "cluster" and a vinyl acetate functionality; and (4) association between a vinyl alcohol cluster and a 4-vinylpyridine functionality. Equilibrium constants are: $K_2 = 109$ L/mol; $K_B = 197$ L/mol; $K_C = 52$ L/mol; and $K_A = 60$ L/mol.

3.1.2.2. Intermolecular forces in polymer-phenoxy blends

Blends comprised of the polymer resulting from the reaction of epichlorohydrin and bisphenol A (referred to as poly(hydroxy ether of bisphenol A) or "phenoxy") have been extensively investigated. The structure of phenoxy is shown in Figure 3-2. This linear condensation polymer lends itself to blend miscibility studies due to its solubility, a trait
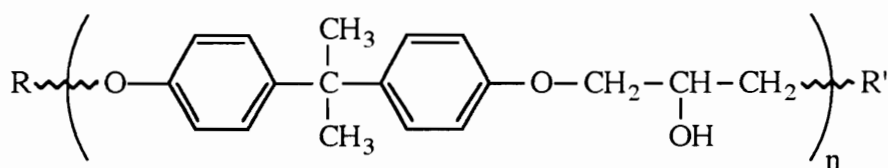
Figure 3-2: The structure of a repeat unit of poly(hydroxy ether of bisphenol A) (phenoxy)

that the crosslinked epoxy resin does not possess. Phenoxy is considered to be a model system for the corresponding epoxy resin (94) because it incorporates analogous functional groups along its partially aliphatic, partially aromatic backbone. Phenoxy resins have been blended with a myriad of polymers, including: poly(N-vinylpyrrolidinone) (95), aliphatic polyesters (94, 96-98), poly(ethylene oxide) (94, 99-100), poly(vinylpyridine) (101), poly(styrene-co-acrylonitrile) (102), poly(ether sulfone) (103), and poly(ether ketone) (104).

Coleman et al. (96) has quantified equilibrium constants between the "phenoxy" polymers and the aliphatic polyester poly(ε-caprolactone). In this elegant and multistep experiment, Coleman et al. first employed the method of Coggeshall and Saier (105) to

determine the equilibrium constants for dimerization and chain-like self association of the secondary aliphatic alcohol 2-propanol. FTIR studies and modeling calculations were then performed on solutions of 2-propanol and phenyl methyl ether in cyclohexane to determine the equilibrium constants of hydrogen bonding between the secondary aliphatic alcohol and an ether group. Subsequently, 1,3-diphenoxy-2-propanol (a close analogue to the repeat unit of phenoxy) was evaluated by FTIR to determine the value of the equilbrium constants when the ether and secondary hydroxyl group were present in the same molecule. The self-association equilibrium constants determined for 1,3-diphenoxy-2-phenol were applied to phenoxy and studies of phenoxy-poly(ε-caprolactone) blends were commenced. The competitive equilibria present in this study are shown in Figure 3-3 and the values of the equilibrium constants at 25 °C were determined to be: dimerization (K_2) 12.0 L/mol; chain-like multimer formation (K_B) 10.8 L/mol; hydroxyl-ether formation (K_E) 2.9 L/mol; and hydroxyl-carbonyl formation (K_A) 7.9 L/mol. Clearly the hydroxyl-hydroxyl self association is stronger than the hydroxyl-ether self association or hydroxyl-carbonyl interassociation in the phenoxy-poly(ε-caprolactone) system. In contrast, however, Coleman et al. (94) found that the intermolecular interaction occurring in phenoxy-poly(ethylene oxide) blends was stronger than the phenoxy self association.
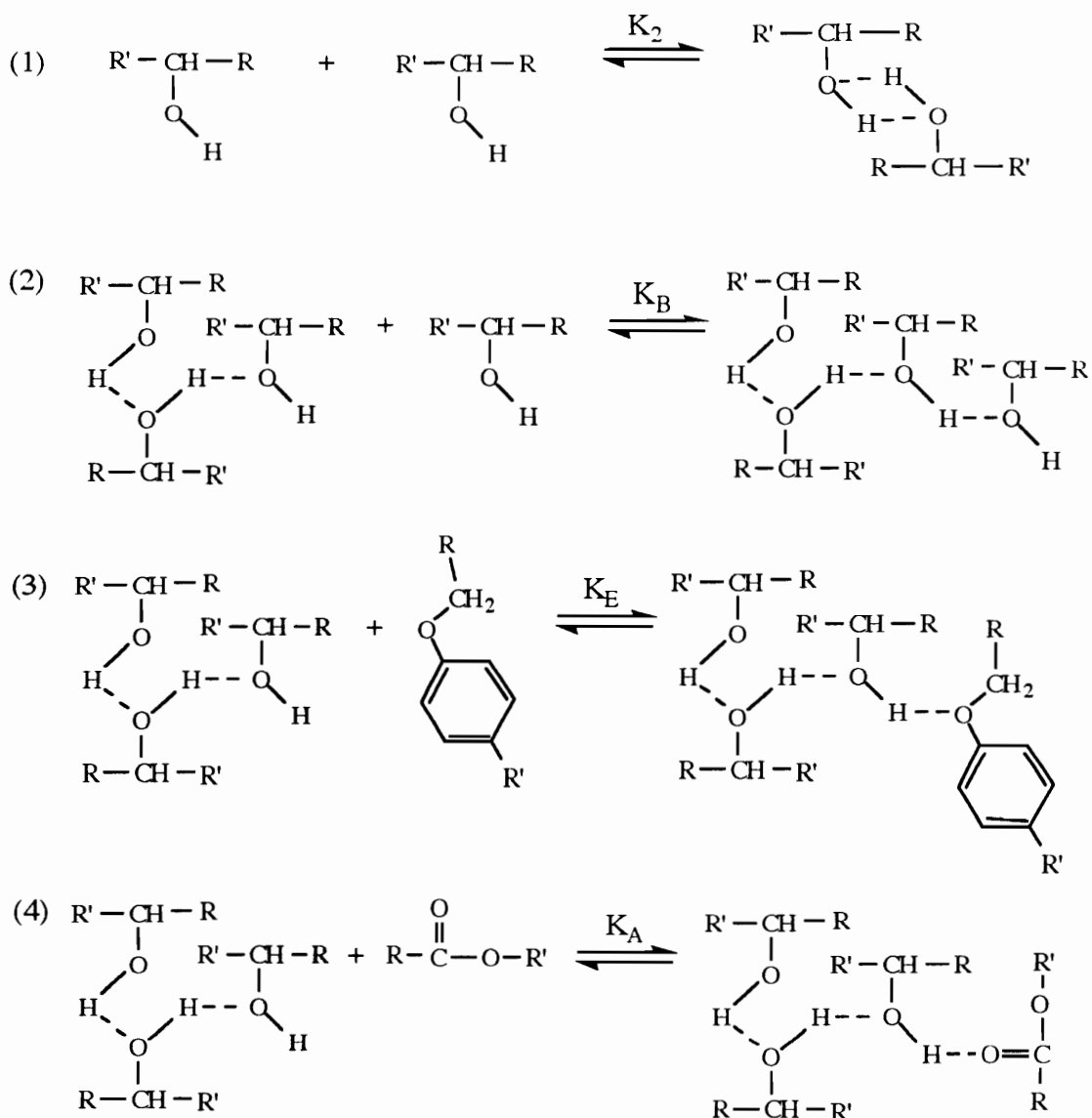
Figure 3-3: Equilibrium constants for associations between phenoxy and poly(ε-caprolactone). (1) phenoxy bimolecular self association between hydroxyl groups; (2) phenoxy chain-like self association of hydroxyl functionalities to form a phenoxy "cluster"; (3) phenoxy cluster association with an ether group of phenoxy; and (4) phenoxy cluster association with a carbonyl functionality of poly(ε-caprolactone). The values of the equilibrium constants are: K_2 = 12.0 L/mol, K_B = 10.8 L/mol, K_E = 2.9 L/mol, and K_A = 7.9 L/mol.

3.1.3. Toughening of epoxy resin networks with engineering thermoplastics

3.1.3.1.　　Two phase epoxy-thermoplastic systems

Traditionally epoxies have been toughened with elastomers such as carboxyl-terminated poly(butadiene-co-acrylonitrile) rubbers (see above section 3.1.1.). Drawbacks to this method included sacrifice of high temperature performance and decreased flexural modulus in order to gain fracture toughness. Ductile aliphatic thermoplastics such as poly(ε-caprolactone) (106), poly(vinyl chloride) (107), and poly(vinyl alcohol) (107) have also been used to modify epoxy resins. These aliphatic modifiers showed partial miscibility with the epoxy resin but the final material showed diminished tensile strength and thermal stability.

In the early 1980's, research efforts began to focus on toughening epoxies with tough, thermally stable, aromatic, ductile thermoplastics such as poly(ether sulfone) (108-110), poly(ether-imides) (111, 112), polyimides (113), poly(ether ether ketone)s (114, 115), poly(ether ether sulfone)s (115, 116), and poly(phenylene oxide) (117). These thermoplastics possess high glass transition temperatures so significant improvement in damage tolerance has been achieved without compromising thermal stability. Early work in thermoplastic toughened epoxy resins involved blending nonfunctionalized high performance polymers with epoxies. These materials showed relatively modest improvements in mechanical properties provided that phase separation and good interfacial adhesion occurred (112).

Chemically prereacting a functionalized thermoplastic polymer into the epoxy resin to control the compatibility and interfacial adhesion of the phase-separated network was first performed by McGrath and co-workers (118-120). To covalently bond high performance polymers into the epoxy network resin, Hedrick et al. (118) and Cecere and

McGrath (115) first capped phenol functionalized poly(bisphenol A-sulfone) with a large excess of a diglycidyl ether, such as bisphenol A-diglycidyl ether, using a quaternary ammonium catalyst. The resulting epoxide terminated poly(bisphenol A-sulfone) was subsequently reacted with the diamine 4,4'-diaminodiphenylsulfone and cured at approximately 200 °C. Alternatively, amine terminated poly(bisphenol A-sulfone)s and poly(bisphenol A-ketone)s may be incorporated into epoxy networks (115). The amine terminated polymers are directly reactive with the epoxy prepolymer and do not require a catalyst. Phase separation of the thermoplastic modifier occured after addition of the diamine curing agent, and during network formation. The heterogeneous specimens displayed domains of poly(arylene ether) dispersed in the continuous epoxy matrix. Mechanical testing of these two phase systems has shown that the particles undergo ductile tearing, which is believed to be an energy absorbing mechanism resulting in higher toughness values (121). The morphology of the epoxy-poly(arylene ether) system has a direct correlation to the mechanical properties (115).

3.1.3.2.   Miscible epoxy-thermoplastic systems

Very few high performance thermoplastic modifiers were found to be miscible with the epoxy resin. Polymers miscible with the epoxy resin were by necessity soluble systems possessing polar groups able to interact with the pendant hydroxyl groups present in the epoxy. Biolley et al. (113) evaluated a polyimide with a fluorene group in the repeat unit as a modifier for epoxy resins. The hindered backbone due to the lateral fluorene groups promoted high T_g and solubility of the polymer. Presence of the thermoplastic modifier shifted the cure cycle to longer times but the resulting system was one phase. The improvement in fracture toughness was minimal which Biolley et al. attributed to the high

miscibility between the polyimide and the epoxy resin. This miscibility lead to increased viscosity of the modified epoxy prepolymer. Longer cure times resulted, and the crosslink density was reduced relative to the unmodified thermoset. Finally, the lack of a phase separated morphology precluded dissipative energy absorption which could efficiently be caused by ductile thermoplastic domains dispersed in the epoxy network.

Guo evaluated phenolphthalein-based poly(arylene ether)s in epoxy blend systems (114, 116). Poly(phenolphthalein ether ether sulfone) was found to be miscible with amine cured epoxy resins such as p-DDS cured diglycidyl ether of bisphenol A. Guo reports that this may be due to the opportunity for hydrogen bonding between the hydroxyl groups of the epoxy and the ester or ether groups present in the poly(phenolphthalein ether ether sulfone). This strong intermolecular interaction reduces the free energy of mixing and enhances miscibility. Conversely, poly(phenolphthalein ether ether ketone), although miscible with phenoxy and diglycidyl ether of bisphenol A (DGEBA), was immiscible with the p-DDS amine cured diglycidyl ether of bisphenol A epoxy resin, separating out of the system during the cure cycle.

The miscible cured poly(phenolphthalein ether ether sulfone)/epoxy blend displayed a single glass transition temperature which varied with composition. The glass transition temperatues of the poly(phenolphthalein ether ether sulfone)/DGEBA uncured system accurately fitted the Gordon-Taylor equation (122), written as:

$$T_g = (W_1 T_{g1} + k W_2 T_{g2})/(W_1 + k W_2) \qquad (3\text{-}1)$$

where T_g is the glass transition temperature of the blend, T_{g1} and T_{g2} are the glass transition temperatures of the pure components one and two, and W_1 and W_2 are the weight fractions of components one and two respectively. The value k is a constant for a given miscible binary system and may be taken as a semiquantitative measure of the

strength of interaction between the components of the blend. When k is one, the glass transition temperature of the blend is the weighted average. When k < 1, the Tg of the blend is lower than expected. When k > 1, the Tg of the blend is higher than expected, which suggests strong interactions (103). In the poly(phenolphthalein ether ether sulfone)/DGEBA uncured system the k value was found to be 0.31.

The glass transition temperature of the poly(phenolphthalein ether ether ketone)/DGEBA uncured system differed from that of the uncured poly(phenolphthalein ether ether sulfone)/DGEBA uncured system because the former accurately fitted the Fox equation (123), written as:

$$1/T_g = W_1/T_{g1} + W_2/T_{g2} \qquad (3\text{-}2)$$

where T_g is the glass transition temperature of the blend, W_1 and W_2 are the weight fractions of components one and two respectively, and T_{g1} and T_{g2} are the glass transition temperatures of the pure components one and two. Note that when the constant k of the Gordon-Taylor equation is one, the Gordon-Taylor equation reduces to the Fox equation. Guo reported that despite the excellent fit between experimental data and the Fox equation, positive deviations for tensile moduli suggested that there is enough interaction between the poly(phenolphthalein ether ether ketone)/DGEBA/p-DDS cured system components to decrease the internal mobility significantly.

3.1.4. Organometallic toughening agents

Organotransition metal complexes have been used as accelerators for epoxy resins for several years (124, 125); enhancement of the epoxy mechanical properties arise when

54

metal acetylacetonates are used as the catalyst in the epoxy cure reaction (126, 127). Lin et al. (128) investigated the toughening effect of cobalt acetylacetonate ($Co(acac)_3$) and chromiun acetylacetonate ($Cr(acac)_3$) on epoxy resins. The cured $Cr(acac)_3$ modified epoxy resin had higher fracture toughness relative to the $Co(acac)_3$ modified epoxy resins. This was attributed to the larger radius of the Cr^{3+} cation relative to the Co^{3+} cation. The larger cation interacts more weakly with its negatively charged acetylacetonate ligands, making the organic ligands more available for hydrogen bonding with the hydroxyl groups of the epoxy resin. Zinc, copper, and chromium acrylates have also been incorporated into epoxy resins resulting in improved thermal stability, chemical resistance, and electrical conductivity relative to unmodified epoxy resins (129, 130).

3.2. Introduction: poly(arylene ether)/epoxy miscibility

It is well known that blending a ductile thermoplastic with an epoxy matrix improves the mechanical properties of the resulting matrix resin. Interleaf systems, wherein a discrete layer of resin of very high toughness is added between plies of a standard prepreg and co-cured, have already been developed (131). In these systems, the tough coating remains as a discrete layer throughout the consolidation process and the final composite material possesses superior compression strength after impact. This implies that coating graphite fibers with ductile thermoplastic materials before prepregging with the epoxy resin will also improve mechanical properties of epoxy-graphite fiber composites. It is possible that interlayer materials coated on individual fibers will not only act as tougheners for the epoxy but will also improve adhesion between the epoxy and the graphite fiber. The transition zone between the reinforcing material and the matrix will differ in chemical composition from the matrix. The fiber interface composition may be totally different from the bulk composition (132). In this collaborative research project pursued by groups in both the Chemistry and Engineering Science and Mechanics departments at Virginia Tech, ductile, high performance thermoplastic poly(arylene ether)s are being investigated as sizing treatments for graphite fibers in order to control the interphase structure through a gradient diffusion process.

It is anticipated that the optimum sizing will be not only miscible (or reactive) with the epoxy resin but will have good adhesion to the normally acidic surface of the graphite fiber. This is accomplished by using a sizing with basic groups that will not only hydrogen bond to the pendant hydroxyl groups on the epoxy backbone but also to the graphite fiber. Functional group candidates must possess lone pairs of electrons and/or π bonds which are available for hydrogen bond formation. Several functional group candidates utilized in this study are shown in Figure 1-1.

Lesko et al. (4, 5) demonstrated that poly(vinylpyrrolidinone) (PVP), an amorphous polymer possessing pendant electron rich amide groups, could be used as a sizing material for graphite fibers. The damage tolerance of the composites made with PVP sized graphite fibers were superior to those with unsized fibers. Use of PVP sized fibers in carbon fiber-epoxy composites improved the static compressive strength by 51 % and increased the notch cross ply R = -1 fatigue by two orders of magnitude over epoxy/bisphenol A sizings (4). Although the PVP was both miscible with the epoxy resin and adhered well to the graphite fiber, composites made using this method would have compromised thermal stability and possibly hydrolytic sensitivity due to the aliphatic nature of the poly(vinyl pyrrolidone) backbone and its hydrophilic nature.

Aromatic, thermally stable polymers with analogous electron rich functional groups are now being investigated as sizing materials. Because the sizings must be stable at the elevated epoxy cure temperatures, candidates for this research include amorphous poly(arylene ether)s with basic functional groups, such as poly(arylene ether sulfone), poly(arylene ether phosphine oxide), poly(arylene ether pyridine), and poly(arylene ether sulfoxide). Use of these high performance materials as sizings will not decrease the use temperature of the final epoxy composite. These polymers have been synthesized with and without reactive amine endgroups and the effects of both miscibility and reactivity will be investigated. Initial blend studies of nonreactive bisphenol A based poly(arylene ether)s with epoxy resins were performed to determine miscibility of each modifier in the epoxy resin, and the results are reported here. Miscibility was evaluated by thermal analysis. The presence of a single glass transition temperature in differential scanning calorimetry scans of the epoxy-poly(arylene ether) blend was taken as an indication of a miscible single phase system. Figure 3-4, which outlines the miscibility and reactivity of the polymers, illustrates the logic of the investigation. A polymer from each block of the table will be investigated to determine its effectiveness as a sizing material.
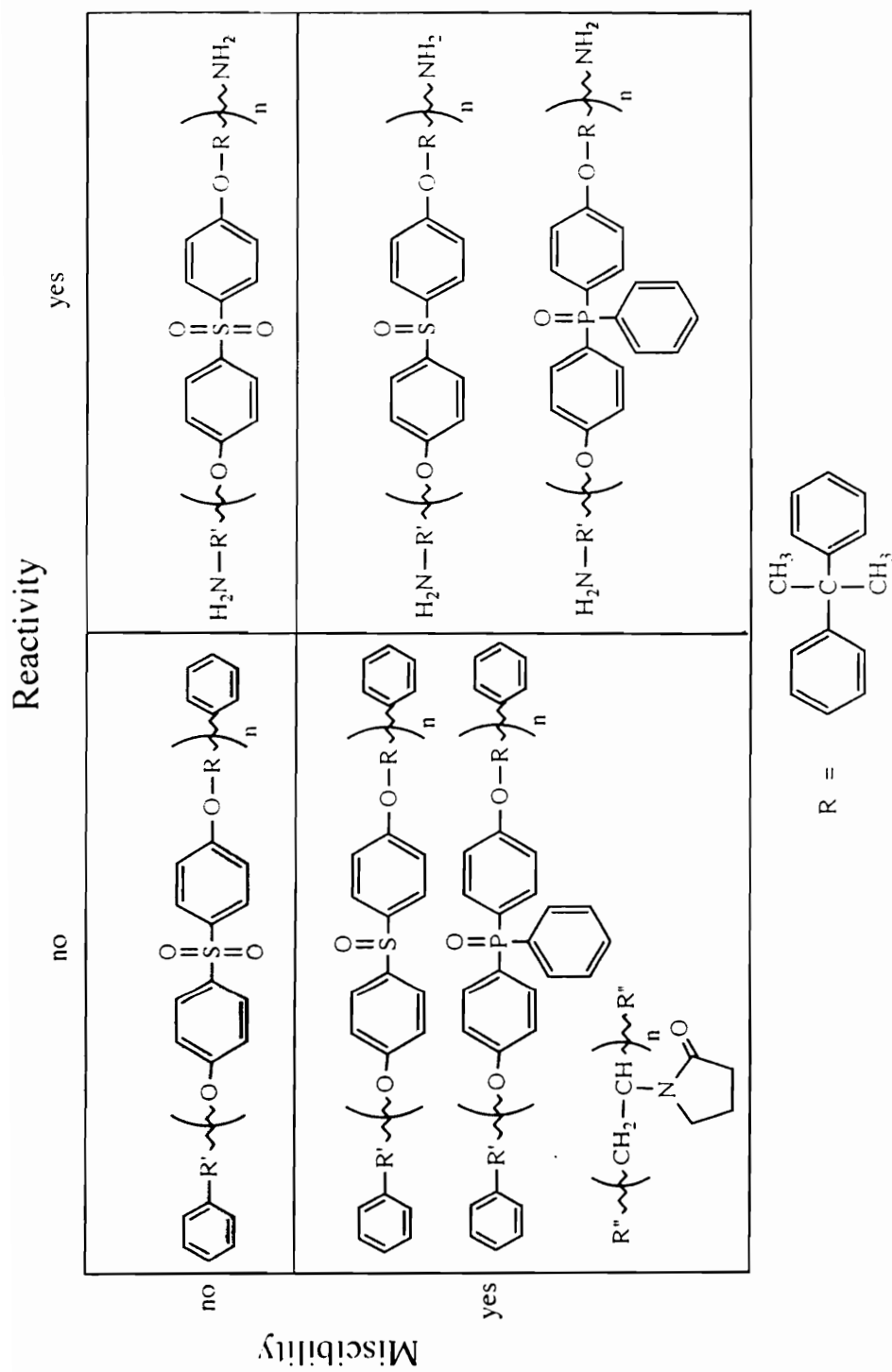
Figure 3-4: Miscibility and reactivity of poly(arylene ether)s with epoxy thermosets

58

3.3.   Preparation of epoxy-poly(arylene ether) blends

3.3.1. Materials for epoxy synthesis

The EPON 828 diepoxide was obtained from Shell Chemical Company and used as received. The diamine, p-diaminodiphenylsulfone (p-DDS), was obtained from Aldrich Chemical Company and used as received. The epoxy equivalent weight (EEW) of EPON 828 is 189 g/mole.

3.3.2. Synthesis of EPON 828/p-DDS epoxy thermosets

The parts by weight of diamine to be used with 100 parts by weight of diepoxide to form the epoxy resin were calculated using the formula:

$$\frac{\dfrac{\text{MW diamine}}{\text{\# of active H's}}}{\text{EEW}} \times 100 \quad = \text{ g diamine} \qquad (3\text{-}3)$$

$$\text{e. g.} \quad \frac{\dfrac{248.3}{4}}{189} \times 100 \quad = \quad 32.8 \text{ g} \qquad (3\text{-}4)$$

Thus 32.8 g of p-DDS must be reacted with 100 g of EPON 828 to form the epoxy thermoset.

EPON 828 (2.5 g) was weighed into a test tube. EPON 828 is a viscous fluid at room temperature but the viscosity decreases dramatically when heated. The test tube containing EPON 828 was placed in an oil bath held at 130 °C. Subsequently 0.82 g of p-DDS was added to the warm EPON 828 and the mixture was stirred using a metal spatula until dissolution of the p-DDS into the liquid EPON 828 was complete. The clear yellow homogeneous solution was poured into a heated aluminum weighing dish and placed in a convection oven preheated to 130 °C. The cure cycle used was 4 hours at 130 °C followed by 2 hours at 220 °C. After the six hour cure cycle the oven was turned off and the samples were allowed to slowly return to room temperature over time. The final epoxy thermoset formed a brittle, pale yellow film.

3.3.3. Synthesis of EPON 828/p-DDS/poly(arylene ether) epoxy blends

Epoxy/poly(arylene ether) blends were synthesized to contain 20 weight percent of the poly(arylene ether) modifer. Blends were made using the following nonfunctionalized bisphenol A based poly(arylene ether)s: Udel™ (poly(arylene ether sulfone)), poly(arylene ether phosphine oxide), poly(arylene ether pyridine), poly(arylene ether sulfoxide), poly(3F-bis A/sulfone), poly(6F-bis A/sulfone), and the copolymers poly(arylene ether quinoxaline-co-sulfone) and poly(arylene ether quinoxaline-co-sulfoxide). The hydroquinone-based poly(arylene ether sulfoxide) was also studied. All polymers were synthesized in Virginia Tech laboratories except Udel™, which was donated by Amoco Chemical Company.

EPON 828 (2.5 g) was weighed into a test tube and heated to 130 °C in an oil bath. The poly(arylene ether) (0.83 g) was added to the test tube; the mixture was stirred and heated until the poly(arylene ether) dissolved (usually requiring 30 minutes). The clear

solution became very viscous after dissolution of the poly(arylene ether). The p-DDS was then added to the homogeneous EPON 828/poly(arylene ether) solution; the solution was stirred until the diamine was completely dissolved. The blend solution was poured into a mold, heated in a convection oven for four hours at 130 °C and 2 hours at 220 °C, and then allowed to slowly cool to room temperature.

The epoxy blends of poy(arylene ether phosphine oxide) and poly(arylene ether sulfoxide) (with both bisphenol A and hydroquinone as the diol) formed clear dark yellow hard films. The epoxy/poly(arylene ether pyridine) blend was transparent and deep red in color. All other epoxy films were cloudy.

3.3.4. Thermal analysis of EPON 828/p-DDS/poly(arylene ether) blends

Thermogravimetric analysis (TGA) and differental scanning calorimetry (DSC) experiments were performed on all poly(arylene ether)s and poly(arylene ether)/epoxy blends. TGA was performed using a Perkin-Elmer Thermogravimetric Analyzer 7 operating in air atmosphere with a heating rate of 10 °C/minute. DSC was conducted with a Perkin-Elmer DSC-7 operating under a nitrogen atmosphere. DSC heating rates were 10 °C/minute in all experiments. Only data from the second heat was evaluated.

3.3.5. Preparation of infrared samples of poly(arylene ether)s and epoxy/poly(arylene ether) blends

Infrared spectroscopy samples were prepared on potassium bromide salt plates. It is crucial that the polymer film is thin and transparent for accurate infrared spectroscopy

measurement. The poly(arylene ether) infrared spectroscopy specimens were prepared by first dissolving the polymer of interest in chloroform at 1 % solids. Two drops of this solution was placed on a KBr plate and the ensemble placed in a vacuum oven at room temperature. Evaporation of the chloroform solvent left a clear, uniform film of the poly(arylene ether) on the salt plate. Samples were stored in a desiccator before infrared spectroscopy measurements were performed.

The epoxy and epoxy/poly(arylene ether) blend infrared spectroscopy samples were also prepared on potassium bromide salt plates. The epoxy homopolymer and the poly(arylene ether)/EPON-828/p-DDS blends were prepared at 130 °C following the above procedure. One drop of the transparent epoxy or the epoxy/poly(arylene ether) solution was placed on a heated KBr plate; a second KBr plate was placed on top of the ensemble and firmly pressed in place to create a sandwich containing a thin layer of precured epoxy resin mixed with the poly(arylene ether) of interest. The salt plates coated with the epoxy/poly(arylene ether) blends were placed in an oven and held at 130 °C for 4 hours followed by 220 °C for 2 hours. The samples were allowed to slowly cool to room temperature then stored in a desiccator until use.

3.4.   Results and Discussion

Epon 828/p-DDS epoxy resins were synthesized with and without high
performance poly(arylene ether) modifiers. The reaction scheme for the synthesis of
unmodified epoxy resin is shown in Figure 3-5.

In order to synthesize modified epoxies, the desired quantity of poly(arylene ether)
modifier was completely dissolved in the EPON 828 prepolymer prior to addition of the
diamine curing agent (Figure 3-6). This ensured that the uncured epoxy system was
homogeneous, and that any immiscibility evident in the cured epoxy resin was a result of
phase separation of the poly(arylene ether) from the epoxy during the curing stage of the
reaction. The structures of the poly(arylene ether)s used in the epoxy blend studies are
shown in Figure 3-7.

3.4.1. Thermal analysis of poly(arylene ether)/epoxy blends

All poly(arylene ether)s and epoxy-poly(arylene ether) blends had 5 % weight loss
values in excess of 500 °C by TGA under nitrogen atmosphere. The thermal analysis data
is tabulated below in Table 3-1. Four poly(arylene ether)s appeared to form miscible
blends with epoxy under the conditions tested: poly(Bis A/phosphine oxide), poly(Bis
A/sulfoxide), poly(HQ/sulfoxide) and poly(Bis A/pyridine). Blends of the epoxy resin
cured with p-DDS with these four poly(arylene ether)s exhibited DSC traces with only one
intermediate T_g value in between those of the homopolymers. Poly(arylene ether Bis
3F/sulfone) may also be miscible with the epoxy thermoset. However, the glass transition
temperatures of each of the components of the blend were similar, and thus changes in the

diglycidyl ether of bisphenol A

4,4'-diaminodiphenylsulfone
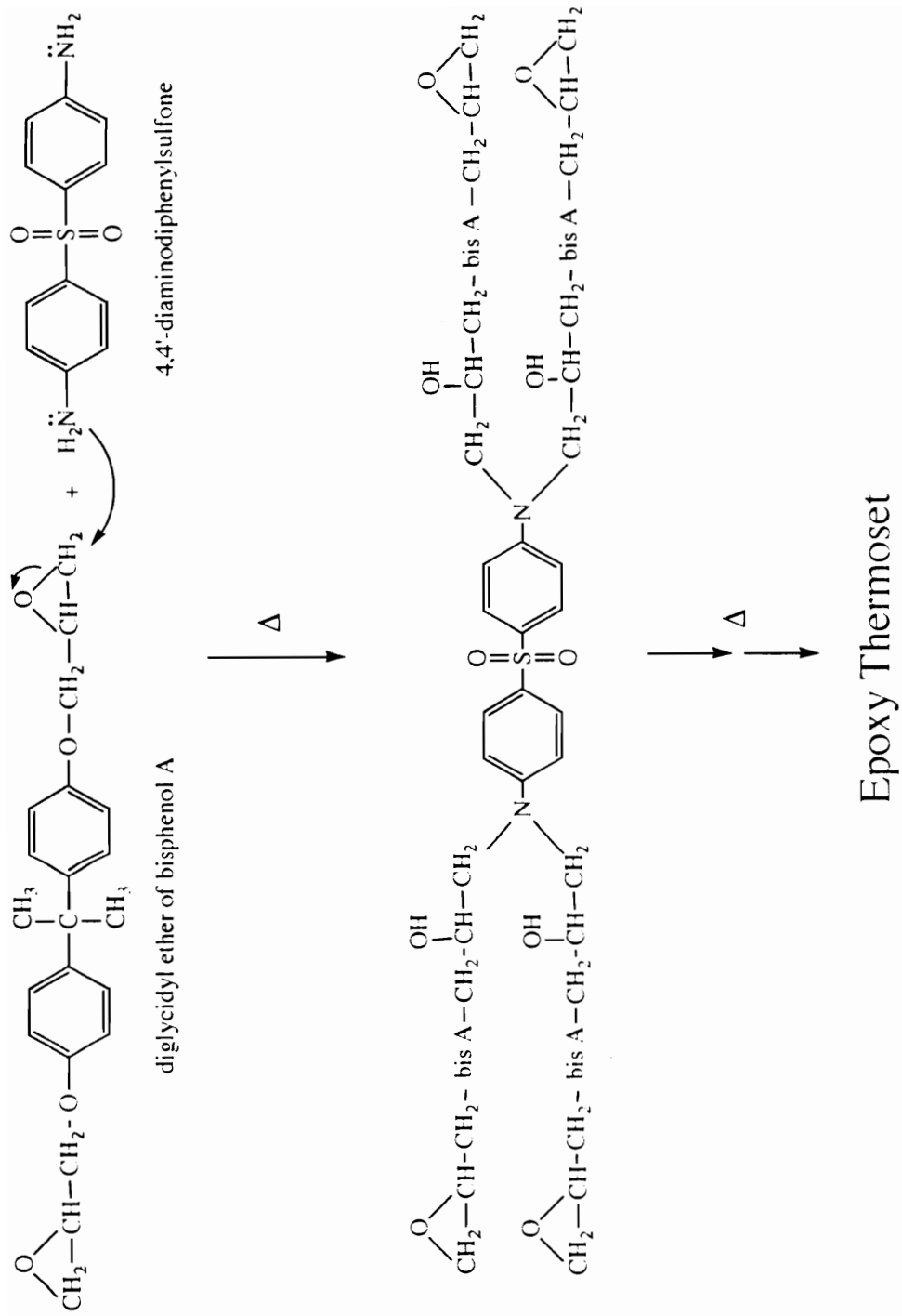
Epoxy Thermoset

Figure 3-5: Synthesis of an epoxy thermoset

64

Figure 3-6: Synthesis of EPON 828 epoxy modified with poly(arylene ether sulfoxide)
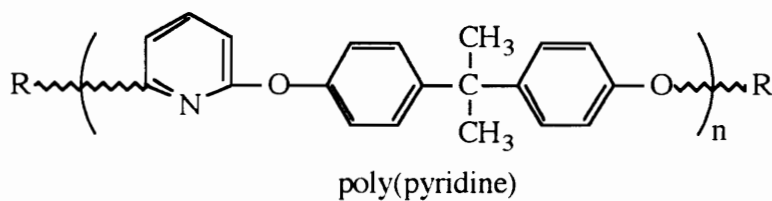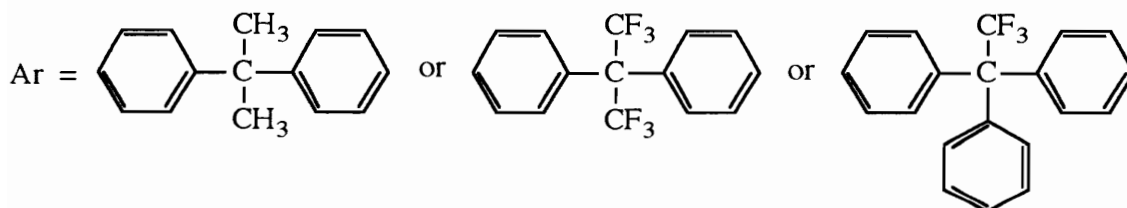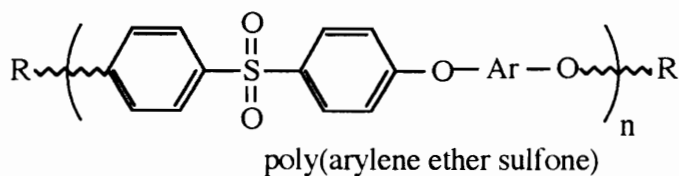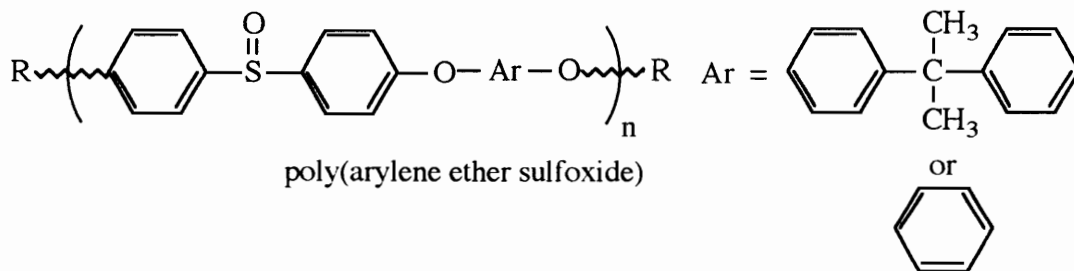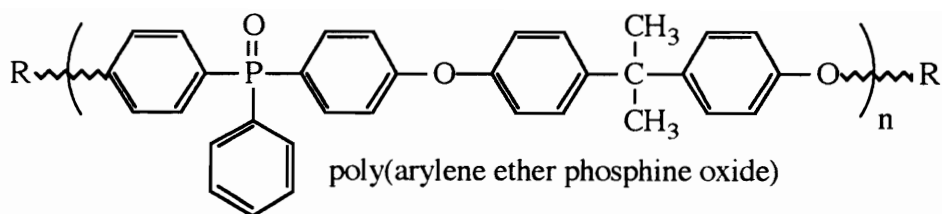
Figure 3-7: Poly(arylene ether)s evaluated for miscibility with EPON 828 epoxy resins

T_g of the blend were not obvious. The epoxy blends of poly(arylene ether phosphine oxide), poly(arylene ether sulfoxide), and poly(arylene ether Bis 3F/sulfone) formed clear, dark, hard, yellow films. The epoxy/poly(pyridine) blend was transparent and deep red. Epoxy blends of Udel™, poly(arylene ether Bis 6F/sulfone), and poly(arylene ether quinoxaline) (homopolymers and copolymers) formed yellowish films with opalescent surfaces. The cloudiness apparent in these films could be indicative of phase separation. This conclusion is supported by the evidence of multiple glass transition temperatures in the DSC scans of opalescent blends.

Table 3-1: Thermal analysis data for poly(arylene ether)s and epoxy-poly(arylene ether) blends

modifier (molecular weight)	T_g (modifier) °C	T_g (blend) °C	miscible?
none	---	213 (epoxy control)	----
Udel™ (20 K)	195	broad, multiple	no
Bis A/sulfoxide (20 K)	169	200	yes
Bis A/pyridine (3K)	100	155	yes
Bis A/phosphine oxide (15 K)	195	208	yes
HQ/sulfoxide (21 K)	172	188	yes
Bis 6F/sulfone (20 K)	205	187, 215	no
Bis 3F/sulfone (high MW)	200	202	??
Bis A/0.4 quinoxaline/0.6 SO	177	177, 213	no

The DSC scan of the miscible epoxy/poly(arylene ether sulfoxide) blend is shown in Figure 3-8.
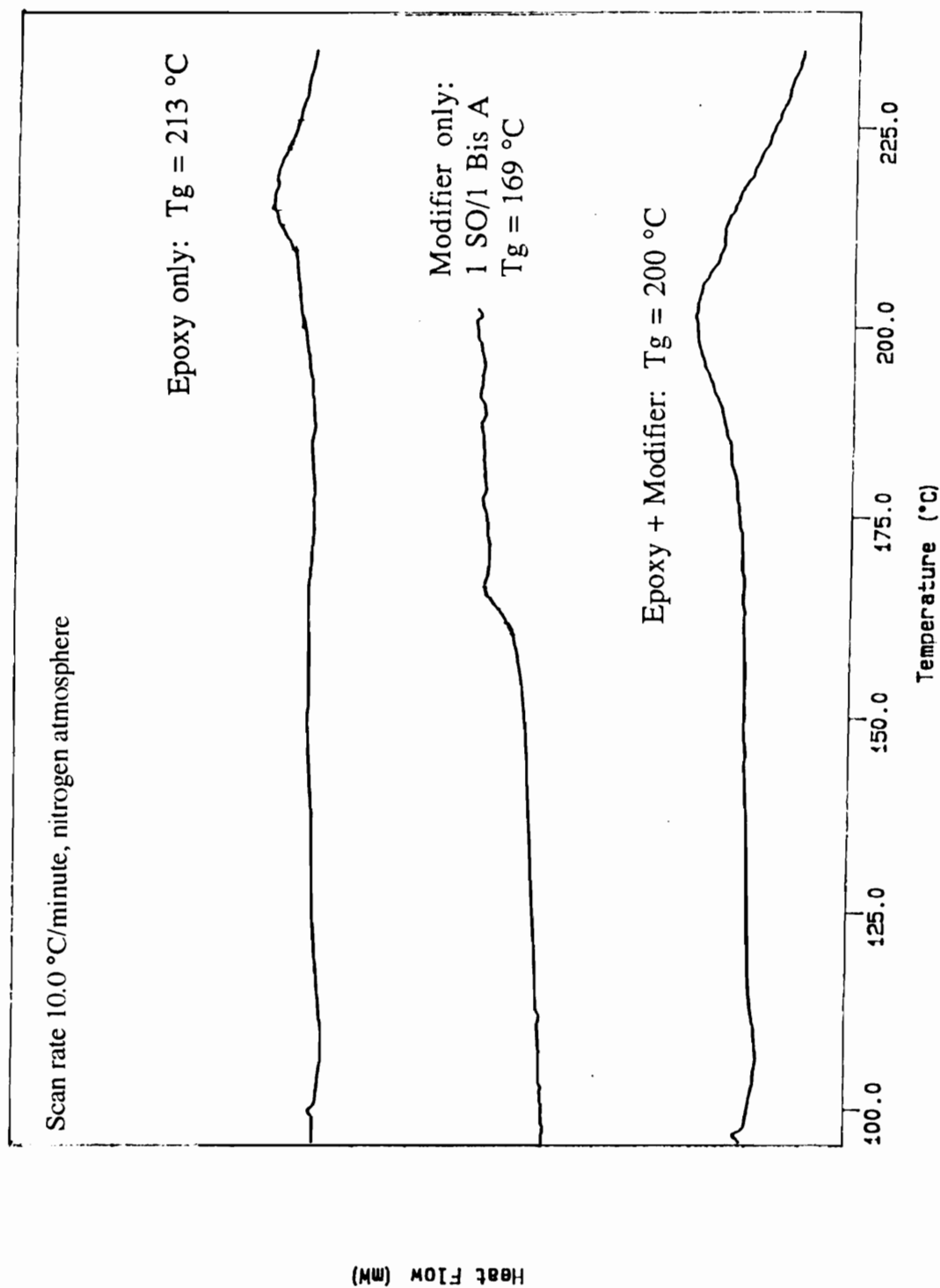
Figure 3-8: Differential scanning calorimetry of EPON 828 epoxy, modifier, and modified epoxy

3.4.2. Microscopy of poly(arylene ether)/epoxy blends

Transmission electron microscopy was performed on two of the poly(arylene ether)/epoxy blends to corroborate the misciblity evidence concluded from the differential scanning calorimetry data. Poly(Bis A/sulfoxide) and reactive poly(Bis A/sulfone) blends (20 weight percent) in EPON 828/p-DDS epoxy resin showed remarkably different morphologies by TEM. The micrograph of the poly(Bis A/sulfoxide)/epoxy blend showed a single phase, miscible system at 6400 times magnification. The blend of the reactive poly(Bis A/sulfone) with epoxy had a diverse morphology at the same magnification. Macrophase separation between the poly(Bis A/sulfone) and the epoxy was clearly evident; however, micron size domains of epoxy existed in the polysulfone continous phase and vice versa. This may be the cause of the multiple T_g pattern seen in the DSC of the epoxy/nonreactive polysulfone blend; various levels of diffusion of each phase into each other could lead to partial miscibility and corresponding variations in T_g.

3.4.3. Intermolecular interactions responsible for miscibility of poly(arylene ether)s based on sulfoxide, phosphine oxide, and pyridine in epoxy resin

The miscibility of the poly(arylene ether sulfoxide), poly(arylene ether phosphine oxide), and poly(arylene ether pyridine) may be attributed to the basicity of the functional groups along the backbone of each polymer. Polymers known to be miscible with amine cured epoxy resins include polyimides (113) and phenolphthalein-based poly(arylene ether sulfone)s (116). Both of these materials possess carbonyl and other functionalities which are available for hydrogen bonding with the secondary hydroxyl groups in the epoxy resin.

Direct measure of basicity of a functional group may provide information on hydrogen bonding capability of this functional group. Bordwell (133) reported the

equilibrium acidity constants shown in Table 3-2. These pK_a values indicate that indeed dimethyl sulfoxide and 4-methylpyridine are more basic than dimethyl sulfone or acetone. No information was available for the phosphine oxide functionality; however, it should be similar to the sulfoxide functionality. Clearly sulfoxide and pyridine functionalities will form stronger hydrogen bonds with the secondary hydroxyl groups present in the epoxy network than will sulfone or carbonyl groups. These intermolecular attractive forces are crucial to polymer-polymer miscibility as they provide a negative enthalpy to the mixing thermodynamics and contribute to a negative free energy of mixing.

Table 3-2: Equilibrium acidities in DMSO at 25 °C (133)

compound	pK_a (in DMSO at 25 °C)
acetone	26.5
dimethylsulfone	31.1
water	31.2
dimethylsulfoxide	35
4-methylpyridine	35
phosphine oxide-containing compounds	no data available

3.4.4. Comparison of 3F- versus 6F-bisphenol poly(arylene ether sulfone)s

The fluorinated poly(arylene ether sulfone)s, synthesized using 6F-bisphenol and 3F-bisphenol in place of bisphenol A, were blended with epoxy thermosetting resins to evaluate the role of the electronegative fluorine atoms on epoxy-poly(arylene ether) miscibility. The results of the experiment were unclear because the glass transition

temperatures of the fluorinated poly(arylene ether)s were close to the T_g of the epoxy thermoset. The poly(arylene ether Bis 3F/sulfone) may have been miscible with the epoxy while the poly(arylene ether Bis 6F/sulfone) appeared to be immiscible. One possible explanation is depicted in Figure 3-9. The electronegative fluorines induce a partial positive
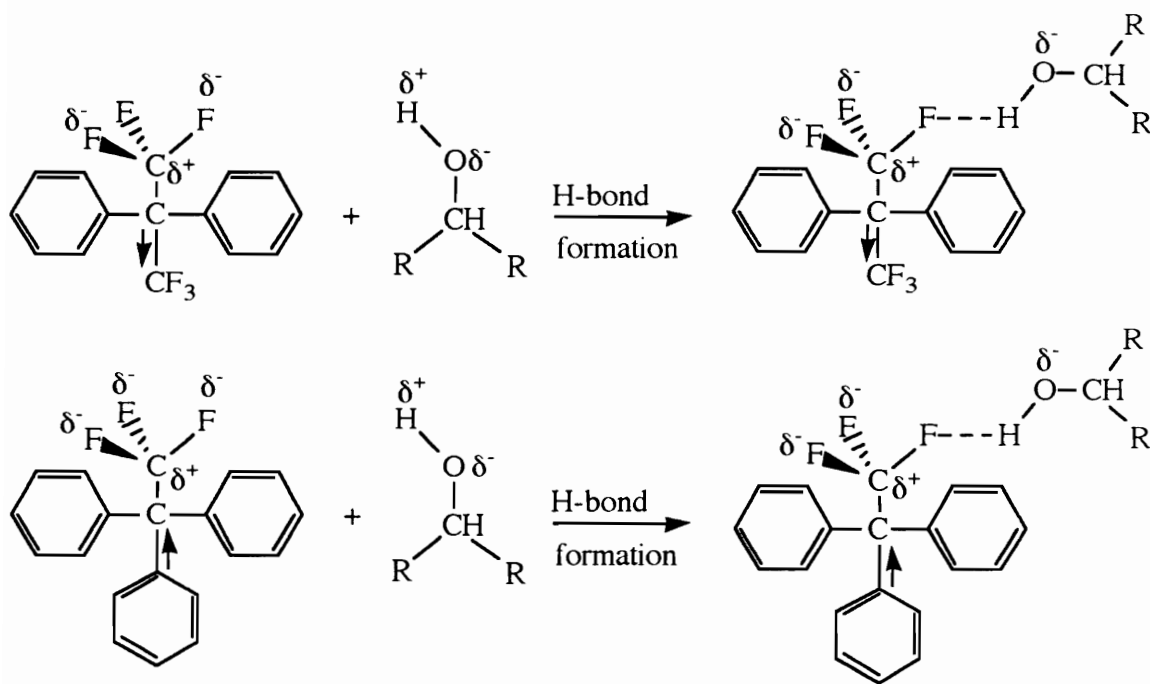
Figure 3-9: Hydrogen bond formation in 3F- and 6F-bisphenol systems

charge on the attached carbon. When a hydrogen bond forms between a fluorine and a hydrogen of an alcohol, the carbon becomes more positive because the electrons on the fluorine are now partially donated to the hydrogen. The nearby phenyl groups on the 3F-bisphenol will stabilize the positive carbon by an inductive effect. Conversely, the additional CF_3 ligand of the 6F-bisphenol is electron withdrawing and will destabilize the

partially positive carbon by an inductive effect. Thus the additional CF$_3$ group in the 6F-bisphenol will inhibit hydrogen bond formation. This may in turn lead to reduced miscibility of the 6F bisphenol (relative to the 3F-bisphenol) in the epoxy resin which contains pendant secondary hydroxyl groups.

3.4.5. Discussion of quinoxaline-based copolymers

The quinoxaline/sulfoxide copolymer, wherein the ratio of functional groups was 0.6 molar equivalents sulfoxide to 0.4 molar equivalents of quinoxaline, was not miscible in the epoxy resin despite the high ratio of sulfoxide functionalities in the polymer. Thus the addition of only a small amount of the rigid quinoxaline unit was enough to counteract the poly(arylene ether sulfoxide)'s miscibility with the epoxy resin. These results were surprising, in light of the fact that poly(arylene ether pyridine) was highly miscible in the epoxy resin. However, the two nitrogens of the quinoxaline group, flanked by phenyl linkages, may not have the accessibility required for adequate hydrogen bond formation. Furthermore, the polar functionality of the polyquinoxaline was imprisoned in a fused heterocyclic ring system; this lack of mobility may also have an effect on the polymer-polymer miscibility as the slow moving chains may not be able to effectively entangle during the curing stage.

3.4.6. Infrared spectroscopy of the poly(arylene ether)/epoxy blends

Infrared spectroscopy was performed in an effort to corroborate the possible hydrogen bonding between the functional groups and the epoxy resin shown in the DSC

results. It is well known that hydrogen bonding tends to shift a stretch to lower frequencies in infrared spectroscopy and samples were made to evaluate the extent of the shift. Stretches on the homopolymers were first identified. Sulfone S-O stretches were found at 1300 and 1150 cm^{-1}; the sulfoxide functionality showed a stretch at 1050 cm^{-1} corresponding to the S-O bond; the phosphine oxide P-O stretched at 1180 cm^{-1}; and the pyridine spectrum had a C-N stretch at 1590 cm^{-1}. The epoxy homopolymer, however, showed strong stretches across the region of 970 to 1350 cm^{-1}. Thus the sulfone, phosphine oxide, sulfoxide, and pyridine stretches were obscured in the blends (80 epoxy/20 poly(arylene ether) (w/w)) and no conclusion about hydrogen bonding could be formed from the infrared spectroscopy study.

3.5. Conclusions

Poly(arylene ether phosphine oxide), poly(arylene ether sulfoxide), and poly(bis A/pyridine) are miscible in EPON 828/p-DDS epoxy resin. These high performance polymers are candidates for sizings because they do not degrade at curing temperatures for the epoxy and should not lower the use temperature of the resulting epoxy composites. The strong epoxy-poly(arylene ether) intermolecular attractive forces should promote diffusion and mixing of the sizing material with the epoxy before and during the cure stage of the reaction. Thus the interphase between the epoxy and the graphite fiber may have a tough, ductile, gradient layer of poly(arylene ether) toughening agent to strengthen the interface between the two components of the composite material. The enhanced properties of the interlayer may improve the properties of the composite as a whole because often the interlayer is the most failure-prone region of the epoxy-graphite fiber composite.

CHAPTER 4

^{1}H NMR studies: hydrogen bond formation between hydrogen donors and electron rich nitrogen- and oxygen-containing model compounds

4.1   Literature review

The phenomenon of intermolecular hydrogen bond formation is evident in the changes of many physical properties such as melting point, sublimation energy, dielectric constant, and spectral behavior of the molecules involved (134). The "hydrogen bond" concept was first applied by Huggins and independently by Latimer and Rodebush in the 1920's to explain a regularity in molecular structures of polar compounds (135). Since the late 1950's a wealth of spectroscopic studies of hydrogen bond formation has appeared in the literature (136). An introduction to hydrogen bonds and some highlights of research in hydrogen bond formation are presented here.

4.1.1. Principles of hydrogen bonding

A hydrogen bond is an intermolecular interaction in which a hydrogen atom that is bonded to an electronegative atom is attracted to an unshared electron pair on another electronegative atom. This special class of intermolecular dipole-dipole attractive forces of the type A-H $\cdots$ B most often occurs when A and B are electronegative atoms such as fluorine, chlorine, oxygen, sulfur, or nitrogen. A is referred to as the electron acceptor and B is the electron donor. The H $\cdots$ B bond distance is intermediary between the length of the

corresponding covalent bond and the sum of the van der Waal radii of the two atoms. For example, in ice, the H··O hydrogen bond has a length of 1.77 Å while the the O-H covalent bond length in ice is 0.99 Å and sum of the van der Waals radii of O and H is 2.50 Å (137). Hydrogen bonds are also known to occur when a hydrogen bonded to an electronegative atom interacts with the p-orbital electrons of a π-bonded system (138). Hydrogen bond strengths range from 5 to 25 kJ/mole (137) and are characterized by a few well-defined structural regularities: very close approach of the two atoms A and B, linearity of the bond (angle AHB $\approx$ 180°), and an increase of polarity of the AH bond (135). At room temperature the interconversion time between complexed and noncomplexed states in hydrogen bonded systems is small, approximately 10^{-8} seconds (139).

4.1.2. Methods for quantitative study of hydrogen bond formation

Hydrogen bond formation can be readily quantitated by calorimetric methods (140) or by spectroscopic methods including infrared, Raman, nuclear magnetic, and emission spectroscopy (89). Infrared spectroscopy is the most straightforward method for the detection of hydrogen bonds (89). The formation of a hydrogen bond X-H··Y shifts the stretching mode (v_{XH}) and its harmonics to lower frequencies and also causes an increase in the intensity and half-band width of the fundamental v_{XH}. The frequency shift, Δv_{XH}, has been correlated with various chemical and physical properties including base strength of donors.

Hydrogen bond formation is also recognized by a characteristic downfield shift of the nuclear magnetic resonance signal of the proton in the hydrogen bond. However, the lifetime of a hydrogen bond lies in the range of 10^{-11} to 10^{-5} seconds, and IR and NMR

require time scales of the order of 10^{-13} and 10^{-2} seconds respectively to average out differences in vibrational frequencies and differences in magnetic resonance frequencies (141). Therefore, with the IR technique one can detect separate hydrogen bonds directly while by NMR one can only obtain information from averaged hydrogen bonds. This difference leads to several different features in IR and NMR measurements (142).

Vinogradav and Linnell summarized the strengths and shortcomings of both IR and NMR spectroscopies for use in hydrogen bond studies (143). Their observations are as follows:

(i).   NMR is useful for hydrogen bond studies involving specific protons, even in cases of weak hydrogen bonding. For weak hydrogen bonding, IR peak overlap is serious.

(ii).   NMR and IR are equally useful in 1:1 complex studies.

(iii).   NMR can be used in aqueous systems, while the presence of water eliminates many of the useful IR spectral regions even with the help of curve fitting.

(iv).   Rates of hydrogen bond formation and dissociation may be studied by NMR but not by IR.

(v).   In self-association, each hydrogen bonded species can be distinguished by IR, but band broadening and overlapping, vibrational coupling and anharmonicity do complicate the interpretation of IR results.

(vi).   Very dilute solutions, gases, and solids may be studied by IR and equilibrium constants can be calculated directly from experimental data with fewer simplifying assumptions than NMR requires.

All in all, IR is the more powerful technique and much more literature information is available on thermodynamics of hydrogen bond formation as studied by infrared spectroscopy. However, NMR is the more facile method for evaluaton of hydrogen bond formation in aqueous systems. Thus this is the method chosen for studying hydrogen bond formation between bases and water in the model compound/DMSO/water system used in this research.

4.1.3. Basic principles of ^{1}H NMR

Nuclear magnetic resonance spectroscopy (NMR) is the most powerful technique for structural analysis available to the organic chemist. With the aid of NMR it is possible to define the environment of practically all commonly occurring functional groups. NMR may be used for quantitative determination of compounds in mixtures and is thus of great use for following the progress of a chemical reaction. Moreover, NMR will often yield kinetic and thermodynamic parameters for certain types of chemical processes. The principal limitations of this method are its inherently low sensitivity and difficulty in acquiring information on solid state materials (144).

4.1.3.1.   The nucleus

NMR spectra are obtained through measurement of the energy gaps between states of different energy. The analysis requires the presence of an external magnetic field and concerns nuclei rather than electrons. Every nucleus has a spin quantum number I which can be zero, an integer, or a half integer, e. g. 0, 1/2, 1, 3/2, etc (145). The value of the

spin quantum number is governed by the shape of the nuclear charge and the number and type of nucleons. A nucleus with a spinning charge ($I \neq 0$) will generate a magnetic field. Then, when an external magnetic field is applied to the spinning nucleus, the nucleus will orient itself in different directions relative to the external field. The number of directions that the nucleus can orient itself is related to the spin quantum number, I, of the nucleus through the relationship $2I + 1$.

There are three principal groups of nuclei:

1) $I = 0$ (nonspinning nuclei). These have no magnetic moment and are composed of even numbers of protons and neutrons, e. g. ^{12}C, ^{16}O. These nuclei are invisible by nuclear magnetic resonance spectroscopy.

2) $I = 1/2$ (spherical spinning charges). These nuclei have a magnetic moment but no electric quadrupole. This group is by far the most important from the chemical point of view. Chemically useful nuclei in this group include: ^{1}H, ^{13}C, ^{19}F, ^{29}Si, ^{31}P, and ^{15}N. The number of different orientations a spin 1/2 nucleus may adopt when subjected to an external magnetic field is: $2I + 1$, or 2.

3) $I > 1/2$ (nonspherical spinning charges). These nuclei have both magnetic dipoles and electron quadropoles. Examples include: $I = 1$: ^{2}H, ^{14}N; $I = 3/2$: ^{11}B, ^{35}Cl, ^{37}Cl, ^{7}Li; $I = 2$: ^{36}Cl, ^{58}Co; $I = 5/2$: ^{25}Mg, ^{27}Al, ^{17}O. Nuclei in this group may show multipeak behavior (adopt more than two orientations) in an NMR spectrum even though they are in an equivalent chemical environment.

The spin-1/2 nuclei are the most important family of nuclei for NMR measurement and are the group of concern in this research. The energy required to flip a spin-1/2 nucleus from one orientation to the other orientation (also referred to as the energy gap corresponding to the spin flip or *resonance*) is calculated by the equation:

$$\Delta E = h\nu \qquad (4\text{-}1)$$

where h is Planck's constant and ν is the NMR frequency (e. g. 400 MHz). Thus a spin flip may be observed by holding the spectrometer magnetic field constant while systematically varying the frequency; often referred to as "sweeping the frequency".

4.1.3.2.   Measurement of the chemical shift

The chemical shift (δ) of a nucleus is the difference between its resonance frequency and that of a reference standard. The typical reference for ^1H NMR spectroscopy is tetramethylsilane, $(CH_3)_4Si$, a nonreactive compound with 12 equivalent protons. The proton resonance of TMS is assigned the value of 0 ppm on the ppm scale. Other resonances are typically downfield of TMS, meaning that higher spectrometer frequencies are required to induce the nuclei to resonate. The chemical shift of the proton of interest is converted from frequency (Hz) to the universally used, unitless ppm value using the equation:

$$\delta_{ppm} = \frac{\text{chemical shift in Hz downfield of TMS}}{\text{spectrometer frequency in Hz}} \times 10^6 \qquad (4\text{-}2)$$

The advantage of the ppm scale is that shifts reported on it are independent of the applied field. Typical values for chemical shifts range from 0 to 12 ppm for protons in ^1H NMR spectroscopy.

4.1.3.3.   Factors influencing the chemical shift

The chemical shifts occurs because the resonance frequency of a nucleus depends not upon the gross field (H_o) between the poles of the magnet of an NMR spectrometer, but on the actual field felt by the resonating nucleus. The actual field felt by the nucleus is related to the spectrometer field through the relationship:

$$H_{nucl} = H_o(1 - \sigma) \tag{4-3}$$

where σ is the shielding constant for the particular situation. Shielding may be explained in the following manner. Consider an isolated hydrogen atom: a nucleus possessing one electron and one proton. When the hydrogen atom is subjected to a spectrometer magnetic field, H_o, as shown in Figure 4-1, the 1s electron will circulate analogously to a current in an electric loop. This circular current will induce another magnetic field, H_e, which, in the region of the nucleus, will oppose the spectrometer magnetic field H_o. Thus the overall magnetic field felt by the nucleus is less than that imposed by the spectrometer, and the proton is said to be "shielded" by the electron. On the other hand, when the hydrogen atom is bonded to a carbon, the electron density is shifted somewhat toward the more
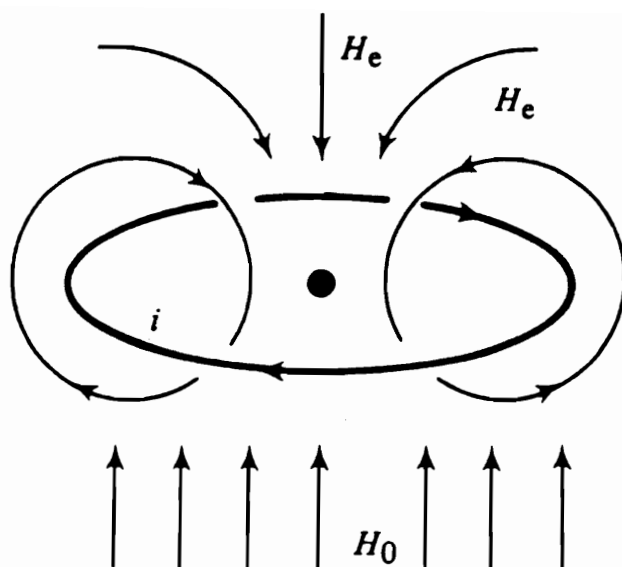
Figure 4-1: Shielding of a proton by the electon in an isolated hydrogen atom (144)

electronegative carbon. The reduced electron density present in the sigma bonded hydrogen will induce a lesser opposing magnetic field, H_e than in the case of the proton alone. Thus the overall magnetic field felt by the hydrogen (bonded to a carbon) will be greater than that felt by the proton alone, and the hydrogen bonded to a carbon is said to be "deshielded". The chemical shift of a deshielded hydrogen moves farther downfield from TMS because a lower spectrometer frequency is required to induce the nucleus to resonate. It follows that the lower the electron density about the hydrogen, the more deshielded the hydrogen is.

Another important factor influencing the chemical shift, other than deshielding by bonding, is the influence of magnetically anisotropic neighboring groups. A group is said to be magnetically anisotropic if the circulation of electrons within it under the influence of

a magnetic field depends on its orientation to this field. The classic example of a magnetically anisotropic environment is benzene. If the planar sigma bonded structure of the benzene molecule is perpendicular to the applied magnetic field, the delocalized π electrons will circulate, causing a ring current. This ring current induces secondary magnetic field which is additive to the applied magnetic field H_o at the periphery of the benzene ring, causing the benzene hydrogens to be deshielded. However, if the planar sigma bonded structure of the benzene ring is parallel to the applied field then no circulation of electrons takes place. Thus benzene is magnetically anisotropic. Overall the chemical shift of benzene protons is much farther downfield than one would expect from mere electron density arguments due to this generation of ring current under an applied magnetic field.

4.1.3.4.   Effect of hydrogen bond formation on the chemical shift

The formation of hydrogen bonds usually lowers the electron density around the proton involved in hydrogen bonding (146). Thus, hydrogen bonding deshields the proton involved, and its resonance is shifted downfield away from TMS. When using NMR for structural determination, three classes of information are extracted from the ^1H NMR spectra: chemical shifts, signal multiplicity, and signal intensity. In hydrogen bonding studies, thermodynamic data is wrapped up in the chemical shift value alone. In an actual measurement, the change in the observed chemical shift, $\Delta\delta_{obs}$, can arise from various sources (147):

$$\Delta\delta_{obs} = \Delta\delta_h + \Delta\delta_w + \Delta\delta_a + \Delta\delta_b \qquad (4\text{-}4)$$

where $\Delta\delta_h$ reflects the change due to the hydrogen bonding, while $\Delta\delta_w$, $\Delta\delta_a$, and $\Delta\delta_b$ arise from changes in van der Waal's forces, magnetic anistropy of solvent molecules, and bulk susceptibility of the solvents respectively. However, the only significant contribution to the change in observed chemical shift is $\Delta\delta_h$; the other factors are negligible. Evaluation of the change in observed chemical shift with hydrogen bonding has been vigorously pursued over several decades and thousands of publications. For this reason only a brief overview of hydrogen bonding by both infrared spectroscopy and nuclear magnetic resonance spectroscopy (for both aqueous systems and systems involving compounds of interest to this research) is presented here.

4.1.4. Hydrogen bond studies of aqueous systems

Water has been shown to exert dramatic influences on the kinetic and thermodynamic properties of solutes in solution (148) and an enormous and continuous effort to understand solute-water interactions in aqueous solution has hallmarked recent years. It is now known that the solute dictates the nature of interaction with the water molecules; the equilibrium constant of hydrogen bond complex formation is sensitive to structural properties of the solutes such as presence of internal hydrogen bonds, positional isomerism, and diastereoism (149). The hydrogen bond in the liquid state is notoriously difficult to describe relative to hydrogen bonds in the highly disordered gaseous state or the highly ordered crystalline state. Structural information on liquids is always statistical in nature due to the complex equilibria and short-range order present in the liquid state (146). Thus the mobility of the liquid ensures that the distribution of intermolecular distances and

intermolecular attractive forces is constantly shifting and only average values may be elucidated from raw data.

4.1.4.1.   The structure of liquid water

The structure of liquid water has historically been controversial. Early workers considered liquid water to be an equilibrium of the sort (150, 151):
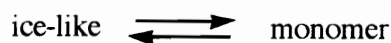
$$\text{ice-like} \rightleftharpoons \text{monomer}$$

wherein monomeric water engages in no hydrogen bond formation while a water molecule in an ice-like cluster can possess one, two, three, or four hydrogen bonds. Alternatively, Buijs and Choppin investigated the infrared spectrum of water in the 1.16 to 1.25 μ region and suggested that the three bands present were due to the presence of three types of water molecules: those having zero, one, and two hydrogen bonds, respectively, to neighboring molecules (152).

Quantitative interpretation of spectroscopic results in hydrogen bond studies is often hampered by the fact that water participates in several simultaneous equilibria via a self association mechanism. Throughout the years, a great deal of research effort has focused on separating the species in equilibrium and characterizing the physical properties of the individual components of liquid water. Schneider, Bernstein, and Pople (153) measured the resonance position of the water hydrogen in the liquid phase at various temperatures relative to the resonance position in the gas phase and used this comparison to derive a value for the "liquid association shift". Schneider et al. suggested that this contribution to

the shift was related to the formation of hydrogen bonds present in the liquid state but not in the gaseous state.

Hindman (154) elaborated that there was more than just the "liquid association" responsible for the difference in signal of the gaseous water relative to liquid water. Hindman's theory evolved around the concept that many interactions affect the shielding in a condensed phase (155). The total shielding constant may be calculated using the equation:

$$\sigma_i = \sigma_o + \sigma_d + \sigma_a + \sigma_f \qquad (4\text{-}5)$$

where σ_i is the total shielding constant and is equal to the sum of σ_o (intramolecular shielding constant), σ_d (the bulk diamagnetic susceptibility constant), σ_a (the molecular susceptibility of neighboring molecules in an anisotropic system), and σ_f (the contribution to the shielding due to the electric-field effects of the charge distributions in the neighboring molecules on the atom in question). Factors important in the multi-faceted σ_f term included van der Waals forces, polarizability, external electric field, and the effect of repulsive overlap on the shielding. Through elegant experimentation and calculations, Hindman derived the shielding effects for monomeric water. Using these values Hindman determined that about twenty percent of water molecules exist as monomeric water at 25 °C. This value corroborated that of Buijs and Choppin determined by infrared spectroscopy (152). In contrast, Stevenson (156) concurrently evaluated the ultraviolet absorption spectrum of water and determined that between 0 °C and 100 °C the nonhydrogen bonded water monomer in liquid water is less than 1 percent. Stevenson also reported that the equilibrium constant for the formation of $(H_2O)_{monomer}$ from $(H_2O)_{polymer}$ at 25.5 °C was 1.33×10^{-3}.

Hindman also deconvoluted the shifts of the various types of hydrogens present in water (154) and found that the shift of monomeric water was 0.56 ppm relative to methane, e. g., 0.79 ppm relative to TMS. Schneider, Bernstein, and Pople (157) reported that the chemical shift of monomeric water was 0.83 ppm downfield from TMS. Lin reported that the shift of the hydrogen in "monomeric water", that is, the shift of a nonhydrogen bonded hydrogen in water, δ_h, ranged between 0.300 and 0.430 ppm relative to TMS depending on the different kinds of measurements and considerations (158). The shift of the hydrogen which is hydrogen bonded to another molecule of water, δ_{bo}, was found to range from 5.43 to 5.57 ppm (158).

Muller and Simon (159) evaluated the concentration of monomeric water in carbon tetrachloride/dioxane mixtures as shown in Figure 4-2. To perform this experiment, low mole fractions (less than 10^{-3}) of water were dissolved in solutions of systematically varied concentrations ranging from zero equivalents of dioxane to 100 equivalents of carbon tetrachloride to the opposite extreme of zero equivalents carbon tetrachloride to 100 equivalents dioxane. It is well known that at low base concentrations, a 1:1 water:base complex is formed in the nonpolar carbon tetrachloride medium, while at higher base concentrations, complexes involving one water molecule and two base molecules are formed (160). Accordingly, Muller and Simon's results demonstrated that dioxane can complex with zero, one, or two water molecules, depending on the solvent composition. At 30 °C, formation of the 1:1 water:dioxane complex was fifteen times more favorable than formation of the 1:2 water:dioxane complex as evidenced by the fact that the equilibrium constant for the formation of the 1:1 complex, K_1, was 12.1 while K_2 was 0.82. Muller and Simon also evaluated the shift of monomeric water to be 1.08 ppm relative to TMS.
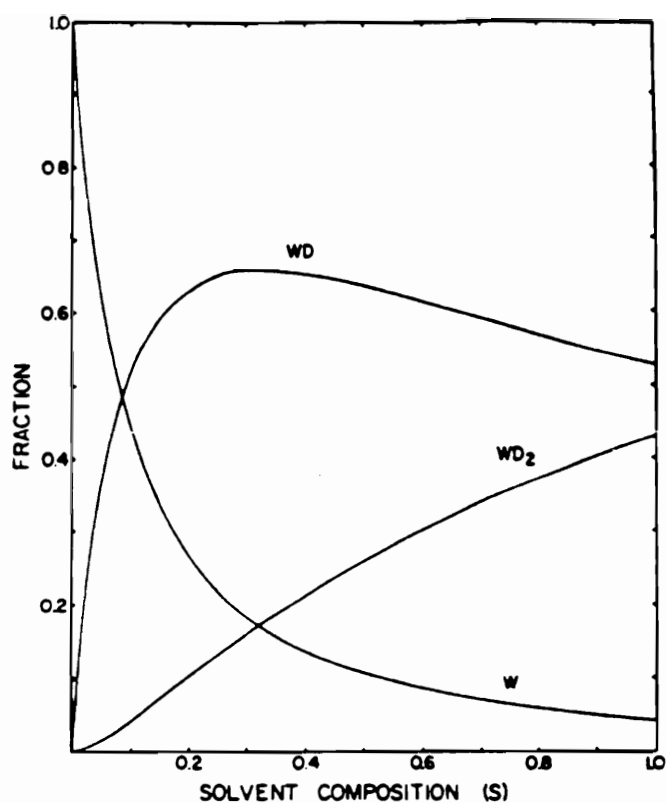
Figure 4-2: The concentrations of monomeric water (W), 1:1 water:dioxane complex (WD), and 1:2 water dioxane complex (WD$_2$) (159) as a function of solvent composition from S = 0 dioxane/1 CCl$_4$ to S = 1 dioxane/0 CCl$_4$

Using the same method to determine equilibrium constants, Nishimura et al. (161) evaluated the hydrogen bonding of water with tributylphosphate, a stronger hydrogen acceptor than dioxane. At 35 °C, K$_1$, the equilibrium constant for formation of the 1:1 water:tributylphosphate complex was 50; K$_2$, the equilibrium constant for formation of the 1:2 water:tributylphosphate complex was 6.8.

4.1.4.2.   Water/dimethylsulfoxide systems

Molecular complex equilibria data between donors and acceptors have been of interest for decades as investigations of association constant data and other thermodynamic parameters have progressed. Systems of biological significance have received widespread attention; the importance of dimethylsulfoxide (DMSO) within chemistry, biotechnology, and medicine has motivated a number of investigations of the molecular properties of DMSO/water mixtures. The DMSO/water mixture represents one of the more complicated binary systems as it has a self associating component (water) plus a second component (DMSO) capable of forming hydrogen bonds with the first component. Some important features of DMSO/water solution chemistry are discussed here.

An early paper by Cowie and Toporowski (162) reported viscosities, densities, and refractive indices of DMSO/water solutions at three different temperatures across mole fractions ranging from 0 DMSO/100 water to 100 DMSO/0 water. In addition to nonideal physical properties, the solutions also showed negative deviations of heats of mixing. Cowie and Toporowski suggested that the large deviations from ideality, with maxima at approximately 30 to 40 mole percent DMSO, were due to the association of the liquids through hydrogen bonding. The greater degree of association in water/DMSO mixtures relative to water alone was attributed by Cowie and Toporowski to the polar sulfoxide group which they hypothesized could complex with two molecules of water. The bond order of the sulfur-oxygen bond is not known. The true structure of DMSO may be considered to be a hybrid between the two resonance structures of DMSO shown in Figure 4-3, with a partial negative charge on the oxygen and a partial positive charge on the sulfur.

Luzar (163) and Puranik et al. (164) evaluated the contribution of hydrogen bonds to dielectric properties of the mixture. Puranik et al. (164) evaluated the static permittivity values of a systematically varied series of DMSO/water solutions. At 25 °C, the static
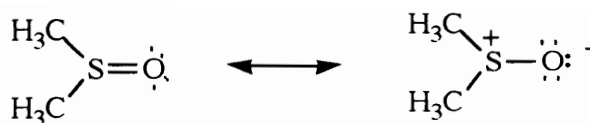
Figure 4-3: Resonance forms of dimethylsulfoxide

permittivity values ranged from 48.4 for the 100 DMSO/0 water solution to 79.5 for the 100 water/0 DMSO solution. The data showed a positive deviation from a straight line: the increase from pure DMSO up to 70 % DMSO was pronounced, followed by a more gradual increase thereafter to the static permittivity of water. Using this data, Puranik et al. determined the dipole moments of water and DMSO molecules to be 2.10 and 4.36 D respectively at 25 °C (1 D $\approx$ 3.34 x 10^{-30} Cm), about 10 % larger than the values for the gaseous water and DMSO molecules.

The structure of the DMSO:water complex in solution is still controversial. It is well known that DMSO forms a stable hydrate in the crystalline state (1 DMSO: 3 H_2O) (165). Furthermore, addition of small amounts of DMSO to water is accompanied by formation of highly polar aggregates and by a breakdown of the "liquid lattice" of water (166). However, the exact structure and molecular dynamics of the DMSO:water complex have not been elucidated until recent years.

Luzar (167) first described the complex to be a nearly tetrahedral arrangement of two or three water molecules hydrogen bonded to one DMSO molecule. However, the degree to which coordination of DMSO by water can be regarded as a long lived complex is not known. In order to evaluate the structure of DMSO/water mixtures, Luzar and Chandler (168) investigated the structure and hydrogen bond dynamics of water/dimethylsulfoxide mixtures using computer simulations. The results of these force field calculations, which agreed well with earlier neutron diffraction experiments (169)

showed that the number of water-water hydrogen bonds diminished with increasing DMSO concentration, signaling a disruption of water's hydrogen bond network beyond the range of nearest neighbors. DMSO also bonds with water more strongly than water bonds to water which is manifested by a longer average lifetime for water-DMSO hydrogen bonds than for water-water hydrogen bonds. The solvated DMSO is, on the average, bonded to two waters, and the average angle between the two hydrogen bonds in the $DMSO:2H_2O$ aggregate is nearly tetrahedral. Preliminary results in hydrogen bonding dynamics yielded lifetimes of hydrogen bonds in pure water and in a 1:2 DMSO:water mixture at 298 K as reported in Table 4-1.

Table 4-1: Hydrogen bond lifetimes, τ_{HB}, and the transition state theory estimate of that time, τ_{TST}, for water-water pairs in pure water, water-water pairs in the 1:2 DMSO:water mixture, and the water-DMSO pairs in the 1:2 DMSO:water mixture at 298 K in picoseconds (168)

	τ_{HB}/ps	τ_{TST}/ps
water-water pair in pure water	1.20 ± 0.08	0.20 ± 0.01
water-water pair in 1:2 DMSO:water mixture	3.3 ± 0.3	0.45 ± 0.03
water-DMSO pair in 1:2 DMSO:water mixture	4.8 ± 0.9	0.80 ± 0.06

4.1.5. Basic electron donors in hydrogen bond studies

Very few researchers have investigated water as the "acid" in hydrogen bonding studies with the electron donors of interest in this research: diphenylsulfone, diphenylsulfoxide, pyridine, and triphenylphosphine oxide. More commonly, the thermodynamics of hydrogen bonding of these bases have been determined using hydrogen donors such as phenol or aliphatic alcohols (170-172). A brief overview of hydrogen bonding studies using diphenylsulfone, diphenylsulfoxide, pyridine, and triphenylphosphine oxide as electron donors is reported here.

The most extensive studies of hydrogen bonding have included phosphorous containing molecules as electron donors, perhaps due to their biological importance. The family of phosphorylated molecules are generally good complexing ligands with a number of important uses and applications, and are particularly well known as extracting agents for metallic ions (173). However, over the years a number of researchers have evaluated the ability of many other oxygen- and nitrogen-containing bases to form strong hydrogen bonds with proton donating compounds. In the early 1960's, Joesten and Drago (174) and Aksnes and Gramstad (175) derived equilibrium constants for the complex formation between phenol and a variety of nitrogen and oxygen donors including phosphine oxide, pyridine, sulfone, and sulfoxide containing compounds. Values obtained in these studies are shown in Table 4-2. The researchers attempted to correlate Δv_{OH}, the shift of the OH stretch to lower frequencies upon complexation, with the calculated equilibrium constants at 25 °C. From this data Joesten and Drago (174) concluded that the spectral shifts in general cannot be accurately used to calculate equilibrium constants over a wide range of compounds. However, this relationship can be linear over narrow, chemically related groups of proton donors and acceptors (176).

Eyman and Drago (177) investigated the change in chemical shift as a function of donor strength by nuclear magnetic resonance spectroscopy. The goal of this research was to correlate data obtained in infrared spectroscopy methods with that acquired using NMR spectroscopy. It was shown that the hydrogen bond shift for phenol-base hydrogen bonding interactions having $-\Delta H$ from 3 to 10 kcal/mole was linearly related to Δv_{O-H} and δ_{obsd} except for donors in which large anisotropy effects are present. Eyman and Drago's data are included with the data of Joesten et al. and Aksnes et al. in Table 4-2. Eyman and Drago's enthalpy values obtained using NMR measurements showed slight discrepancies compared to the data obtained via IR spectroscopy. However, the relative hydrogen bonding strength of certain functional groups is clearly demonstrated. Bases forming weak hydrogen bonds with phenol (i.e. $-\Delta H$ of hydrogen bond formation is less than 5 kcal/mole) include acetone, acetonitrile, tetramethylene sulfone, and tetrahydrofuran. Bases forming moderate strength hydrogen bonds with phenol include trimethylphosphate, DMSO, NMP, and DMAc. Bases strongly hydrogen bonding to phenol include trimethylphosphine oxide, triphenylphosphine oxide, triethylamine, pyridine, and tetramethylene sulfoxide.

The functionalities of interest in this research may be approximately ranked by hydrogen bonding ability as: sulfone < sulfoxide < phosphine oxide ≤ pyridine. The observed shift is plotted as a function of negative change in enthalpy for select data from Table 4-2, as shown in Figure 4-4. However, while the sulfone, sulfoxide, and phosphine oxide-containing hydrogen bond adducts with phenol show a linear relationship between the chemical shift of the adduct proton and the $-\Delta H$ of adduct formation, the pyridine adduct does not fall into line with the other bases. The difference was proposed by Eyman and Drago (177) to be due to the large anisotropy of pyridine which shifted the hydrogen of phenol farther downfield than expected. This may be explained by the electronic structure

Table 4-2: Frequency shifts, chemical shifts, enthalpy values, and equilibrium constants for phenol:base 1:1 adducts (174-181)

Base	$\Delta \nu_{O-H}$ (cm^{-1})	δ_{obsd} (30°C)[c]	$-\Delta H$(kcal/mol)	K (25 °C)
CH_3CN	178[a]	6.62	3.2[a], 3.5[c]	5.0[a]
Ph_2CO	175[g]		4.40[g]	7.70[g]
$(CH_3)_2CO$	193[a]	7.87	3.3[a], 3.7[c]	13.5[a]
$(CH_3)_3PO$	464[a]	10.00	7.4[a], 8.1[c]	1480[a]
Et_3N	553[a]	10.45	9.2[a], 9.5[c]	89[a]
$(CH_3O)_3PO$	315[b]	8.35	5.3[b], 5.7[c]	182.9[b]
Ph_3PO	430[b]	10.10	6.7[b], 7.5[c]	1055[b]
C_5H_5N	465[b]	10.88	7.5[b], 8.1[c]	64.0[b]
$(CH_2)_4SO$	400[d]	8.93	7.0[c]	
$(CH_3)_2SO$	359[a]	8.90	6.4[c], 8.0[f]	230 (20 °C)[f]
NMP	341[e]	9.42	6.1[c]	
DMAc	345[a]	9.45	6.2[c]	
$(CH_2)_4O$	305[c]	8.05	5.5[c]	
$(CH2)_4SO_2$	181[a]	6.93	3.5[c]	
$(C_6H_5)_2SO$	294[f]		5.76[f]	70 (20 °C)[f]

a) M. D. Joesten and R. S. Drago, J. Am. Chem. Soc., 1962, 84, 3817
b) G. Aksnes and T. Gramstad, Acta. Chem. Scand., 1960, 14, 1485
c) D. P. Eyman and R. S. Drago, J. Am. Chem. Soc., 1966, 88(8), 1617
d) R. S. Drago, B. Wayland, and R. L. Carlson, J. Am. Chem. Soc., 1963, 85, 3125
e) J. H. Bright, R. S. Drago, D. M. Hart, and S. K. Madan, Inorg. Chem., 1965, 4, 18
f) T. Gramstad, Spectrochim. Acta, 1963, 19, 829
g) S. Singh, A. S. N. Murthy, and C. N. R. Rao, Trans. Faraday Soc., 1966, 62, 1056
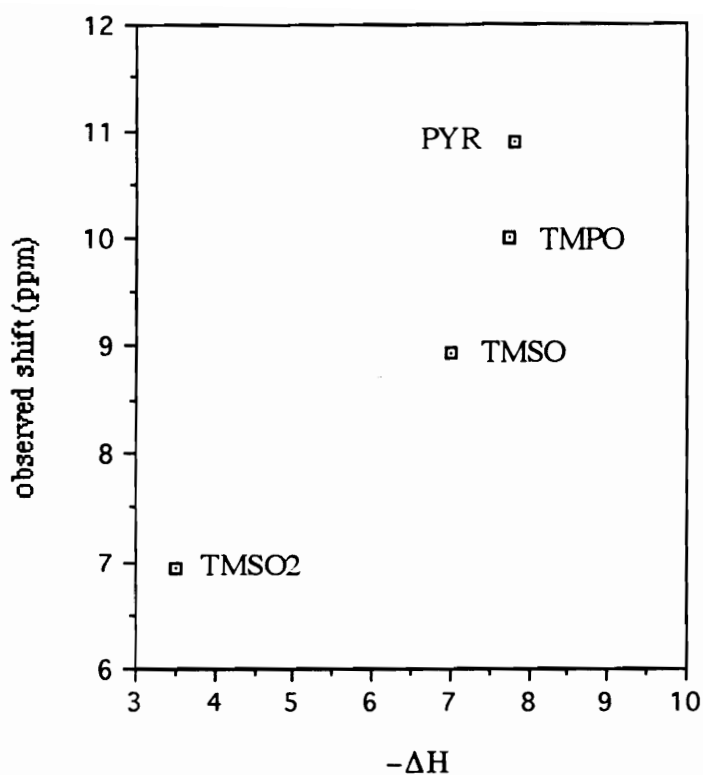
Figure 4-4: Observed shift of the acidic hydrogen in phenol:base complexes (downfield of TMS) as a function of enthalpy (kcal/mol) for tetramethylene sulfone, tetramethylene sulfoxide, trimethylphosphine oxide, and pyridine complexes (174, 175, 177)
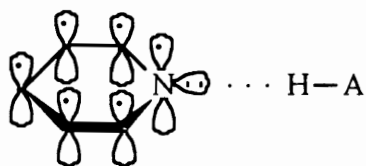
Figure 4-5: A schematic representation of π- and σ-bonds in pyridine showing the nonbonded pair of electrons in the sp^2 orbital involved in hydrogen bond formation

94

of pyridine which is shown in Figure 4-5. The nitrogen of the pyridine molecule is sp^2

hybridized; the sole p electron is incorporated into the aromatic π-structure while the

nonbonded pair of electrons on nitrogen are contained in an sp^2 atomic orbital.

Nuclear magnetic resonance spectroscopy was also employed by Hadzi and

Smerkolj to evaluate equilibrium constants of chloroacetic acids with oxygen bases in much

the same manner (182). The chemical shifts of the 1:1 acid:base adducts between

monochloroacetic acid and a variety of oxygen bases (downfield of TMS), as well

as the calculated equilibrium constants of complex formation are shown in Table 4-3. The

Table 4-3: Chemical shifts of complexes of monochloroacetic acid (MCA) and oxygen donors (downfield of TMS) and equilibrium constants of association for these complexes (182)

Base	adduct shift (ppm)	K (L/mol)
none (monomeric MCA)	6.94	-------
3,5-dichloropyridine	13.56	1.95×10^3
diphenylsulfoxide	12.27	6.24×10^3
dibenzylsulfoxide	12.55	9.93×10^3
triphenylphosphine oxide	13.51	3.78×10^4
trioctylphoshine oxide	14.16	7.03×10^4

monomer chemical shift of monochloroacetic acid was determined from the dilution curve

of the acid in carbon tetrachloride. The graphical representation of this data is shown in

Figure 4-6. It is interesting to note that once again the pyridine shows anomalous behavior

relative to other bases. In this research the relationship between the base strength and

chemical shift of the adducts is linear except for the 3,5-dichloropyridine:monochloroacetic acid complex. Hadzi proposed that this is due in part to the induced ring currents in the pyridine ring. This corroborates the results obtained for the complexation of pyridine with phenol wherein the pyridine showed anomalous behavior due to anisotropy (177). Furthermore, it is apparent that aliphatic bases hydrogen bond more strongly than their aromatic analogues. For example, dimethylsulfoxide (and dibenzylsulfoxide) accept hydrogen bonds more readily than diphenylsulfoxide (183) while trimethylphosphine oxide (and trioctylphosphine oxide) form hydrogen bonds more readily than triphenylphosphine oxide.
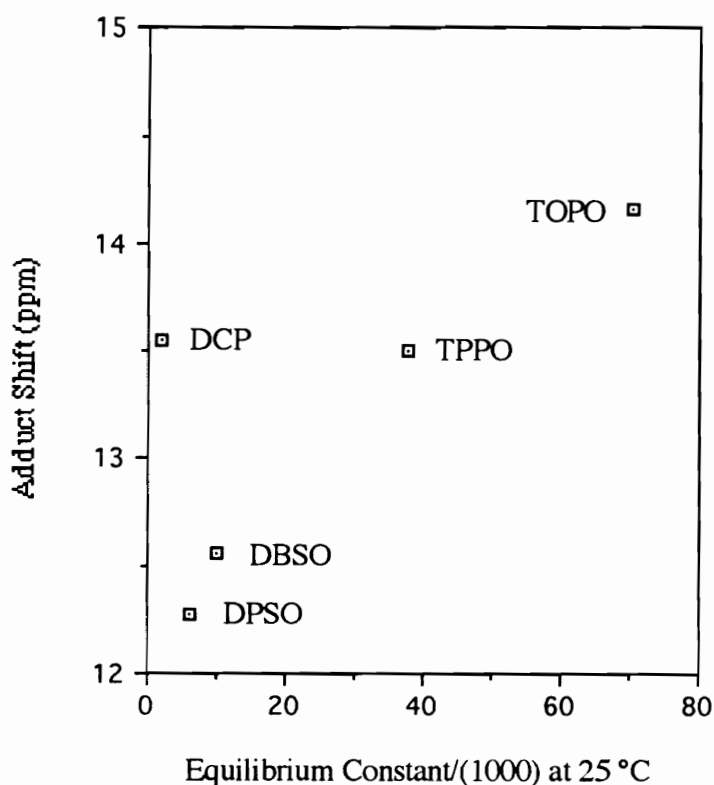
Figure 4-6: Shift of monochloroacetic acid:oxygen base 1:1 complex with respect to the equilibrium constant for the complex formation for the compounds diphenylsulfoxide, dibenzylsulfoxide, triphenylphosphine oxide, 3,5-dichloropyridine, and trioctylphosphine oxide (182)

The interest in hydrogen bonding ability of various oxygen and nitrogen donors has continued into current times. Kamlet et al. (184) have revolutionized the calculation of interaction parameters through development of three scales of solute or solvent properties. This method, which has been applied to a broad spectrum of compounds, involes a π^* scale of molecular dipolarity/polarizability, an α scale of molecular hydrogen bond acidities (ability to accept an electron pair in a solvent-solute or solute-solute hydrogen bond), and a β scale of hydrogen bond basicities (ability to donate an electron pair). These parameters may be used, in conjuction with experimental infrared spectral data, to predict large numbers of diverse physiochemical properties of solutes and solvents through linear solvation energy relationships.

Abraham et al. (185) have tabulated a large number of parameters of this type including π_2^H, the solute dipolarity/polarizability, and α_2^H and β_2^H, the effective solute hydrogen bonding acidity and basicity. Selected values, determined by Abraham et al. using gas chromatographic methods, are shown in Table 4-4. It is interesting to note that although quinoxaline has a much higher polarizability than pyridine, its ability to accept hydrogen bonds is not much greater (0.59 compared to 0.52). This is incongruent in the fact that quinoxaline has two nitrogen atoms available for hydrogen bonding whereas pyridine has only one. This may be partially explained by the fact that after quinoxaline forms one hydrogen bond, the entire structure becomes distorted as the molecule undergoes an electron density redistribution. The hydrogen bond forces the molecule to readjust bond lengths and bond angles within the quinoxaline plane and molecular symmetry is lost (186). The second hydrogen bond thus will not form as readily as the first.

The method of Kamlet et al. (184) developed to calculate solute interaction parameters may also be applied to a series of related compounds to evaluate contributions of different substituents to the overall hydrogen bonding ability of a molecule. Taft et al. (187) used this method to calculate hydrogen bond acceptor basicities for the family of

Table 4-4: Values for π_2^H (the solute dipolarity/polarizability), α_2^H (the effective solute hydrogen bonding acidity), and β_2^H (the effective solute hydrogen bonding basicity) (185)

solute	π_2^H	α_2^H	β_2^H
diphenylether	1.08	0.00	0.20
water	0.45	0.82	0.35
benzophenone	1.50	0.00	0.50
pyridine	0.84	0.00	0.52
quinoxaline	1.20	0.00	0.59
diphenylsulfone	2.15	0.00	0.70
dimethylsulfone	1.70	0.00	0.76
N,N-dimethylacetamide	1.33	0.00	0.78
dimethyl sulfoxide	1.74	0.00	0.88

XYZP=O phosphine oxide compounds. A multiple substituent parameter equation was derived using early infrared spectroscopy data for shifts of phenol stretches in phenol-base complexes to examine the structure-property relationships in this series of compounds (188-190). This mathematical expression, shown in Equation 4-6, calculates β (ability to donate an electron pair) values where σ_α is the substituent polarizability, σ_F is the substituent field effect, and σ_R is the substituent resonance effect. The calculated values correlated well with experimental spectral data. Furthermore, this correlation demonstrates that the field/inductive effects of substituents (σ_F values) play the major role in hydrogen

$$\beta = (0.84 \pm 0.02) - (0.08 \pm 0.01)\Sigma\sigma_\alpha - (0.46 \pm 0.01)\Sigma\sigma_F - (0.17 \pm 0.01)\Sigma\sigma_R \qquad (4\text{-}6)$$

bond accepting ability of the phosphine oxides. The substituent polarizability term (σ_α) indicates that the P=O dipole will induce a dipole in a polarizable substituent, thus increasing the value of β. Similarly, the resonance effect term (σ_R) demonstrates that since the P=O group is a π-electron acceptor, π-electron donor substituents increase the β value. However, steric twisting from coplanarity reduces π-electron donating ability of substituents and thus the σ_R values are not strictly additive with successive substitution. Taft et al. tabulated substituent parameters for a multitude of aliphatic, aromatic, and halogenic substituents possible in XYZP=O compounds; selected values are shown in Table 4-5.

Table 4-5: Substituent parameters used in calculation of hydrogen bond accepting abilties of XYZP=O compounds (187)

substituent	σ_α	σ_F	σ_R
H	0.00	0.00	0.00
CH_3	-0.35	0.00	-0.08
C_2H_5	-0.49	0.00	-0.07
n-C_4H_9	-0.57	0.00	-0.07
CH_3O	-0.17	0.25	-0.42
C_2H_5O	-0.23	0.25	-0.45
n-C_4H_9O	-0.27	0.25	-0.46
C_6H_5	-0.81	0.10	-0.22
C_6H_5O	-0.38	0.38	-0.32
F	0.13	0.44	-0.25
Cl	-0.43	0.45	-0.17

From Equation 4-6, hydrogen bonding abilities of various XYZP=O compounds may be approximated. The results of several calculations are shown in Table 4-6. Calculation shows that triphenylphosphine oxide is more basic than trimethylphosphine oxide, although experiments have shown that the opposite is true. This may be due to the fact that the resonance effect (σ_R) of the phenyl substituent is not strictly additive with subsequent substitution due to the steric twisting which results when bulky ligands are added to the phosphine oxide center and so the $\Sigma\sigma_R$ term is erroneously large in the calculation of β for $Ph_3P=O$.

Table 4-6: Hydrogen bonding abilities (β) for several phosphine oxide-containing bases calculated from the substituent polarizabilities σ_α, inductive effects σ_F, and resonance effects σ_R using Equation 4-6

compound	$\Sigma\sigma_\alpha$	$\Sigma\sigma_F$	$\Sigma\sigma_R$	β
$(CH_3)_3PO$	-1.05	0.00	-0.24	0.96
Ph_3PO	-2.43	0.30	-0.66	1.01
$(PhO)_3PO$	-1.14	1.14	-0.96	0.57
$Ph_2(CH_3)PO$	-1.97	0.2	-0.52	0.99
$PhCl_2PO$	-1.67	1.00	-0.56	0.61

4.1.6. Molecular modeling of triphenylphosphine oxide:acid adducts

The previous section of this report concerned itself with the thermodynamics of hydrogen bond formation between oxygen and nitrogen bases with acids. Interest in the actual geometrical structure of the acid:base adduct has also persisted; however, there is little data in the literature on the structures of acid:base adducts wherein pyridine-, sulfone-, and sulfoxide-containing compounds serve as bases. The structure of the phosphine oxide:acid adduct has generated the most interest over the years and thus a discussion of molecular modeling will be confined to the structure of the triphenylphosphine oxide:acid adduct.

Elucidation of the structure of the phosphine oxide:acid adduct has been pursued over several decades. In the 1960's the structure of the complex formed between triphenylphosphine oxide and pentafluorophenol in solution was hypothesized by Gramstad and Van Binst (191) to be either a hydrogen bonded complex of the sort P=O ·· H-O possessing partial charges on the atoms, or a proton transfer complex of structure P=OH ·· O equipped with full charges on the atoms. The first isolation of 1:1 adducts between phosphine oxide-containing bases and substituted peroxybenzoic acids was reported in the mid 1970's, when crystalline complexes between triphenylphosphine oxide and nitrated or chlorinated peroxybenzoic acids were obtained at subambient temperatures (192). Gramsted et al. pursued the structure of the triphenylphosphine oxide/pentafluorophenol complex first investigated in the 1960's, and recently published X-ray crystallographic data of a crystalline triphenylphosphine oxide/pentafluorophenol complex (193). This data verified the exact nature of the bond between the two components in the solid state. The structure elucidated by Gramstad et al. is shown in Figure 4-7 and some of the bond angles are tabulated in Table 4-7.
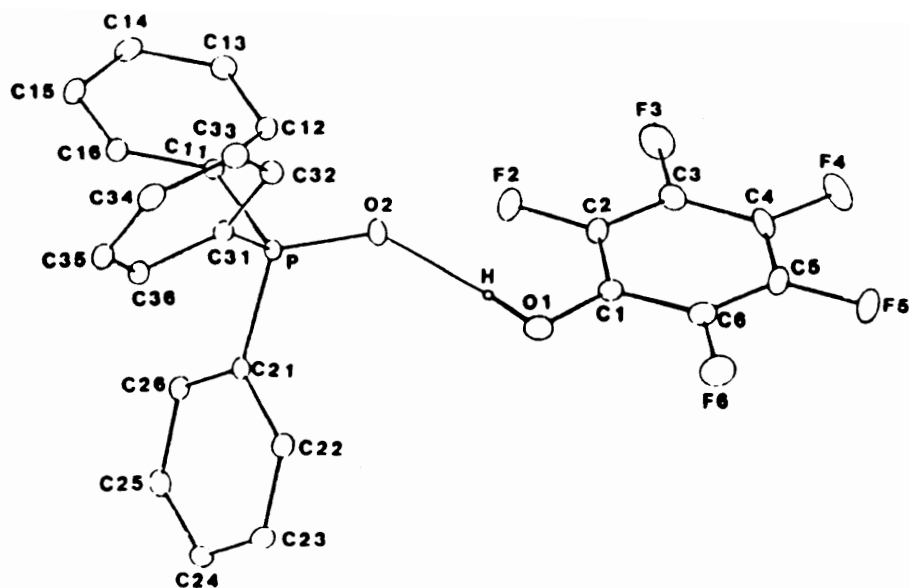
Figure 4-7: The hydrogen bonded complex between pentafluorophenol and triphenyl phosphine oxide (P, O2 and O1 are in the plane of the paper) (193)

The torsional angles between the phenyl rings of the hydrogen bonded triphenyl phosphine oxide/pentafluorophenol complex were found to be as follows: H-O1-C(phenyl) 24.1°; O2-P-C11(phenyl) 19.5 °; O2-P-C21(phenyl) 53.5 °; and O2-P-C31(phenyl) 24.0 °. In comparison, the nonhydrogen bonded orthorhombic triphenyl phosphine oxide possesses torsional angles of: 21.1, 59.3, and 24.1 in the solid state (194). This indicates that upon hydrogen bond formation, the propeller-like triphenylphosphine oxide adjusts to a slightly more planar configuration. Finally, the interatomic bond lengths of the hydrogen bonded atoms indicated that there was no proton transfer. The bond lengths were: O1-H (0.86 Å), H . . O2 (1.79 Å), and O1-O2 (2.645 Å).

Table 4-7: Bond angles in the hydrogen bonded complex between pentafluorophenol and triphenylphosphine oxide (193)

Atoms involved in bond	Bond angle (°)
O1-H··O2	174
C1-O1-H	112
O2-P-C11	111.5
O2-P-C21	112.9
O2-P-C31	111.4
C11-P-C21	107.1
C21-P-C31	105.8
C31-P-C11	107.9

4.2   Introduction to hydrogen bonding calculations

The basic premise of this research is that the ability of certain functional groups to hydrogen bond with hydroxyl groups may be ranked by ^{1}H nuclear magnetic resonance spectroscopy. Because polymer-polymer miscibility is governed by intermolecular interactions, comprehension of functional group hydrogen bonding ability will play a crucial role in the choice of blend modifiers for certain systems. Ultimately, the propensity of certain polymers (such as poly(arylene ether)s equipped with functionalities such as phosphine oxide, sulfone, sulfoxide, or pyridine) to hydrogen bond to the pendant secondary hydroxyl groups of epoxy networks will be investigated. However, the fundamental research concerning the hydrogen bonding of model compounds to water must be laid out first as the foundation to this project. Herein is described the fundamental research and analysis method used to evaluate the ability of functional groups such as phosphine oxide, sulfoxide, sulfone, and pyridine to hydrogen bond with water.

The organic compounds of interest are not water soluble; thus an aqueous/organic binary system was necessary to perform the solution ^{1}H NMR measurements. Deuterated dimethylsulfoxide was chosen as the organic component not only because of its ready availability but also because the model compounds are DMSO soluble. Use of a binary DMSO-d_6/water solvent system complicated the investigation because the hydrogen bonding molecular dynamics included not only water self association but also DMSO-water hydrogen bonds. These effects must first be accounted for before the hydrogen bonding between water and the model compound can be evaluated. A description of the problem follows.

When water and DMSO are combined in a solution, two different hydrogen bonding equilibria arise: a molecule of water can hydrogen bond either to another molecule

of water or to a molecule of DMSO as depicted in Figure 4-8. The equilibrium constants

for these equilibria will be referred to as K_o and K_n respectively. Furthermore, the shift of
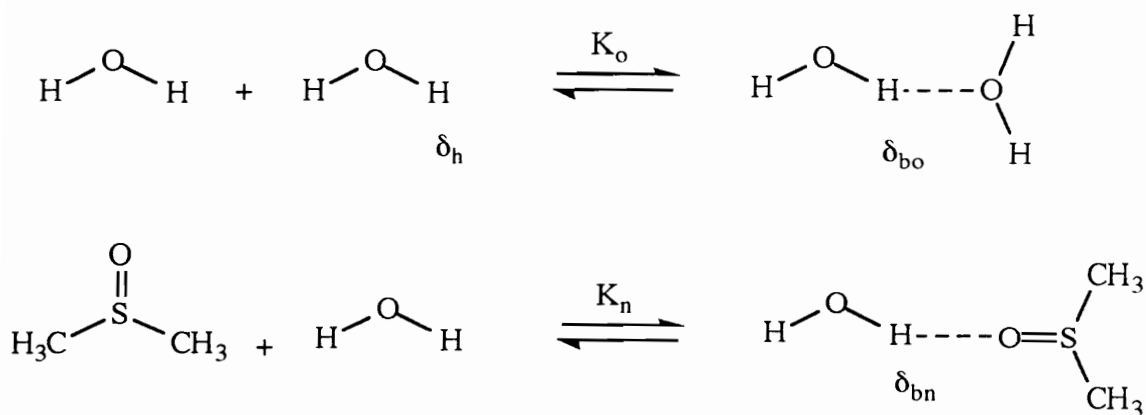
Figure 4-8: Possible hydrogen bonding equilibria present in a DMSO/water solution

the water peak in the NMR spectrum is due to the weighted average of three discrete types

of water protons: free water (the water hydrogen is not hydrogen bonded); a hydrogen that

is H-bonded to another molecule of water; and a hydrogen that is H-bonded to a molecule

of DMSO. The first two shifts, δ_h and δ_{bo}, were taken from the literature. The goal of this

calculation is to determine experimentally and mathematically the shift of the water H-

bonded to DMSO, δ_{bn}, and the equilibrium constants, K_o and K_n, for the hydrogen

bonded complex formation. These values may then be applied to the ternary

water/DMSO/model compound system for derivation of parameters associated with

interaction of water with the model compound.

Three equilibria are possible in the ternary DMSO-d6/water/model compound system: water H-bonding to water (equilibrium constant K_o); water H-bonding to DMSO-d6 (with equilibrium constant K_n); and water hydrogen bonding to the model compound (with equilibrium constant K_p). The three competing equilibria are shown in Figure 4-9. The chemical shift of the water proton in this ternary system would be a weighted average
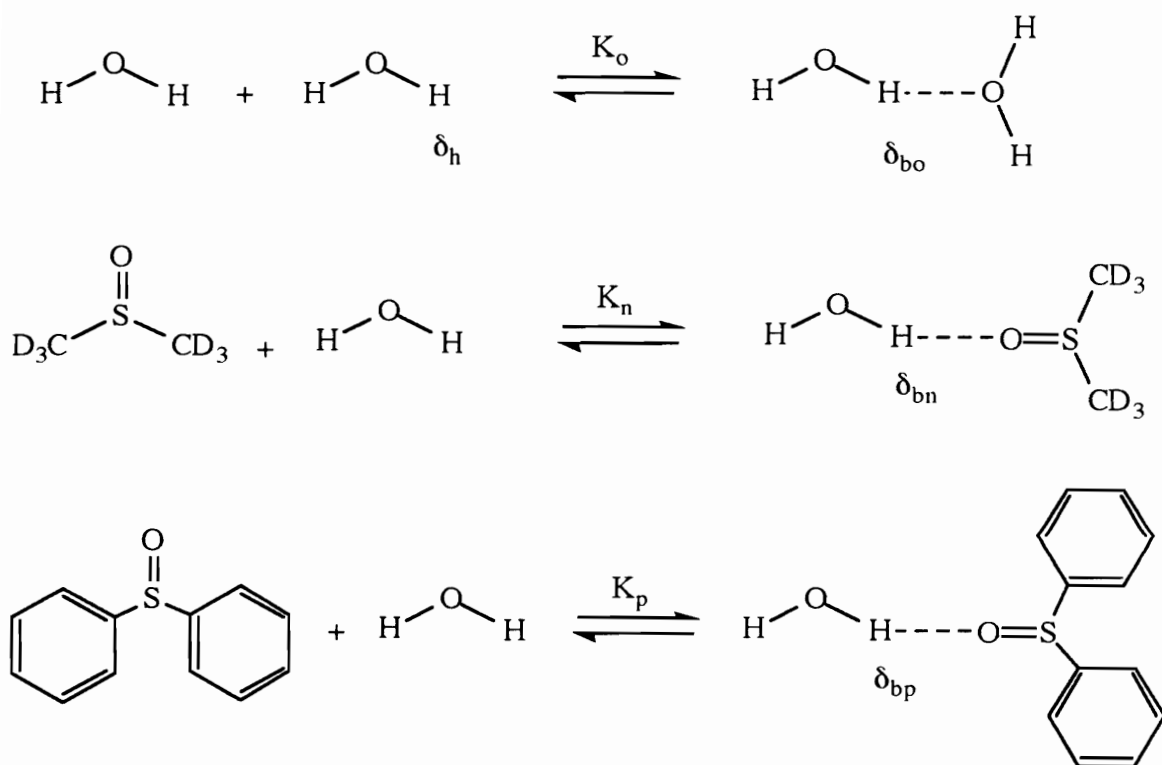
Figure 4-9: Three competing equilibria present in the water/DMSO-d6/model compound solution. Here the model compound is shown as diphenylsulfoxide.

of four different types of hydrogens: free hydrogen (δ_h); hydrogen H-bonded to water (δ_{bo}); hydrogen H-bonded to DMSO-d6 (δ_{bn}); and hydrogen H-bonded to the model compound (δ_{bp}). Thus the observed shift, δ, of the system would be:

$$\delta = \Sigma F_i \delta_i \qquad (4\text{-}7)$$

where F_i is the mole fraction of each particular kind of hydrogen and δ_i is the chemical shift of that specific species. The mole fractions values, F_i, may be expressed in terms of equilibrium constants and the original concentrations of the donors and acceptors. The shifts of the individual species, δ_i, may also be derived from experimental ^{1}H NMR spectra. The mathematical method for calculation of these unknown equilibrium constants and chemical shifts, K_o, K_n, δ_{bn}, K_p, and δ_{bp}, is taken from Lin's Ph.D. thesis (195). Lin derived and used this method to evaluate the hydrogen bonding between polyimide carbonyls and water in the water/NMP/polyimide ternary system. The enthalpy and entropy of hydrogen bond formation may be successively calculated using the equation:

$$\ln K = (-\Delta H/R)(1/T) + \Delta S/R \qquad (4\text{-}8)$$

by plotting the equilibrium constant of the complex formation as a function of reciprocal experimental temperature in Kelvin, where R is the gas constant. The slope and the intercept will give enthalpy and entropy respectively. Calculation of the enthalpy of hydrogen bond formation was not pursued in this research; all experimental spectra were obtained at one temperature.

Lin proposed the following simplifying assumptions for the calculation of equilibrium constants and chemical shifts (196):

1)   A hydrogen bond is formed between a proton donor and a proton acceptor site. Equilibrium of the hydrogen bonding is considered as that between the donor and the acceptor site.

2)   Only the change in chemical shift caused by hydrogen bonding is considered. The changes caused by the other factors such as van der Waal's interactions are neglected.

3)   Only the hydrogen bonding between water protons and oxygen atoms in DMSO-d_6 will be considered. Only hydrogen bonding between water protons and the model compound functional groups will be considered. Other hydrogen bonding may exist but will be ignored.

4)   In a X=O group (X = C, P, or S), there are two lone electron pairs and one π-bond orbital capable of forming hydrogen bonds with water protons. Their ability to hydrogen bond is averaged out, i. e., the ability of hydrogen bonding of each lone electron pair and the π-bond orbital is considered to be the same.

        The water/DMSO system shown in Figure 4-8 was first evaluated. Lin's equations (195) for the calculations of hydrogen bonding parameters are shown in this Introduction section. The application of these equations to achieve the parameters of interest, using spreadsheet logistics, is explained in the Experimental section.

4.2.1. Calculations for the water/DMSO-d_6 binary solutions

For the water/DMSO-d_6 solutions, the initial mole fraction of the proton donors and acceptors can be expressed as:

$$F^{\circ}_h = N^{\circ}_h/N^{\circ}_t \qquad (4\text{-}9)$$

$$F^{\circ}_o = X_o N^{\circ}_o/N^{\circ}_t \qquad (4\text{-}10)$$

$$F^{\circ}_n = X_n N^{\circ}_n/N^{\circ}_t \qquad (4\text{-}11)$$

where F°_h, F°_o, and F°_n are the initial mole fractions of water protons, proton acceptors of the water oxygen and DMSO oxygen respectively. N°_h, N°_o, and N°_n are the intial number of moles of water protons, water oxygen atoms, and DMSO carbonyl groups, respectively. X_o and X_n are the "functionalities" hydrogen bonding for the water oxygen and the DMSO oxygen, and N_t is the total moles of donors and acceptors. The functionality for the water oxygen, X_o, is taken as two, because each water oxygen possesses two lone pairs of electrons and can partake in two hydrogen bonds. The functionality of the DMSO oxygen, X_n, is three; each of the two lone pairs as well as the sulfur-oxygen π bond can partake in hydrogen bonding with water protons.

The total moles of donors and acceptors, N_t, can be calculated using the expression:

$$N^{\circ}_t = N^{\circ}_h + X_o N^{\circ}_o + X_n N^{\circ}_n \qquad (4\text{-}12)$$

taking into account water as both a donor and acceptor, and DMSO as hydrogen bond acceptor. The mole fractions of free water protons, F_h, and hydrogen bonded complexes, F_{bo} and F_{bn}, at equilibrium can be expressed as:

$$F_h = N_h / N^{\circ}{}_t \qquad (4\text{-}13)$$

$$F_{bo} = N_{bo} / N^{\circ}{}_t \qquad (4\text{-}14)$$

$$F_{bn} = N_{bn} / N^{\circ}{}_t \qquad (4\text{-}15)$$

where N_h, N_{bo}, and N_{bn} are the number of moles of free water protons, water protons hydrogen bonded to water, and water protons hydrogen bonded to DMSO respectively. Of course the initial number of hydrogens in the system, $F^{\circ}{}_h$, is related to the hydrogen bonded hydrogens by the expression:

$$F^{\circ}{}_h = F_h + F_{bo} + F_{bn} \qquad (4\text{-}16)$$

This expression may be rearranged to:

$$F_h = F^{\circ}{}_h - F_{bo} - F_{bn} \qquad (4\text{-}17)$$

and:

$$F_h = F^{\circ}{}_o - F_{bo} - F_{bn} \qquad (4\text{-}18)$$

because $F°_o$, the initial mole fraction of hydrogen bond acceptors on oxygen (i. e. two per water molecule), is equal to $F°_h$, the initial mole fraction of water protons (also two per water molecule).

The equilibrium constants may now be expressed in terms of concentrations as shown in Figure 4-10. Here F_n is the mole fraction of free DMSO proton acceptors, F_{bn} is the mole fraction of water hydrogen bonded to DMSO, and F_h is the mole fraction of free water protons.
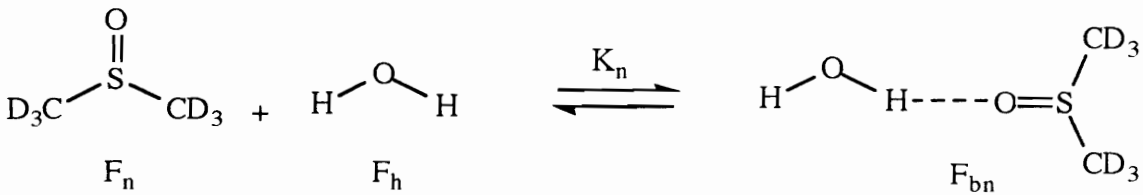
Figure 4-10: The equilibrium between water and DMSO-d_6

It follows that the mole fraction of free DMSO proton acceptors, F_n, is equal to:

$$F_n = F°_n - F_{bn} \qquad (4\text{-}19)$$

where $F°_n$ is the initial number of DMSO proton acceptors and F_{bn} is the number of complexed DMSO proton acceptors. The equilibrium constant for the reaction shown in Figure 4-10 is:

$$K_n = \frac{F_{bn}}{(F_h)(F_n)} \qquad (4\text{-}20)$$

which with substitution of previously derived expressions for F_h and F_n translates to:

$$K_n = \frac{F_{bn}}{(F^\circ_o - F_{bo} - F_{bn})(F^\circ_n - F_{bn})}$$

(4-21)

Similarly, for the water self association equilibrium shown in Figure 4-11:
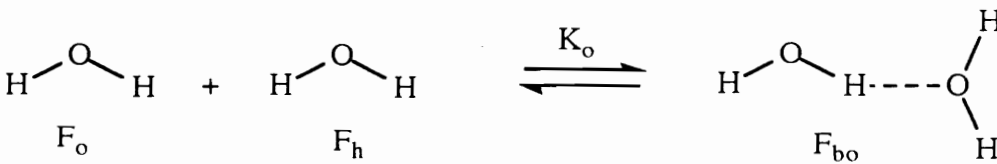
Figure 4-11: The self association equilibrium of water

the equation for K_o is determined to be:

$$K_o = \frac{F_{bo}}{(F_h)(F_o)}$$

(4-22)

or:

$$K_o = \frac{F_{bo}}{(F^\circ_o - F_{bo} - F_{bn})(F^\circ_o - F_{bo})}$$

(4-23)

Now the equilibrium constants and fractions of hydrogen bonded complexes are expressed in terms of original concentrations. When Equation 4-23 is solved for F_{bo}, as shown by Lin, the result is:

$$F_{bo} = \frac{K_o F^{\circ}_o F_{bn}}{K_n \left[F^{\circ}_n - F_{bn}\left(1 - \frac{K_o}{K_n}\right)\right]}$$

(4-24)

When Equation 4-21 is solved for F_{bn} a polynomial equation results. Using some simplifications, Lin utilized the quadratic equation to arrive at the expression for F_{bn} shown below:

$$A = 1 + \frac{F^{\circ}_o K_o}{F^{\circ}_n K_n}$$

(4-25)

$$B = \frac{1}{K_n} + F^{\circ}_n + F^{\circ}_o + F^{\circ}_o \left[\frac{K_o}{K_n}\right]$$

(4-26)

$$C = F^{\circ}_n F^{\circ}_o$$

(4-27)

Then:

$$F_{bn} = \frac{B - \sqrt{B^2 - 4AC}}{2A}$$

(4-28)

The calculated values can be applied to the equation for the observed chemical shift:

$$\delta = \Sigma F_i \delta_i \qquad (4\text{-}29)$$

or, more specifically:

$$\delta \;=\; \frac{F_h}{F^\circ_h}\,\delta_h \;+\; \frac{F_{bo}}{F^\circ_h}\,\delta_{bo} \;+\; \frac{F_{bn}}{F^\circ_h}\,\delta_{bn} \qquad (4\text{-}30)$$

This equation translates to (with $F^\circ_o = F^\circ_h$):

$$\delta \;=\; \frac{1}{F^\circ_o}\,[(F^\circ_o - F_{bo} - F_{bn})\delta_h + F_{bo}\delta_{bo} + F_{bn}\delta_{bn}] \qquad (4\text{-}31)$$

where δ_h, δ_{bo}, and δ_{bn} are the characteristic chemical shifts of the free water protons, water protons hydrogen bonded to water, and water protons hydrogen bonded to DMSO respectively. The δ_h and δ_{bo} values reported by Lin (197) are 0.37 ppm and 5.43 ppm respectively. The observed chemical shift, δ, is measured experimentally, F_{bo} and F_{bn} are known in terms of the equilibrium constants K_o and K_n as shown in Equations 4-24 and 4-28, and F°_o can be calculated using Equation 4-10. Using this equation, the desired equilibrium constants, K_o and K_n, as well as the chemical shift of the water proton that is hydrogen bonded to water, δ_{bn}, may be calculated. The method is explained in the Experimental section and involves systematic variation of the three unknown values (K_o, K_n, and δ_{bn}) with itierative calculations to find which set of three values produces a

chemical shift value closest to the chemical shift observed experimentally across a broad concentration range of DMSO-d_6/water solutions.

4.2.2. Calculations for the water/DMSO-d_6/model compound ternary solutions

The same methodology is used to analyze the ternary water/DMSO-d_6/model compound system with a few minor changes in the calculations. For the water/DMSO-d_6/model compound solutions, the initial mole fraction of the proton donors and acceptors can be expressed as:

$$F^\circ_h = N^\circ_h/N^\circ_t \qquad\qquad (4\text{-}32)$$

$$F^\circ_o = X_o N^\circ_o/N^\circ_t \qquad\qquad (4\text{-}33)$$

$$F^\circ_n = X_n N^\circ_n/N^\circ_t \qquad\qquad (4\text{-}34)$$

$$F^\circ_p = X_p N^\circ_p/N^\circ_t \qquad\qquad (4\text{-}35)$$

where F°_h, F°_o, F°_n, and F°_p are the initial mole fractions of water protons and proton acceptors of the water oxygen, the DMSO oxygen, and the model compound respectively, N°_h, N°_o, N°_n, and N°_p are the intial number of moles of water protons, water oxygens, DMSO carbonyl groups, and model compound functional groups, respectively. X_o, X_n, and X_p are the "functionalities" of hydrogen bonding for the water oxygen, the DMSO

115

oxygen, and the model compound functional group; N_t is the total moles of donors and acceptors. The functionality for the water oxygen, X_o, is taken as two, because each water oxygen possesses two lone pairs of electrons and can partake in two hydrogen bonds. The functionality of the DMSO oxygen, X_n, is three; each of the two lone pairs as well as the sulfur-oxygen π bond can partake in hydrogen bonding with water protons. For the model compounds, the functionalities were taken as: pyridine: 1; sulfone: 6; sulfoxide: 3; and phosphine oxide: 3.

The total moles of donors and acceptors, N_t, can be calculated using the expression:

$$N^\circ_t = N^\circ_h + X_o N^\circ_o + X_n N^\circ_n + X_p N^\circ_p \qquad (4\text{-}36)$$

taking into account water as both a donor and acceptor, DMSO as hydrogen bond acceptor, and the model compound as a hydrogen bond acceptor. The mole fractions of free water protons, F_h, and hydrogen bonded complexes, F_{bo}, F_{bn}, and F_{bp}, at equilibrium can be expressed as:

$$F_h = N_h/N^\circ_t \qquad (4\text{-}37)$$

$$F_{bo} = N_{bo}/N^\circ_t \qquad (4\text{-}38)$$

$$F_{bn} = N_{bn}/N^\circ_t \qquad (4\text{-}39)$$

$$F_{bp} = N_{bp}/N^\circ_t \qquad (4\text{-}40)$$

where N_h, N_{bo}, N_{bn}, and N_{bp} are the number of moles of free water protons, water protons hydrogen bonded to water, water protons hydrogen bonded to DMSO, and water

protons hydrogen bonded to the model compound, respectively. Of course the initial number of hydrogens in the system, F°_h, is related to the hydrogen bonded hydrogens by the expression:

$$F^{\circ}_h = F_h + F_{bo} + F_{bn} + F_{bp} \qquad (4\text{-}41)$$

This expression may be rearranged to:

$$F_h = F^{\circ}_h - F_{bo} - F_{bn} - F_{bp} \qquad (4\text{-}42)$$

and:

$$F_h = F^{\circ}_o - F_{bo} - F_{bn} - F_{bp} \qquad (4\text{-}43)$$

because F°_o, the initial mole fraction of hydrogen bond acceptors on oxygen (i. e. two per water molecule), is equal to F°_h, the initial mole fraction of water protons (also two per water molecule).

The calculation of the equilibrium constants for the formation of the water-water complex and the water-DMSO complex were shown in the previous section of the Introduction. Now the equilibrium constant for the formation of the complex between water and the model compound may also be expressed in terms of concentrations as shown in Figure 4-12. Diphenylsulfoxide is shown in this example, however, the same calculation will be applied to each of the model compounds. Here F_p is the mole fraction of free model compound proton acceptors, F_{bp} is the mole fraction of water hydrogen bonded to the model compound, and F_h is the mole fraction of free water protons.
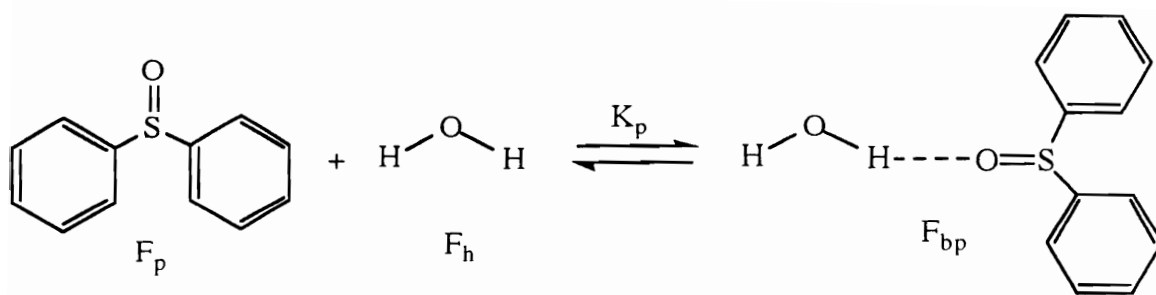
Figure 4-12: The equilibrium between water and diphenylsulfoxide

It follows that the mole fraction of free model compound proton acceptors, F_p, is equal to:

$$F_p = F^{\circ}_p - F_{bp} \qquad (4\text{-}44)$$

where F°_p is the initial number of model compound proton acceptors and F_{bp} is the number of complexed DMSO proton acceptors. The equilibrium constant for the above equation is:

$$K_p = \frac{F_{bp}}{F_h F_p} \qquad (4\text{-}45)$$

which with substitution of previously derived expressions for F_h and F_p translates to:

$$K_p = \frac{F_{bp}}{(F^{\circ}_o - F_{bo} - F_{bn} - F_{bp})(F^{\circ}_p - F_{bp})} \qquad (4\text{-}46)$$

The equilibrium constants for the water-water and water-DMSO-d_6 hydrogen bond formation in the ternary sytem, K_o and K_p, may be derived in a similar manner. They are merely expanded forms of Equations 4-23 and 4-21:

$$K_o = \frac{F_{bo}}{(F^{\circ}_o - F_{bo} - F_{bn} - F_{bp})(F^{\circ}_o - F_{bo})} \qquad (4\text{-}47)$$

$$K_n = \frac{F_{bn}}{(F^{\circ}_o - F_{bo} - F_{bn} - F_{bp})(F^{\circ}_n - F_{bn})} \qquad (4\text{-}48)$$

Equation 4-46 and Equation 4-47 are readily solved to obtain F_{bp} and F_{bo} as functions of equilibrium constants and original concentrations. The final solutions to the equations are shown below:

$$F_{bp} = \frac{K_p F^{\circ}_p F_{bn}}{K_n \left[F^{\circ}_n - F_{bn}\left(1 - \frac{K_p}{K_n}\right)\right]} \qquad (4\text{-}49)$$

$$F_{bo} = \frac{K_o F^{\circ}_o F_{bn}}{K_n \left[F^{\circ}_n - F_{bn}\left(1 - \frac{K_o}{K_n}\right)\right]} \qquad (4\text{-}50)$$

The relationship for F_{bn} is once again a second order polynomial which may be derived from Equation 4-48 (after some simplifying approximations) using the quadratic equation and the following values of A, B, and C:

$$A = 1 + \frac{F^\circ_o K_o}{F^\circ_n K_n} + \frac{F^\circ_p K_p}{F^\circ_n K_n} \qquad (4\text{-}51)$$

$$B = \frac{1}{K_n} + F^\circ_n + F^\circ_o + F^\circ_o\left[\frac{K_o}{K_n}\right] + F^\circ_p\left[\frac{K_p}{K_n}\right] \qquad (4\text{-}52)$$

$$C = F^\circ_n F^\circ_o \qquad (4\text{-}53)$$

then:

$$F_{bn} = \frac{B - \sqrt{B^2 - 4AC}}{2A} \qquad (4\text{-}54)$$

The calculated mole fraction values can be applied to the equation for the observed chemical shift:

$$\delta = \Sigma F_i \delta_i \qquad (4\text{-}55)$$

or, more specifically:

$$\delta = \frac{F_h}{F^\circ_h}\delta_h + \frac{F_{bo}}{F^\circ_h}\delta_{bo} + \frac{F_{bn}}{F^\circ_h}\delta_{bn} + \frac{F_{bp}}{F^\circ_h}\delta_{bp} \qquad (4\text{-}56)$$

This equation translates to (with $F^\circ_o = F^\circ_h$):

$$\delta = \frac{1}{F^\circ_o} \left[(F^\circ_o - F_{bo} - F_{bn})\delta_h + F_{bo}\delta_{bo} + F_{bn}\delta_{bn} + F_{bp}\delta_{bp} \right]$$

(4-57)

Here δ_h and δ_{bo} are literature values for the characteristic chemical shifts of the free water protons and water protons hydrogen bonded to water (197). The chemical shift of a water proton hydrogen bonded to DMSO-d_6, δ_{bn}, was calculated in the previous section, as were K_o and K_n, the equilibrium constants for the formation of the water-water complex and the water-DMSO complex. Knowledge of the equilibrium constants K_o and K_n permits the calculation of F_{bo} and F_{bn}. Thus the only unknowns in the above Equation 4-57 are F_{bp} and δ_{bp}, the mole fraction water hydrogens complexed to the model compound and the shift of the hydrogen that is hydrogen bonded to the model compound respectively. F_{bp} is known as a function of K_p, and thus a spreadsheet calculation is set up using systematically varying values in sets of K_p and δ_{bp} as explained in the Experimental section. The values of K_p and δ_{bp} that give a calculated δ value the most closely approximating the experimental δ value across a wide range of solution compositions are chosen as the true values.

4.3.   Experimental methods: determination of hydrogen bonding ability of electron rich

oxygen- and nitrogen-containing model compounds with water

4.3.1 Preparation of DMSO-d_6/water solutions for ^{1}H NMR evaluation

The interactions of DMSO-d_6 with water were first thoroughly evaluated prior to undertaking the study of ternary DMSO-d_6/water/model compound solutions. Eighteen water/DMSO-d_6 solutions were prepared with concentrations ranging from 0.01 mole fraction water in DMSO-d_6 to 0.73 mole fraction water in DMSO-d_6. The DMSO-d_6 (Aldrich Chemical Co., purchased as 99.5 % pure with no TMS reference) was vacuum distilled from calcium hydride to afford scrupulously anhydrous solvent for the dilutions and sample preparation. Distilled water was used to prepare the experimental solutions. Wilmad 508 pp NMR tubes with threaded necks were oven dried, and then sealed with a cap and septum and flame dried before use. The sealed tube was weighed, DMSO-d_6 was added via syringe, and the weight of the added DMSO-d_6 was determined. Water was thereafter added by syringe and the tube was reweighed. The weights of water and DMSO-d_6 in each tube were determined and the mole fractions of each were calculated. Tetramethylsilane (TMS) reference (0.1 mL) was added to each tube and ^{1}H nuclear magnetic resonance spectroscopy was performed on each sample using a Varian Unity 400 MHz NMR. Instrumental parameters used were: number of transients (nt) was 48, the temperature was 25 °C, and the pulse width was 1 μsec. The shift of the water peak in each sample was referenced to the TMS peak (which was set to 0 ppm).

4.3.2. Preparation of ternary DMSO-d$_6$/water/model compound systems for ^{1}H NMR evaluation

After establishing the parameters for the binary DMSO-d$_6$/water solution, ternary DMSO-d$_6$/water/model compound systems may be evaluated. The ternary NMR samples were prepared in much the same way as the binary DMSO-d$_6$/water samples. The DMSO-d$_6$ was vacuum distilled from calcium hydride to afford scrupulously anhydrous solvent for the sample preparation. The triphenylphosphine oxide was recrystallized from diethyl ether. The diphenylmethylphosphine oxide was recrystallized from ethanol/water (80/20). The diphenylsulfone and the diphenylsulfoxide were purchased from Aldrich Chemical Company and recrystallized from diethyl ether. All solid materials were dried in a vacuum oven to constant weight before use. The pyridine was purchased from Fisher Chemical Company and distilled from potassium hydroxide.

A stock solution of 3 weight percent distilled water in distilled DMSO-d$_6$ was prepared in a flame dried roundbottom flask sealed with a septum. In separate flamed dried roundbottom flasks, ternary solutions were prepared by dissolving each of the five model compounds in the 97/3 (w/w) DMSO-d$_6$/water solution to afford 15 weight percent solutions of model compounds in aqueous DMSO-d$_6$.

The series of seven NMR samples with varied concentrations of model compound in aqueous DMSO-d$_6$ was prepared in flame dried NMR tubes sealed with septa and screw caps for each of the five model compounds. The sealed NMR tube was weighed on the analytical balance, charged with the 15 weight percent solution of model compound in aqueous DMSO-d$_6$, and reweighed. Then a known weight of the 97/3 (w/w) DMSO-d$_6$/water stock solution was added to the NMR tube. TMS (0.1 mL) was added to each tube to complete the sample preparation. Weights of each of the components of the ternary system, model compound, DMSO-d$_6$, and water, were calculated and converted to mole

fractions for further calculations. ^{1}H NMR spectra were obtained on a Varian Unity NMR operating at 400 MHz with 48 transients, a pulse width of 1 μsec, and the temperature locked to 25 °C. The water peak was referenced to the TMS peak held at 0 ppm. Multiple runs of one sample were performed, with sample ejection, relocking, and reshimming between runs to evaluate reproducibility of the ^{1}H NMR results for a single sample solution. Among the five runs of one sample, only the thousandths place in the ppm value varied.

Molecular modeling calculations were performed on triphenylphosphine oxide and diphenylmethylphosphine oxide to determine the lowest energy conformation of each molecule. The semi-empirical AM1 minimization modeling was performed using Spartan modeling software developed by Wavefunction, Inc. on a Silicon Graphics Personal Iris computer.

4.3.3. Mathematical evaluation of ^{1}H NMR data from DMSO-d_6/water solutions

The raw data obtained from the ^{1}H NMR spectra included the shift of the water proton with respect to the concentration of water in the DMSO-d_6/water solutions and the shift of the water proton with respect to the concentration of model compound in the DMSO-d_6/water 97/3 solutions. This information was mathematically evaluated using the equations outlined in the Introduction section; equilibrium constants for the formation of hydrogen bonded complexes and shifts of the protons involved in these complexes were obtained. The logistics for the spreadsheet calculations were complicated and are thus explained in this Experimental section.

4.3.3.1.   Preparation of "tailored" data from the experimental data for the DMSO
            d_6/water solutions

The weights and moles of both water and DMSO-d_6 in each sample, as well as the
mole fraction of water in each sample and the experimental ^{1}H NMR data are shown in
Table 4-8. This raw data was used to determine how the shift of the water proton varied
with the mole fraction of water in the sample as shown in Figure 4-13.

Table 4-8: Raw data for the DMSO-d_6/water samples: content and mole fraction of water
in each sample and shift of the water proton by ^{1}H NMR spectroscopy at 25 °C

Sample No.	g DMSO-d_6	mmoles DMSO-d_6	mg H_2O	mmoles H_2O	X H_2O	δ H_2O (ppm)
1	1.1766	14.0	63.6	3.5	0.20	3.58
2	1.0486	12.5	58.0	3.2	0.21	3.59
3	0.8624	10.3	26.0	1.4	0.12	3.47
4	1.3261	15.8	7.3	0.4	0.03	3.35
5	0.8196	9.7	440.7	24.5	0.72	4.46
6	0.8089	9.6	35.0	1.9	0.17	3.53
7	0.8154	9.7	78.1	4.3	0.31	3.74
8	0.8217	9.8	158.9	8.8	0.47	4.01
9	1.034	12.3	38.4	2.1	0.15	3.50
10	0.6915	8.2	407.3	22.6	0.73	4.48
11	0.7298	8.7	308.2	17.1	0.66	4.35
12	1.4907	17.7	13.2	0.7	0.04	3.36
13	1.4798	17.6	12.3	0.7	0.04	3.37
14	1.9596	23.3	3.5	0.2	0.008	3.33
15	1.1569	13.8	53.4	3.0	0.18	3.56
16	1.0648	12.7	25.6	1.4	0.10	3.47
17	0.9695	11.5	242.8	13.5	0.539	4.12
18	1.1058	13.1	155.8	8.6	0.40	3.88
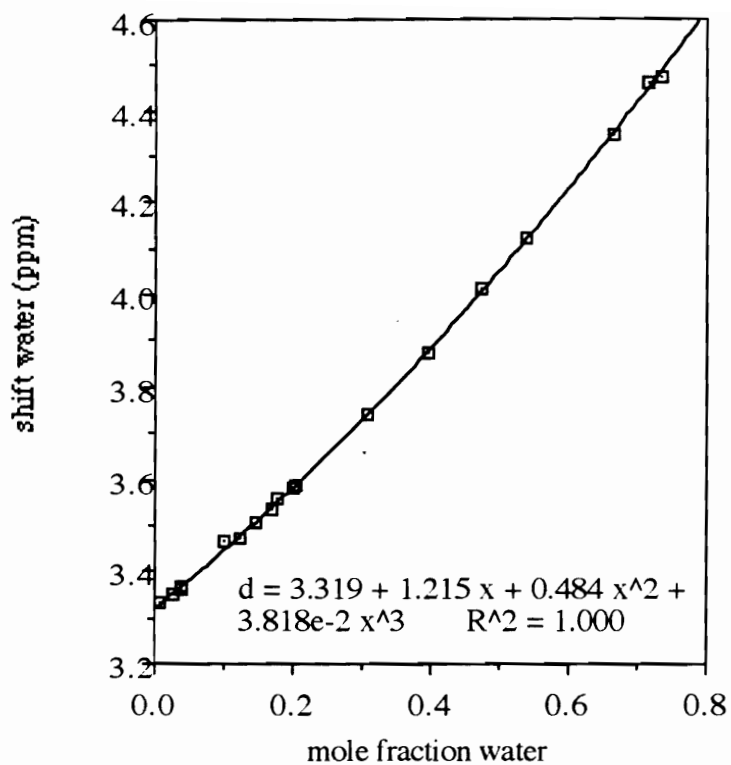
Figure 4-13: The chemical shift of water downfield from TMS with respect to the mole fraction of water in DMSO-d_6/water solutions at 25 °C

The equation for the curve shown in Figure 4-13 was determined to be:

$$\delta = 3.319 + 1.215\,(X_{H2O}) + 0.484(X_{H2O})^2 + 0.0381(X_{H2O})^3 \quad \text{with } R^2 = 1.0 \qquad (4\text{-}58)$$

where δ is the experimental shift of the water peak (in ppm) determined by ^{1}H NMR and X_{H2O} is the mole fraction of water in the DMSO-d_6/water solution. R^2 is the correlation coefficient of the mathematical equation to the experimental data points.

Equation 4-58 for the experimental data was used to prepare the "tailored" data shown in Table 4-9, where values for the moles of DMSO-d_6 were held constant at 0.01 moles and the mole fraction of water was varied from 0.1 to 0.7 in increments of 0.1. These values closely match the experimental values shown in Table 4-8 and thus the shift of the water proton was precisely calculated using Equation 4-58.

Table 4-9: "Tailored" data for the DMSO-d_6/water solutions: systematic variation of mole fraction water values to calculate the shift of water from Equation 4-58

mol DMSO-d_6	mol fracxn H_2O	calculated shift for H_2O (ppm)
0.01	0.00	3.319
0.01	0.10	3.445
0.01	0.20	3.582
0.01	0.30	3.728
0.01	0.40	3.885
0.01	0.50	4.052
0.01	0.60	4.230
0.01	0.70	4.420

The goal of the first part of the mathematical evaluation of the DMSO-d_6/water ^{1}H NMR data was to determine thermodynamic and spectroscopic parameters for these solutions. Thus the values in Table 4-9 were used to set up the calculations for the shift of

water that is hydrogen bonded to the DMSO (δ_{bn}) and equilibrium constants of two interactions: water H-bonded to water (K_o) and water H-bonded to DMSO (K_n). All spreadsheets were created on a MacIntosh IIsi using *Excel 4.0* (version 3) and a detailed description of spreadsheet formatting follows.

4.3.3.2.   Calculations of moles and mole fractions of hydrogen bonding donors and acceptors in the DMSO-d6/water solutions

The values from Table 4-9 were used to calculate other parameters for the DMSO-d6/water solutions. The results of these subsequent calculations are shown in Table 4-10 and a description of the calculations follows. The number of moles of water can be calculated from the values of moles DMSO-d6 and mole fraction water, knowing that the mole fraction of water is equal to the ratio of the moles water over the total moles:

$$X_{H2O} = \frac{\text{moles } H_2O}{(\text{moles } H_2O + \text{moles DMSO-d6})} \tag{4-59}$$

This equation can then be rearranged to determine the number of moles of water directly:

$$\text{moles } H_2O = \frac{(X_{H2O})(\text{moles DMSO-d6})}{1 - X_{H2O}} \tag{4-60}$$

These values obtained from Equation 4-60 were inserted into Table 4-10 (column 3) for use in subsequent calculations. A detailed description of the following calculations is

reported in Lin's thesis (195) and also outlined in the Introduction section of this thesis. The value of N°_t, the total number of moles of hydrogen bonding donors and acceptors, may be calculated using the expression:

$$N^{\circ}_t = N^{\circ}_h + X_o N^{\circ}_o + X_n N^{\circ}_n \qquad (4\text{-}12)$$

where N°_h is the total moles of hydrogen atoms in the solution (equal to two times the total moles of water), N°_o is the total moles of oxygen atoms (from water) in the solution (equal to the number of moles of water), and N°_n is the total moles of oxygen atoms (from DMSO-d_6) in the solution (equal to the number of moles of DMSO-d_6). The value of X_o, the functionality of the oxygen atom in water, is taken as 2. This assumes that each lone pair of the oxygen atom in water is equally able to act as a hydrogen bond acceptor. The functionality of the oxygen atom in DMSO-d_6, X_n, is taken as 3, because the p-p π bonding orbital in the sulfur-oxygen double bond can act as a hydrogen bond acceptor as well as each of the two lone pairs of electrons on the oxygen. The values for N°_t, calculated using Equation 4-12, were inserted into Table 4-10 (column 5).

Finally, the initial mole fractions of the hydrogen bonding donors and acceptors can be calculated, using the ratios:

$$F^{\circ}_h = N^{\circ}_h / N^{\circ}_t \qquad (4\text{-}9)$$

$$F^{\circ}_o = (X_o N^{\circ}_o)/N^{\circ}_t \qquad (4\text{-}10)$$

$$F^{\circ}_n = (X_n N^{\circ}_n)/N^{\circ}_t \qquad (4\text{-}11)$$

where F°_h is the initial mole fraction of hydrogen bond donor atoms in the solution, F°_o is the initial mole fraction of hydrogen bond acceptors (in water) in the solution, and F°_n is the initial mole fraction of hydrogen bond acceptors (in DMSO-d_6) in the solution. The calculated values for these mole fractions are also shown in Table 4-10 (columns 6-8). The parameters shown in Table 4-10 may be used to calculate the desired values: the equilibrium constant of the interaction of water hydrogen bonded to water (K_o), the equilibrium constant of the interaction of water hydrogen bonded to DMSO (K_n), and the shift of the water hydrogen bonded to DMSO (δ_{bn}). The methodology for this detailed iterative calculation follows.

Table 4-10: Calculated parameters for DMSO-d_6/water solutions including the total initial number of donors and acceptors ($N^{\circ}t$), the initial mole fraction of hydrogen bond donors in water (F°_h), and the initial mole fraction of hydrogen bond acceptors in water (F°_o) and in DMSO-d_6 (F°_n)

mole DMSO-d_6	X H_2O	mmole H_2O	δ H_2O (ppm)	$N^{\circ}t$	F°_h	F°_o	F°_n
0.01	0.00	0.0	3.319	0.030	0.000	0.000	1.000
0.01	0.10	1.1	3.445	0.034	0.065	0.065	0.871
0.01	0.20	2.5	3.582	0.040	0.125	0.125	0.750
0.01	0.30	4.3	3.728	0.047	0.182	0.182	0.636
0.01	0.40	6.7	3.885	0.057	0.235	0.235	0.529
0.01	0.50	10.0	4.052	0.070	0.286	0.286	0.429
0.01	0.60	15.0	4.230	0.090	0.333	0.333	0.333
0.01	0.70	23.3	4.420	0.123	0.378	0.378	0.243

4.3.3.3. Calculation of δ_{bn}, K_o, and K_n for the binary DMSO-d_6/water solutions

The calculation for the three unknowns, δ_{bn}, K_o, and K_n, is fairly complex and must be performed using a computer program. Here the data was compiled using an iterative approach with the MacIntosh spreadsheet program Excel 4.0. The spreadsheets for these calculation were set up as follows. A separate spreadsheet was created for each mole fraction of water in DMSO-d_6, so a total of seven spreadsheets was formed, one corresponding to each of $X_{H2O} = 0.1$, $X_{H2O} = 0.2$, $X_{H2O} = 0.3$, and so forth. Thus seven spreadsheets were required for the calculation of the parameters for the water/DMSO-d_6 solutions. A portion of one sample spreadsheet for the concentration $X_{H2O} = 0.1$ is shown in Table A-1.

The values K_n (equilibrium constant for the water-DMSO-d_6 hydrogen bond), K_o (equilibrium constant for the water-water hydrogen bond), and δ_{bn} (the shift of the water proton that is hydrogen bonded to DMSO-d_6) comprise the three unknowns. Each spreadsheet was developed to test 1000 different combinations of the three unknowns. To create 1000 different sets of the unknowns, the values were varied as follows (see Table A-1). A range of values of K_n was chosen (for example, from 39.8 to 66.8 in increments of 3 [note that the initial tests should have much wider value ranges for each of the paramters K_n, K_o, and δ_{bn}, so that the true value will lie somewhere within the chosen range!]). The first 100 rows of the K_n column of the spreadsheet contained the value 39.8, the next 100 rows of this column contained the value 42.8, the next 100 rows of K_n column contained the value 45.8, and so on until the 1000 cells in the K_n column were filled. Next a range of values for K_o was chosen (for example, from 29.5 to 56.5 in increments of 3). The first 10 rows of the column for K_o would read 29.5, 32.5, 35.5, 38.5, 41.5, 44.5, 47.5, 50.5, 53.5, 56.5. This pattern was repeated 99 more times to fill the 1000 cells in the K_o

column. To fill the δ_{bn} column, chosen values were varied in groups of ten. For example, the first ten rows of the δ_{bn} column was assigned the value 3.33, the next ten rows the value 3.34, the next ten rows the value 3.35, increasing the δ_{bn} value by 0.01 ppm every ten rows until the first one hundred rows of the δ_{bn} column were filled. Then the values in the first one hundred rows were copied into the remaining 900 rows to complete the δ_{bn} column. The spreadsheet was thus set up with 1000 unique sets of the three unknown values. This format is demonstrated in Table A-1, which is 1/8 of the spreadsheet corresponding to the mole fraction 0.1 of water in DMSO-d_6. The same set of K_n, K_o, and δ_{bn} values was used for each of the seven spreadsheets (each spreadsheet corresponded to a different mole fraction of water in the DMSO/water solution: 0.1, 0.2, 0.3, 0.4, 0.5, 0.6, and 0.7).

The next two columns of Table A-1 are F°_o and F°_n, calculated as shown previously (Equations 4-10 and 4-11 and Table 4-10). These numerical values were input into the spreadsheet directly. All subsequent values shown in the spreadsheet (Table A-1) were calculated within the format of the spreadsheet by inserting the equation into the appropriate column and copying 1000 times so it existed in each row. This was the method used to calculate the values A, B, and C, which are subsequently used in the calculation of F_{bn}, the mole fraction of hydrogen bonding acceptors in DMSO. The equation for the calculation of F_{bo}, the mole fraction of hydrogen bonding acceptors in water, was also placed directly into the spreadsheet and copied down the 1000 rows, so as the K_o and K_n values varied down the spreadsheet, so did the calculated value of F_{bo}. The detailed derivation of these equations was explained previously by Lin (195) and is also discussed in the Introduction section of this thesis. The equations for A, B, and C were inserted into the spreadsheet and copied down the 1000 rows. The equations are as follows:

$$A = 1 + \frac{F^\circ_o K_o}{F^\circ_n K_n}$$

(4-25)

$$B = \frac{1}{K_n} + F^\circ_n + F^\circ_o + F^\circ_o \left[\frac{K_o}{K_n} \right]$$

(4-26)

$$C = F^\circ_n F^\circ_o$$

(4-27)

As the values input for K_o and K_n varied down the spreadsheet, the results for A, B, and C also varied, as shown in Table A-1. The values for F_{bn} also varied down the spreadsheet, because F_{bn} is linked to the A, B, and C values through:

$$F_{bn} = \frac{B - \sqrt{B^2 - 4AC}}{2A}$$

(4-28)

Note that the positive route of the quadratic equation gave unreasonable results so only the negative route was used to calculate F_{bn} values. F_{bo} was also systematically calculated for each of the 1000 sets of values in the spreadsheet. F_{bo} is calculated using the expression:

$$F_{bo} = \frac{K_o F^\circ_o F_{bn}}{K_n \left[F^\circ_n - F_{bn} \left(1 - \frac{K_o}{K_n} \right) \right]}$$

(4-24)

which was directly put into the spreadsheet. The expression for the theoretical shift, δ_{th}, was also placed in the spreadsheet:

$$\delta_{th} = \frac{1}{F^{\circ}_{o}} \left[(F^{\circ}_{o} - F_{bo} - F_{bn})\delta_h + F_{bo}\delta_{bo} + F_{bn}\delta_{bn} \right] \qquad (4\text{-}31)$$

Here δ_h is the shift of the proton of water when it is "free" or not hydrogen bonded to any other species in the solution and δ_{bo} is the shift of the proton of water when it is hydrogen bonded to another molecule of water. A range of literature values for δ_h and δ_{bo} have been reported (154). Here the values used were 0.37 ppm and 5.43 ppm respectively. Upon performing the spreadsheet calculation, 1000 different values for δ_{th} resulted, each corresponding to a different set of the systematically varied K_o, K_n, and δ_{bn} values. Each calculated δ_{th} value was compared to the experimental δ value across all concentrations, as discussed in the section below.

4.3.3.4. Calculation of the "norm" value

The theoretical shift, δ_{th}, was compared to the experimental shift of the DMSO-d_6/water solution for each of the seven mole fractions of water used. The 1000 theoretical shift values of each of the seven spreadsheets were copied into an eighth spreadsheet, Table A-2, to calculate the "norm" value (the amount that the theoretical value deviated from the experimental value across the entire sample composition range). The norm was calculated using the equation:

$$\text{norm} = [\ \Sigma(\delta_{th} - \delta)^2\ ]^{1/2} \tag{4-61}$$

The spreadsheet was then sorted with respect to norm values and inspected to find which values of K_n, K_o, and δ_{bn} yielded the lowest norm values. The values of K_n, K_o, and δ_{bn} corresponding to the lowest norm values were considered to be the best fit combination of the three unknowns. New, narrower value ranges were constructed around these best fit values and applied to the set of seven spreadsheets (each corresponding to a different mole fraction of water in DMSO-d_6) to again calculate theoretical norm values. This reiterative process was continued to find the set of the three values, K_n, K_o, and δ_{bn} which gave the closest theoretical shift values relative to the experimental values across all mole fractions of water in DMSO-d_6. After 45 iterations of this calculation, the norm value for the binary DMSO-d_6/water system was reduced to 0.0092. This was the lowest norm obtained; the best fit parameters corresponding to this norm value were: $K_n = 52$, $K_o = 48$, and $\delta_{bn} = 3.38$ ppm.

4.3.3.5.   Error analysis of the binary DMSO-d_6/water solution calculations

4.3.3.5a.   Error inherent in the mathematical calculation

Literature values for δ_h range from 0.30 to 0.43 ppm and values for δ_{bo} range from 5.43 to 5.57. In the calculations performed here to yield the constants K_o, K_n, and δ_{bn}, δ_h was held constant at 0.37 ppm while δ_{bo} was held constant 5.43 ppm. To calculate the error inherent in the calculation of K_n, K_o, and δ_{bn} for the DMSO-d_6/water solutions,

the extremes of each range of values were input into the equations while holding the δ_{bn} value constant.

4.3.3.5b.   Error inherent in the experimental values

The ^{1}H NMR spectrometer used to evaluate the shift of water in the DMSO-d_6/water solutions was accurate to 0.01 ppm while the analytical balance used to measure quantities of DMSO-d_6 and water in the sample solutions was accurate to 0.001 g. First, the effect of a 0.001 g error on the mole fraction of water in the solution was evaluated by adding 0.001 g to each of the experimental weight values in Table 4-8 (columns 2 and 4). The maximum change in mole fraction of water was calculated to be 0.004. The mole fraction water values obtained in this manner were input into equation 4-58 to calculate the observed shift when assuming a weighing error of 0.001 g. The maximum change in the chemical shift value was found to be 0.01 ppm. This value was added to the spectrometer error of 0.01 ppm to yield a maximum chemical shift error of 0.02 ppm. The effect of a 0.001 g weighing error also changed F°_{o} and F°_{n} values (calculated from Equations 4-10 and 4-11) a maximum value of 0.002.

To determine the effect of the weighing and spectrometer error on the calculated values of K_o, K_n, and δ_{bn}, the values for F°_{o}, F°_{n}, and observed shift in the spreadsheet tables were changed by + 0.002, + 0.002, and + 0.02 respectively (in each of the seven spreadsheets representing each of the mole fractions of DMSO-d_6/water). The iterative calculations were repeated by varying K_o, K_n, and δ_{bn} values to minimize the norm value.

4.3.4. Ternary H-bonding systems

4.3.4.1. The structure of the hydrogen bond accepting model compounds

After calculation of the equilibrium constants for the formation of water-water and water-DMSO-d_6 complexes, a third species (another hydrogen bond acceptor) may be added to the solution. This introduces two new variables, the equilibrium constant for the formation of the new water-acceptor complex, as well as the shift of the water hydrogen that is hydrogen bonded to this acceptor. Calculation of these new parameters may be performed in much the same manner as previously discussed.

The structures of the hydrogen bond accepting model compounds are depicted in Figure 4-14. Note that all of these compounds have lone electron pairs able to accept hydrogen bonds. The experimental ^{1}H NMR data obtained for the water/DMSO-d_6/diphenylsulfoxide solutions is shown in Figure 4-15.
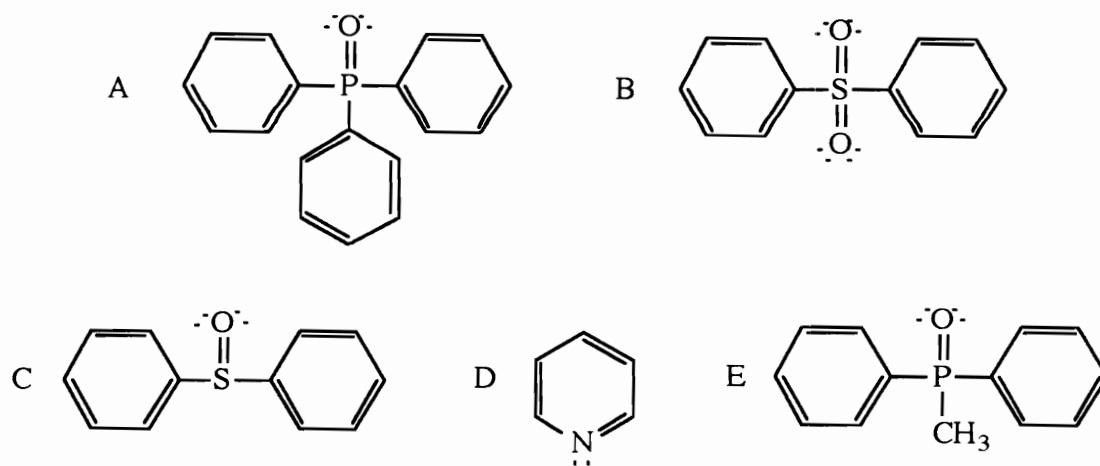
Figure 4-14: The hydrogen bond accepting model compounds used in NMR studies: (A) triphenylphosphine oxide; (B) diphenylsulfone; (C) diphenylsulfoxide; (D) pyridine; and (E) diphenylmethylphosphine oxide
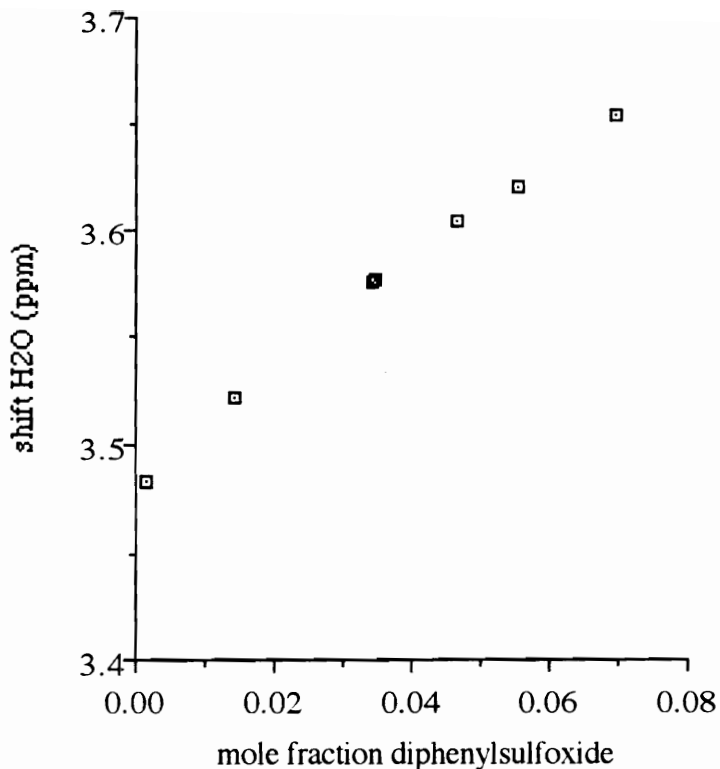
Figure 4-15: Experimental ^{1}H NMR data for the diphenylsulfoxide/DMSO-d6/water solutions: chemical shift of the water proton (downfield from TMS) as a function of mole fraction diphenylsulfoxide in 97/3 DMSO-d6/H2O at 25 °C

4.3.4.2.   Spreadsheet calculations of moles and mole fractions of H-bond donors and acceptors in the ternary system

The following calculations were performed using Excel version 4.0 on a MacIntosh IIsi. The total number of moles of hydrogen bonding donors and acceptors was calculated using the equation:

138

$$N°_t = N°_h + X_o N°_o + X_n N°_n + X_p N°_p \qquad (4\text{-}36)$$

This equation is a variation of Equation 4-12, with the minor addition of the product of $N°_p$, (the total moles of model compound in the solution) and X_p (the functionality of the model compound). Functionalities varied among the model compounds. The functionality values used in the calculations were: $X_p = 3$ for phosphine oxide and sulfoxide, $X_p = 6$ for sulfone, and $X_p = 1$ for pyridine. In each case the functionality was determined by the number of lone pairs possessed by each hydrogen bond accepting group plus the number of π bonds available for H-bonding. The resulting $N°_t$ values are shown in Table 4-11.

The initial mole fractions of the hydrogen bonding donors and acceptors are:

$$F°_h = N°_h/N°_t \qquad (4\text{-}32)$$

$$F°_o = (X_o N°_o)/N°_t \qquad (4\text{-}33)$$

$$F°_n = (X_n N°_n)/N°_t \qquad (4\text{-}34)$$

$$F°_p = (X_p N°_p)/N°_t \qquad (4\text{-}35)$$

The first three equations were explained earlier. Equation (4-35) shows the calculation of $F°_p$, the initial mole fraction of hydrogen bond acceptors (on the model compound) in the

solution, where X_p is the functionality of the model compound being evaluated and N°_p is the initial number of moles of model compound functional groups (in all cases equal to the number of moles of model compound). The initial mole fractions of hydrogen bond donors and acceptors are shown in Table 4-11 as calculated for the diphenylsulfoxide/DMSO-d_6/water solutions. These values may now be used to calculate the desired values: the shift of water hydrogen bonded to the model compound (δ_{bp}) and the equilibrium constant of the interaction of water hydrogen to the model compound (K_p).

Table 4-11: Calculated mole fraction data for hydrogen bond donors and acceptors in diphenylsulfoxide/water/DMSO-d_6 solutions across the experimental composition range

mol fraction DPSO	δ H_2O	N°_t	F°_h	F°_o	F°_n	F°_p
0.0696	3.65	0.0331	0.0766	0.0766	0.7799	0.0669
0.0466	3.60	0.0374	0.0784	0.0784	0.7983	0.0448
0.0141	3.52	0.0416	0.0810	0.0810	0.8245	0.0135
0.0346	3.58	0.0389	0.0794	0.0794	0.8080	0.0332
0.0014	3.48	0.0383	0.0820	0.0820	0.8347	0.0013
0.0554	3.62	0.0309	0.0777	0.0777	0.7913	0.0532
0.0344	3.58	0.0358	0.0794	0.0794	0.8082	0.0330

4.3.4.3.   Calculations of δ_{bp} and K_p for the DMSO-d_6/water/model compound ternary solutions

Two unknowns may be calculated from the experimental ^1H NMR data of the ternary water/DMSO-d_6/model compound solutions: the shift of the water hydrogen

bonded to the model compound (δ_{bp}) and the equilibrium constant of the hydrogen bonding interaction between water and the model compound, K_p. The same systematic approach is used to perform these calculations using an interative process with the MacIntosh spreadsheet Excel 4.0. Seven spreadsheets are necessary for each model compound because ^{1}H NMR data was collected at seven different sample concentrations. A sample spreadsheet is shown in Table A-3, which shows data and calculations for a sample consisting of 0.035 mole fraction diphenylsulfoxide in 97/3 DMSO-d_6/water.

The calculations for the ternary solutions were less complex than calculations for the binary DMSO-d_6/water systems. This time there were only two unknowns in each solution so only 100 unique combinations of the two unknowns were necessary for each iterative calculation. The spreadsheets for the model compounds were thus one tenth of the size of the spreadsheets used to calculate the parameters for the DMSO-d_6/water binary system. The discrete sets of the unknown values were formulated and input into the spreadsheet by the same system used in the preparation of the DMSO-d_6/water spreadsheets.

The following equations were copied into the spreadsheet in the appropriate columns. To calculate the value of F_{bn}, the mole fraction of water bound to DMSO-d_6 molecules, once again the quadratic formula was used. The equations for the A, B, and C, shown here in the expanded form required in the ternary system, were copied into the spreadsheets. The equation for F_{bn} was also copied into the spreadsheet. As the input values of K_p were varied over the course of the iterative calculations, the computed values for A, B, and C, and subsequently F_{bn}, varied. The equations were placed in the spreadsheet as follows:

$$A = 1 + \frac{F^\circ_o K_o}{F^\circ_n K_n} + \frac{F^\circ_p K_p}{F^\circ_n K_n} \tag{4-51}$$

$$B = \frac{1}{K_n} + F^\circ_n + F^\circ_o + F^\circ_o \left[\frac{K_o}{K_n} \right] + F^\circ_p \left[\frac{K_p}{K_n} \right] \tag{4-52}$$

$$C = F^\circ_n F^\circ_o \tag{4-53}$$

and:

$$F_{bn} = \frac{B - \sqrt{B^2 - 4AC}}{2A} \tag{4-54}$$

The equations for F_{bo}, the mole fraction of hydrogen bonding acceptors in water, and F_{bp}, the mole fraction of hydrogen bonding acceptors in the model compound, were also placed in the spreadsheet:

$$F_{bo} = \frac{K_o F^\circ_o F_{bn}}{K_n \left[F^\circ_n - F_{bn} \left(1 - \frac{K_o}{K_n} \right) \right]} \tag{4-50}$$

142

$$F_{bp} = \cfrac{K_p F^\circ_p F_{bn}}{K_n \left[F^\circ_n - F_{bn}\left(1 - \cfrac{K_p}{K_n}\right)\right]}$$

(4-49)

Finally, the theoretical shift, δ_{th}, was calculated from the equation:

$$\delta_{th} = \frac{1}{F^\circ_o} \left[(F^\circ_o - F_{bo} - F_{bn})\delta_h + F_{bo}\delta_{bo} + F_{bn}\delta_{bn} + F_{bp}\delta_{bp} \right]$$

(4-57)

δ_{bn} (the shift of water H-bonded to DMSO) was calculated here to be 3.38 ppm, δ_h and δ_{bo} are literature values, and the unknown δ_{bp} is the shift of the proton of water when it is hydrogen bonded to a molecule of the model compound. δ_{th} changes with each set of δ_{bp} and K_p values input into the program and its deviation from the experimental value (across the entire concentration range) is evaluated using the norm function (Equation 4-61) as explained in the previous section. For example, after 37 iterations of the diphenylsulfoxide/DMSO-d_6/water data, the lowest norm value obtained was 0.0095 which corresponded to values of δ_{bp} of 5.13 ppm with a K_p of 107.6.

4.3.4.4.   Error analysis for the model compound ternary system calculations

4.3.4.4a.   Error inherent in the mathematical calculation

Error analysis was performed on the mathematical calculations by inputting both the minimum and maximum values for δ_h and δ_{bo} into the calculation for the equilibrium constant K_p and shift δ_{bp}. From fitting calculations, Lin found that the optimum values for

δ_h and δ_{bo} were 0.37 ppm and 5.43 ppm respectively. Literature values range from 0.30 to 0.43 ppm for δ_h and 5.43 to 5.57 ppm for δ_{bo}. Using the method devised by Lin, error in the calculations here was ascertained by replacing the values of 0.37 ppm and 5.43 ppm with the values of 0.43 ppm and 5.57 ppm while holding δ_{bp} constant and repeating the spreadsheet calculations to determine the best fit values of K_p for each of the model compounds.

4.3.4.4b.   Error inherent in the experimental values

First, the error inherent in locking and shimming the ^{1}H NMR spectrometer was determined by inserting one sample five times with relocking and reshimming each time before measuring the chemical shift of water in the DMSO-d_6/model compound/water solution. The measured chemical shift value for water (in ppm) varied only in the thousandths place each time so locking and shimming was not a source of experimental error.

Experimental error arose from weighing the sample quantities and from ^{1}H NMR field drift. The ^{1}H NMR spectrometer used to evaluate the shift of water in the DMSO-d_6/water solutions was assumed to be accurate to 0.01 ppm while the analytical balance used to measure quantities of DMSO-d_6 and water in the sample solutions was assumed accurate to 0.001 g. The effect of a 0.001 g error on the mole fraction of model compound in the solution was evaluated by adding 0.001 g to each of the experimental weight values. The maximum change in mole fraction of model corresponded to an error in the chemical shift value of 0.01 ppm. This value was added to the spectrometer error of 0.01 ppm to yield a maximum chemical shift error of 0.02 ppm. The value 0.02 ppm was added to the observed chemical shift values across the entire concentration range. The effect of a 0.001 g weighing error also changed F°_o, F°_n, and F°_p values (calculated from Equations 4-33, 4-

34, and 4-35) a maximum value of 0.0002, 0.0004, and 0.0001 respectively. The values for F°_{o}, F°_{n}, and F°_{p} were changed in the model compound spreadsheets across the entire concentration range. Other equations were changed as a result of the experimental error inherent in the DMSO-d_6/water experiment. The previously calculated experimental errors for K_o, K_n, and δ_{bn} were found to be $\pm$ 6.5, $\pm$ 6.2, and $\pm$ 0.01 respectively. The maximum experimental values of K_o = 54, K_n = 58, and δ_{bn} = 3.9 were input into equations in the spreadsheet for the calculation of "A" (Equation 4-51), "B" (Equation 4-52), F_{bo} (Equation 4-50), F_{bp} (Equation 4-49), and δ (Equation 4-57). The iterative calculations were repeated by varying K_p and δ_{bp} values to minimize the norm value across the entire concentration range of model compound/DMSO-d_6/water solutions for each of the model compounds.

4.4.   Results and Discussion

4.4.1. Binary DMSO-d$_6$/water systems

The raw data obtained for the ^{1}H NMR results of eighteen different DMSO-d$_6$/water solutions is shown in Figure 4-16. The shift of the water moves farther downfield away from TMS as the mole fraction of water increases across the entire
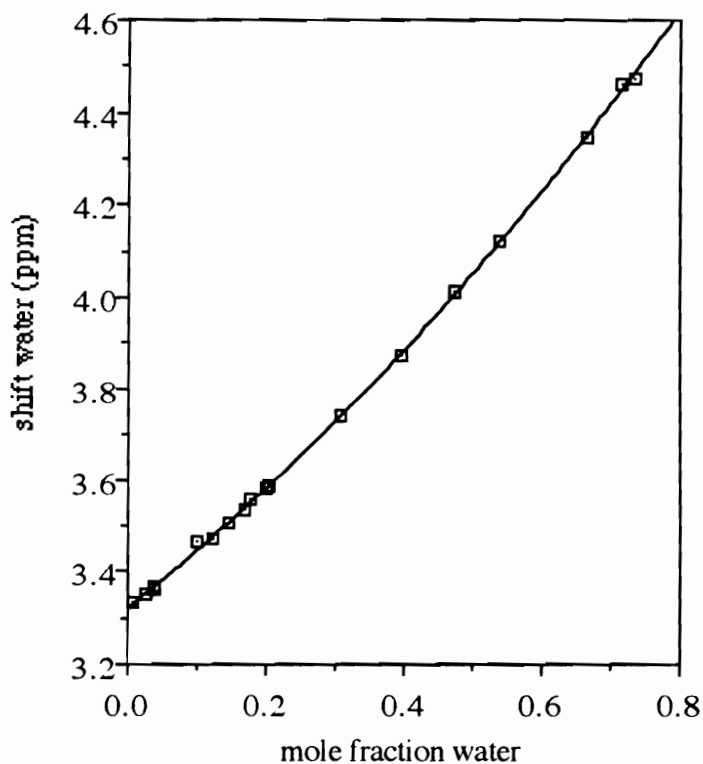
Figure 4-16: Shift of water relative to TMS as a function of added mole fraction water in DMSO-d$_6$ at 25 °C

concentration range of DMSO-d_6/water solutions investigated. This increased deshielding of the water proton with increased water concentration is synonymous with increased hydrogen bonding of the water protons.

Figure 4-17 shows typical ^{1}H NMR spectra of two DMSO-d_6/water mixtures superimposed upon one another, part of the data used to construct the graph in Figure 4-16. The water peak is a singlet, due to averaging of signals of the different types of water hydrogens present in the solution. The shift of the water hydrogen bonded to water, δ_{bo}, is shown at 5.4 ppm, and the shift of the "free" water hydrogen, δ_h, is 0.37 ppm. Finally, the shift of the water proton that is hydrogen bonded to DMSO-d_6, δ_{bn}, is 3.38 ppm. This was the value produced by the iterative spreadsheet calculations as discussed in the Experimental section. Note that the experimental ^{1}H NMR shift of the water proton moves closer to the resonance frequency of pure water as the mole fraction of water in the sample increases.

The iterative spreadsheet calculations were set up using the ^{1}H NMR data for the shifts of the water peak relative to the mole fractions of water and DMSO-d_6 in the solutions. Evaluation of the systematically varied DMSO-d_6/water solutions provided, after 45 iterations, the results: K_n = 52, K_o = 48, and δ_{bn} = 3.38 ppm. Values reported by Lin for the same calculation using the oxygen base N-methylpyrrolidinone (NMP) in place of DMSO-d_6 as the hydrogen bond acceptor, are shown in Table 4-12. DMSO has been known to form exceedingly strong hydrogen bonds with water for many years; apparently DMSO-d_6 hydrogen bonds with water much more strongly than does NMP. The mathematical error analysis for values of K_o and K_n resulted in errors of $\pm$ 11.0 and $\pm$ 12.2 respectively for the equilibrium constants. The experimental error (from spectrometer and weighing inaccuracies) resulted in errors of $\pm$ 6.5, $\pm$ 6.2, and $\pm$ 0.01 ppm for values of K_o, K_n, and δ_{bn} respectively. The error values shown in Table 4-12 represent of the sum of error from both mathematical and experimental sources for each calculated value.
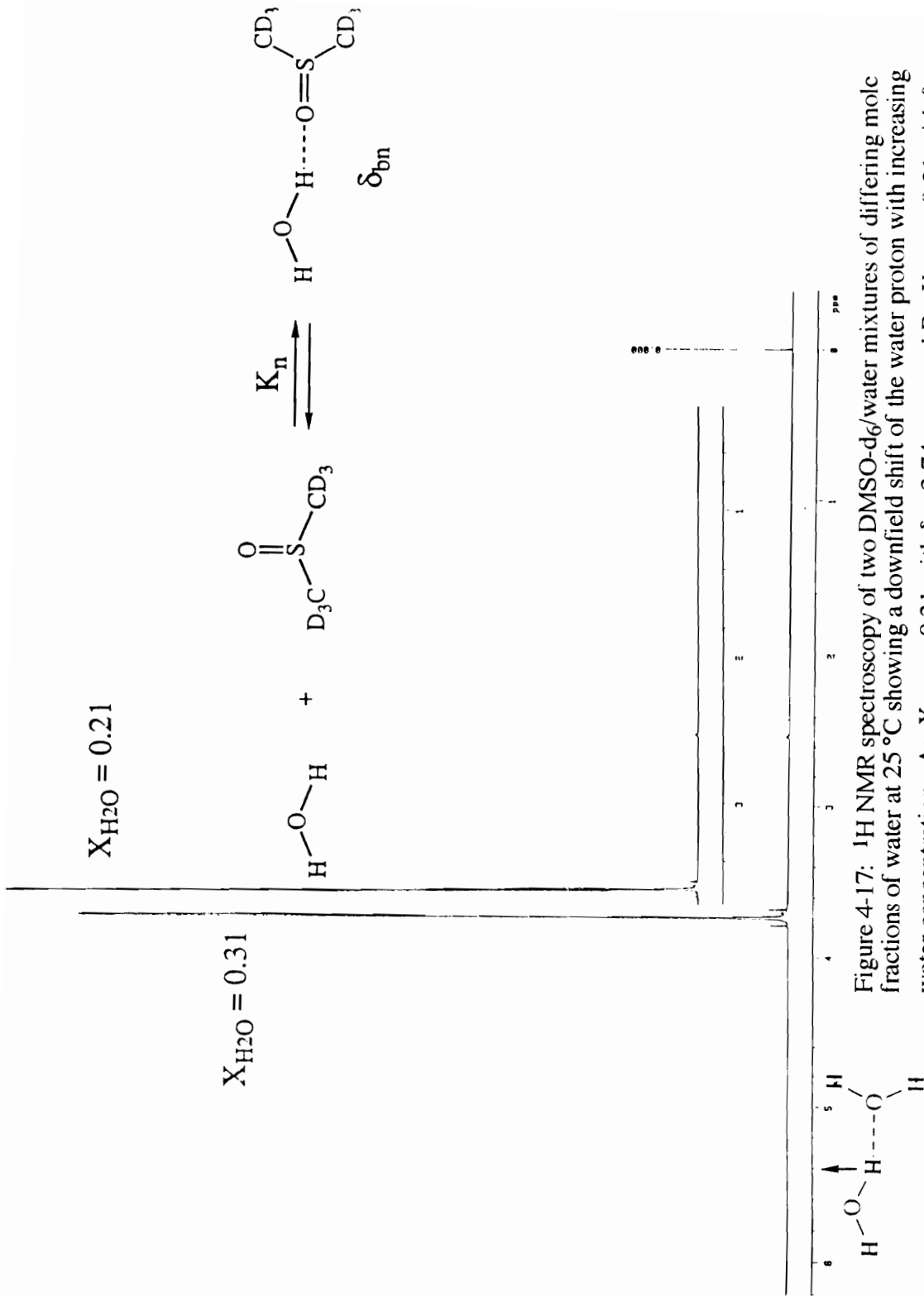
Figure 4-17: ^1H NMR spectroscopy of two DMSO-d_6/water mixtures of differing mole fractions of water at 25 °C showing a downfield shift of the water proton with increasing water concentration. A: $X_{H2O} = 0.31$ with $\delta = 3.74$ ppm; and B: $X_{H2O} = 0.21$ with $\delta = 3.59$ ppm.

The norm value, a test of closeness of theoretical calculated values to the experimental values, was 0.0092, indicating good agreement between the values. A comparison of experimental and calculated values using the best fit parameters of δ_{bn} = 3.38 ppm, K_o = 48, K_n = 52 is shown in Figure 4-18. Because several minima and maxima exist in the norm equation, a broad range of K_o and K_n values were tested, while holding δ_{bn} constant at 3.38 ppm, to verify that the computations were correct. The test for minima and maxima used all possible combinations of values of K_n ranging from 1 to 100 with values of K_o ranging from 1 to 70. The results are shown in Table A-4 and also validated the calculated values of K_o = 48 and K_n = 52.

The shift calculated for water hydrogen bonded to DMSO (δ_{bn}) is entirely reasonable, since literature values for the shift of "free" water is 0.37 ppm and the shift of water H-bonded to water is 5.43 ppm. The overall shift of the water in the experimental solution is the weighted average of all types of water hydrogens present, "free", hydrogen bonded to other molecules of water, and hydrogen bonded to molecules of DMSO. Experimental shift values for the broad range of solution concentrations (from 0.008 to 0.73 mole fraction water in DMSO-d_6) ranged from 3.33 ppm to 4.48 ppm respectively. When the solution contains a large amount of water, as in the latter case, the shift of the hydrogen of water approaches that of the pure water-water H-bond (δ_{bo}), 5.43 ppm. When there is very little water in the DMSO-d_6/water solution (as in the former case where X_{H2O} is 0.008), the shift of the water in this solution (3.33 ppm) approaches the calculated shift of water bonded solely to DMSO (δ_{bn}), calculated to be 3.38 ppm. Note that the largest mole fraction of water in DMSO-d_6 measureable by this technique was X_{H2O} = 0.73, because TMS was insoluble in ^{1}H NMR solutions of higher water concentrations.

Table 4-12: Equilibrium constants for hydrogen bonding of water to water (K_o), water to oxygen bases (K_n), and shift of the hydrogen (δ_{bn}) involved in the water-NMP complex (198) compared to parameters for water-DMSO-d_6 hydrogen bonding interactions and solubility parameters (199)

oxygen base	Temp (°C)	δ_{bn} (ppm)	K_o	K_n	δ (Mpa)$^{1/2}$
NMP	21	3.19	22.2 ± 3.4	24.9 ± 3.2	23.1
NMP	30	3.19	17.0 ± 2.6	20.1 ±2.1	23.1
DMSO-d_6	25	3.38 ± 0.01	48 ± 17.5	52 ± 18.4	
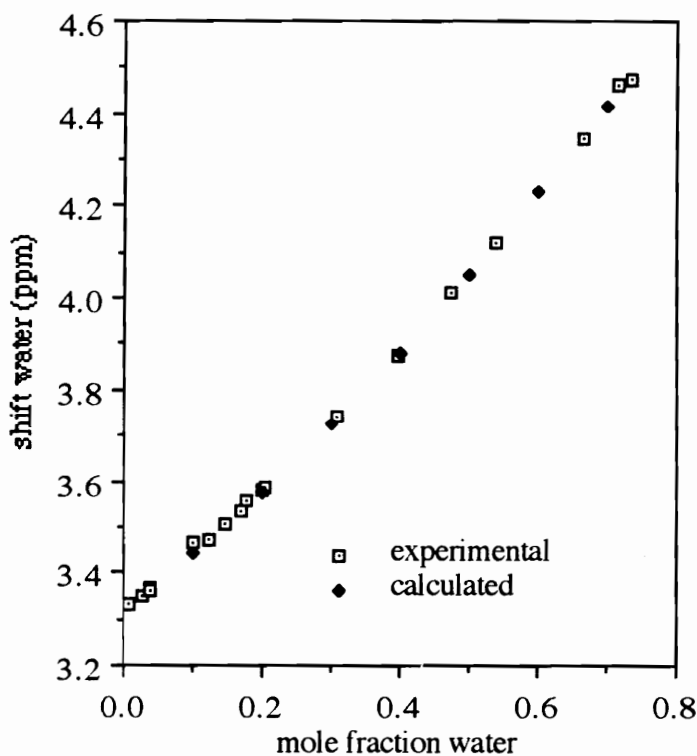
Figure 4-18: Experimental and calculated values for the shift of water in DMSO-d_6/water solutions (downfield from TMS) as a function of mole fraction water at 25 °C. The calculated shifts correspond to parameters of δ_{bn} = 3.38 ppm, K_o = 48, and K_n = 52. The excellent goodness of fit was represented by a norm value of 0.0092.

4.4.2. Ternary DMSO-d_6/water/model compound systems

The chemical shift of water, in a systematically varied series of solutions comprising model compounds dissolved in a 97/3 w/w DMSO-d_6/water solution, was evaluated using ^{1}H NMR spectroscopy at 25 °C. For each model compound: triphenylphosphine oxide (TPPO) (two trials), diphenylsulfoxide (DPSO), diphenylsulfone (DPSO2), pyridine, and diphenylmethylphosphine oxide (DPMPO), the shift of the water proton was plotted as a function of mole fraction model compound as shown in Figures 4-19 through 4-23. Two experiments using TPPO as the model compound were performed to verify reproducibility of the data. In each case, the water resonance moved downfield away from TMS as the mole fraction of model compound increased.

Figure 4-24 shows typical ^{1}H NMR spectra of two DMSO-d_6/water/diphenyl-sulfoxide mixtures superimposed upon one another, part of the data used to construct the graph in Figure 4-20. As in the case of the binary DMSO-d_6/water solution, the water peak in the ternary solution is a singlet, due to the averaging of the signals of the different types of water hydrogens present in the solution. There are three competing equilibria in the DMSO-d_6/water/diphenylsulfoxide solution: water-water hydrogen bond formation, water-DMSO-d_6 hydrogen bond formation, and water-diphenylsulfoxide hydrogen bond formation. In Figure 4-24, the shift of the water hydrogen bonded to water, δ_{bo}, is at 5.43 ppm, the shift of the "free" water hydrogen, δ_h, is 0.37 ppm, and the shift of the water proton that is hydrogen bonded to DMSO-d_6, δ_{bn}, is 3.38 ppm. The shift of the hydrogen that is complexed to diphenylsulfoxide, δ_{bp}, is 5.13 ppm. This was the value produced by the iterative spreadsheet calculations as discussed in the Experimental section. It is evident from Figure 4-24 that, as the mole fraction of diphenylsulfoxide is increased, the water
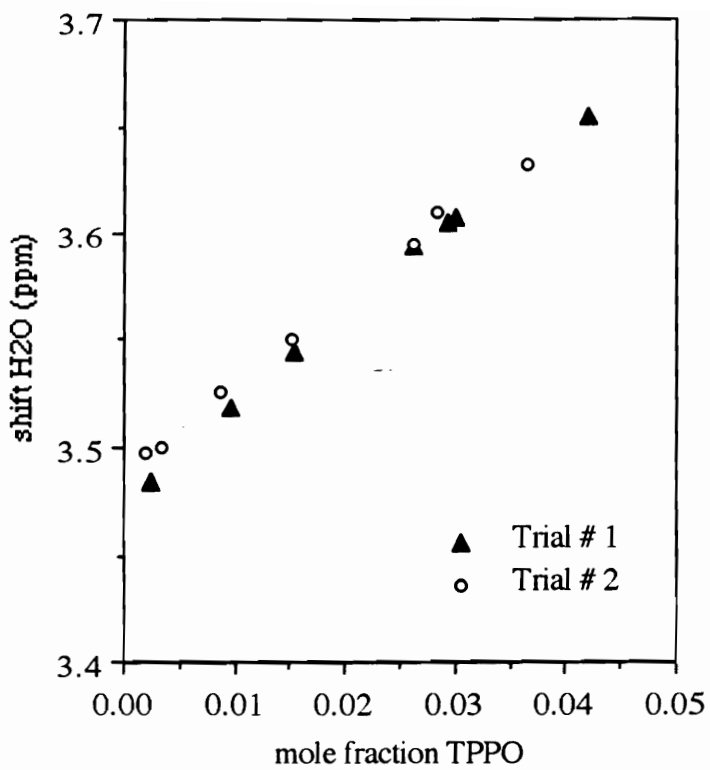
Figure 4-19: Shift of water at 25 °C in a DMSO-d$_6$/water (97/3 w/w) solution relative to TMS as a function of added triphenylphosphine oxide (two trials)
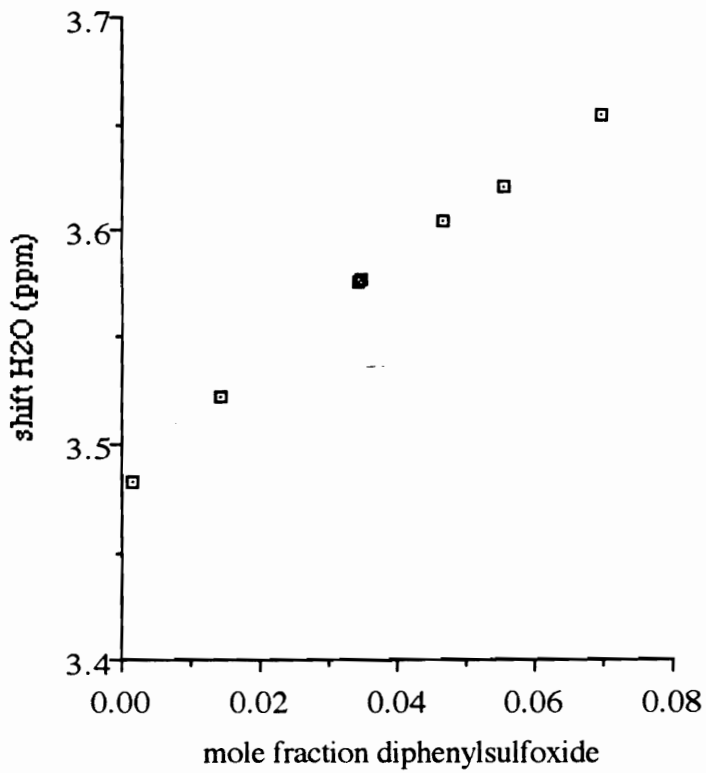
Figure 4-20: Shift of water at 25 °C in a DMSO-d_6/water (97/3 w/w) solution relative to TMS as a function of mole fraction diphenylsulfoxide
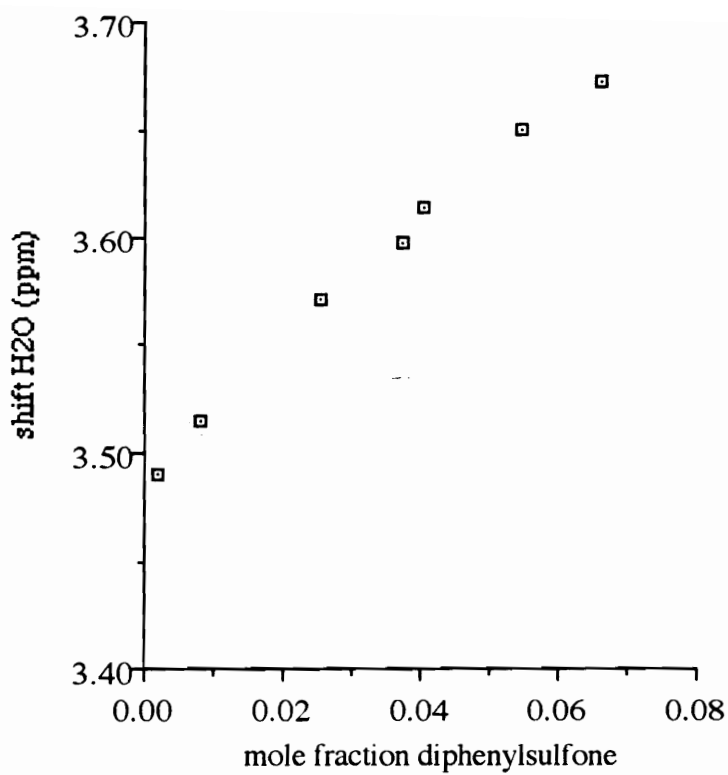
Figure 4-21: Shift of water at 25 °C in a DMSO-d_6/water (97/3 w/w) solution relative to TMS as a function of mole fraction diphenylsulfone
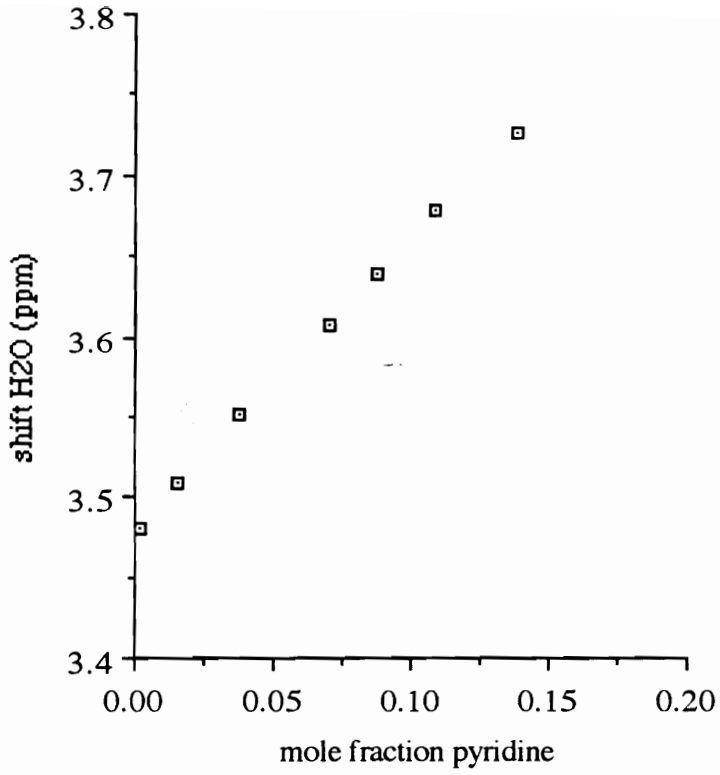
Figure 4-22: Shift of water at 25 °C in a DMSO-d$_6$/water (97/3 w/w) solution relative to TMS as a function of mole fraction pyridine
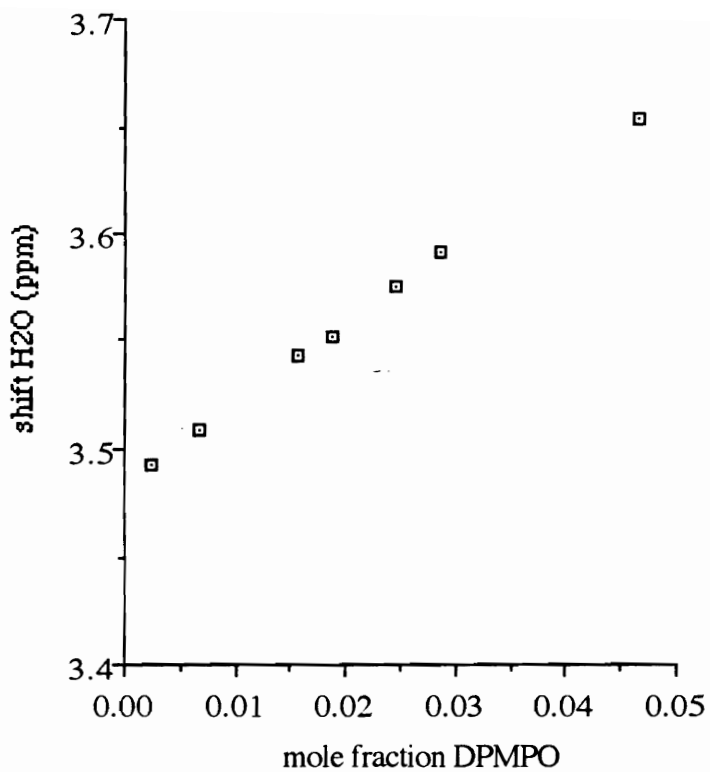
Figure 4-23: Shift of water at 25 °C in a DMSO-d_6/water (97/3 w/w) solution relative to TMS as a function of mole fraction diphenylmethylphosphine oxide
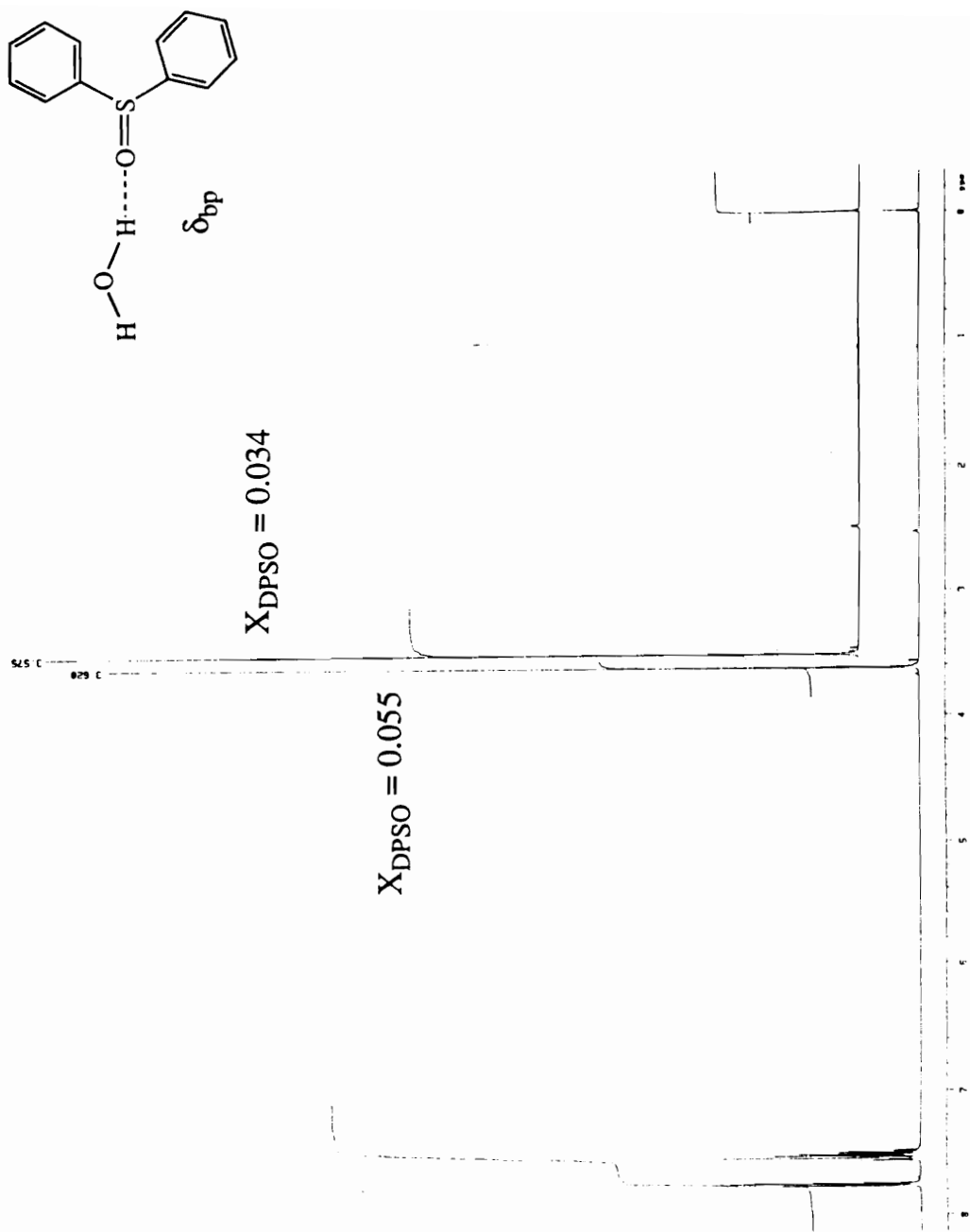
Figure 4-24: ^{1}H NMR spectroscopy of two solutions of differing mole fraction diphenylsulfoxide dissolved in 97/3 w/w DMSO-d6/water at 25 °C. A: $X_{DPSO} = 0.055$ with $\delta = 3.62$ ppm; and B: $X_{DPSO} = 0.034$ with $\delta = 3.58$ ppm.

peak moves downfield. This is due to an increased likelihood of formation of the water-diphenylsulfoxide hydrogen bond complex coupled with decreased formation of water-water and water-DMSO-d_6 complexes and a decreased concentration of "free" water. Thus the averaged chemical shift of the water proton is increasingly deshielded due to the increasing amount of hydrogen bond formation with the electronegative sulfoxide moiety.

The results based on the experimental ^1H NMR data are outlined in Table 4-13. For each model compound, the equilibrium constant of water-model compound complex formation (K_p values) and the shift of the hydrogen bonded to the model compound (δ_{bp} values) were evaluated. The norm, an evaluation of fit between experimental and

Table 4-13: Equilibrium constants, chemical shifts of the proton involved in the water-model compound complex, and norm values calculated for the ternary DMSO-d_6/water/model compound systems at 25 °C

model compound	K_p	δ_{bp} (ppm)	calculated norm
TPPO (trial 1)	55.4 ± 27.6	7.35 ± 0.44	0.0104
TPPO (trial 2)	75.2	6.60	0.0097
DPMPO	61.7 ± 12.3	6.60 ± 0.29	0.0038
pyridine	143.5 ± 25.9	6.06 ± 0.14	0.0091
DPSO	107.6 ± 23.9	5.13 ± 0.12	0.0095
DPSO2	92.4 ± 24.2	4.69 ± 0.06	0.1416

theoretical shift values, is also reported. As norm values approach zero, the calculated shift of water in the DMSO-d_6/water/model compound solution approaches the experimental shift in the solution of the same composition.

The error in the calculation was determined using two methods, mathematical and experimental. The mathematical error was evaluated by replacing the literature values for δ_h and δ_{bo} (0.37 and 5.43 ppm respectively) with the maximum values for δ_h and δ_{bo} (0.43 and 5.57 ppm respectively). The spreadsheet calculations were repeated, varying K_p to find the lowest norm value, while holding the shift value δ_{bp} constant. The mathematical error analysis for values of K_p resulted in errors of $\pm$ 6.7, $\pm$ 9.1, $\pm$ 20.2, $\pm$ 20.7, and $\pm$ 16.4 respectively for TPPO (trial 1), DPMPO, pyridine, DPSO, and DPSO2. The experimental error was determined by translating weighing and spectrometer errors to chemical shift error and evaluating the effect of change in chemical shift on the calculated values for K_p and δ_{bp}. The experimental errors (from spectrometer and weighing inaccuracies, cumulative from the binary DMSO-d_6/water experimental results) for K_p values were $\pm$ 20.9, $\pm$ 3.2, $\pm$ 5.7, $\pm$ 3.2 and $\pm$ 7.8 for TPPO (trial 1), DPMPO, pyridine, DPSO, and DPSO2 respectively. The error values for K_p shown in Table 4-13 represent of the sum of error from both mathematical and experimental sources for each calculated value. The error for the chemical shift values shown in Table 4-13 is calculated from experimental sources.

The best fit calculated shift of water in DMSO-d_6/water/model compound solutions relative to the experimental data is shown in Figures 4-25 through 4-30.
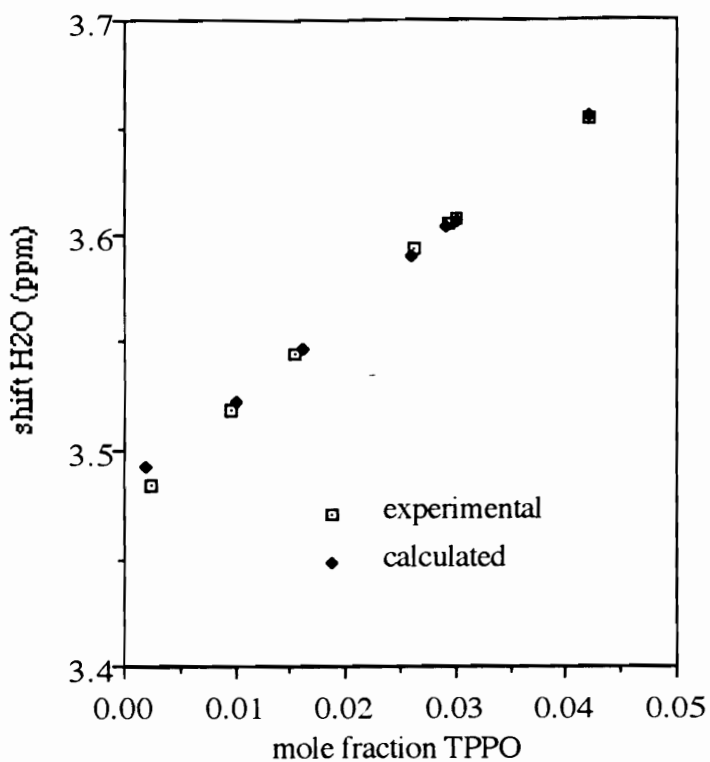
Figure 4-25: First trial experimental and calculated values for the shift of water in DMSO-d_6/water/TPPO solutions (downfield from TMS) as a function of mole fraction TPPO at 25 °C. The calculated shifts correspond to parameters of δ_{bp} = 7.35 ppm and K_p = 55.4. The excellent fit was described by a norm value of 0.010.
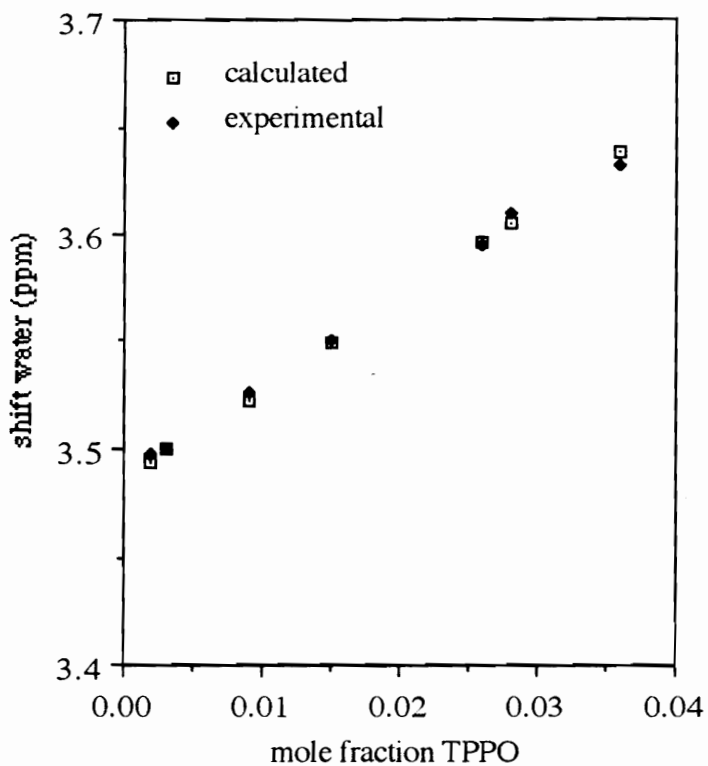
Figure 4-26: Second trial experimental and calculated values for the shift of water in DMSO-d_6/water/TPPO solutions (downfield from TMS) as a function of mole fraction TPPO at 25 °C. The calculated shifts correspond to parameters of δ_{bp} = 6.60 ppm and K_p = 75.2. The excellent fit was described by a norm value of 0.0097.
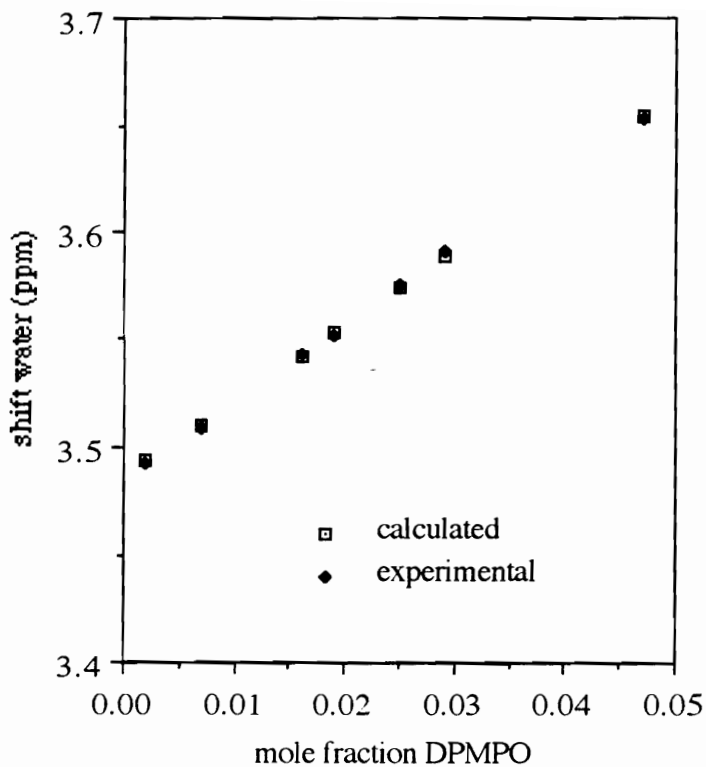
Figure 4-27: Experimental and calculated values for the shift of water in DMSO-d_6/water/DPMPO solutions (downfield from TMS) as a function of mole fraction DPMPO at 25 °C. The calculated shifts correspond to parameters of $\delta_{bp} = 6.60$ ppm and $K_p = 61.7$. The excellent fit was described by a norm value of 0.0038.
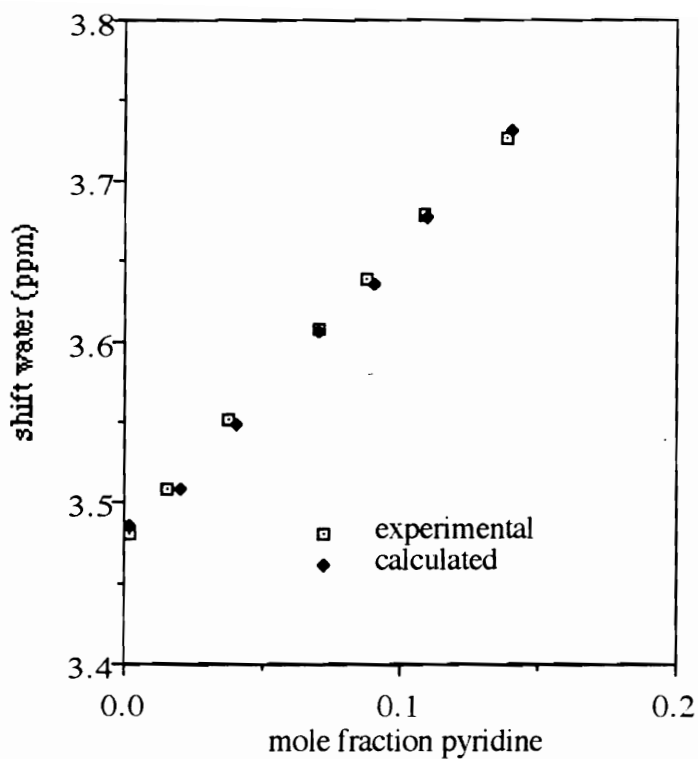
Figure 4-28: Experimental and calculated values for the shift of water in DMSO-d_6/water/pyridine solutions (downfield from TMS) as a function of mole fraction pyridine at 25 °C. The calculated shifts correspond to parameters of δ_{bp} = 6.06 ppm and K_p = 143.5. The excellent fit was described by a norm value of 0.0091.
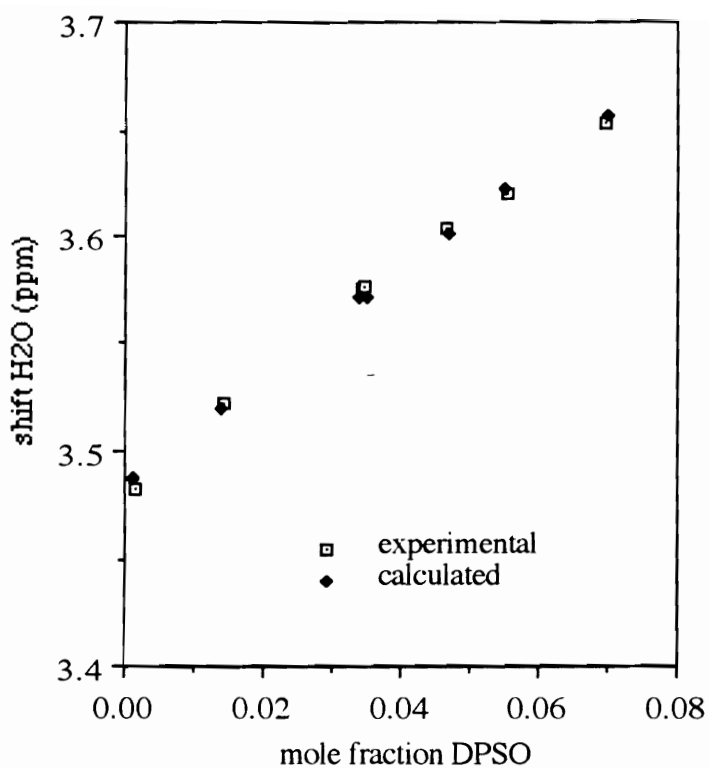
Figure 4-29: Experimental and calculated values for the shift of water in DMSO-d_6/water/DPSO solutions (downfield from TMS) as a function of mole fraction DPSO at 25 °C. The calculated shifts correspond to parameters of $\delta_{bp} = 5.13$ ppm and $K_p = 107.6$. The excellent fit was described by a norm value of 0.0095.
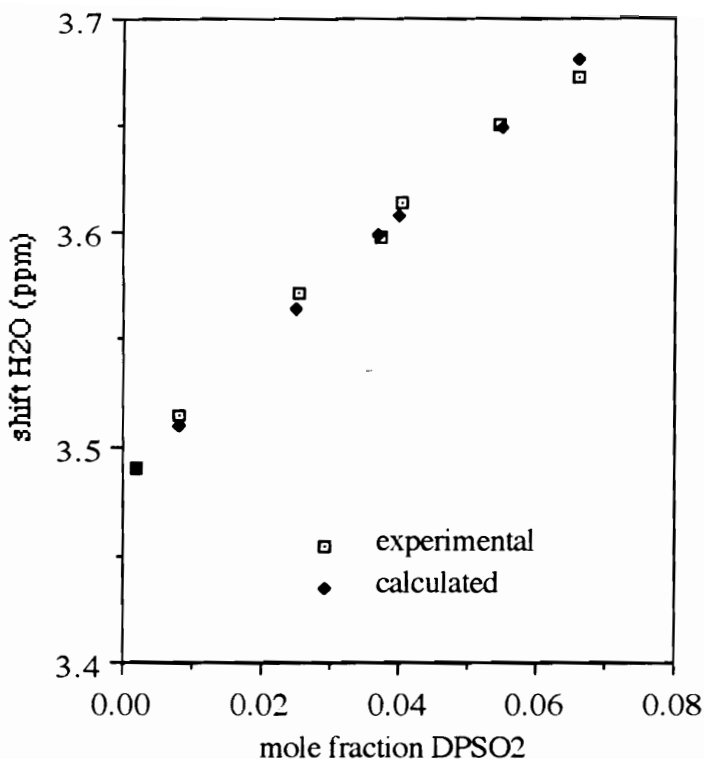
Figure 4-30: Experimental and calculated values for the shift of water in DMSO-d_6/water/DPSO2 solutions (downfield from TMS) as a function of mole fraction DPSO2 at 25 °C. The calculated shifts correspond to parameters of $\delta_{bp} = 4.69$ ppm and $K_p = 92.4$. The fit was described by a norm value of 0.142.

The relationship between the shift of the complexed hydrogen as a function of equilibrium constant for the complex formation for the different model compounds is shown in Figure 4-31. The equilibrium constants for the water-model compound complex formation (K_p values) obtained for the diphenylsulfone, diphenylsulfoxide, and pyridine

clearly rank these compounds in terms of hydrogen bonding ability. For example, the high equilibrium constant for the formation of the pyridine-water complex (143.5) agrees with the deshielded downfield shift of the proton of the complex (δ_{bp} = 6.06 ppm). Thus it is apparent that pyridine hydrogen bonds more strongly with water than does diphenylsulfone
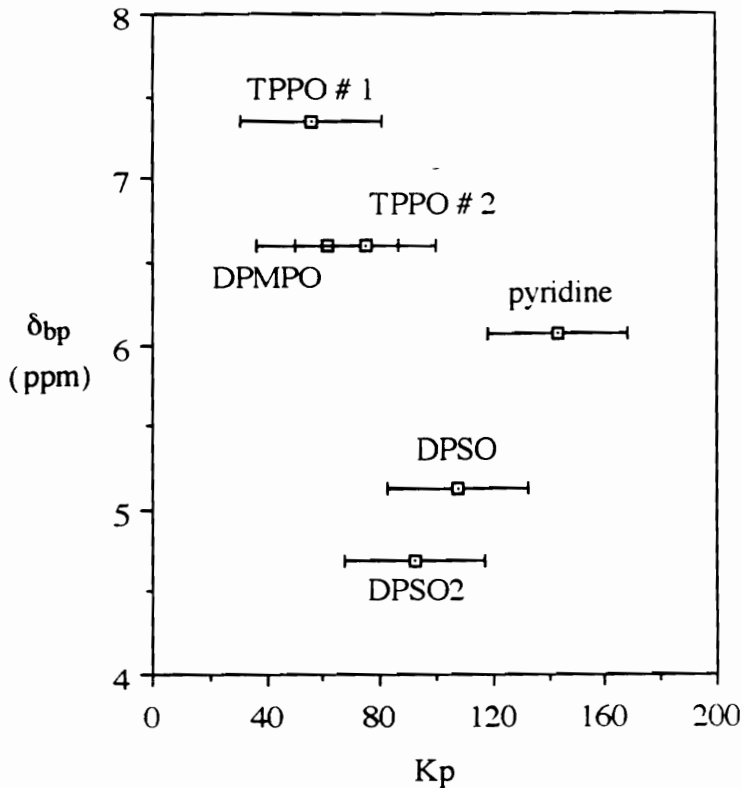
Figure 4-31: Shift of the proton hydrogen bonded to the model compound as a function of equilibrium constant for the complex formation for triphenylphosphine oxide (TPPO #1, TPPO #2), pyridine, diphenyl sulfoxide (DPSO), diphenylmethylphosphine oxide (DPMPO), and diphenyl sulfone (DPSO2) dissolved in 97/3 DMSO-d_6/water at 25 °C

and diphenylsulfoxide. It is also apparent that diphenylsulfoxide hydrogen bonds more strongly than diphenylsulfone with water. This suggests that the hydrogen bonding ability of two polymers of similar molecular weight and structure, one possessing sulfoxide linkages (i. e., poly(arylene ether sulfoxide)) and the other possessing sulfone linkages (i.

e., poly(arylene ether sulfone)), could be analogously ranked using this system. Thus it is not a surprise that poly(Bis A-sulfoxide) is miscible with an epoxy resin possessing secondary hydroxyl groups whereas poly(Bis A-sulfone) is immiscible with the same epoxy resin under the same conditions. This idea is substantiated by the work of Coleman, Xu, and Painter (92) wherein the hydrogen bonding ability of ester-containing model compounds was found to vary systematically with polyesters of analogous structures.

The raw data of the two trial runs of the triphenylphosphine oxide (Figure 4-19) showed good reproducibility of the NMR experiment. The slight deviation in the curves may be due to the fact that the stock DMSO-d_6/water solution concentrations were slightly different between the two trials. In the first trial the concentration of the DMSO-d_6/water solution was 3.05 weight percent water while in trial two the DMSO-d_6/water solution was 3.10 weight percent water. This would explain the deviation between the two runs which increased at lower weight percent model compound. However, when the K_p and δ_{bp} values for the two trials for the triphenylphosphine oxide were calculated, the deviation for the two runs was much more severe as shown in Table 4-14. One possibility for the poor reproducibility of the calculations may be based on the fact that the calculations were performed on the actual experimental data points rather than on a best fit line describing the set of data points (see Figure 4-32). Minor deviations from linearity for a single ^{1}H NMR sample, due to a possible weighing or handling error, could have drastically affected the calculation.

Table 4-14: Reproducibility of the DMSO-d6/water/triphenylphosphine oxide calculations for K_p and δ_{bp} based on ^{1}H NMR data

model compound	K_p	δ_{bp} (ppm)	calculated norm
TPPO (trial 1)	55.4 ± 6.7	7.354	0.0104
TPPO (trial 2)	75.2	6.60	0.0097
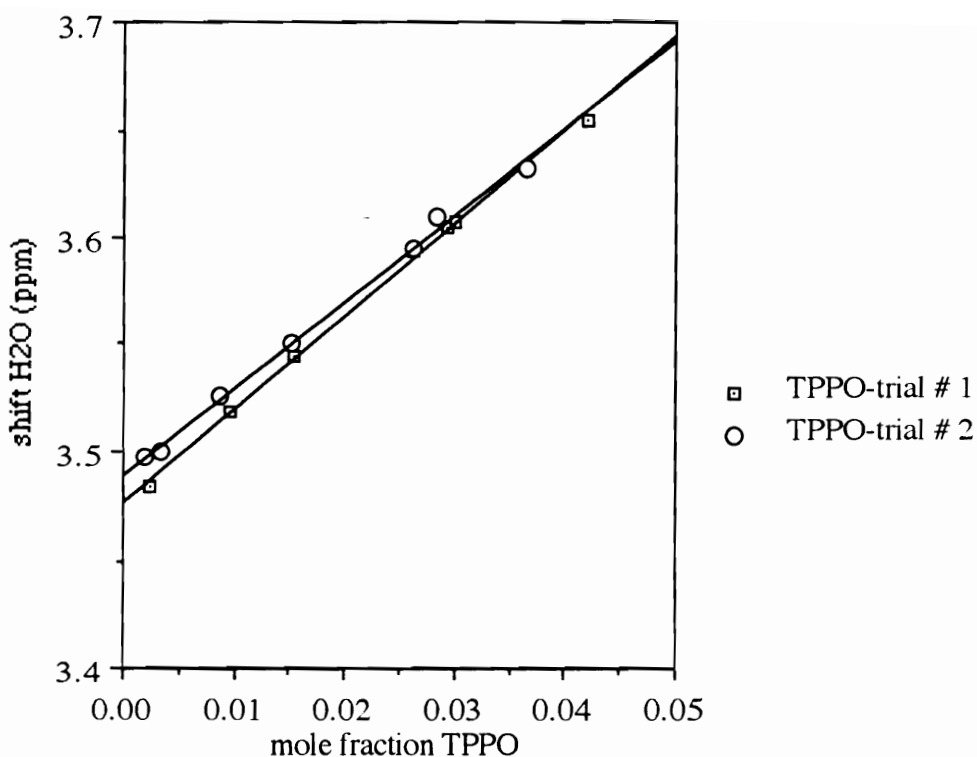
Figure 4-32: Comparison of best fit lines for the two trials of the DMSO-d$_6$/water/triphenylphosphine oxide ^{1}H NMR experiment

Neither phosphine oxide-containing model compound fit into the linear series of values defined by the diphenylsulfone, diphenylsulfoxide, and pyridine as shown in Figure 4-31. The equilibrium constant for the hydrogen bonded complex is lower (55.4 or 75.2) than that found for the other three model compounds. Conversely, the shift of the proton hydrogen bonded to triphenylphosphine oxide, 7.35 ppm, lies within the aromatic range of

shifts. This deviation from the linear path defined by diphenylsulfone, diphenylsulfoxide, and pyridine, indicates that the water-phosphine oxide interaction may be following another pathway altogether. One possibility is that the hydrogen which is hydrogen bonded to the phosphine oxide moiety is also under the influence of the phenyl rings of TPPO. As shown in Figure 4-33, a computer modeled triphenylphosphine oxide molecule, the phenyl rings in this sterically hindered structure are rotated; long range coupling may be possible between an aromatic hydrogen and the water hydrogen in the hydrogen bonded complex. Furthermore, a phenyl ring in the proximity of the hydrogen bonded water may also deshield the proton involved in complexation. This would once again be evidenced by a anomalous downfield shift in the water-triphenylphosphine oxide complex with respect to complexes formed from the other less hindered model compounds.

The computer modeled diphenylmethylphosphine oxide is depicted in Figure 4-34. The structure of this molecule is much less hindered than the triphenylphosphine oxide. This should permit more facile complexation of the phosphine oxide moiety with water; a result which seems to be indicated by a higher equilibrium constant of hydrogen bond formation for the diphenylmethylphosphine oxide relative to triphenylphosphine oxide (61.7 relative to 55.4).
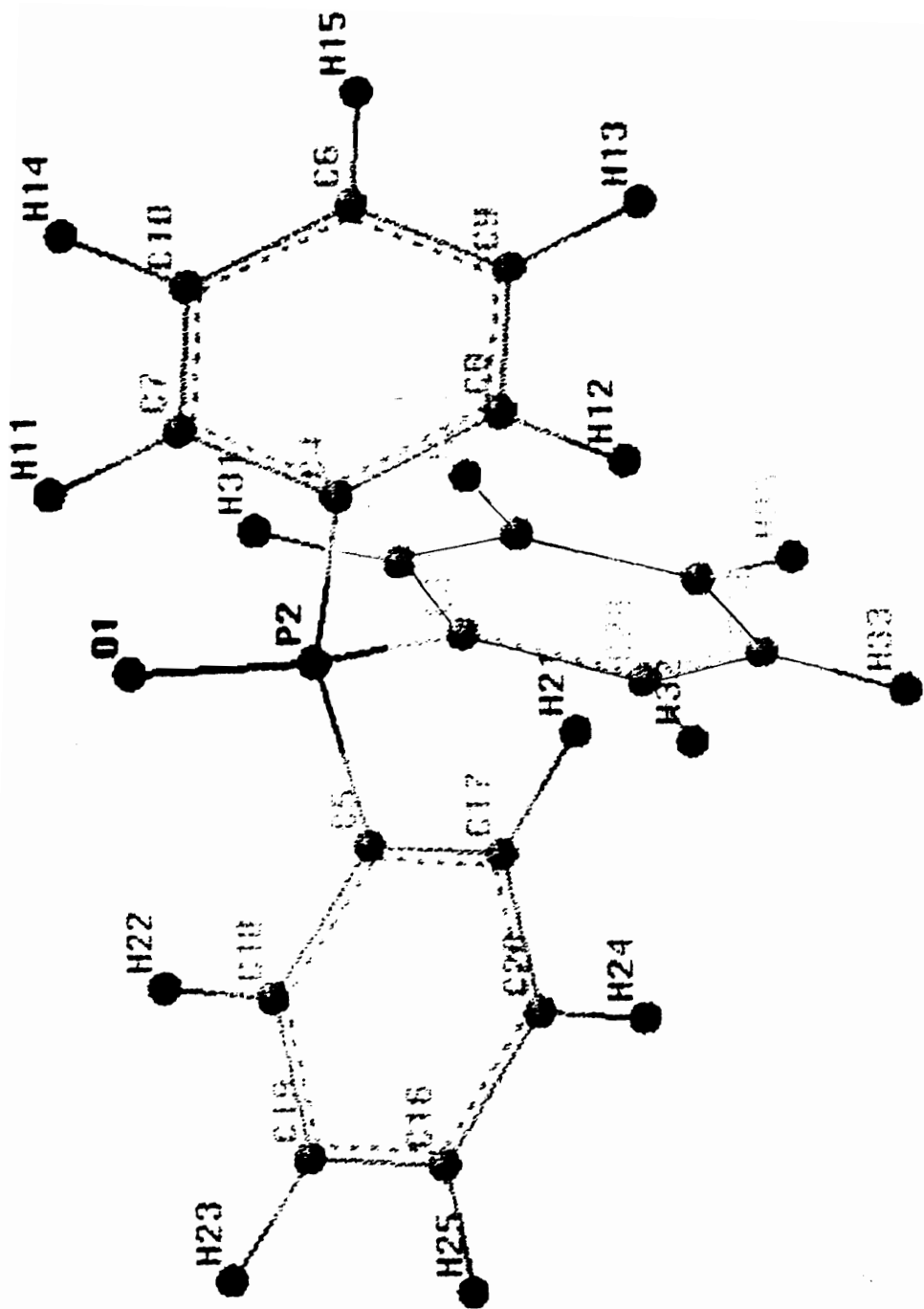
Figure 4-33: Semi-empirical AM1 minimization modeling of triphenylphosphine oxide using Spartan modeling software (Wavefunction, Inc.)
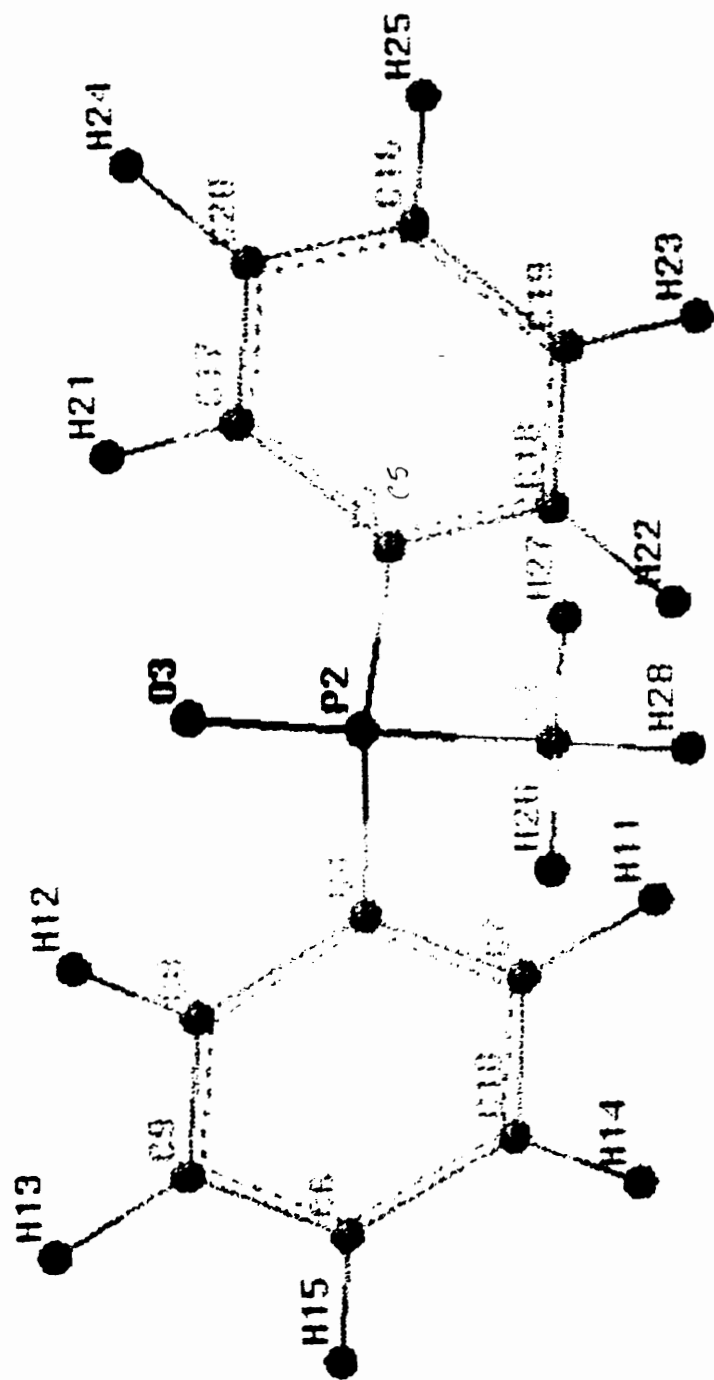
Figure 4-34: Semi-empirical AM1 minimization modeling of diphenylmethylphosphine oxide using Spartan modeling software (Wavefunction, Inc.)

171

4.5.   Conclusions

The DMSO-d_6 was found to hydrogen bond strongly with water as demonstrated by the large equilibrium constant for the formation of the DMSO-d_6-water complex of $K_n =$ 52 at 25 °C.   In the calculations of parameters of the binary DMSO-d_6-water solutions the functionality of the DMSO-d_6, X_n, was set to three.   This assumes that DMSO-d_6 possesses three different hydrogen bonding sites: two due to the lone pairs of electrons and one due to the sulfur-oxygen π-bond, but this was not proven.   However, the fit of the calculated values to the experimental data was quite close (Figure 4-18).   Lin (200) showed that for H_2O-NMP solutions, the calculated shift did not accurately mirror the experimental shift when the functionality of the hydrogen bonding ligand was incorrectly chosen.   Thus the choice of $X_n = 3$ for DMSO-d_6 was probably accurate despite the unknown bond order of the sulfur-oxygen linkage.

The calculated equilibrium constants and shifts for the complexed proton in the DMSO-d_6/water solutions were applied to calculations of similar parameters for the DMSO-d_6/water/model compound solutions.   Once again an assumption was made: that the DMSO-d_6/water interactions were unchanged by the presence of the model compounds.   At the low mole fractions of added model compound this was probably the case.   Moreover, the calculated shift mirrored the experimental shift across the entire concentration range, so this assumption was also taken as valid.

By ^{1}H NMR studies, the model compounds were ranked in hydrogen bonding ability as: pyridine > diphenylsulfoxide > diphenylsulfone.   Triphenylphosphine oxide and diphenylmethylphosphine oxide did not fit the trend and the hydrogen bonding ability of these compounds cannot be ranked with respect to the other three model compounds. Eyman and Drago's published values for the enthalpy of hydrogen bond formation between phenol and compounds with the same functional groups, shown in Table 4-2 and Figure 4-

4, followed the same qualitative trend as the compounds used in this research. However, in this data pyridine was the outlier in hydrogen bonding studies of compounds with similar functional groups.

CHAPTER 5

Benzoin condensation of bisaldehydes

5.1.   Literature review of the benzoin condensation reaction

5.1.1. Benzoin applications

Benzoin and its derivatives are widely used for commercial applications where a free radical source is requisite. Photooxidation of benzoin under oxygen cleaves the unstable α-hydroxyketone functionality and yields benzaldehyde, perbenzoic acid, and hydrogen peroxide (201). Benzoin is thus widely used as a photoinitiator in the coatings and printings industries for photocurable coatings, varnishes, printing inks, and paints (202). Inoue et al. (203) demonstrated that benzoin can also initiate the polymerization of methyl methacrylate in a pyridine-carbon tetrachloride solvent system.

5.1.2. Mechanism of the benzoin condensation in protic conditions

The benzoin condensation reaction, wherein two aldehyde moieties are coupled via a multistep mechanism to form an α-hydroxy carbonyl compound, has been known since 1903 (204). The reaction between two aldehydes is catalyzed by a species which not only acts as a nucleophile on the electrophilic aldehyde site, but must also serve as an electron withdrawing group after attachment to the aldehyde functionality. Catalysts for the benzoin condensation include the cyanide ion (205-207), thiazolium salts (208, 209) polymer bound thiazolium salts (210, 211), and bis(thiazolin-2-ylidene)s (212).

Kuebrich et al. (207) used ^{1}H nuclear magnetic resonance and ultraviolet spectroscopies to elucidate the mechanism of the cyanide catalyzed benzoin condensation in protic conditions shown in Figure 5-1. The reactions were performed in absolute methanol with potassium cyanide as the catalyst at 34 °C. Step (1), addition of cyanide to benzaldehyde, is rapid, and $\Delta H_1 = -9.9$ kcal/mol. Rearrangement of this adduct to form the cyanocarbanion intermediate, shown in Step (2), is slow, with $\Delta H_2 = +10$ kcal/mol. The resonance stabilized cyanocarbanion intermediate, also referred to as the "active aldehyde" intermediate, is relatively stable. Furthermore, attack of this active aldehyde on an electrophilic site (such as another molecule of benzaldehyde) proceeds through a "loose" transition state (213). In the "loose" transition state, the bond between the carbanionic carbon and the electrophile is quite weak, so that the structures of both moieties of the transition state remain little changed from their reactant condition, implying a lack of selectivity of the active aldehyde intermediate in its reactions with electrophiles. In Step (3), the cyanocarbanion releases its partial bond with the hydrogen of the methanol solvent and forms a carbon-carbon bond with another molecule of benzaldehyde. The enthalpy of Step (3) is $\Delta H_3 = +10$ kcal/mol; because there is an entropic preference for reaction with methanol rather than benzaldehyde this is the rate determining step for the cyanide catalyzed benzoin condensation of benzaldehyde in methanol. Subsequent rearrangement of the dimer adduct and loss of cyanide to regenerate the catalyst is rapid.
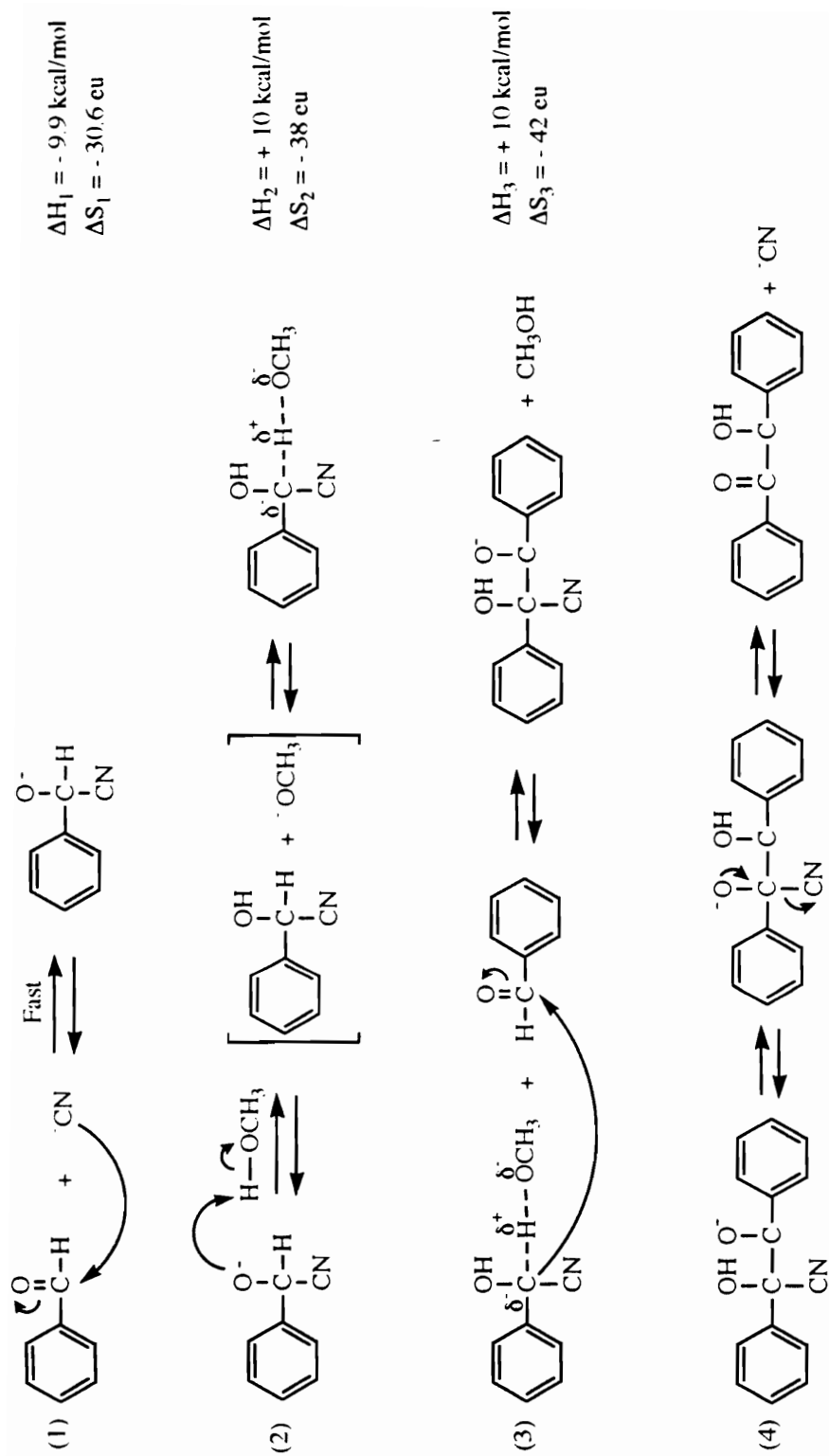
Figure 5-1: Mechanism of the cyanide catalyzed benzoin condensation of benzaldehyde in methanol

176

5.1.3. Tetraalkylammonium cyanides as catalysts in the benzoin condensation reaction

Solodar (214) found that tetraalkylammonium cyanides in aqueous solution catalyze the benzoin condensation reaction. Tetraethylammonium cyanide can be prepared from tetraethylammonium chloride (215) although Solodar's more general procedure permits synthesis of tetrabutylammonium cyanide and tetrapropylammonium cyanide as well by passing tetraalkylammonium bromides through a basic ion exchange resin in the cyanide form (216). White and Baizer (217) investigated tetraalkylammonium cyanides as nucleophilic and basic reagents in nonaqueous media such as acetonitrile and tetrahydrofuran. White and Baizer found that the benzoin condensation reaction proceeds at room temperature using 1 mmol of tetrabutylammonium cyanide with 50 mmol benzaldehyde in 5 mL tetrahydrofuran and produces a 81 % yield of pure benzoin. Quaternary ammonium salts and crown ethers have also been used as phase transfer catalysts to perform the benzoin condensation in benzene (218). Polymer supported quaternary ammonium cyanides have been used as catalysts in the benzoin condensation reaction (219).

5.1.4. Oxidation of benzoins to form benzils

Benzil compounds, or α-diketone compounds, are needed in quantity and at a reasonable price to use in the preparation of polyquinoxalines: thermoplastic, high-temperature, heat-stable adhesives (220). Bisbenzoins may be prepared as precursors to the tetraketone monomers used in poly(phenyl quinoxaline) synthesis reactions. (221, 222). The benzoin functionality is easily oxidized to benzil by a number of mild reagents.

The tradeoff exists because if the oxidizing reagent is too strong, the unstable α-hydroxyketone carbon-carbon bond will cleave.

A number of workers have shown that α-hydroxyketones are oxidized by metal ions or metal complexes in alkaline solution. Water and Marshall (223), Kinoshita (224), and Gampp and Zuberbuhler (225) have shown that cupric salts serve as oxidizing agents. Adolf and Hamilton (226) investigated the iron (III) catalyzed oxidation of acetoin by oxygen and hydrogen peroxide and Hammond and Wu (227) studied the autoxidation of benzoin in methanol catalyzed by nickel acetate. Tsuruya et al. (228) evaluated the oxidative effect of cobalt salts such as cobalt (II) $(acac)_2$ and cobalt (II) nitrate on benzoin. They found that the oxidation activity was appreciably dependent on the cobalt (II) salt used and that cobalt (II) nitrate was the most active for benzoin oxidation in acetonitrile solvent. Hodali and El-Zaru (229) reported the oxidation of substituted benzoins by octacyanomolybdate (V) in alkaline medium. The following trend in rate of oxidation was observed: o,o'-dichlorobenzoin > p,p'-dichlorobenzoin > m,m'-dimethoxybenzoin > benzoin > p,p'-dimethoxybenzoin > o,o'-dimethoxybenzoin. This indicates that electron donating groups decreased the rate of benzoin oxidation to benzil.

Other workers have investigated the oxidation of benzoins in the absence of metal ions and metal complexes. VanDyke and Pritchard (230) reported that benzoins are oxidized to benzils using dimethylsulfoxide in the presence of acetic anydride at room temperature. Seventy to ninety percent yields of dicarbonyl compounds were obtained using this method. Ogata and Tezuka (231) found that nitric acid oxidation of benzoin produces benzil in low yields.

In general, metal (II), solvent, or acid catalyzed methods of benzoin oxidation to form benzil produce low yields of material with subsequent rigorous purification steps to

remove residual catalyst. Other synthesis routes to tetraketone monomers are currently under investigation (220, 232, 233).

5.1.5. Synthesis of polybenzoin and polybenzil materials

One literature reference reported the synthesis of polybenzoin materials using the potassium cyanide catalyzed benzoin condensation reaction on difunctional terephthalaldehyde in 50/50 methanol/water (v/v) (234). The molar ratio catalyst to monomer used was 5 equivalents KCN to 1 equivalent terephthaladehyde; the reaction was performed at 1.5 % solids in the aqueous methanol reaction medium. The polymer obtained was subsequently oxidized to polybenzil in aqueous acetic acid or aqueous nitric acid. Both the polybenzoin and the polybenzil were soluble in DMSO and in strong protic acids such as sulfuric acid, trifluoroacetic acid, and methanesulfonic acid but were insoluble in N,N'dimethylformamide, N-methyl-2-pyrrolidinone, phenol, and m-cresol. Inherent viscosity data obtained for the polymers was: η_{inh} was 0.4 dL/g for both the polybenzoin and the corresponding polybenzil as measured in DMSO at 30 °C from a solution of concentration 0.5 g polymer per 100 mL DMSO.

5.2. Introduction

Current synthetic approaches to polyquinoxaline materials include condensation of tetraamines with tetraketone monomers and incorporation of the quinoxaline moiety into a monomer that is polymerizable by nucleophilic aromatic substitution. The limitations of the first method include the potential carcinogenicity and expense of the tetraamine and the tetraketone monomers. Poly(arylene ether) syntheses of quinoxaline-containing monomers such as 2,3-bis(4-fluorophenyl)quinoxaline are difficult to push to high molecular weight due to the low reactivity of the monomer and diminutive solubility of the resulting polymer.

A different approach (Figure 5-2), designed to afford a synthetic pathway circumventing the multi-step monomer syntheses requisite for the classical polyquinoxaline materials, was investigated in this research. Spectroscopic results indicate that readily available aromatic dialdehydes (terephthalaldehyde and isophthalaldehyde) can be directly condensed to poly(benzoin) oligomers at room temperature using a catalytic level of organic cyanide in dry polar aprotic solvents.

Attempts to oxidize the resultant polymers to the corresponding poly(benzil)s using known oxidizing reagents failed. The materials obtained after oxidation steps were very low molecular weight, indicating the possibility that the unstable benzoin moiety was cleaved during the oxidation.
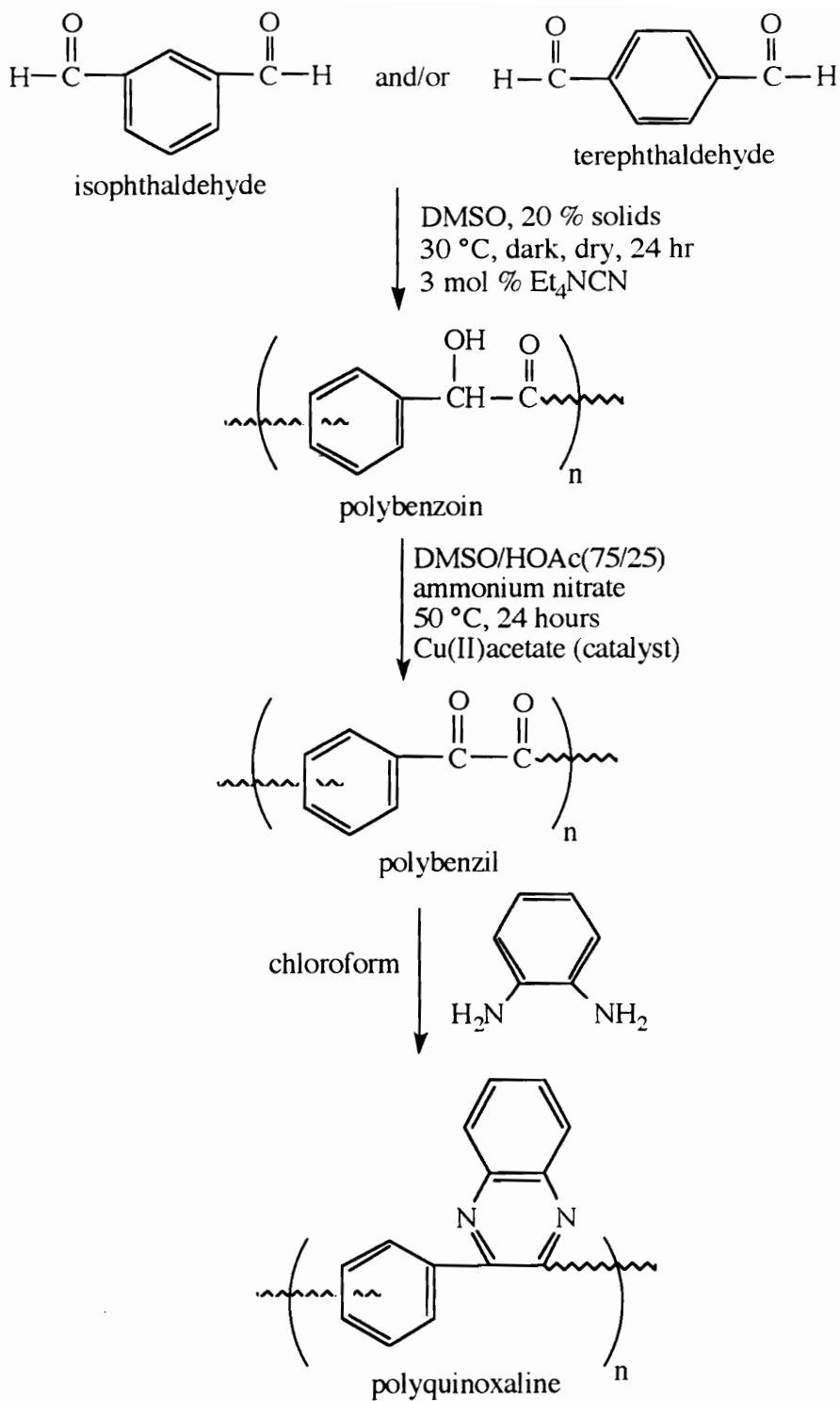
Figure 5-2: Synthesis of polyquinoxaline materials via the benzoin condensation route

181

5.3. Synthesis of polybenzoin materials

5.3.1. Purification of monomers and reagents

Isophthaldehyde (Lancaster) and terephthaldehyde (Aldrich) were recrystallized from water and dried at room temperature *in vacuo* for 24 hours before use. Dimethyl sulfoxide (DMSO) was obtained from Fisher, stirred over calcium hydride for 16 hours, and vacuum distilled. Tetraethylammonium cyanide (Et_4NCN) was obtained from Aldrich, charged to a preweighed roundbottom flask, and dried in a room temperature vacuum oven for two hours prior to use. 3-Bromobenzaldehyde was stirred over calcium hydride and vacuum distilled. Copper (II) acetate (Aldrich), ammonium nitrate (Fisher), and acetic acid (Fisher) were used as received.

5.3.2. Polybenzoin Synthesis

Polymers were synthesized either with uncontrolled molecular weight or a stoichiometric quantity of an endcapping reagent, 3-bromobenzaldehyde, was added to control the molecular weight of the polybenzoin oligomers. Homopolymers of either isophthalaldehyde or terephthalaldehyde, as well as copolymers of the two dialdehydes, were synthesized. The reactions were performed both in roundbottom flasks and in Wilmad 508 pp NMR tubes capped with septa and screw tight lids.

5.3.2.1.   Polybenzoin synthesis reactions performed in NMR tubes

Reactions were performed in NMR tubes to monitor more precisely the the effect of catalyst type and concentration, the effect of temperature, and the effect of anhydrous conditions. Reactions of both isophthalaldehyde and terephthalaldehyde were evaluated. Concentrations of the catalysts (potassium cyanide or tetraethylammonium cyanide) ranged from 0.1 mole percent to 5 mole percent. Temperatures were varied from 30 °C to 100 °C.

Reaction solutions were prepared using a stock solution of either dry isophthalaldehyde or dry terephthalaldehyde at 16 weight percent solids in DMSO-d_6. A stock solution of either 2 weight percent tetraethylammonium cyanide in DMSO-d_6 was prepared or a stock solution of 2 weight percent KCN in 95/5 DMSO-d_6/water was prepared. A known weight of the stock solution of dialdehyde was added via syringe to the flame dried, sealed and capped NMR tube, followed by a known weight of the the catalyst solution. The initial reaction solutions were evaluated by ^{1}H NMR, then placed in constant temperature oil baths and ^{1}H NMR spectra were measured periodically. The disappearance of the aldehyde proton at 10.0 ppm and the appearance of the benzoin alcohol and methine protons at 5.7 - 6.7 ppm were monitored over time.

5.3.2.2.   Reactions in roundbottom flasks

The weight of the tetraethylammonium cyanide catalyst was ascertained after drying and the catalyst was dissolved in DMSO to afford a 5 % solution (w/v). The dialdehyde of interest, isophthaldehyde or terephthaldehdye, was dissolved at 20 % solids in DMSO in a roundbottom flask. The endcapping reagent for the controlled molecular weight polymerizations was added at this time, via syringe. All the flasks were equipped with

septa, flushed for 5 minutes with a steady flow of nitrogen, and maintained under a positive pressure nitrogen blanket. After dissolution of the monomers and the catalyst, a known volume of the catalyst/DMSO solution was added to the monomer/DMSO solution via syringe to afford three mole percent Et$_4$NCN relative to moles of dialdehyde monomer (1.5 mol % catalyst relative to aldehyde units). The flasks were covered with aluminum foil and held at 30 °C in an oil bath for 24 hours while the disappearance of the aldehyde peak at 10.0 ppm was monitored by ^{1}H NMR. The polymer was precipitated into vigorously stirring water, collected in a Buchner funnel, and dried at room temperature under vacuum.

5.3.3. Synthesis of polybenzil materials

The dry polybenzoin was redissolved in a solution of DMSO and acetic acid (75:25) in a roundbottom flask equipped with a septum. Ammonium nitrate (1.5 eq) was added to the solution and allowed to dissolve while a 2 % (w/v) solution of copper(II) acetate in DMSO was prepared. A known volume of the copper acetate solution was added to the polymer solution to afford 0.01 equivalents of Cu^{2+} relative to benzoin moiety. The reaction flask was held at 50 °C in an oil bath; the septum was peirced with a needle running to a mineral oil bubbler. The disappearance of the methine and hydroxyl peaks at 6.0 to 6.5 ppm were monitored by ^{1}H NMR. After 24 hours, the oxidized polymer, polybenzil, was precipitated into water, redissolved in DMSO, and reprecipitated into water.

5.3.4. Instrumentation

All nuclear magnetic resonance spectroscopy was performed on a Varian Unity spectrometer operating at 400 MHz. Distilled DMSO-d_6 was used in all cases as the NMR solvent. Correlation spectroscopy (COSY) experiments used a standard double quantum filtered COSY sequence with an acquisition time of 0.167 s and f_1 dimension resolution of 7.65 Hz. Total correlation spectroscopy (TOCSY) parameters included an acquisition time of 0.149 seconds with a resolution in the f_1 dimension of 24.1 Hz. The TOCSY mixing time was 125 milliseconds. Both COSY and TOCSY experiments utilized a sine bell weighting function shifted by $\pi/3$. Transition temperatures were evaluated on a Perkin-Elmer DSC 7 differential scanning calorimeter while the 5 % weight loss values for the polymers were determined using a Perkin-Elmer TGA 7 thermogravimetric analyzer. Intrinsic viscosity measurements were performed in N-methylpyrrolidinone at 25 °C using an Ubbelhode viscometer.

5.4. Results and Discussion

The proposed synthesis route to polyquinoxalines via the benzoin condensation first involved synthesis of a polybenzoin, followed by oxidation of this material to a polybenzil, and finally reacting the polybenzil with ortho-phenylene diamine to achieve a polyquinoxaline material. The reaction scheme is illustrated in Figure 5-2. In this synthesis methodology, the first step, preparation of the polybenzoin precursor, was optimized using the conditions described in the experimental section. Optimum conditions for the oxidation of this material to the polybenzil, however, were never developed. In all cases, an oxidation procedure rigorous enough to oxidize the alcohol to the ketone, seemingly cleaved the polymer chain.

The detailed synthesis scheme shown in Figure 5-3 shows the complex equilibrium necessary for the benzoin condensation reaction to take place. Many factors were found to effect the equilibrium, including reaction temperature, percent cyanide catalyst used, and presence of water in the reaction medium. The equilibrium benzoin condensation reaction proceeded to greater than 99.5 % conversion for both terephthalaldehyde and isophthalaldehyde under conditions using 3 % Et₄NCN catalyst relative to dialdehyde in anhydrous reaction medium at 30 °C. The resulting polybenzoin material was a pale yellow color.

^{1}H NMR was used to identify conditions under which the aldehyde reacts essentially quantitatively. The benzoin condensation reaction proceeds to greater than 99.3 % conversion for both terephthalaldehyde and isophthalaldehyde under the well-defined conditions described in the experimental section (and illustrated in Figure 5-2). The reaction of isophthalaldehyde with tetraethylammonium cyanide was monitored at different catalyst levels, different temperatures, and under protic and aprotic conditions. Catalyst
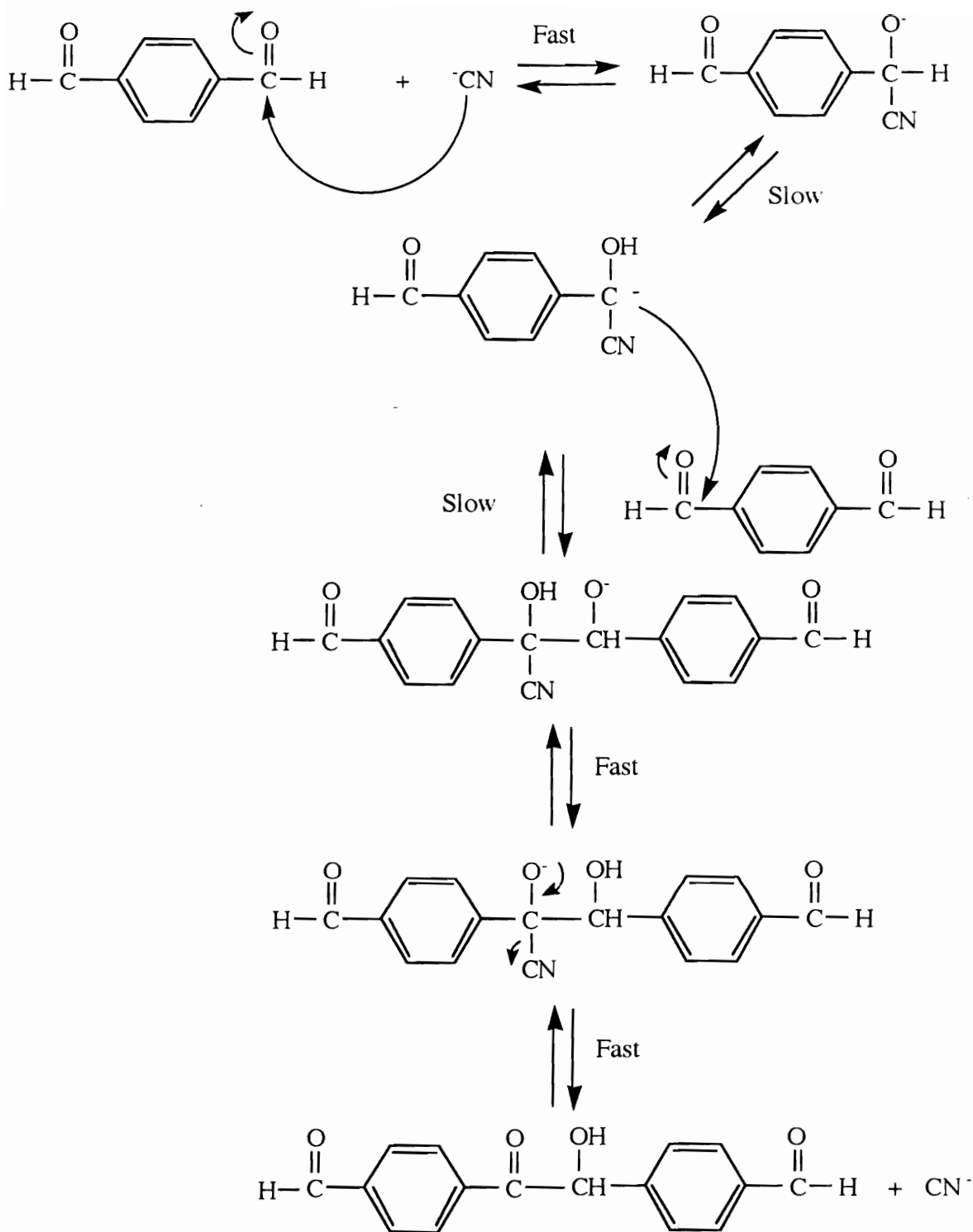
Figure 5-3: Equilibrium benzoin condensation reaction

concentrations ranging from 0.1 mole % to 15 mole % (relative to moles of dialdehyde) were evaluated; the concentration of 3 mole % was optimum for minimizing the amount of cyanide utilized while achieving high percent conversion in the desired time frame. Elevated reaction temperatures (40 °C to 100 °C) never afforded greater than 95 % conversion of monomer to polymer while lower temperatures (0 °C) afforded no conversion of monomer to polymer. ^{1}H NMR spectra of high temperature reaction mixtures showed appearance of a peak between 4.3 and 4.7 ppm, perhaps due to decomposition of the tetraethylammonium cyanide catalyst via a Hoffman degradation mechanism.

Evaluation of protic conditions (non-distilled solvent, non-dried catalyst) relative to aprotic conditions (rigorously dried solvent, catalyst, and monomer) demonstrated that the reaction proceeded to 99+ % conversion under aprotic conditions (Figure 5-4). The reaction performed under protic conditions (containing residual water) stopped at less than 95 % conversion at identical temperatures and percent catalyst. This could be related to the hydrogen transfer in the equilibrium mechanism. The presence of a proton in the reaction solution, other than the proton on the molecule undergoing the reaction, may inhibit the equilibrium from progressing.

The polybenzoins precipitated as fibrous pale yellow polymers in water. They were soluble in polar aprotic solvents such as DMSO, NMP, DMAc, and DMF, but insoluble in ethanol, chloroform, tetrahydrofuran, chlorobenzene, and toluene. Soxhlet extraction in order to remove residual cyanide catalyst was an inappropriate method for purification because the polymers turned into viscous fluids upon soxhlet extraction with methanol.

Two dimensional nuclear magnetic resonance spectroscopy techniques (correlation (COSY) and total correlation (TOCSY) spectroscopy experiments) of the polybenzoins prepared from isophthaldehyde demonstrated strong correlation between the major aromatic resonances labeled in this spectrum. A representative TOCSY spectrum is shown in Figure

Figure 5-4: ^{1}H NMR spectrum of aprotic isophthalaldehyde benzoin condensation reaction
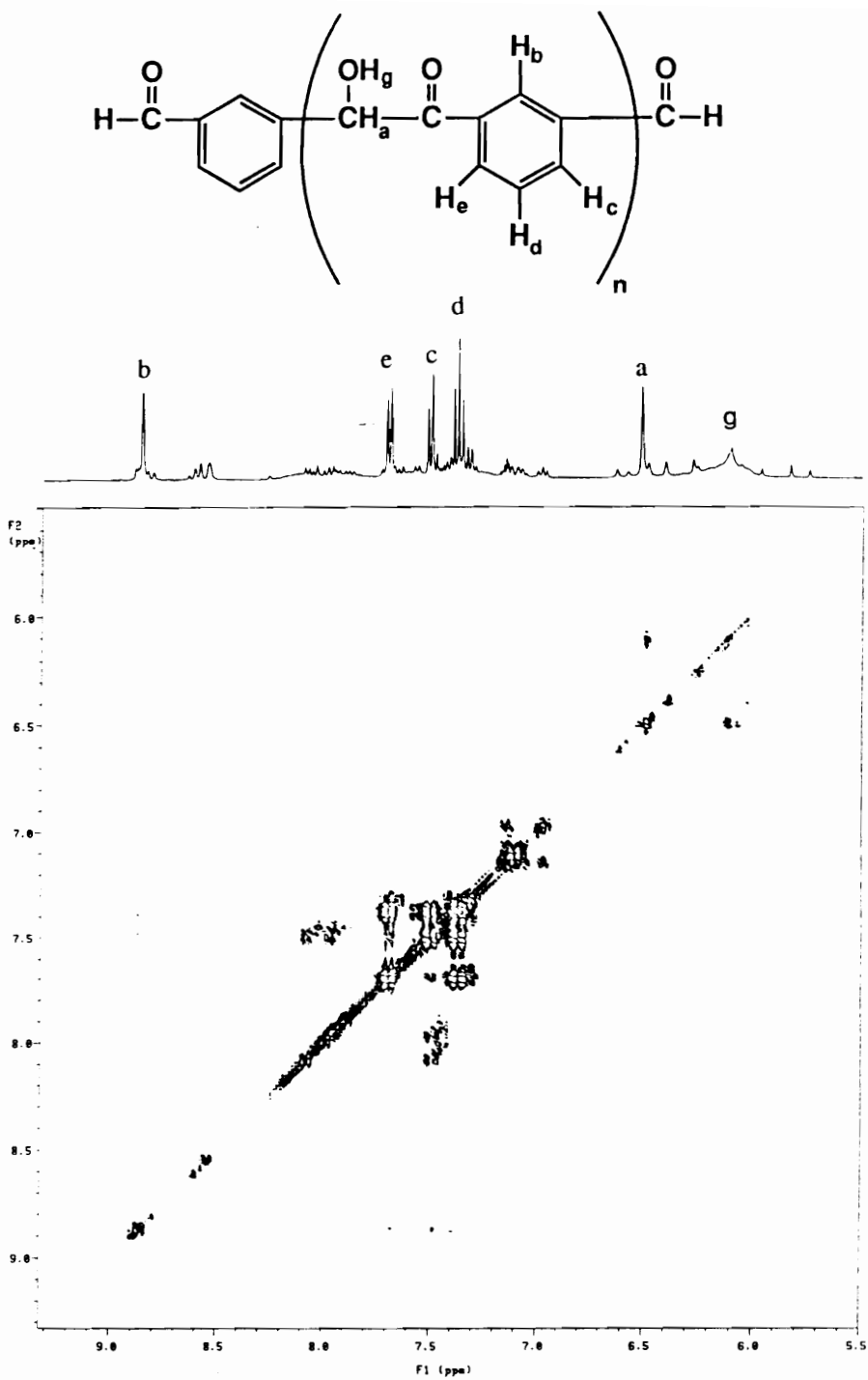
Figure 5-5: Total correlation spectroscopy of polybenzoin of isophthalaldehyde in DMSO-d6 (400 MHz NMR spectrometer)

5-5. The multiplicities and shifts of the peaks suggest that the primary aromatic ring formed in the polybenzoin structure possesses both a carbonyl and a methine substituent. The presence of two distinct doublets, at 7.7 and 7.5 ppm, are indicative of the protons ortho to the carbonyl and ortho to the methine respectively. The triplet at 7.4 ppm is assigned to the proton meta to both the methine and carbonyl substituent and split by the two adjacent protons. The singlet at 8.9 ppm is due to the proton ortho to both the methine and the carbonyl. These results suggest that the aromatic rings of the final polybenzoin structure are set up in a "head-to-tail" fashion. This may be due to equilibration after a statistical polymerization via base promoted tautomer exchange.

Thermal analysis of the uncontrolled molecular weight polybenzoin of terephthaldehyde yielded 5 % weight loss values of 300 °C by TGA under a nitrogen atmosphere with a scan rate of 10 °C/minute. The uncontrolled molecular weight polybenzoin of terephthaldehyde possessed a glass transition temperature of 145 °C (Figure 5-6), while the uncontrolled molecular weight polybenzoin comprised of 90 % terephthaloyl units and 10 % isophthaloyl units had a glass transition temperature of 138 °C (Figure 5-7). Physical data for polybenzoins of terephthaldehyde are presented in Table 5-1. The intrinsic viscosity data shows that high molecular weight polybenzoins were not obtained. This is a direct contradiction of the report by Adb-Alla (234) of high molecular weight polybenzoin synthesis.

Table 5-1: Intrinsic viscosity, TGA, and DSC data for terephthalaldehyde, isophthalaldehyde, and mixed iso/tere polybenzoins of uncontrolled molecular weights

Polybenzoins	$[\eta]^{25\,°C}$ (NMP, dL/g)	5 % wgt loss(°C)	T_g (°C)
tere	0.09	300	145
90 tere/10 iso (w/w)	0.08	325	138
iso	0.08		
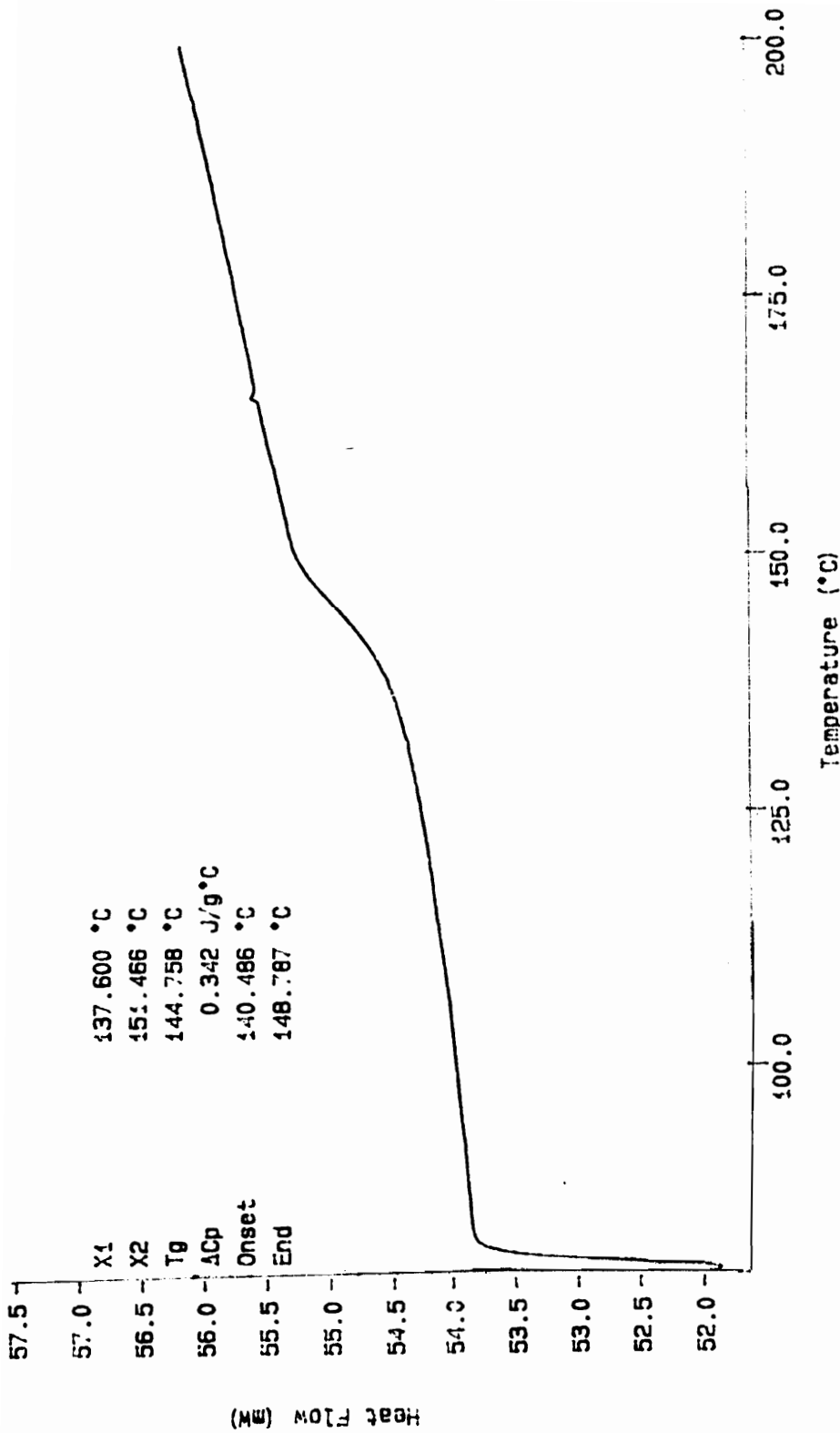
Figure 5-6: Differential scanning calorimetry of polybenzoin of terephthalaldehyde (scan

rate 10 °C/minute under a nitrogen atmosphere)

X1	137.600	°C
X2	151.466	°C
Tg	144.758	°C
ΔCp	0.342	J/g°C
Onset	140.486	°C
End	148.787	°C
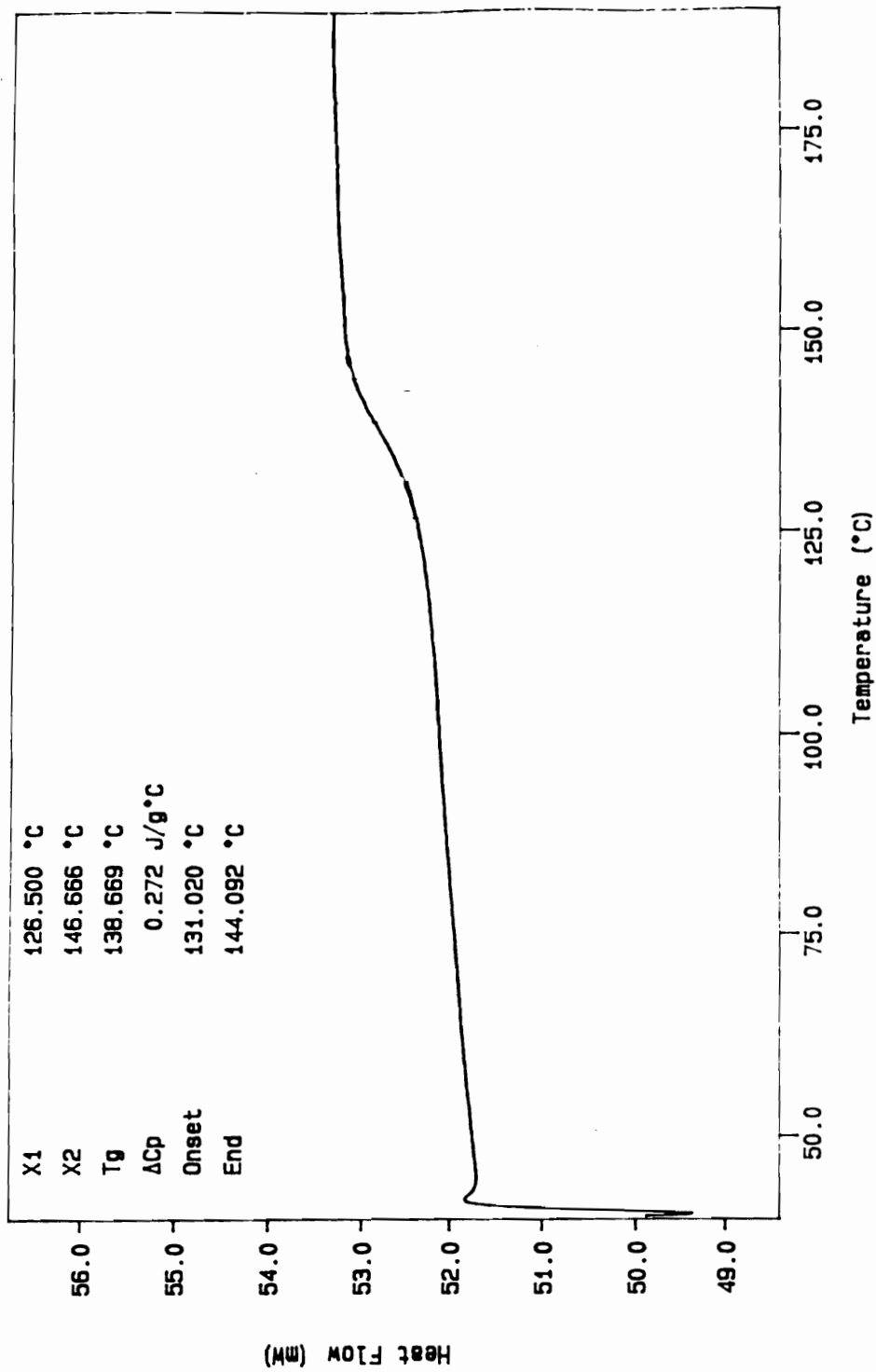
Figure 5-7: Differential scanning calorimetry of polybenzoin of 90/10

tere/isophthalaldehyde (scan rate 10 °C/minute under a nitrogen atmosphere)

X1	126.500 °C
X2	146.666 °C
Tg	138.669 °C
ΔCp	0.272 J/g°C
Onset	131.020 °C
End	144.092 °C

Attempts to oxidize the polybenzoin to polybenzil were unsuccessful. The oxidation procedure was tailored (by ^{1}H NMR) to be rigorous enough to oxidize all of the α-hydroxy-ketone to α-diketone yet not so rigorous as to break up the relatively unstable polybenzoin moiety. Several literature oxidation procedures for the oxidation of benzil to benzoin were attempted, including nitric acid oxidation, acetic anhydride/DMSO oxidation, and the Cu^{2+} oxidation described herein. ^{1}H NMR studies of the first two oxidation procedures showed generation of a peak at 10.5 ppm during the oxidation reaction, indicative of aldehyde or perhaps carboxylic acid formation. The Cu^{2+} oxidation procedure required mild heating to afford complete oxidation of the benzoin to the benzil without generation of chain breakage products. The polybenzoin yellow color converted to deep red after oxidation to the polybenzil structures. However, thermogravimetric analysis of the resulting polybenzil showed a diminished thermal stability of the resulting polybenzil relative to the polybenzoin. Furthermore, the polybenzil showed enhanced solubility and was soluble in solvents such as tetrahydrofuran. These two properties indicate that the polybenzil molecular weight could have decreased during the oxidation step.

5.5. Conclusions

The polyquinoxaline precursor materials described herein could lead to important advances in the field of high performance polymers, providing both low cost and ease of polymerization to an important class of materials. However, under the conditions tested, the benzoin condensation reaction of the aromatic dialdehydes terephthalaldehyde and isophthalaldehyde failed to yield high molecular weight polymers. This was in all likelihood due to the complex series of equilibria occuring in the benzoin condensation reaction. High molecular weight materials are only achieved when the polymerization is

pushed to greater than 99.9 percent conversion monomer to polymer; a difficult task for an equilibrium reaction. Furthermore, subsequent oxidation reactions on the polybenzoin material resulted in a decrease of molecular weight, probably due to cleavage of the fragile benzoin functionality.

CHAPTER 6

Conclusions

The thermal analysis data indicated that poly(arylene ether phosphine oxide), poly(arylene ether sulfoxide), and poly(arylene ether pyridine) were miscible with epoxy thermosets while poly(arylene ether sulfone) was not. These results mirrored the information obtained from the ^{1}H NMR calculations which illustrated that diphenylsulfone was the weakest hydrogen bonder of the set of model compounds (triphenylphosphine oxide, diphenylmethylphosphine oxide, pyridine, diphenylsulfoxide, and diphenylsulfone).

The ^{1}H NMR data for the diphenylsulfone, diphenylsulfoxide, and pyridine followed a linear trend for the shift of the proton hydrogen bonded to the model compound with respect to the calculated equilibrium constant of hydrogen bond formation. The phosphine oxide-containing model compounds, on the other hand, did not follow this trend. It is possible that a different mechanism of hydrogen bond complex formation is occurring in the phosphine oxide-containing materials. The experiment was repeated with diphenylmethylphosphine oxide as the hydrogen bond acceptor to ascertain whether the difference between the triphenylphosphine oxide and the other model compounds was due to steric effects caused by the bulky phenyl substituents. The diphenylmethylphosphine oxide, however, yielded results similar to those of triphenylphosphine oxide. This suggests that the difference between the phosphine oxide-containing model compounds and the other model compounds is not due to steric hindrance but may in fact be due to the inherent nature of the phosphine oxide ligand.

The ^{1}H NMR calculations are a useful tool for evaluating hydrogen bonding parameters but have several limitations. First, the hydrogen bond acceptor must be soluble

in the test solution. In this research, the test solution was 97/3 DMSO-d_6/water; the poly(arylene ether)s were insoluble in this solution to any measureable concentration. Due to this constraint, hydrogen bonding studies were performed on model compounds. Furthermore, the hydrogen bond formation in solution results from several hydrogen bonding equilibria; the desired values of the equilibrium constant for hydrogen bond formation between water and the model compound, as well as the shift of the hydrogen that is hydrogen bonded to the model compound, must be deconvoluted from the shift of water in the ternary DMSO-d_6/water/model compound solution. Finally, the basic premise of the two step calculation: first determination of the equilibrium constants for the binary DMSO-d_6/water solution, followed by determination of the constants for the ternary DMSO-d_6/water/model compound solution, assumes that the DMSO-d_6/water equilibrium remains the same despite the addition of the model compound.

CHAPTER 7

Suggested future studies

Additional research is recommended to verify the ability of the ^{1}H NMR

calculations to measure hydrogen bonding potentials of specific functional groups. The

work should be repeated using different concentrations of DMSO-d$_6$/water solutions and at

different temperatures to evaluate ΔH and ΔS for the hydrogen bond formation. This work

will ascertain whether the trends evidenced by the model compounds remain the same

under a variety of conditions. Further investigation into the anomalous solution properties

of the phosphine oxide-containing model compounds will also be of interest. Furthermore,

^{1}H NMR studies utilizing 2-propanol as the hydrogen bond donor would also be of value.

This would identify hydrogen bonding parameters between the functional groups of interest

and a secondary alcohol, more clearly representing the situation occurring when the

poly(arylene ether) hydrogen bonds with an epoxy matrix.

To determine whether poly(arylene ether)s possessing the electron rich functional

groups mimic the hydrogen bonding behavior of model compounds, the approach of

Coleman should be pursued. Coleman used FTIR spectroscopy to evaluate

polyester/phenoxy interactions (94). This method, used to calculate parameters for

poly(arylene ether)/phenoxy blends, should accurately illustrate poly(arylene ether)/epoxy

interactions.

Alternatively, poly(arylene ether)/epoxy interactions may be evaluated by

employing the Gordon-Taylor Equation and thermal analysis on a series of

epoxy/poly(arylene ether) blends with systematically varied compositions. The glass

transition temperature may be plotted as a function of weight percent poly(arylene ether)

and fitted to the Gordon-Taylor Equation to determine whether the poly(arylene ether)/epoxy interactions are favorable.

The long term goal of this collaborative research project is to determine the effect of a ductile sizing material on the mechanical properties of the final epoxy/graphite fiber composite. The graphite fibers must first be sized with the poly(arylene ether) material, then prepregged with epoxy resin and cured. Placing the sized fibers in a dogbone-shaped mold and filling the mold with epoxy resin will produce a sample ready for mechanical testing. Scanning electron microscopy of the fraction surface of the specimen will elucidate how much the poly(arylene ether) diffuses into the epoxy thermoset during cure. The effect of both the sizing and of the gradient ductile/thermoset interphase on the mechanical properties of the composite could thus be evaluated.

Table A-1: A portion of the spreadsheet table used to calculate K_o, K_n, and δ_{bn} for the DMSO-d_6/water ^{1}H NMR samples (8 pages)

Kn	Ko	delta H-DMSO	Init. F water Oxygens	Init. F DMSO oxygens	A	B	C
39.8	29.5	3.33	0.06450	0.87100	1.05489	1.00843	0.05618
39.8	32.5	3.33	0.06450	0.87100	1.06047	1.01330	0.05618
39.8	35.5	3.33	0.06450	0.87100	1.06605	1.01816	0.05618
39.8	38.5	3.33	0.06450	0.87100	1.07163	1.02302	0.05618
39.8	41.5	3.33	0.06450	0.87100	1.07722	1.02788	0.05618
39.8	44.5	3.33	0.06450	0.87100	1.08280	1.03274	0.05618
39.8	47.5	3.33	0.06450	0.87100	1.08838	1.03760	0.05618
39.8	50.5	3.33	0.06450	0.87100	1.09396	1.04247	0.05618
39.8	53.5	3.33	0.06450	0.87100	1.09954	1.04733	0.05618
39.8	56.5	3.33	0.06450	0.87100	1.10513	1.05219	0.05618
39.8	29.5	3.34	0.06450	0.87100	1.05489	1.00843	0.05618
39.8	32.5	3.34	0.06450	0.87100	1.06047	1.01330	0.05618
39.8	35.5	3.34	0.06450	0.87100	1.06605	1.01816	0.05618
39.8	38.5	3.34	0.06450	0.87100	1.07163	1.02302	0.05618
39.8	41.5	3.34	0.06450	0.87100	1.07722	1.02788	0.05618
39.8	44.5	3.34	0.06450	0.87100	1.08280	1.03274	0.05618
39.8	47.5	3.34	0.06450	0.87100	1.08838	1.03760	0.05618
39.8	50.5	3.34	0.06450	0.87100	1.09396	1.04247	0.05618
39.8	53.5	3.34	0.06450	0.87100	1.09954	1.04733	0.05618
39.8	56.5	3.35	0.06450	0.87100	1.10513	1.05219	0.05618
39.8	29.5	3.35	0.06450	0.87100	1.05489	1.00843	0.05618
39.8	32.5	3.35	0.06450	0.87100	1.06047	1.01330	0.05618
39.8	35.5	3.35	0.06450	0.87100	1.06605	1.01816	0.05618
39.8	38.5	3.35	0.06450	0.87100	1.07163	1.02302	0.05618
39.8	41.5	3.35	0.06450	0.87100	1.07722	1.02788	0.05618
39.8	44.5	3.35	0.06450	0.87100	1.08280	1.03274	0.05618
39.8	47.5	3.35	0.06450	0.87100	1.08838	1.03760	0.05618
39.8	50.5	3.35	0.06450	0.87100	1.09396	1.04247	0.05618
39.8	53.5	3.35	0.06450	0.87100	1.09954	1.04733	0.05618
39.8	56.5	3.35	0.06450	0.87100	1.10513	1.05219	0.05618
39.8	29.5	3.36	0.06450	0.87100	1.05489	1.00843	0.05618

39.8	32.5	3.36	0.06450	0.87100	1.06047	1.01330	0.05618
39.8	35.5	3.36	0.06450	0.87100	1.06605	1.01816	0.05618
39.8	38.5	3.36	0.06450	0.87100	1.07163	1.02302	0.05618
39.8	41.5	3.36	0.06450	0.87100	1.07722	1.02788	0.05618
39.8	44.5	3.36	0.06450	0.87100	1.08280	1.03274	0.05618
39.8	47.5	3.36	0.06450	0.87100	1.08838	1.03760	0.05618
39.8	50.5	3.36	0.06450	0.87100	1.09396	1.04247	0.05618
39.8	53.5	3.36	0.06450	0.87100	1.09954	1.04733	0.05618
39.8	56.5	3.36	0.06450	0.87100	1.10513	1.05219	0.05618
39.8	29.5	3.37	0.06450	0.87100	1.05489	1.00843	0.05618
39.8	32.5	3.37	0.06450	0.87100	1.06047	1.01330	0.05618
39.8	35.5	3.37	0.06450	0.87100	1.06605	1.01816	0.05618
39.8	38.5	3.37	0.06450	0.87100	1.07163	1.02302	0.05618
39.8	41.5	3.37	0.06450	0.87100	1.07722	1.02788	0.05618
39.8	44.5	3.37	0.06450	0.87100	1.08280	1.03274	0.05618
39.8	47.5	3.37	0.06450	0.87100	1.08838	1.03760	0.05618
39.8	50.5	3.37	0.06450	0.87100	1.09396	1.04247	0.05618
39.8	53.5	3.37	0.06450	0.87100	1.09954	1.04733	0.05618
39.8	56.5	3.37	0.06450	0.87100	1.10513	1.05219	0.05618
39.8	29.5	3.37	0.06450	0.87100	1.05489	1.00843	0.05618
39.8	32.5	3.38	0.06450	0.87100	1.06047	1.01330	0.05618
39.8	35.5	3.38	0.06450	0.87100	1.06605	1.01816	0.05618
39.8	38.5	3.38	0.06450	0.87100	1.07163	1.02302	0.05618
39.8	41.5	3.38	0.06450	0.87100	1.07722	1.02788	0.05618
39.8	44.5	3.38	0.06450	0.87100	1.08280	1.03274	0.05618
39.8	47.5	3.38	0.06450	0.87100	1.08838	1.03760	0.05618
39.8	50.5	3.38	0.06450	0.87100	1.09396	1.04247	0.05618
39.8	53.5	3.38	0.06450	0.87100	1.09954	1.04733	0.05618
39.8	56.5	3.38	0.06450	0.87100	1.10513	1.05219	0.05618
39.8	29.5	3.39	0.06450	0.87100	1.05489	1.00843	0.05618
39.8	32.5	3.39	0.06450	0.87100	1.06047	1.01330	0.05618
39.8	35.5	3.39	0.06450	0.87100	1.06605	1.01816	0.05618

39.8	38.5	3.39	0.06450		0.87100	1.07163	1.02302	0.05618
39.8	41.5	3.39	0.06450		0.87100	1.07722	1.02788	0.05618
39.8	44.5	3.39	0.06450		0.87100	1.08280	1.03274	0.05618
39.8	47.5	3.39	0.06450		0.87100	1.08838	1.03760	0.05618
39.8	50.5	3.39	0.06450		0.87100	1.09396	1.04247	0.05618
39.8	53.5	3.39	0.06450		0.87100	1.09954	1.04733	0.05618
39.8	56.5	3.39	0.06450		0.87100	1.10513	1.05219	0.05618
39.8	29.5	3.40	0.06450		0.87100	1.05489	1.00843	0.05618
39.8	32.5	3.40	0.06450		0.87100	1.06047	1.01330	0.05618
39.8	35.5	3.40	0.06450		0.87100	1.06605	1.01816	0.05618
39.8	38.5	3.40	0.06450		0.87100	1.07163	1.02302	0.05618
39.8	41.5	3.40	0.06450		0.87100	1.07722	1.02788	0.05618
39.8	44.5	3.40	0.06450		0.87100	1.08280	1.03274	0.05618
39.8	47.5	3.40	0.06450		0.87100	1.08838	1.03760	0.05618
39.8	50.5	3.40	0.06450		0.87100	1.09396	1.04247	0.05618
39.8	53.5	3.40	0.06450		0.87100	1.09954	1.04733	0.05618
39.8	56.5	3.40	0.06450		0.87100	1.10513	1.05219	0.05618
39.8	29.5	3.41	0.06450		0.87100	1.05489	1.00843	0.05618
39.8	32.5	3.41	0.06450		0.87100	1.06047	1.01330	0.05618
39.8	35.5	3.41	0.06450		0.87100	1.06605	1.01816	0.05618
39.8	38.5	3.41	0.06450		0.87100	1.07163	1.02302	0.05618
39.8	41.5	3.41	0.06450		0.87100	1.07722	1.02788	0.05618
39.8	44.5	3.41	0.06450		0.87100	1.08280	1.03274	0.05618
39.8	47.5	3.41	0.06450		0.87100	1.08838	1.03760	0.05618
39.8	50.5	3.41	0.06450		0.87100	1.09396	1.04247	0.05618
39.8	53.5	3.41	0.06450		0.87100	1.09954	1.04733	0.05618
39.8	56.5	3.41	0.06450		0.87100	1.10513	1.05219	0.05618
39.8	29.5	3.42	0.06450		0.87100	1.05489	1.00843	0.05618
39.8	32.5	3.42	0.06450		0.87100	1.06047	1.01330	0.05618
39.8	35.5	3.42	0.06450		0.87100	1.06605	1.01816	0.05618
39.8	38.5	3.42	0.06450		0.87100	1.07163	1.02302	0.05618
39.8	41.5	3.42	0.06450		0.87100	1.07722	1.02788	0.05618

39.8	44.5	3.42	0.06450	0.87100	1.08280	1.03274	0.05618
39.8	47.5	3.42	0.06450	0.87100	1.08838	1.03760	0.05618
39.8	50.5	3.42	0.06450	0.87100	1.09396	1.04247	0.05618
39.8	53.5	3.42	0.06450	0.87100	1.09954	1.04733	0.05618
39.8	56.5	3.42	0.06450	0.87100	1.10513	1.05219	0.05618
39.8	29.5	3.33	0.06450	0.87100	1.05104	1.00332	0.05618
42.8	32.5	3.33	0.06450	0.87100	1.05623	1.00784	0.05618
42.8	35.5	3.33	0.06450	0.87100	1.06142	1.01236	0.05618
42.8	38.5	3.33	0.06450	0.87100	1.06661	1.01688	0.05618
42.8	41.5	3.33	0.06450	0.87100	1.07180	1.02141	0.05618
42.8	44.5	3.33	0.06450	0.87100	1.07699	1.02593	0.05618
42.8	47.5	3.33	0.06450	0.87100	1.08218	1.03045	0.05618
42.8	50.5	3.33	0.06450	0.87100	1.08738	1.03497	0.05618
42.8	53.5	3.33	0.06450	0.87100	1.09257	1.03949	0.05618
42.8	56.5	3.33	0.06450	0.87100	1.09776	1.04401	0.05618
42.8	29.5	3.34	0.06450	0.87100	1.05104	1.00332	0.05618
42.8	32.5	3.34	0.06450	0.87100	1.05623	1.00784	0.05618
42.8	35.5	3.34	0.06450	0.87100	1.06142	1.01236	0.05618
42.8	38.5	3.34	0.06450	0.87100	1.06661	1.01688	0.05618
42.8	41.5	3.34	0.06450	0.87100	1.07180	1.02141	0.05618
42.8	44.5	3.34	0.06450	0.87100	1.07699	1.02593	0.05618
42.8	47.5	3.34	0.06450	0.87100	1.08218	1.03045	0.05618
42.8	50.5	3.34	0.06450	0.87100	1.08738	1.03497	0.05618
42.8	53.5	3.34	0.06450	0.87100	1.09257	1.03949	0.05618
42.8	56.5	3.34	0.06450	0.87100	1.09776	1.04401	0.05618
42.8	29.5	3.35	0.06450	0.87100	1.05104	1.00332	0.05618
42.8	32.5	3.35	0.06450	0.87100	1.05623	1.00784	0.05618
42.8	35.5	3.35	0.06450	0.87100	1.06142	1.01236	0.05618
42.8	38.5	3.35	0.06450	0.87100	1.06661	1.01688	0.05618
42.8	41.5	3.35	0.06450	0.87100	1.07180	1.02141	0.05618
42.8	44.5	3.35	0.06450	0.87100	1.07699	1.02593	0.05618
42.8	47.5	3.35	0.06450	0.87100	1.08218	1.03045	0.05618

Fwater-bonded DMSO	F water-water	theor. shift(.1)	observed shift(.1)
0.05940	0.00332	3.35636	3.445
0.05910	0.00362	3.36595	3.445
0.05880	0.00391	3.37521	3.445
0.05850	0.00420	3.38414	3.445
0.05821	0.00448	3.39275	3.445
0.05792	0.00476	3.40106	3.445
0.05763	0.00503	3.40908	3.445
0.05734	0.00529	3.41681	3.445
0.05706	0.00555	3.42427	3.445
0.05678	0.00581	3.43146	3.445
0.05940	0.00332	3.36557	3.445
0.05910	0.00362	3.37512	3.445
0.05880	0.00391	3.38433	3.445
0.05850	0.00420	3.39321	3.445
0.05821	0.00448	3.40178	3.445
0.05792	0.00476	3.41004	3.445
0.05763	0.00503	3.41801	3.445
0.05734	0.00529	3.42570	3.445
0.05706	0.00555	3.43311	3.445
0.05678	0.00581	3.44027	3.445
0.05940	0.00332	3.37478	3.445
0.05910	0.00362	3.38428	3.445
0.05880	0.00391	3.39344	3.445
0.05850	0.00420	3.40228	3.445
0.05821	0.00448	3.41080	3.445
0.05792	0.00476	3.41902	3.445
0.05763	0.00503	3.42695	3.445
0.05734	0.00529	3.43459	3.445
0.05706	0.00555	3.44196	3.445
0.05678	0.00581	3.44907	3.445
0.05940	0.00332	3.38398	3.445

	0.05910	0.00362	3.39344	3.445
	0.05880	0.00391	3.40256	3.445
	0.05850	0.00420	3.41135	3.445
	0.05821	0.00448	3.41983	3.445
	0.05792	0.00476	3.42800	3.445
	0.05763	0.00503	3.43588	3.445
	0.05734	0.00529	3.44348	3.445
	0.05706	0.00555	3.45081	3.445
	0.05678	0.00581	3.45787	3.445
	0.05940	0.00332	3.39319	3.445
	0.05910	0.00362	3.40260	3.445
	0.05880	0.00391	3.41168	3.445
	0.05850	0.00420	3.42042	3.445
	0.05821	0.00448	3.42885	3.445
	0.05792	0.00476	3.43698	3.445
	0.05763	0.00503	3.44481	3.445
	0.05734	0.00529	3.45237	3.445
	0.05706	0.00555	3.45965	3.445
	0.05678	0.00581	3.46667	3.445
	0.05940	0.00332	3.40240	3.445
	0.05910	0.00362	3.41177	3.445
	0.05880	0.00391	3.42079	3.445
	0.05850	0.00420	3.42949	3.445
	0.05821	0.00448	3.43788	3.445
	0.05792	0.00476	3.44596	3.445
	0.05763	0.00503	3.45375	3.445
	0.05734	0.00529	3.46126	3.445
	0.05706	0.00555	3.46850	3.445
	0.05678	0.00581	3.47548	3.445
	0.05940	0.00332	3.41161	3.445
	0.05910	0.00362	3.42093	3.445
	0.05880	0.00391	3.42991	3.445

0.05850	0.00420	3.43856	3.445
0.05821	0.00448	3.44690	3.445
0.05792	0.00476	3.45494	3.445
0.05763	0.00503	3.46268	3.445
0.05734	0.00529	3.47015	3.445
0.05706	0.00555	3.47735	3.445
0.05678	0.00581	3.48428	3.445
0.05940	0.00332	3.42082	3.445
0.05910	0.00362	3.43009	3.445
0.05880	0.00391	3.43902	3.445
0.05850	0.00420	3.44763	3.445
0.05821	0.00448	3.45592	3.445
0.05792	0.00476	3.46392	3.445
0.05763	0.00503	3.47162	3.445
0.05734	0.00529	3.47904	3.445
0.05706	0.00555	3.48619	3.445
0.05678	0.00581	3.49308	3.445
0.05940	0.00332	3.43003	3.445
0.05910	0.00362	3.43925	3.445
0.05880	0.00391	3.44814	3.445
0.05850	0.00420	3.45670	3.445
0.05821	0.00448	3.46495	3.445
0.05792	0.00476	3.47290	3.445
0.05763	0.00503	3.48055	3.445
0.05734	0.00529	3.48793	3.445
0.05706	0.00555	3.49504	3.445
0.05678	0.00581	3.50189	3.445
0.05940	0.00332	3.43924	3.445
0.05910	0.00362	3.44842	3.445
0.05880	0.00391	3.45725	3.445
0.05850	0.00420	3.46577	3.445
0.05821	0.00448	3.47397	3.445

0.05792	0.00476	3.48187	3.445
0.05763	0.00503	3.48949	3.445
0.05734	0.00529	3.49682	3.445
0.05706	0.00555	3.50388	3.445
0.05678	0.00581	3.51069	3.445
0.05973	0.00312	3.35552	3.445
0.05945	0.00340	3.36467	3.445
0.05916	0.00368	3.37352	3.445
0.05888	0.00395	3.38207	3.445
0.05861	0.00422	3.39033	3.445
0.05833	0.00448	3.39833	3.445
0.05806	0.00474	3.40606	3.445
0.05779	0.00499	3.41353	3.445
0.05752	0.00524	3.42076	3.445
0.05726	0.00548	3.42774	3.445
0.05973	0.00312	3.36478	3.445
0.05945	0.00340	3.37389	3.445
0.05916	0.00368	3.38269	3.445
0.05888	0.00395	3.39120	3.445
0.05861	0.00422	3.39942	3.445
0.05833	0.00448	3.40737	3.445
0.05806	0.00474	3.41506	3.445
0.05779	0.00499	3.42249	3.445
0.05752	0.00524	3.42968	3.445
0.05726	0.00548	3.43662	3.445
0.05973	0.00312	3.37405	3.445
0.05945	0.00340	3.38311	3.445
0.05916	0.00368	3.39186	3.445
0.05888	0.00395	3.40033	3.445
0.05861	0.00422	3.40851	3.445
0.05833	0.00448	3.41642	3.445
0.05806	0.00474	3.42406	3.445

Table A-2: Sample calculation of the "norm" value across seven concentrations of DMSO-d$_6$/water ^{1}H NMR samples (eight pages)

theor. shift(.1)	obs. shift(.1)	theor. shift(.2)	obs. shift(.2)	theor. shift(.3)	obs. shift(.3)	theor. shift(.4)	obs. shift(.4)	theor. shift(.5)
3.356	3.445	3.474	3.582	3.615	3.728	3.784	3.885	3.984
3.366	3.445	3.491	3.582	3.634	3.728	3.797	3.885	3.983
3.375	3.445	3.505	3.582	3.649	3.728	3.807	3.885	3.978
3.384	3.445	3.519	3.582	3.663	3.728	3.814	3.885	3.970
3.393	3.445	3.532	3.582	3.674	3.728	3.818	3.885	3.961
3.401	3.445	3.544	3.582	3.684	3.728	3.820	3.885	3.949
3.409	3.445	3.554	3.582	3.692	3.728	3.820	3.885	3.937
3.417	3.445	3.564	3.582	3.698	3.728	3.819	3.885	3.924
3.424	3.445	3.573	3.582	3.704	3.728	3.816	3.885	3.910
3.431	3.445	3.581	3.582	3.708	3.728	3.813	3.885	3.896
3.366	3.445	3.483	3.582	3.623	3.728	3.791	3.885	3.990
3.375	3.445	3.499	3.582	3.641	3.728	3.804	3.885	3.989
3.384	3.445	3.514	3.582	3.657	3.728	3.814	3.885	3.984
3.393	3.445	3.528	3.582	3.670	3.728	3.820	3.885	3.976
3.402	3.445	3.540	3.582	3.681	3.728	3.824	3.885	3.966
3.410	3.445	3.552	3.582	3.691	3.728	3.826	3.885	3.955
3.418	3.445	3.562	3.582	3.699	3.728	3.826	3.885	3.942
3.426	3.445	3.572	3.582	3.705	3.728	3.825	3.885	3.929
3.433	3.445	3.581	3.582	3.711	3.728	3.822	3.885	3.915
3.440	3.445	3.589	3.582	3.715	3.728	3.819	3.885	3.900
3.375	3.445	3.491	3.582	3.631	3.728	3.798	3.885	3.996
3.384	3.445	3.508	3.582	3.649	3.728	3.811	3.885	3.995
3.393	3.445	3.522	3.582	3.665	3.728	3.821	3.885	3.990
3.402	3.445	3.536	3.582	3.678	3.728	3.827	3.885	3.982
3.411	3.445	3.548	3.582	3.689	3.728	3.831	3.885	3.972
3.419	3.445	3.560	3.582	3.698	3.728	3.833	3.885	3.960
3.427	3.445	3.570	3.582	3.706	3.728	3.832	3.885	3.947
3.435	3.445	3.580	3.582	3.712	3.728	3.831	3.885	3.934
3.442	3.445	3.589	3.582	3.718	3.728	3.828	3.885	3.920
3.449	3.445	3.597	3.582	3.722	3.728	3.824	3.885	3.905
3.384	3.445	3.500	3.582	3.639	3.728	3.806	3.885	4.003

3.393	3.445	3.516	3.582	3.657	3.728	3.818	3.885	4.001
3.403	3.445	3.531	3.582	3.672	3.728	3.828	3.885	3.996
3.411	3.445	3.544	3.582	3.685	3.728	3.834	3.885	3.988
3.420	3.445	3.557	3.582	3.696	3.728	3.837	3.885	3.977
3.428	3.445	3.568	3.582	3.706	3.728	3.839	3.885	3.966
3.436	3.445	3.579	3.582	3.713	3.728	3.839	3.885	3.953
3.443	3.445	3.588	3.582	3.720	3.728	3.837	3.885	3.939
3.451	3.445	3.597	3.582	3.725	3.728	3.834	3.885	3.925
3.458	3.445	3.605	3.582	3.729	3.728	3.830	3.885	3.910
3.393	3.445	3.509	3.582	3.647	3.728	3.813	3.885	4.009
3.403	3.445	3.525	3.582	3.665	3.728	3.825	3.885	4.007
3.412	3.445	3.539	3.582	3.680	3.728	3.834	3.885	4.002
3.420	3.445	3.553	3.582	3.693	3.728	3.840	3.885	3.993
3.429	3.445	3.565	3.582	3.704	3.728	3.844	3.885	3.983
3.437	3.445	3.576	3.582	3.713	3.728	3.845	3.885	3.971
3.445	3.445	3.587	3.582	3.720	3.728	3.845	3.885	3.958
3.452	3.445	3.596	3.582	3.727	3.728	3.843	3.885	3.944
3.460	3.445	3.605	3.582	3.732	3.728	3.840	3.885	3.930
3.467	3.445	3.613	3.582	3.736	3.728	3.836	3.885	3.915
3.402	3.445	3.517	3.582	3.655	3.728	3.820	3.885	4.015
3.412	3.445	3.533	3.582	3.672	3.728	3.832	3.885	4.013
3.421	3.445	3.548	3.582	3.688	3.728	3.841	3.885	4.008
3.429	3.445	3.561	3.582	3.700	3.728	3.847	3.885	3.999
3.438	3.445	3.573	3.582	3.711	3.728	3.850	3.885	3.989
3.446	3.445	3.584	3.582	3.720	3.728	3.852	3.885	3.977
3.454	3.445	3.595	3.582	3.728	3.728	3.851	3.885	3.963
3.461	3.445	3.604	3.582	3.734	3.728	3.849	3.885	3.949
3.468	3.445	3.613	3.582	3.739	3.728	3.846	3.885	3.935
3.475	3.445	3.621	3.582	3.742	3.728	3.842	3.885	3.920
3.412	3.445	3.526	3.582	3.663	3.728	3.827	3.885	4.021
3.421	3.445	3.542	3.582	3.680	3.728	3.839	3.885	4.019
3.430	3.445	3.556	3.582	3.695	3.728	3.848	3.885	4.013

3.439	3.445	3.569	3.582	3.708	3.728	3.854	3.885	4.005
3.447	3.445	3.581	3.582	3.719	3.728	3.857	3.885	3.994
3.455	3.445	3.593	3.582	3.727	3.728	3.858	3.885	3.982
3.463	3.445	3.603	3.582	3.735	3.728	3.858	3.885	3.969
3.470	3.445	3.612	3.582	3.741	3.728	3.855	3.885	3.955
3.477	3.445	3.621	3.582	3.746	3.728	3.852	3.885	3.940
3.484	3.445	3.628	3.582	3.749	3.728	3.848	3.885	3.925
3.421	3.445	3.534	3.582	3.671	3.728	3.834	3.885	4.028
3.430	3.445	3.550	3.582	3.688	3.728	3.846	3.885	4.025
3.439	3.445	3.564	3.582	3.703	3.728	3.855	3.885	4.019
3.448	3.445	3.578	3.582	3.715	3.728	3.861	3.885	4.011
3.456	3.445	3.590	3.582	3.726	3.728	3.864	3.885	4.000
3.464	3.445	3.601	3.582	3.735	3.728	3.865	3.885	3.987
3.472	3.445	3.611	3.582	3.742	3.728	3.864	3.885	3.974
3.479	3.445	3.620	3.582	3.748	3.728	3.862	3.885	3.960
3.486	3.445	3.629	3.582	3.753	3.728	3.858	3.885	3.945
3.493	3.445	3.636	3.582	3.756	3.728	3.854	3.885	3.930
3.430	3.445	3.543	3.582	3.679	3.728	3.841	3.885	4.034
3.439	3.445	3.559	3.582	3.696	3.728	3.853	3.885	4.031
3.448	3.445	3.573	3.582	3.711	3.728	3.862	3.885	4.025
3.457	3.445	3.586	3.582	3.723	3.728	3.867	3.885	4.016
3.465	3.445	3.598	3.582	3.733	3.728	3.870	3.885	4.005
3.473	3.445	3.609	3.582	3.742	3.728	3.871	3.885	3.993
3.481	3.445	3.619	3.582	3.749	3.728	3.870	3.885	3.979
3.488	3.445	3.628	3.582	3.755	3.728	3.868	3.885	3.965
3.495	3.445	3.636	3.582	3.760	3.728	3.864	3.885	3.950
3.502	3.445	3.644	3.582	3.763	3.728	3.860	3.885	3.935
3.439	3.445	3.552	3.582	3.687	3.728	3.848	3.885	4.040
3.448	3.445	3.567	3.582	3.704	3.728	3.860	3.885	4.038
3.457	3.445	3.581	3.582	3.718	3.728	3.869	3.885	4.031
3.466	3.445	3.594	3.582	3.730	3.728	3.874	3.885	4.022
3.474	3.445	3.606	3.582	3.741	3.728	3.877	3.885	4.011

3.482	3.445	3.617	3.582	3.749	3.728	3.877	3.885	3.998
3.489	3.445	3.627	3.582	3.756	3.728	3.876	3.885	3.985
3.497	3.445	3.636	3.582	3.762	3.728	3.874	3.885	3.970
3.504	3.445	3.644	3.582	3.767	3.728	3.870	3.885	3.955
3.511	3.445	3.652	3.582	3.770	3.728	3.866	3.885	3.940
3.356	3.445	3.470	3.582	3.610	3.728	3.785	3.885	3.999
3.365	3.445	3.486	3.582	3.629	3.728	3.800	3.885	4.000
3.374	3.445	3.500	3.582	3.645	3.728	3.811	3.885	3.997
3.382	3.445	3.514	3.582	3.660	3.728	3.819	3.885	3.992
3.390	3.445	3.527	3.582	3.672	3.728	3.825	3.885	3.984
3.398	3.445	3.539	3.582	3.682	3.728	3.828	3.885	3.974
3.406	3.445	3.549	3.582	3.691	3.728	3.830	3.885	3.963
3.414	3.445	3.559	3.582	3.699	3.728	3.830	3.885	3.951
3.421	3.445	3.569	3.582	3.705	3.728	3.828	3.885	3.938
3.428	3.445	3.577	3.582	3.710	3.728	3.826	3.885	3.925
3.365	3.445	3.478	3.582	3.618	3.728	3.792	3.885	4.005
3.374	3.445	3.494	3.582	3.637	3.728	3.807	3.885	4.006
3.383	3.445	3.509	3.582	3.653	3.728	3.818	3.885	4.003
3.391	3.445	3.523	3.582	3.667	3.728	3.826	3.885	3.998
3.399	3.445	3.535	3.582	3.679	3.728	3.831	3.885	3.989
3.407	3.445	3.547	3.582	3.690	3.728	3.835	3.885	3.979
3.415	3.445	3.558	3.582	3.698	3.728	3.836	3.885	3.968
3.422	3.445	3.567	3.582	3.706	3.728	3.836	3.885	3.956
3.430	3.445	3.577	3.582	3.712	3.728	3.835	3.885	3.943
3.437	3.445	3.585	3.582	3.717	3.728	3.832	3.885	3.930
3.374	3.445	3.487	3.582	3.626	3.728	3.799	3.885	4.012
3.383	3.445	3.503	3.582	3.645	3.728	3.814	3.885	4.013
3.392	3.445	3.517	3.582	3.661	3.728	3.825	3.885	4.010
3.400	3.445	3.531	3.582	3.675	3.728	3.833	3.885	4.003
3.409	3.445	3.543	3.582	3.687	3.728	3.838	3.885	3.995
3.416	3.445	3.555	3.582	3.697	3.728	3.841	3.885	3.985
3.424	3.445	3.566	3.582	3.706	3.728	3.843	3.885	3.974

obs. shift(.5)	theor. shift(.6)	obs. shift(.6)	theor. shift(.7)	obs. shift(.7)	Sum of (theor.-obs)^2	Norm
4.052	4.212	4.230	4.450	4.420	0.048	0.220
4.052	4.186	4.230	4.391	4.420	0.039	0.197
4.052	4.157	4.230	4.333	4.420	0.041	0.203
4.052	4.128	4.230	4.277	4.420	0.055	0.234
4.052	4.098	4.230	4.224	4.420	0.077	0.277
4.052	4.069	4.230	4.173	4.420	0.107	0.327
4.052	4.040	4.230	4.125	4.420	0.144	0.379
4.052	4.012	4.230	4.081	4.420	0.186	0.431
4.052	3.984	4.230	4.038	4.420	0.232	0.482
4.052	3.958	4.230	3.999	4.420	0.282	0.531
4.052	4.218	4.230	4.454	4.420	0.041	0.203
4.052	4.191	4.230	4.395	4.420	0.032	0.179
4.052	4.162	4.230	4.337	4.420	0.035	0.186
4.052	4.133	4.230	4.281	4.420	0.048	0.219
4.052	4.103	4.230	4.227	4.420	0.070	0.265
4.052	4.073	4.230	4.176	4.420	0.100	0.317
4.052	4.044	4.230	4.129	4.420	0.137	0.370
4.052	4.016	4.230	4.084	4.420	0.179	0.423
4.052	3.988	4.230	4.041	4.420	0.225	0.474
4.052	3.961	4.230	4.002	4.420	0.275	0.524
4.052	4.223	4.230	4.458	4.420	0.035	0.186
4.052	4.196	4.230	4.399	4.420	0.026	0.160
4.052	4.167	4.230	4.340	4.420	0.028	0.169
4.052	4.137	4.230	4.284	4.420	0.042	0.204
4.052	4.108	4.230	4.231	4.420	0.064	0.253
4.052	4.078	4.230	4.180	4.420	0.094	0.307
4.052	4.049	4.230	4.132	4.420	0.131	0.361
4.052	4.020	4.230	4.087	4.420	0.172	0.415
4.052	3.992	4.230	4.045	4.420	0.218	0.467
4.052	3.965	4.230	4.005	4.420	0.268	0.518
4.052	4.228	4.230	4.462	4.420	0.029	0.170

4.052	4.201	4.230	4.403	4.420	0.020	0.142
4.052	4.172	4.230	4.344	4.420	0.023	0.152
4.052	4.142	4.230	4.288	4.420	0.036	0.191
4.052	4.112	4.230	4.234	4.420	0.059	0.242
4.052	4.082	4.230	4.183	4.420	0.089	0.298
4.052	4.053	4.230	4.135	4.420	0.125	0.353
4.052	4.024	4.230	4.090	4.420	0.166	0.408
4.052	3.996	4.230	4.048	4.420	0.212	0.461
4.052	3.969	4.230	4.008	4.420	0.262	0.512
4.052	4.233	4.230	4.466	4.420	0.024	0.155
4.052	4.206	4.230	4.407	4.420	0.015	0.124
4.052	4.177	4.230	4.348	4.420	0.018	0.135
4.052	4.147	4.230	4.291	4.420	0.032	0.178
4.052	4.117	4.230	4.238	4.420	0.054	0.232
4.052	4.087	4.230	4.186	4.420	0.084	0.289
4.052	4.057	4.230	4.138	4.420	0.120	0.346
4.052	4.028	4.230	4.093	4.420	0.161	0.401
4.052	4.000	4.230	4.051	4.420	0.207	0.455
4.052	3.973	4.230	4.011	4.420	0.256	0.506
4.052	4.239	4.230	4.470	4.420	0.020	0.140
4.052	4.211	4.230	4.411	4.420	0.011	0.106
4.052	4.182	4.230	4.352	4.420	0.014	0.119
4.052	4.152	4.230	4.295	4.420	0.027	0.166
4.052	4.121	4.230	4.241	4.420	0.049	0.222
4.052	4.091	4.230	4.190	4.420	0.079	0.281
4.052	4.061	4.230	4.142	4.420	0.115	0.339
4.052	4.032	4.230	4.096	4.420	0.156	0.395
4.052	4.004	4.230	4.054	4.420	0.202	0.449
4.052	3.977	4.230	4.014	4.420	0.251	0.501
4.052	4.244	4.230	4.475	4.420	0.016	0.126
4.052	4.216	4.230	4.415	4.420	0.008	0.089
4.052	4.187	4.230	4.356	4.420	0.011	0.104

4.052	4.156	4.230	4.299	4.420	0.024	0.155
4.052	4.126	4.230	4.245	4.420	0.046	0.214
4.052	4.096	4.230	4.193	4.420	0.075	0.274
4.052	4.066	4.230	4.145	4.420	0.111	0.333
4.052	4.037	4.230	4.099	4.420	0.152	0.390
4.052	4.008	4.230	4.057	4.420	0.198	0.444
4.052	3.981	4.230	4.017	4.420	0.246	0.496
4.052	4.249	4.230	4.479	4.420	0.013	0.114
4.052	4.221	4.230	4.419	4.420	0.005	0.071
4.052	4.192	4.230	4.359	4.420	0.008	0.090
4.052	4.161	4.230	4.302	4.420	0.021	0.145
4.052	4.130	4.230	4.248	4.420	0.043	0.207
4.052	4.100	4.230	4.197	4.420	0.072	0.269
4.052	4.070	4.230	4.148	4.420	0.108	0.328
4.052	4.041	4.230	4.103	4.420	0.149	0.386
4.052	4.012	4.230	4.060	4.420	0.194	0.440
4.052	3.985	4.230	4.020	4.420	0.242	0.492
4.052	4.254	4.230	4.483	4.420	0.011	0.105
4.052	4.227	4.230	4.422	4.420	0.003	0.055
4.052	4.197	4.230	4.363	4.420	0.006	0.077
4.052	4.166	4.230	4.306	4.420	0.019	0.137
4.052	4.135	4.230	4.252	4.420	0.040	0.201
4.052	4.104	4.230	4.200	4.420	0.070	0.264
4.052	4.074	4.230	4.151	4.420	0.105	0.324
4.052	4.045	4.230	4.106	4.420	0.146	0.382
4.052	4.017	4.230	4.063	4.420	0.190	0.436
4.052	3.989	4.230	4.022	4.420	0.239	0.489
4.052	4.260	4.230	4.487	4.420	0.009	0.097
4.052	4.232	4.230	4.426	4.420	0.002	0.041
4.052	4.202	4.230	4.367	4.420	0.005	0.068
4.052	4.171	4.230	4.310	4.420	0.017	0.131
4.052	4.140	4.230	4.255	4.420	0.039	0.197

4.052	4.109	4.230	4.203	4.420	0.068	0.260
4.052	4.079	4.230	4.155	4.420	0.103	0.321
4.052	4.049	4.230	4.109	4.420	0.143	0.378
4.052	4.021	4.230	4.066	4.420	0.188	0.433
4.052	3.993	4.230	4.025	4.420	0.236	0.486
4.052	4.253	4.230	4.525	4.420	0.059	0.243
4.052	4.229	4.230	4.467	4.420	0.038	0.194
4.052	4.201	4.230	4.408	4.420	0.028	0.167
4.052	4.173	4.230	4.352	4.420	0.029	0.171
4.052	4.144	4.230	4.297	4.420	0.040	0.200
4.052	4.115	4.230	4.245	4.420	0.059	0.243
4.052	4.087	4.230	4.196	4.420	0.086	0.293
4.052	4.059	4.230	4.150	4.420	0.118	0.344
4.052	4.031	4.230	4.106	4.420	0.156	0.394
4.052	4.005	4.230	4.065	4.420	0.197	0.444
4.052	4.259	4.230	4.530	4.420	0.053	0.230
4.052	4.234	4.230	4.471	4.420	0.032	0.178
4.052	4.207	4.230	4.412	4.420	0.022	0.149
4.052	4.178	4.230	4.355	4.420	0.023	0.153
4.052	4.149	4.230	4.301	4.420	0.034	0.185
4.052	4.120	4.230	4.249	4.420	0.053	0.231
4.052	4.091	4.230	4.200	4.420	0.080	0.282
4.052	4.063	4.230	4.153	4.420	0.112	0.335
4.052	4.036	4.230	4.109	4.420	0.149	0.386
4.052	4.009	4.230	4.068	4.420	0.191	0.437
4.052	4.264	4.230	4.534	4.420	0.048	0.218
4.052	4.239	4.230	4.475	4.420	0.027	0.163
4.052	4.212	4.230	4.416	4.420	0.017	0.131
4.052	4.183	4.230	4.359	4.420	0.018	0.136
4.052	4.154	4.230	4.304	4.420	0.029	0.171
4.052	4.125	4.230	4.252	4.420	0.048	0.219
4.052	4.096	4.230	4.203	4.420	0.074	0.273

Table A-3: Sample calculation of best fit parameters (K_p and δ_{bp}) for mole fraction diphenylsulfoxide = 0.035 in 97/3 DMSO-d_6/water (eight pages)

Kp	delta H-SO2	Init. F. SO O's	Init. F water Oxygens	Init. F DMSO oxygens	A	B	C
35	3.5	0.03324	0.07938	0.80799	1.1179	1.0019	0.0641
35	4	0.03324	0.07938	0.80799	1.1179	1.0019	0.0641
35	4.5	0.03324	0.07938	0.80799	1.1179	1.0019	0.0641
35	5	0.03324	0.07938	0.80799	1.1179	1.0019	0.0641
35	5.5	0.03324	0.07938	0.80799	1.1179	1.0019	0.0641
35	6	0.03324	0.07938	0.80799	1.1179	1.0019	0.0641
35	6.5	0.03324	0.07938	0.80799	1.1179	1.0019	0.0641
35	7	0.03324	0.07938	0.80799	1.1179	1.0019	0.0641
35	7.5	0.03324	0.07938	0.80799	1.1179	1.0019	0.0641
35	8	0.03324	0.07938	0.80799	1.1179	1.0019	0.0641
40	3.5	0.03324	0.07938	0.80799	1.1219	1.0051	0.0641
40	4	0.03324	0.07938	0.80799	1.1219	1.0051	0.0641
40	4.5	0.03324	0.07938	0.80799	1.1219	1.0051	0.0641
40	5	0.03324	0.07938	0.80799	1.1219	1.0051	0.0641
40	5.5	0.03324	0.07938	0.80799	1.1219	1.0051	0.0641
40	6	0.03324	0.07938	0.80799	1.1219	1.0051	0.0641
40	6.5	0.03324	0.07938	0.80799	1.1219	1.0051	0.0641
40	7	0.03324	0.07938	0.80799	1.1219	1.0051	0.0641
40	7.5	0.03324	0.07938	0.80799	1.1219	1.0051	0.0641
40	8	0.03324	0.07938	0.80799	1.1219	1.0051	0.0641
45	3.5	0.03324	0.07938	0.80799	1.1258	1.0083	0.0641
45	4	0.03324	0.07938	0.80799	1.1258	1.0083	0.0641
45	4.5	0.03324	0.07938	0.80799	1.1258	1.0083	0.0641
45	5	0.03324	0.07938	0.80799	1.1258	1.0083	0.0641
45	5.5	0.03324	0.07938	0.80799	1.1258	1.0083	0.0641
45	6	0.03324	0.07938	0.80799	1.1258	1.0083	0.0641
45	6.5	0.03324	0.07938	0.80799	1.1258	1.0083	0.0641
45	7	0.03324	0.07938	0.80799	1.1258	1.0083	0.0641
45	7.5	0.03324	0.07938	0.80799	1.1258	1.0083	0.0641
45	8	0.03324	0.07938	0.80799	1.1258	1.0083	0.0641
50	3.5	0.03324	0.07938	0.80799	1.1298	1.0116	0.0641

mol F SO=.035

50	4	0.03324	0.07938	0.80799	1.1298	1.0116	0.0641
50	4.5	0.03324	0.07938	0.80799	1.1298	1.0116	0.0641
50	5	0.03324	0.07938	0.80799	1.1298	1.0116	0.0641
50	5.5	0.03324	0.07938	0.80799	1.1298	1.0116	0.0641
50	6	0.03324	0.07938	0.80799	1.1298	1.0116	0.0641
50	6.5	0.03324	0.07938	0.80799	1.1298	1.0116	0.0641
50	7	0.03324	0.07938	0.80799	1.1298	1.0116	0.0641
50	7.5	0.03324	0.07938	0.80799	1.1298	1.0116	0.0641
50	8	0.03324	0.07938	0.80799	1.1298	1.0116	0.0641
55	3.5	0.03324	0.07938	0.80799	1.1338	1.0148	0.0641
55	4	0.03324	0.07938	0.80799	1.1338	1.0148	0.0641
55	4.5	0.03324	0.07938	0.80799	1.1338	1.0148	0.0641
55	5	0.03324	0.07938	0.80799	1.1338	1.0148	0.0641
55	5.5	0.03324	0.07938	0.80799	1.1338	1.0148	0.0641
55	6	0.03324	0.07938	0.80799	1.1338	1.0148	0.0641
55	6.5	0.03324	0.07938	0.80799	1.1338	1.0148	0.0641
55	7	0.03324	0.07938	0.80799	1.1338	1.0148	0.0641
55	7.5	0.03324	0.07938	0.80799	1.1338	1.0148	0.0641
55	8	0.03324	0.07938	0.80799	1.1338	1.0148	0.0641
60	3.5	0.03324	0.07938	0.80799	1.1377	1.0180	0.0641
60	4	0.03324	0.07938	0.80799	1.1377	1.0180	0.0641
60	4.5	0.03324	0.07938	0.80799	1.1377	1.0180	0.0641
60	5	0.03324	0.07938	0.80799	1.1377	1.0180	0.0641
60	5.5	0.03324	0.07938	0.80799	1.1377	1.0180	0.0641
60	6	0.03324	0.07938	0.80799	1.1377	1.0180	0.0641
60	6.5	0.03324	0.07938	0.80799	1.1377	1.0180	0.0641
60	7	0.03324	0.07938	0.80799	1.1377	1.0180	0.0641
60	7.5	0.03324	0.07938	0.80799	1.1377	1.0180	0.0641
60	8	0.03324	0.07938	0.80799	1.1377	1.0180	0.0641
65	3.5	0.03324	0.07938	0.80799	1.1417	1.0212	0.0641
65	4	0.03324	0.07938	0.80799	1.1417	1.0212	0.0641
65	4.5	0.03324	0.07938	0.80799	1.1417	1.0212	0.0641

mol F SO=.035

65	5	0.03324	0.07938	0.80799	1.1417	1.0212	0.0641
65	5.5	0.03324	0.07938	0.80799	1.1417	1.0212	0.0641
65	6	0.03324	0.07938	0.80799	1.1417	1.0212	0.0641
65	6.5	0.03324	0.07938	0.80799	1.1417	1.0212	0.0641
65	7	0.03324	0.07938	0.80799	1.1417	1.0212	0.0641
65	7.5	0.03324	0.07938	0.80799	1.1417	1.0212	0.0641
65	8	0.03324	0.07938	0.80799	1.1417	1.0212	0.0641
70	3.5	0.03324	0.07938	0.80799	1.1457	1.0244	0.0641
70	4	0.03324	0.07938	0.80799	1.1457	1.0244	0.0641
70	4.5	0.03324	0.07938	0.80799	1.1457	1.0244	0.0641
70	5	0.03324	0.07938	0.80799	1.1457	1.0244	0.0641
70	5.5	0.03324	0.07938	0.80799	1.1457	1.0244	0.0641
70	6	0.03324	0.07938	0.80799	1.1457	1.0244	0.0641
70	6.5	0.03324	0.07938	0.80799	1.1457	1.0244	0.0641
70	7	0.03324	0.07938	0.80799	1.1457	1.0244	0.0641
70	7.5	0.03324	0.07938	0.80799	1.1457	1.0244	0.0641
70	8	0.03324	0.07938	0.80799	1.1457	1.0244	0.0641
75	3.5	0.03324	0.07938	0.80799	1.1497	1.0276	0.0641
75	4	0.03324	0.07938	0.80799	1.1497	1.0276	0.0641
75	4.5	0.03324	0.07938	0.80799	1.1497	1.0276	0.0641
75	5	0.03324	0.07938	0.80799	1.1497	1.0276	0.0641
75	5.5	0.03324	0.07938	0.80799	1.1497	1.0276	0.0641
75	6	0.03324	0.07938	0.80799	1.1497	1.0276	0.0641
75	6.5	0.03324	0.07938	0.80799	1.1497	1.0276	0.0641
75	7	0.03324	0.07938	0.80799	1.1497	1.0276	0.0641
75	7.5	0.03324	0.07938	0.80799	1.1497	1.0276	0.0641
75	8	0.03324	0.07938	0.80799	1.1497	1.0276	0.0641
80	3.5	0.03324	0.07938	0.80799	1.1536	1.0308	0.0641
80	4	0.03324	0.07938	0.80799	1.1536	1.0308	0.0641
80	4.5	0.03324	0.07938	0.80799	1.1536	1.0308	0.0641
80	5	0.03324	0.07938	0.80799	1.1536	1.0308	0.0641
80	5.5	0.03324	0.07938	0.80799	1.1536	1.0308	0.0641

mol F SO=.035

80	6	0.03324	0.07938	0.80799	1.1536	1.0308	0.0641
80	6.5	0.03324	0.07938	0.80799	1.1536	1.0308	0.0641
80	7	0.03324	0.07938	0.80799	1.1536	1.0308	0.0641
80	7.5	0.03324	0.07938	0.80799	1.1536	1.0308	0.0641
80	8	0.03324	0.07938	0.80799	1.1536	1.0308	0.0641

mol F SO=.035

Fwater-bonded DMSO	F water-water	F-water-SO	theor. shift(.035)	obs. shift(.035)
0.0694	0.0063	0.0020	3.4841	3.576
0.0694	0.0063	0.0020	3.4966	3.576
0.0694	0.0063	0.0020	3.5091	3.576
0.0694	0.0063	0.0020	3.5216	3.576
0.0694	0.0063	0.0020	3.5341	3.576
0.0694	0.0063	0.0020	3.5466	3.576
0.0694	0.0063	0.0020	3.5591	3.576
0.0694	0.0063	0.0020	3.5716	3.576
0.0694	0.0063	0.0020	3.5841	3.576
0.0694	0.0063	0.0020	3.5966	3.576
0.0691	0.0063	0.0022	3.4837	3.576
0.0691	0.0063	0.0022	3.4978	3.576
0.0691	0.0063	0.0022	3.5120	3.576
0.0691	0.0063	0.0022	3.5261	3.576
0.0691	0.0063	0.0022	3.5402	3.576
0.0691	0.0063	0.0022	3.5543	3.576
0.0691	0.0063	0.0022	3.5684	3.576
0.0691	0.0063	0.0022	3.5825	3.576
0.0691	0.0063	0.0022	3.5966	3.576
0.0691	0.0063	0.0022	3.6107	3.576
0.0689	0.0063	0.0025	3.4832	3.576
0.0689	0.0063	0.0025	3.4989	3.576
0.0689	0.0063	0.0025	3.5146	3.576
0.0689	0.0063	0.0025	3.5302	3.576
0.0689	0.0063	0.0025	3.5459	3.576
0.0689	0.0063	0.0025	3.5616	3.576
0.0689	0.0063	0.0025	3.5773	3.576
0.0689	0.0063	0.0025	3.5930	3.576
0.0689	0.0063	0.0025	3.6087	3.576
0.0689	0.0063	0.0025	3.6244	3.576
0.0687	0.0062	0.0027	3.4825	3.576

mol F SO=.035

0.0687	0.0062	0.0027	3.4997	3.576
0.0687	0.0062	0.0027	3.5169	3.576
0.0687	0.0062	0.0027	3.5342	3.576
0.0687	0.0062	0.0027	3.5514	3.576
0.0687	0.0062	0.0027	3.5686	3.576
0.0687	0.0062	0.0027	3.5858	3.576
0.0687	0.0062	0.0027	3.6031	3.576
0.0687	0.0062	0.0027	3.6203	3.576
0.0687	0.0062	0.0027	3.6375	3.576
0.0684	0.0062	0.0030	3.4816	3.576
0.0684	0.0062	0.0030	3.5004	3.576
0.0684	0.0062	0.0030	3.5191	3.576
0.0684	0.0062	0.0030	3.5378	3.576
0.0684	0.0062	0.0030	3.5565	3.576
0.0684	0.0062	0.0030	3.5753	3.576
0.0684	0.0062	0.0030	3.5940	3.576
0.0684	0.0062	0.0030	3.6127	3.576
0.0684	0.0062	0.0030	3.6315	3.576
0.0684	0.0062	0.0030	3.6502	3.576
0.0682	0.0062	0.0032	3.4806	3.576
0.0682	0.0062	0.0032	3.5008	3.576
0.0682	0.0062	0.0032	3.5210	3.576
0.0682	0.0062	0.0032	3.5412	3.576
0.0682	0.0062	0.0032	3.5614	3.576
0.0682	0.0062	0.0032	3.5816	3.576
0.0682	0.0062	0.0032	3.6018	3.576
0.0682	0.0062	0.0032	3.6220	3.576
0.0682	0.0062	0.0032	3.6422	3.576
0.0682	0.0062	0.0032	3.6624	3.576
0.0680	0.0062	0.0034	3.4795	3.576
0.0680	0.0062	0.0034	3.5011	3.576
0.0680	0.0062	0.0034	3.5228	3.576

mol F SO=.035

0.0680	0.0062	0.0034	3.5444	3.576
0.0680	0.0062	0.0034	3.5660	3.576
0.0680	0.0062	0.0034	3.5877	3.576
0.0680	0.0062	0.0034	3.6093	3.576
0.0680	0.0062	0.0034	3.6309	3.576
0.0680	0.0062	0.0034	3.6526	3.576
0.0680	0.0062	0.0034	3.6742	3.576
0.0677	0.0061	0.0037	3.4782	3.576
0.0677	0.0061	0.0037	3.5012	3.576
0.0677	0.0061	0.0037	3.5243	3.576
0.0677	0.0061	0.0037	3.5473	3.576
0.0677	0.0061	0.0037	3.5704	3.576
0.0677	0.0061	0.0037	3.5934	3.576
0.0677	0.0061	0.0037	3.6165	3.576
0.0677	0.0061	0.0037	3.6395	3.576
0.0677	0.0061	0.0037	3.6625	3.576
0.0677	0.0061	0.0037	3.6856	3.576
0.0675	0.0061	0.0039	3.4768	3.576
0.0675	0.0061	0.0039	3.5012	3.576
0.0675	0.0061	0.0039	3.5256	3.576
0.0675	0.0061	0.0039	3.5501	3.576
0.0675	0.0061	0.0039	3.5745	3.576
0.0675	0.0061	0.0039	3.5989	3.576
0.0675	0.0061	0.0039	3.6233	3.576
0.0675	0.0061	0.0039	3.6477	3.576
0.0675	0.0061	0.0039	3.6721	3.576
0.0675	0.0061	0.0039	3.6966	3.576
0.0673	0.0061	0.0041	3.4753	3.576
0.0673	0.0061	0.0041	3.5010	3.576
0.0673	0.0061	0.0041	3.5268	3.576
0.0673	0.0061	0.0041	3.5526	3.576
0.0673	0.0061	0.0041	3.5783	3.576

mol F SO=.035

0.0673	0.0061	0.0041	3.6041	3.576
0.0673	0.0061	0.0041	3.6298	3.576
0.0673	0.0061	0.0041	3.6556	3.576
0.0673	0.0061	0.0041	3.6814	3.576
0.0673	0.0061	0.0041	3.7071	3.576

Table A-4: Test of a broad range of K_o and K_n values to find minima in the "norm" equation. δ_{bn} was held constant at 3.38 ppm, while K_n was varied from 1 to 100 and K_o was varied from 1 to 70. Iterative calculations were performed on every possible combination of K_o and K_n values. The theoretically calculated δ value was compared to the experimental δ value across the seven sample concentrations using the norm function. Best fit values were $K_n = 53$ and $K_o = 49$ with a norm of 0.01.

Trial #	K_n range	K_o range	best fit K_n	best fit K_o	δ_{bn} (ppm)	norm
1	1 to 100	1 to 10	36	10	3.38	0.57
2	1 to 100	11 to 20	33	20	3.38	0.27
3	1 to 100	21 to 30	39	30	3.38	0.13
4	1 to 100	31 to 40	46	40	3.38	0.05
5	1 to 100	41 to 50	53	49	3.38	0.01
6	1 to 100	51 to 60	55	51	3.38	0.02
7	1 to 100	61 to 70	63	61	3.38	0.05

REFERENCES

1. A. L. Ogden, M. W. Hyer, J. T. Muellerleile, G. T. Wilkes, and A. C. Loos, Proc. Am. Soc. Composites, 5th Technical Conf., Technomic Publishing Co., Inc., Lancaster, 1990, p. 249

2. E. M. Silverman, J. E. Sathoff, and W. C. Forbes, SAMPE J., 1989, 25(5), 39

3. M. Molyneux, Composites, 1983, 14(2), 87

4. J. J. Lesko, R. E. Swain, J. M. Cartwright, J. W. Chin, K. L. Reifsnider, D. A. Dillard, and J. P. Wightman, J. Adhesion, 1994, 45, 43

5. H. Zhuang, H. Oyama, R. Bucher, M. Hochella, J. Lesko, A. Loos, J. McGrath, K. Reifsnider, and J. Wightman, Polymer Preprints, 1995, 36(1), 819

6. T. Lin, Ph. D. Dissertation, Virginia Tech, 1993, p. 29

7. J. E. Harris and R. N. Johnson in "Encylcopedia of Polymer Science and Engineering," H. F. Mark, N. M. Bikales, C. G. Overberger, G. Menges, and J. I. Kroschwitz, eds., Vol. 13, John Wiley and Sons, NY, 1985, p. 196-211)

8. J. L. Hedrick, D. K. Mohanty, B. C. Johnson, R. Viswanathan, J. A. Hinkley, and J. E. McGrath, J. Polym. Sci.: Polym. Chem. Edn., 1986, 23, 287

9. J. March, "Advanced Organic Chemistry", 3rd ed., John Wiley & Sons, 1985

10. R. N. Johnson, A. G. Farnham, R. A. Clendinning, W. F. Hale, and C. N. Merriam, J. Polym. Sci. Part A-1, 1967, 5, 2375

11. J. R. Babu, A. E. Brink, M. Konas, and J. S. Riffle, Polymer, 1994, 35(23), 4949

12. C. D. Smith, H. J. Grubbs, H. F. Webster, J. P. Wightman, and J. E. McGrath, High Perf. Polym., 1991, 3(4), 211

13. J. Hedrick, R. Twieg, T. Matray, and K. Carter, Macromolecules, 1993, 26, 4833-4839

14. H. M. Relles, C. M. Orlando, D. R. Heath, R. W. Schluenz, J. S. Manello, and S. Hoff, J. Polym. Sci.: Polym. Chem. Edn., 1977, 15, 2441-2451

15. T. E. Atwood, D. A. Barr, G. G. Faasey, V. J. Leslie, A. B. Newton, and J. B. Rose, Polymer, 1977, 18, 354

16. K. R. Lyon, J. F. Geibel, and J. E. McGrath, Proc. Am. Chem. Soc. Div. Polym. Mater. Sci. Eng., 1991, 65, 249

17. J. G. Hilborn, J. W. Labadie, and J. L. Hedrick, Macromolecules, 1990, 23, 2854-2861

18. J. L. Hedrick, Polym. Bull., 1991, 25, 543-550

19. K. R. Carter, H. Jonsson, R. Twieg, R. D. Miller, and J. L. Hedrick, Polym. Prepr., 1992, 33(1), 388

20. A. E. Brink, M. C. Lin, and J. S. Riffle, Chemistry of MATERIALS, 1993, 5, 925-929

21. D. M. White, T. Takekoshi, F. J. Williams, H. M. Relles, P. E. Donahue, H. J. Klopfer, F. R. Loucks, J. S. Manello, R. O. Matthews, and R. W. Schluenz, J. Polym. Sci.: Polym. Chem. Edn., 1981, 19, 1635-1658

22. E. Bonaparte, Masters Thesis, Virginia Tech, 1994

23. A. E. Brink, Ph.D. Dissertation, Virginia Tech, 1994

24. R. N. Johnson, A. G. Farnham, R. N. Clendinning, W. F. Hale, and C. N. Merriam, J. Polym. Sci., A-1, 1967, 5, 2374

25. W. Wrasidlo, J. Polym. Sci. A-1, 1970, 8, 1107

26. P. Sanseau, A. Schlitz, G. Rabilloud, and L. Verdet, Electrochem. Soc. Ext. Abstr., 1987, 87-2, 665

27. P. M. Hergenrother, Polym. Eng. Sci., 1976, 16, 303

28. J. W. Labadie and J. L. Hedrick, J. Polym. Sci.: Part A: Polym. Chem. Edn., 1989, 27, 2951-2962

29. P. Hergenrother in "Encyclopedia of Polymer Science and Engineering", V. 13, John Wiley & Sons, NY, 1988, p. 55-87

30. O. Hinsberg, Ber. Dent. Chem. Ges., 1884, 17, 318 and V. Korner, Ber. Dent. Chem. Ges., 1884, 17, 573

31. G. P. deGaudemaris and B. J. Sillion, J. Poly. Sci., Part B, 1964, 2, 203

32. P. M. Hergenrother and H. H. Levine, J. Polym. Sci., Part A-1, 1967, 5, 1453

33. J. W. Connell and P. M. Hergenrother, Polym. Prepr., 1988, 29(1), 172

34. J. W. Connell and P. M. Hergenrother, Polymer, 1992, 33(17), 3739

35. J. L. Hedrick and J. W. Labadie, Proc. ACS Div. Polym. Mat. Sci. Eng., 1988, 59, 42-45

36. J. L. Hedrick and J. W. Labadie, Macromolecules, 1990, 23, 23

37. J. L. Hedrick and J. W. Labadie, Macromolecules, 1988, 21(6), 1883

38. J. L. Hedrick and J. W. Labadie, Macromolecules, 1990, 23(6), 1561

39. J. W. Labadie, J. L. Hedrick, and S. K. Boyer, J. Polym. Sci.: Part A: Polym. Chem., 1992, 30, 519-523

40. J. Hedrick, R. Twieg, T. Matray, and K. Carter, Macromolecules, 1993, 26, 4833-4839

41. K. W. Stickney, J. R. Babu, and J. S. Riffle, Proc. of the Adhesion Soc. 16th Annual Mtg., Williamsburg, VA, 1993, p. 271

42. K. R. Carter, H. Jonsson, R. Twieg, R. D. Miller, and J. L. Hedrick, Polym. Prepr., 1992, 33(1), 388

43. J. W. Labadie, J. L. Hedrick, K. Carter, R. Twieg, Polym. Bull., 1993, 30, 25

44. a) J. W. Connell, J. G. Smith, Jr., and J. L. Hedrick, Proc. ACS Div. Polym. Mat. Eng. Sci., 1993, 69, 289; b) C. D. Smith, Ph. D. Dissertation, Virginia Tech, 1991

45. J. L. Hedrick, J. W. Labadie, and T. P. Russell, Macromolecules, 1991, 24, 4559-4566

46. J. L. Hedrick, J. W. Labadie, T. P. Russell, and T. Palmer, Polymer, 1991, 32(5), 950

47. P. M. Hergenrother and S. J. Havens, Macromolecules, 1994, 27, 4659-4664

48. T. Yamamoto, T. Kanbara, N. Ooba, and S. Tomaru, Chem. Lett., 1994, 9, 1709-1712

49. K. Chmil and U. Scherf, Makromol. Chem., 1993, 194, 1377-1386

50. N. Miyaura, T. Yanagi, A. Suzuki, Synth. Commun., 1981, 11, 513

51. R. N. Johnson, A. G. Farnham, R. A. Clendinning, W. F. Hale, and C. N. Merriam, J. Polym. Sci., 1967, 5, 2575

52. T. Fujisawa, M. Kakutani, and N. Kobayashi, Polym. Lett., 1971, 9, 91-94

53. J. R. Babu, A. E. Brink, M. Konas, and J. S. Riffle, Polymer, 1994, 35(23), 4949

54. N.J. Leonard and L. E. Sutton, J. Am. Chem. Soc., 1948, 70, 1564

55. A. E. Grulke, in "Polymer Handbook", 3rd ed., J. Brandup and E. H. Immergut, eds., John Wiley and Sons, NY, 1989, VII, 519

56. L. V. McAdams J. A. Gannon in "Encyclopedia of Polymer Science and Engineering," Vol. 6, H. F. Mark, N. M. Bikales, C. G. Overberger, G. Menges, and J. I. Kroschwitz, eds., John Wiley and Sons, NY p. 322-382

57. I. Y. Chang, 37th Int. SAMPE Symp., March 9-12, 1992, p. 1276

58. E. H. Rowe, A. R. Siebert, and R. S. Drake, Modern Plastics, 1970, 47, 110

59. J. N. Sultan and F. J. McGarry, Polym. Eng. Sci., 1973, 13, 29

60. A. J. Kinloch, S. J. Shaw, D. A. Tod, and D. L. Hunston, Polymer, 1983, 24, 1341

61. R. A. Pearson and A. F. Yee, J. Mater. Sci., 1986, 21, 2475

62. D. Verchere, H. Sautereau, J. P. Pascault, S. M. Moschiar, C. C. Riccardi, and R. J. J. Williams, J. Appl. Polym. Sci., 1990, 41, 467

63. L. T. Manzione, J. K. Gillham, and C. A. McPherson, J. Appl. Polym. Sci., 1981, 26, 889

64. C. K. Riew, E. H. Rowe, and A. R. Siebert, Adv. Chem. Ser., 1976, 154, 326

65. P. Bussi and H. Ishida, J. Appl. Polym. Sci., 1994, 53, 441-454

66. P. Bussi and H. Ishida, Polymer, 1994, 35(5), 956

67. N. Biolley, T. Pascal, and B. Sillion, Polymer, 1994, 35(3), 558

68. R. S. Slysh, Am. Chem. Soc. Adv. Chem. Ser., 1970, 92, 108

69. J. S. Riffle, I. Yilgor, C. Tran, G. L. Wilkes, J. E. McGrath, and A. K. Banthia, Am. Chem. Soc. Symp. Ser., 1983, 221, 21

70. S. Gazit and J. P. Bell, Am. Chem. Soc. Symp. Ser., 1983, 221, 55

71. J. Mijovic, E. M. Pearce, and C.-C. Foun, Am. Chem. Soc. Adv. Chem. Ser., 1984, 208, 293

72. T. J. Kemp, A. Wilford, O. W. Howarth, and T. C. P. Lee, Polymer, 1992, 33(9), 1860

73. O. Olabisi, L. M. Robeson, and M. T.Shaw, "Polymer-Polymer Miscibility", Academic Press, NY, 1979

74. D. R. Paul and S. Newman, eds., "Polymer Blends", Academic Press, NY, 1978

75. C. Qin, A. T. N. Pires, and L. A. Belfiore, Polym. Commun., 1990, 31, 177

76. G. C. Maitland, M. Rigby, E. B. Smith, and W. W. Wakeham, "Intermolecular Forces--Their Origin and Determination", Oxford University Press (Clarendon), London and New York, 1981

77. F. W. Billmeyer, Jr., "Textbook of Polymer Science", Wiley-Interscience, NY, 1984, p. 14

78. G. Odian, "Principles of Polymerization", 2nd ed., John Wiley and Sons, NY, 1981, p. 32

79. S. P. Ting, B. J. Bulkin, and E. M. Pearce, J. Polym. Sci., Polym. Chem. Ed., 1981, 19, 1451

80. S. R. Fahrenholtz and T. K. Kwei, Macromolecules, 1981, 14, 1076

81. C. Leonard, J. L. Halary, and L. Monnerie, Polymer, 1985, 26, 1507

82. E. J. Moskala, D. F. Varnell, and M. M. Coleman, Polymer, 1985, 26, 228

83. X. Zhang, K. Takegoshi, and K. Hikichi, Polymer, 1992, 33(4), 712

84. X. Zhang, K. Takegoshi, and K. Hikichi, Polymer J., 1991, 23, 79

85. D. L. Van der Hart, W. L. Earl, and A. N. Garroway, J. Magn. Reson., 1981, 44, 361

86. J. Grobelny, D. M. Rice, F. E. Karasz, and W. J. MacKnight, Macromolecules, 1990, 23, 2139

87. J. L. White and P. A Mirau, Macromolecules, 1994, 27, 1648-1650

88. P. A. Mirau, H. Tanaka, F. A. Bovey, Macromolecules, 1988, 21, 2929

89. A. S. N. Murthy and C. N. R. Rao, Appl. Spectrosc. Rev., 1968, 2, 69-191

90. G. Ruggeri, R. Bertani, M. Aglietto, A. D'Alessio, and E. Benedetti, Polymer International, 1994, 34, 1-6

91. M. M. Coleman, J. F. Graf, P. C. Painter, "Specific Interactions and the Miscibility of Polymer Blends", Technomic Publishing, Inc., Lancaster, PA, 1991

92. M. M. Coleman, Y. Xu, and P. C. Painter, Macromolecules, 1994, 27, 127-134

93. L. C. Cesteros, J. R. Isasi, and I. Katime, Macromolecules, 1993, 26, 7256-7262

94. M. M. Coleman and E. J. Moskala, Polymer, 1983, 24, 251

95. C. J. Tsang, J. C. Clark, S. T. Wellinghoff, and W. G. Miller, J. Polym. Sci.: Part B: Polym. Phys., 1991, 29, 247-259

96. M. M. Coleman, X. Yang, P. C. Painter, and J. F. Graf, Macromolecules, 1992, 25, 4414-4424

97. M. Alberdi, E. Espi, M. J. Fernandez-Berridi, and J. J. Iruin, Polymer Journal, 1994, 26(9), 1037-1046

98. S. H. Goh, S. Y. Lee, and S. M. Low, Macromolecules, 1994, 27, 6736-6739

99. L. M. Robeson, W. F. Hale, and C. N. Merriam, Macromolecules, 1981, 14, 1644

100. M. Iriarte, E. Espi, A. Etxeberria, M. Valero, M. J. Fernandez-Berridi, and J. J. Iruin, Macromolecules, 1991, 24(20), 5546

101. A. M. de Ilarduya, J. L. Eguiburu, E. Espi, J. J. Iruin, M. J. Fernandez-Berridi, Makromol. Chem., 1993, 194, 501-510

102. M. Vanneste and G. Groeninckx, Polymer, 1994, 35(1), 162

103. V. B. Singh and D. J. Walsh, J. Macromol. Sci. Phys., 1986, B25(1-2), 65-87

104. Q. Guo, J. Huang, B. Li, T. Chen, H. Zhang, and Z. Feng, Polymer, 1991, 32, 58

105.   N. D. Coggeshall and D. L. Saier, J. Am. Chem. Soc., 1951, 73, 5414

106.   J. N. Clark, J. H. Daly, and A. Garton, J. Appl. Polym. Sci., 1984, 29, 3381-3390

107.   D. Feldman, J. Appl. Polym Sci., 1984, 29, 515-531

108.   J. L. Hedrick, Ph. D. dissertation, Virginia Tech, 1988

109.   R. S. Raghava, Soc. Adv. Mater. Proc. Eng. 28th Nat. Symp., 1983, p. 367-375

110.   C. B. Bucknall and I. I. Partridge, Polymer, 1983, 24, 639

111.   J. Daimant and R. J. Moulton, 29th Natl. SAMPE Symp., 1984, 29, 422

112.   D. J. Hourston and J. M. Lane, Polymer, 1992, 33(7), 1379

113.   N. Biolley, T. Pascal, and B. Sillion, Polymer, 1994, 35(3), 558

114.   Q. Guo, J. Huang, B. Li, T. Chen, H. Zhang, and Z. Feng, Polymer, 1991, 32(1), 58

115.   J. A. Cecere and J. E. McGrath, Polym. Prepr., 1986, 27(1), 299

116.   Q. Guo, Polymer, 1993, 34(1), 70

117.   R. A. Pearson and A. F. Yee, J. Appl. Polym. Sci., 1993, 48, 1051-1060

118.   J. L. Hedrick, I. Yilgor, G. L. Wilkes, and J. E. McGrath, Polym. Bull., 1985, 13, 201

119.   a) J. L. Hedrick, I. Yilgor, J. C. Hedrick, G. L. Wilkes, and J. E. McGrath, Soc. Adv. Mater. Proc. Eng. 30th Nat. Symp., 1985, p. 947-958; b) T. H. Yoon, S. C. Liptak, D. B. Priddy, Jr., and J. E. McGrath, J. Adhesion, 1994, 45, 191-203

120.   J. L. Hedrick, I. Yilgor, M. Jurek, J. C. Hedrick, G. L. Wilkes, and J. E. McGrath, Polymer, 1991, 32(11), 2020

121.   E. M. Yorkgitis, N. S. Eiss, Jr., C. Tran, G. L. Wilkes, and J. E. McGrath, in "Advances in Polymer Science: Epoxy Resin and Composites I", V. 72, K. Dusek, ed., Springer-Verlag, NY, 1985, p. 70-109

122.   M. Gordon and J. S. Taylor, J. Appl. Chem., 1952, 2, 495

123.   T. G. Fox, Bull. Am. Phys. Soc., 1956, 1, 123

124.   J. D. B. Smith, J. Appl. Polym. Sci., 1981, 26, 979

125.   L. S. Frankel, US Pat. 4 237 242, 1980

126.   P. V. Reddy, R. Thiagarajan, and M. C. Ratra, J. Appl. Polym. Sci., 1990, 41, 319

127.   D. M. Stoakley and A. K. St. Clair, J. Appl. Polym. Sci., 1986, 31, 225

128.   K.-F. Lin, W.-Y. Shu, and T.-L. Wey, Polymer, 1993, 34(10), 2162

129.   M. Anand and A. K. Srivastava, Polymer, 1993, 34(13), 2860

130. M. Anand and A. K. Srivastava, J. Appl. Polym. Sci., 1994, 51(2), 203

131. R. B. Krieger, Nat. SAMPE Symp., 1985, 30, 1570

132. M.-F. Grenier-Loustalot and P. Grenier, Polymer, 1992, 33(6), 1187

133. F. G. Bordwell, Acc. Chem. Res., 1988, 21, 456

134. A. K. Chandra and A. B. Sannigrahi, J. Phys. Chem., 1965, 69(8), 2494

135. P. Schuster in "Encyclopedia of Physical Science and Technology", 2nd ed., Volume 7, R. A. Meyers, ed., Academic Press, Inc., San Diego, 1992, p. 727

136. D. Hadzi (ed.), "Hydrogen Bonding", Pergamon Press, New York, 1959 and G. C. Pimentel and A. L. McClellan, "The Hydrogen Bond", Freeman, San Francisco, 1960

137. R. J. Gillespie, D. A. Humphreys, N. C. Baird, and E. A. Robinson, "Chemistry", 2nd ed., Allyn and Bacon, Boston, 1989, p. 593-594

138. S. Suzuki, P. G. Green, R. E. Bumgarner, S. Dasgupta, W. A. Goddard III, G. A. Blake, Science, 1992, 257, 942

139. J. A. Pople, W. G. Schneider, and J. J. Bernstein, "High Resolution Nuclear Magnetic Resonance," McGraw-Hill Book Co., Inc., New York, 1959, Chapter 15

140. D. Neerinck, A. Van Audenhaege, L. Lamberts, and P. Huyskens, Nature, 1968, 218, 461-462

141. J. C. Davis Jr. and K. K. Deb, Advan. Magn. Resonance, 1970, 4, 201

142. S. N. Vinogradov and R. H. Linnell, "Hydrogen Bonding", Van Nostrand Reinhold Co., New York, 1971, p. 88

143. S. N. Vinogradov and R. H. Linnell, "Hydrogen Bonding", Van Nostrand Reinhold Co., New York, 1971, p. 100

144. S. Sternhell in "Instrumental Analysis", H. H. Bauer, G. D. Christian, and J. D. O'Reilly, eds., Allyn and Bacon, Inc., Boston, 1978, Ch. 12

145. P. W. Atkins, "Physical Chemistry", 4th ed., W. H. Freeman and Co., New York, 1990, Ch. 18

146. P. Schuster, "The Hydrogen Bond: Recent Developments in the Theory and Experiments", P. Schuster, G. Zundel, and C. Sandorfy, eds., North-Holland Publishing Co., Amsterdam, 1976, p. 73

147. I. R. Lantzke, in "Physical Chemistry of Organic Solvent Systems", A. K. Covinton and T. Dickinson, eds., Plenum Press, London, 1973, p. 483

148. F. Franks, ed., "Water: A Comprehensive Treatise", Plenum Press, New York, 1975

149. R.-S. Tsai, W. Fan, N. El Tayar, P.-A. Carrupt, B. Testa, and L. B. Kier, J. Am. Chem. Soc., 1993, 115, 9632-9639

150. G. Nemethy and H. A. Scheraga, J. Phys. Chem., 1962, 36, 3382

151. R. P. Marchi and H. Eyring, J. Phys. Chem., 1964, 68, 221

152. K. Buijs and G.R. Choppin, J. Chem. Phys., 1963, 39, 2035

153. W. G. Schneider, H. J. Bernstein, and J. A. Pople, J. Chem. Phys., 1958, 28, 601

154. J. C. Hindman, J. Chem. Phys., 1966, 44(12), 4582

155. M. J. Stephen, Mol.Phys., 1958, 1, 223

156. D. P. Stevenson, J. Phys. Chem., 1965, 69(7), 2145

157. W. G. Schneider, H. J. Bernstein, and J. A. Pople, J. Chem. Phys., 1958, 28, 601

158. T. Lin, Ph. D. Dissertation, Virginia Tech, 1993, p. 26

159. N. Muller and P. Simon, J. Phys. Chem., 1967, 71(3), 568

160. S. C. Mohr, W. D. Wilk, and G. M. Barrow, J. Am. Chem. Soc., 1965, 87, 3048

161. N. Nishimura, C. H. Ke, and N. C. Li, J. Am. Chem. Soc., 1968, 90(2), 234

162. J. M. G. Cowie and P. M. Toporowski, Can. J. Chem., 1961, 39, 2240

163. A. Luzar, J. Mol. Liq., 1990, 46, 221

164. S. M. Puranik, A. C. Kumbharkhane, and S. C. Mehrotra, J. Chem. Soc. Faraday Trans., 1992, 88(3), 433-435

165. D. H. Rasmussen and A. P. Mackenzie, Nature (London), 1968, 220, 1315

166. J. J. Lindberg and C. Majani, Acta Chem. Scand., 1963, 17, 1477

167. A. Luzar, J. Chem. Phys., 1989, 91, 3603

168. A. Luzar and D. Chandler, J. Chem. Phys., 1993, 98(10), 8160

169. A. K. Soper and A. Luzar, J. Chem. Phys., 1992, 97, 1320

170. A. K. Chandra and A. B. Sannigrahi, J. Phys. Chem., 1965, 69(8), 2494

171. D. P. Stevenson, J. Am. Chem. Soc., 1962, 84(15), 2849

172. A. Kivinen, J. Murto, S. Liljequist, and S. Vaara, Acta Chem. Scand. A, 1975, 29(10), 911-918

173. J.-C. Harge, H. El Abdallaoui, and P. Rubini, Magn. Res. Chem., 1993, 31, 752-757

174. M. D. Joesten and R. S. Drago, J. Am. Chem. Soc., 1962, 84, 3817

175. G. Aksnes and T. Gramstad, Acta. Chem. Scand., 1960, 14, 1485

176. G. C. Pimentel and A. L. McClellan, Ann. Rev. Phys. Chem., 1971, 22, 347

177. D. P. Eyman and R. S. Drago, J. Am. Chem. Soc., 1966, 88(8), 1617

178. R. S. Drago, B. Wayland, and R. L. Carlson, J. Am. Chem. Soc., 1963, 85, 3125

179. J. H. Bright, R. S. Drago, D. M. Hart, and S. K. Madan, Inorg. Chem., 1965, 4, 18

180. T. Gramstad, Spectrochim. Acta, 1963, 19, 829

181. S. Singh, A. S. N. Murthy, and C. N. R. Rao, Trans. Faraday Soc., 1966, 62, 1056

182. D. Hadzi and R. Smerkolj, J. Chem. Soc. Faraday Transactions I, 1976, 72, 1188

183. P. Ruostesuo, P. Pirila-Honkanen, and S. Kaartinen, Spectrochim. Acta, 1988, 44A(4), 359-362

184. M. J. Kamlet, R. M. Doherty, J.-L. M. Abboud, M. H. Abraham, and R. W. Tft, CHEMTECH, 1986, 16, 566

185. M. H. Abraham, H. S. Chadha, G. S. Whiting, and R. C. Mitchell, J. Pharm. Sci., 1994, 83(8), 1085

186. K. Wozniak, T. M. Krygowski, E. Grech, W. Kolodziejski, and J. Klinowski, J. Phys. Chem., 1993, 97, 1862-1867

187. R. W. Taft, W. J. Shuely, R. M. Doherty, and M. J. Kamlet, J. Org. Chem., 1988, 53, 1737-1741

188. T. Gramstad and J. Sandstrom, Spectrochim. Acta, Part A, 1969, 25A, 31

189. O. A. Raevskii, M. M. Gilyazov, and Y. A. Levin, Zh. Obshch. Khim., 1983, 53, 1720

190. E. M. Arnett, E. J. Mitchell, and T. S. S. R. Murty, J. Am. Chem. Soc., 1974, 96, 3875

191. T. Gramstad and G. Van Binst, Spectrochim. Acta, 1966, 22, 1681

192. B. Plesnicar, R. Kavcic, and D. Hadzi, J. Molec. Struct., 1974, 20, 457-460

193. T. Gramstad, S. Husebye, and K. Maartmann-Moe, Acta Chem. Scand. B, 1986, 40B, 26-30

194. G. Bandoli, G. Bortolozzo, D. A. Clemente, U. Croatto, and C. J. Panattoni, J. Chem. Soc. A., 1970, 2778

195. T. Lin, Ph. D. Dissertation, Virginia Tech, 1993

196. ibid, pp. 29-30

197. ibid, pp. 56

198. ibid, p. 58

199. A. E. Grulke, in "Polymer Handbook", 3rd ed., J. Brandup and E. H. Immergut, eds., John Wiley and Sons, NY, 1989, VII, 519

200. T. Lin, Ph. D. dissertation, Virginia Tech, 1993, p. 59

201. Y. Sawaki and Y. Ogata, J. Am. Chem. Soc., 1981, 103(8), 2049

202. S. P. Pappas, Prog. Org. Coat., 1974, 2, 333

203. K. Inoue, K. Machizuki, and T. Tanigaki, Polym. J., 1977, 9(4), 349-353

204. A. J. Lapworth, J. Chem. Soc., 1903, 83, 995

205. A. J. Lapworth, J. Chem. Soc., 1904, 85, 1206

206. E. Stern, Z. Phys. Chem., 1905, 50, 519

207. J. P. Kuebrich, R. L. Schowen, M. Wang, and M. E. Lupes, J. Am. Chem. Soc., 1971, 93, 1214

208. T. Ugai, R. Tanaka, and T. Dokawa, J. Pharm. Soc. Jpn., 1943, 63, 296

209. R. Breslow, J. Am. Chem. Soc., 1958, 80, 3719

210. H. J. Van den Berg, G. Challa, and U. K. Pandit, J. Mol. Cat., 1989, 51, 1-12

211. K. Karimian, F. Mohanazadeh, and S. Rezai, J. Heterocyclic Chem., 1983, 20, 1119

212. B. Lachmann, H. Steinmaus, and H. W. Wanzlick, Tetrahedron, 1971, 27, 4085

213. J. P. Kuebrich and R. L. Schowen, J. Am. Chem. Soc., 1971, 93(5), 1220

214. J. Solodar, Tetrahedron Letters, 1971, 3, 287

215. S. Andreades and E. W. Zahnow, J. Am. Chem. Soc., 1969, 91, 4181

216. J. Solodar, Synth. Inorg. Metal-Org. Chem., 1971, 1(2), 141-143

217. D. A. White and M. M. Baizer, J. Chem. Soc. Perkin Trans. 1, 1973, 19, 2230

218. J. Castells, F. Pujol, H. Llitjos, and M. Moreno-Manas, Tetrahedron, 1982, 38(3), 337-346

219. C. C. Leznoff and J. Y. Wong, Can. J. Chem., 1973, 51(22), 3756-64

220. S. Havens, C. C. Yu, D. Draney, and C. S. Marvel, J. Polym. Sci.: Polym. Chem. Edn., 1981, 19, 1349-1356

221. R. H. Kratzer, K. L. Paciorek, and D. W. Karle, J. Org. Chem., 1976, 41, 2230

222. unsure of patent number: G. Rabilloud and B. Sillion, Ger. Pat.: DE 3019500, Nov. 27, 1980

223. B. A. Marshall and W. A. Waters, J. Chem. Soc., 1960, 2, 392

224. K. Kinoshita, Bull. Chem. Soc. Jpn., 1959, 32, 777

225. H. Gampp and A. D. Zuberbuhler, J. Mol. Cat., 1980, 7, 81-88

226. P. K. Adolf and G. A. Hamilton, J. Am. Chem. Soc., 1971, 93, 3420

227. G. S. Hammond and C.-H. S. Wu, J. Am. Chem. Soc., 1973, 95, 8215

228. S. Tsuruya, T. Masuoka and M. Masai, J. Mol. Cat., 1981, 10, 21-32

229. H. A. Hodali and R. A. El-Zaru, Polyhedron, 1990, 9(18), 2299-2304

230. M. VanDyke and N. D. Pritchard, J. Org. Chem., 1967, 32, 3204

231. Y. Ogata and H. Tezuka, Tetrahedron, 1970, 26, 5593-5599

232. S. E. Wentworth, Proc. 11th Nat'l SAMPE Tech. Conf., 1979, p. 752

233. J. March, Advanced Organic Chemistry, 3rd ed., John Wiley and Sons, NY, 1985, p. 1077

234. M. A. Abd-Alla, Makromol. Chem., 1991, 192, 277-283

VITA

The author, Katherine Weber Stickney, was born in Dover, New Hampshire, on December 5, 1963. The daughter of Dr. and Mrs. James H. Weber, she lived in Durham, N. H., and attended the University of New Hampshire after graduation from high school. Katherine received her B. S. in Chemistry (with a minor in French), Magna Cum Laude, from the University of New Hampshire in 1986. After graduation she worked for two years in Bausch & Lomb's rigid gas permeable contact lens division in Wilmington, Massachusetts, where her work involved the synthesis and characterization of new contact lens materials. Katherine left Bausch & Lomb in 1987 in order to serve as a United States Peace Corps volunteer in Togo, West Africa, where she taught high school physics and chemistry in French until 1989.

In January 1990, Katherine enrolled in the doctoral program of chemistry at Virginia Tech, in Blacksburg, Virginia, where she engaged in course work and research under the guidance of Professor J. S Riffle. The title of her doctoral dissertation is "Hydrogen Bonding as it Relates to Miscibility of High Performance Poly(arylene ether)s with Epoxy Resins". She expects to graduate in August 1995, with a Ph. D. in Chemistry from Virginia Tech. Her immediate plans after graduation include a Visiting Professorship of Chemistry at the University of Indianapolis, in Indianapolis, Indiana.

236